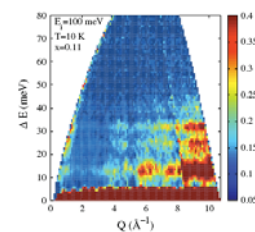
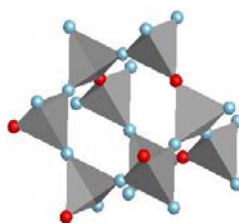
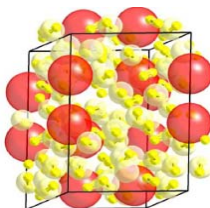
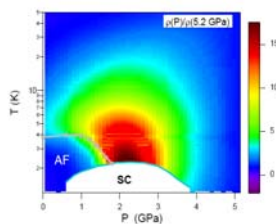
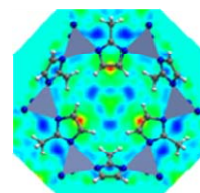
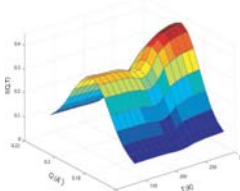
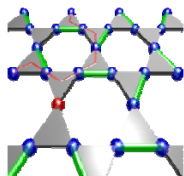
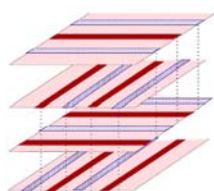


NEUTRON SCATTERING CONTRACTORS' MEETING

JULY 18-21, 2010

AIRLIE CONFERENCE CENTER
WARRENTON, VA



OFFICE OF BASIC ENERGY SCIENCES
DIVISION OF MATERIALS SCIENCES
AND ENGINEERING



U.S. DEPARTMENT OF
ENERGY

On the Cover

Top Row, Left to Right

Nature of stacking of stripe planes in the low temperature tetragonal phase of $\text{La}_{15/8}\text{Ba}_{1/8}\text{CuO}_4$
Courtesy: John Tranquada, Brookhaven National Lab

Existence of Spinons in a $S=1/2$ “kagome” antiferromagnet.
Courtesy: Collin Broholm, Johns Hopkins University

Confined water maintained in its liquid state in uniform cylindrical nanopores exhibits a density minimum at -63°C .
Courtesy: Sow-Hsin Chen, MIT

Difference Fourier analysis, showing the main- H_2 absorption sites (red circles) in ZIF8 are near the top of C-C bond of the linker and not the metal center.
Courtesy: Taner Yildirim, NIST

Bottom Row, Left to Right

As CeRhIn_5 's magnetic transition (AF) is tuned toward zero temperature by applied pressure, a dome of superconductivity (SC) emerges. The dark red area above the dome's maximum reflects very strong isotropic scattering of electrons by quantum excitations. Coincidence of most intense scattering and the maximum temperature for superconductivity provides strong evidence for a new, unconventional pairing mechanism.
Courtesy: Joe Thompson and John Sarrao, LANL

A novel compound $\text{Xe}(\text{H}_2)_7$ with the highest number of hydrogen molecules per chemical formula unit known to date forms above 40K bar pressure and surprisingly remains stable even up to 2.5M bar. High resolution structure of this compound reveals that the xenon atoms coalesce into pairs that are surrounded by hydrogen molecules.
Courtesy: M. Somayazulu and Rus Hemley, Carnegie Institute of Washington

Neutron Diffraction of CdCr_2O_4 above a critical field of 28 T on its ordering into the $\text{P4}_3\text{32}$ spin configuration. Blue and red spheres represent the magnetic moments oriented parallel and anti-parallel to the field, respectively.
Courtesy: S.-H. Lee, University of Virginia

Inelastic neutron scattering data as a function of Q and E for $\text{LaFeAsO}_{1-x}\text{F}_x$ shows that the phonon density of states is not consistent with conventional superconductivity.
Courtesy: D Mandrus, ORNL; P.C. Canfield and R. McQueeney, Ames Lab

This document was produced under contract number DE-AC05-06OR23100 between the U.S. Department of Energy and Oak Ridge Associated Universities.

Foreword

This volume comprises the scientific content of the 2010 Neutron Scattering Contractors Meeting sponsored by the Division of Materials Sciences and Engineering (DMS&E) in the Office of Basic Energy Sciences (BES) of the U.S. Department of Energy (DOE). This meeting on July 18-21, 2010 at the Airlie Conference Center, Warrenton, VA, is the second in the series, covering the projects funded by the Neutron Scattering Program. The first meeting held on October 16-19, 2007 included both X-ray and Neutron Scattering programs. BES DMS&E has a long tradition of supporting a comprehensive scattering program in recognition of the high impact these tools have in discovery and use-inspired research. The size of the BES Scattering program has grown to the point where X-ray scattering now has a separate program and contractors meeting parallel to neutron scattering.

The DMS&E Neutron Scattering CRA supports basic research using neutron scattering, spectroscopy, and imaging for materials research, primarily at major BES-supported user facilities. Neutron scattering serves as one of the primary tools for characterizing the atomic, electronic and magnetic structures and excitations of materials. Information on structure and dynamics becomes the basis for identifying new materials and describing mechanisms underlying their unique behavior. Other key aspects of this activity are the development and improvement of next-generation instrumentation involving innovative focusing optics, novel detectors, sample environments, data analysis tools, and the production and application of polarized neutrons. Topical areas highlighted in this contractors meeting include Superconductivity, Magnetism, Systems under Nanoconfinement, Soft Matter and Advanced tools for focusing and polarization. Also included are the facility updates on new tools and techniques that service the basic research needs of various BES research initiatives.

The purpose of the contractors meeting is to bring together researchers funded by BES in the Neutron Scattering research area, to facilitate the exchange of new results and research highlights, to foster new ideas and collaborations among the participants, and to identify needs of the research community. The meeting will also help DMS&E to assess the state of the program, chart future directions, and identify programmatic needs.

We thank all the meeting participants for their active contributions in sharing their ideas and research accomplishments. Sincere thanks are also due to the speakers from other BES programs involved with neutron scattering in multi-disciplinary research. The advice and help of the Meeting Chairs, John Tranquada and Tonya Kuhl, in planning for the meeting are deeply appreciated. We sincerely thank Christie Ashton, Kerry Gorey in DMS&E and Lee-Ann Tally at the Oak Ridge Institute of Science and Education for their outstanding work in all aspects of the meeting organization.

Thiyaga P. Thiyagarajan and Helen Kerch
Division of Materials Sciences and Engineering
Office of Basic Energy Sciences
Office of Science
U.S. Department of Energy

Table of Contents

Foreword	i
Table of Contents	ii
Agenda	vii
Session I – Superconductivity (I) Sessions	
Frustrated Magnetism & Superconductivity	
<i>C. Broholm, N. P. Armitage, R J. Cava, O. Tchernyshyov, and Z. Tesanovic</i>	1
Complex Electronic Materials	
<i>J. D. Thompson, E. D. Bauer, R. Movshovich, F. Ronning and J. L. Sarrao</i>	5
Using Neutron as a Probe to Study Magnetic Excitations in Strongly Correlated Electron Materials	
<i>Pengcheng Dai</i>	9
Session II – Superconductivity (II)	
Electronic Structure and Physical Properties of Iron-Based Superconductors – Results from Theory and Open Questions	
<i>David J. Singh</i>	13
Correlations and Competition Between the Lattice, Electrons, and Magnetism	
<i>R. J. McQueeney, V. P. Antropov, A. I. Goldman, B. N. Harmon, A. Kreyssig, D. Vaknin, and J. L. Zarestky</i>	14
Orbital Correlations, Frustration, and Nanoscale Correlations in Transition Metal Compounds	
<i>S. Rosenkranz, R. Osborn, E.A. Goremychkin, O. Chmaisson, H. Claus, D.Y. Chung, M.G. Kanatzidis, J.F. Mitchell, M.R. Norman, J.C. Campuzano, A. D. Christianson, M. D. Lumsden, D.L. Abernathy, T. Guidi, R.I. Bewley, P. Manuel, L.C. Chapon, and D. Reznik</i>	23
Neutron Scattering Studies of High-Temperature Superconductors and Related Systems	
<i>John M. Tranquada, Genda Gu, Markus Hücker, Guangyong Xu, and Igor Zaliznyak</i>	27

Session III – Interfaces and Nanoconfinement

Fluid Interface Reactions, Structures and Transport (FIRST) Energy Frontier Research Center <i>David J. Wesolowski</i>	31
Neutron and X-Ray Scattering Studies of the Liquid- Liquid Transition in Supercooled Confined Water and the Dynamics of Biomolecular Assemblies <i>Sow-Hsin Chen</i>	32
Neutron Scattering Studies of Classical and Quantum Fluids in Porous Media <i>Henry R. Glyde</i>	36
From Fundamental Understanding to Predicting New Nanomaterials for High-Capacity Hydrogen Storage <i>Taner Yildirim and Jack E. Fischer</i>	40

Session IV – Magnetism

Material Synthesis and Spectroscopy/Diffraction Studies of Multiferroics: Towards Enhanced Tc and Spin/Lattice Coupling <i>S-W Cheong, Rutgers University</i>	44
Magnetic Behavior in Constrained Geometries <i>S. G. E. te Velthuis, Axel Hoffmann, J. S. Jiang, Goran Karapetrov, Cristina Visani, Norbert Nemes, Jacobo Santamaria and Maria Iavarone</i>	48
A Global Understanding of Magnetic Phase Separation in Doped Cobaltites <i>Chris Leighton</i>	52
A Unified Effort for Crystal Growth, Neutron Scattering, and X-ray Scattering Studies of Novel Correlated Electron Materials <i>Young Lee</i>	56

Session V – Soft Matter

Neutron and X-ray Scattering Studies of Multi-Component Phospholipid Bilayers and Multilayers <i>Sunil K. Sinha, Yicong Ma, Gang Chen, A.N. Parikh, Zhang Jiang, Mrinmay Mukhopadhyay, David Worcester, Curt DeCaro and Laurence Lurio</i>	60
--	----

Structure-Property Relationships of Polymer Brushes in Restricted Geometries and their Utilization as Ultra-low Friction Lubricants <i>Tonya Kuhl and Roland Faller</i>	62
Application of small angle neutron scattering and phase sensitive neutron reflectometry to polymer-based solar cells <i>Michael E. Mackay</i>	66
Neutron Spin Echo studies of Hemoglobin and Myoglobin: Multiscale Internal Dynamics <i>Jyotsana Lal, Peter Fouquet, Marco Maccarini, and Lee Makowski</i>	67
Session VI – Advanced Capabilities (Sources, Optics, Instrumentation)	
New Instruments and New Science at SNS and HFIR at Oak Ridge <i>Stephen Nagler</i>	68
Advanced Capabilities and Enhancements at the Lujan Neutron Scattering Center <i>Thomas Proffen</i>	69
Neutron Microfocusing Optics and Applications <i>Gene E. Ice and Judy W. L. Pang</i>	70
Polarized ^3He in Neutron Scattering <i>W. M. Snow and T. R. Gentile</i>	74
Inelastic X-ray Scattering at Third Generation Synchrotron Sources: Present Activities and Future Plans <i>J. P. Hill</i>	78
Poster Sessions	
Poster Session I	79
Poster Session II	81
Poster Abstracts	
Structure/Property Relationships in Complex Oxides <i>O. Chmaissem, B. Dabrowski, and R. Osborn</i>	83

Atomic and Mesoscopic Study of Metallic Glasses <i>T. Egami, J. R. Morris, E. P. George, and D. M. Nicholson</i>	87
Control of Structure-Property Relationships in Complex Oxides by Designed Strain <i>M. R. Fitzsimmons, J. Olamit and S. Singh</i>	91
Neutron and X-Ray Studies of Spin and Charge Manipulation in Magnetic Nanostructures <i>Eric E. Fullerton and Sunil Sinha</i>	95
Vibrational Thermodynamics of Materials <i>Brent Fultz</i>	99
Polarized ^3He in Neutron Scattering <i>W. M. Snow and T. R. Gentile</i>	103
Towards New Extremes in Neutron Diffraction <i>M. Guthrie, R. Boehler, X. Chen, D. Mao, C. A. Tulk, A. F. Moreira Dos Santos, J. Molaison, and N. Pradham</i>	104
Photoelectron Spectroscopy of Transuranics <i>J. J. Joyce, T. Durakiewicz, and K. S. Graham</i>	105
Investigation of the spin-glass regime between the antiferromagnetic and superconducting phases in $\text{Fe}_{1+y}\text{SexTe}_{1-x}$ <i>N. Katayama, S. Ji, D. Louca, S.-H. Lee, M. Fujita, T. J. Sato, J. S. Wen, Z. J. Xu, G. D. Gu, G. Xu, Z. W. Lin, M. Enoki, S. Chang, K. Yamada and J.M. Tranquada</i>	109
Optics for Advanced Neutron Imaging and Scattering <i>B. Khaykovich, M. V. Gubarev, Y. Bagdasarova, B. D. Ramsey, and D. E. Moncton</i>	112
Quantum Critical Behavior in $\text{Ce}(\text{Ni}_{0.935}\text{Pd}_{0.065})_2\text{Ge}_2$ <i>Jon Lawrence and Eric Bauer</i>	116
Neutron Scattering Study of Geometrically Frustrated Spinels and Unconventional Superconductors <i>S. H. Lee</i>	120

Neutron Scattering Studies of Vortex Matter in Type-II Superconductors <i>X. S. Ling, Helen A. Hanson, Xi Wang, I. K. Dimitrov, J. Shi, B. B. Maranville, C. F. Majkrzak, M. Laver, U. Keiderling, and M. Russina</i>	124
Spin Transitions, Phase Competition and Ordering in Perovskite Oxides <i>Despina Louca</i>	128
Designer phase transitions in lithium-based spinels <i>Wouter Montfrooij</i>	132
Neutron and X-ray Scattering Group: Instrumentation and Outreach <i>R. Osborn, S. Rosenkranz, S. G. E. te Velthuis, U. Perez-Salas, D.L. Abernathy, and F. Ye</i>	136
Behavior of Lipid Mixtures: From Lipid Rafts to Protein Crystallization <i>U. Perez-Salas, S. Garg, D. Hanson, P. Laible, P. Bulter, and L. Porcar</i>	140
Self-Assembly of Conjugated Polymer Networks <i>K. Weigandt, J. Richards, G. Newbloom and D. C. Pozzo</i>	144
Development of New Methods for Studying Nanostructures using Neutron Scattering <i>Roger Pynn</i>	147
Coherent Transport in Nafion and Other Superprotonic Conductors <i>George Reiter</i>	151
Novel Molecular Materials for Hydrogen Storage Applications <i>Maddury Somayazulu, Timothy Stroebel, Raja Chellappa, Viktor V Struzhkin and Russell J Hemley</i>	155
Author Index	159

Neutron Scattering Contractors Meeting

*U. S. Department of Energy
Office of Basic Energy Sciences*

July 18-21, 2010

Program Chair: Thiyaga P. Thiyagarajan

Meeting Chairs: John Tranquada (BNL) and Tonya Kuhl (University of California, Davis)

SUNDAY, JULY 18

6:00 – 8:00 pm Registration
7:30 – 8:30 pm ***** Dinner *****

MONDAY, JULY 19

7:00 – 8:00 am ***** Breakfast*****
7:30 – 8:00 am Registration
8:00 – 8:30 am *Welcome*
Division and Program Updates
Linda Horton, Director, Division of Materials Science and Engineering
Thiyaga P. Thiyagarajan and Helen Kerch
Program Management, DMSE Neutron Scattering

Session I **Superconductivity (I)**
Chair: John Tranquada, BNL

8:30 – 9:00 am Collin Broholm, JHU
Frustrated Magnetism & Superconductivity
9:00 – 9:30 am Joe Thompson, LANL
Complex Electronic Materials
9:30 – 10:00 am Pengcheng Dai, University of Tennessee, Knoxville
*Using Neutron as a Probe to Study Magnetic Excitations
In Strongly Correlated Electron Materials*
10:00 – 10:30 am ***** Break *****

Session II**Superconductivity (II)**

Chair: John Sarrao, LANL

- 10:30 – 11:00 am David Singh, ORNL (Invited)
Electronic Structure and Physical Properties of Iron-Based Superconductors – Results from Theory and Open Questions
- 11:00 – 11:30 am Robert McQueeney, Ames Lab
Correlations and Competition Between the Lattice, Electrons, and Magnetism
- 11:30 – 12:00 Noon Stephan Rosenkranz, ANL
Orbital Correlations, Frustration, and Nanoscale Correlations in Transition Metal Compounds
- 12:00 – 12:30 PM John Tranquada, BNL
Neutron Scattering Studies of High-Temperature Superconductors and Related Systems
- 12:30 – 1:30 pm ***** Lunch *****
- 1:30 – 3:00 pm **Interaction & Discussions**
- 3:00 – 5:00 pm **Poster Session I**
- 6:00 – 7:00 pm ***** Dinner *****

Session III**Interfaces and Nanoconfinement**

Chair: Tonya Kuhl, University of California, Davis

- 7:00 – 7:30 pm David Wesolowski, ORNL (Invited)
Fluid Interface Reactions, Structures and Transport (FIRST) Energy Frontier Research Center
- 7:30 – 8:00 pm Sow-Hsin Chen, MIT
Neutron and X-Ray Scattering Studies of the Liquid-Liquid Transition in Supercooled Confined Water and the Dynamics of Biomolecular Assemblies
- 8:00 – 8:30 pm Henry Glyde, University of Delaware
Neutron Scattering Studies of Classical and Quantum Fluids in Porous Media
- 8:30 – 9:00 pm Taner Yildirim, University of Pennsylvania/NIST
From Fundamental Understanding to Predicting New Nanomaterials for High-Capacity Hydrogen
- 9:00 – 10:00 pm **Continuation of Poster Session I**

TUESDAY, JULY 20

7:00 – 8:00 am ***** Breakfast *****

Session IV

MAGNETISM

Chair: Takeshi Egami, University of Tennessee, Knoxville

8:00 – 8:30 am S-W Cheong, Rutgers University
Material Synthesis and Spectroscopy/Diffraction Studies of Multiferroics: Towards Enhanced Tc and Spin/Lattice Coupling

8:30 – 9:00 am Suzanne te Velthuis, ANL
Magnetic Behavior in Constrained Geometries

9:00 – 9:30 am Chris Leighton, University of Minnesota
A Global Understanding of Magnetic Phase Separation in Doped Cobaltites

9:30 – 10:00 am Young Lee, MIT
Neutron Scattering Study of Geometrically Frustrated Spinels and Unconventional Superconductors

10:00 – 10:30 am ***** Break *****

Session V

Soft Matter

Chair: Dean Myles, ORNL

10:30 – 11:00 am Sunil Sinha – University of California, San Diego (Invited)
Neutron and X-ray Scattering Studies of Multi-Component Phospholipid Bilayers and Multilayers

11:00 – 11:30 am Tonya Kuhl – University of California, Davis
Structure-Property Relationships of Polymer Brushes in Restricted Geometries and their Utilization as Ultra-low Friction Lubricants

11:30 – 12:00 Noon Michael Mackay, Delaware, University of Delaware (Invited)
Application of small angle neutron scattering and phase sensitive neutron reflectometry to polymer-based solar cells

12:00 – 12:30 pm Jyotsana Lal, ANL (Invited)
Neutron Spin Echo studies of Hemoglobin and Myoglobin: Multiscale Internal Dynamics

12:30 – 1:30 pm ***** Lunch *****

1:30 – 3:00 pm	Interaction & Discussions
3:00 – 5:30 pm	<i>Poster Session II</i>
6:00 – 7:00 pm	***** Dinner *****
Session VI	Advanced Capabilities (Sources, Optics, Instrumentation) Chair: David Mao, Carnegie Institute of Washington, Washington, D.C.
7:00 – 7:30 pm	Steve Nagler, ORNL (Invited) <i>New Instruments and New Science at SNS and HFIR at Oak Ridge</i>
7:30 – 8:00 pm	Thomas Proffen, LANL (Invited) <i>Advanced Capabilities and Enhancements at the Luja Neutron Scattering Center</i>
8:00 – 8:30 pm	Gene Ice, ORNL <i>Neutron Microfocusing Optics and Applications</i>
8:30 – 9:00 pm	W. M. Snow, Indiana University <i>Polarized ³He in Neutron Scattering</i>
9:00 – 9:30 pm	John Hill, BNL (Invited) <i>Inelastic X-ray Scattering at Third Generation Synchrotron Sources: Present Activities and Future Plans</i>
9:30 – 10:00 pm	<i>Discussions on Neutron Scattering Growth Areas</i> Moderators: John Tranquada, BNL and Tonya Kuhl, UCD

WEDNESDAY, JULY 21

7:30 – 9:00 am	***** Breakfast *****
9:00 – 10:00 am	Interaction & Discussions
10:00	***** Adjourn *****

Session I

Superconductivity (I)

Frustrated Magnetism & Superconductivity

C. Broholm (broholm@jhu.edu)^{1,2}, N. P. Armitage¹, R J. Cava³, O. Tchernyshyov¹ & Z. Tesanovic¹

¹ Department of Physics and Astronomy, Johns Hopkins University, Baltimore, MD 21218

² NIST Center for Neutron Research, NIST, Gaithersburg, MD 20899

³ Department of Chemistry, Princeton University, Princeton, NJ 08544

Research Scope

The Institute for Quantum Matter combines materials synthesis, advanced spectroscopy, and theory to explore materials dominated by strong electronic correlations. Central aspects of the correlated electron problem may be realized in frustrated magnets with low spin quantum number. We are also examining superconductivity near magnetic instabilities in copper oxides, iron pnictides, and heavy fermion systems.

Recent Progress

Disorder profoundly impacts strongly correlated states of frustrated magnets. Cava and Dutton sharply controlled impurities in highly frustrated chromium based antiferromagnetic oxides [6]. β -CaCr₂O₄ (Fig. 1) contains weakly interacting frustrated spin chains with suppressed ordering. Fig. 1 shows the effects of site and bond centered doping in β -CaCr_{2-2x}Ga_{2x}O₄ and β -Ca_{1-y}Cr₂O₄. Both dopants reduce frustration ($f=|\theta|/T_N$) and enhance χ . While Ga substitution for Cr suppresses antiferromagnetism, calcium deficiency induces static ferrimagnetism beyond T_N indicating holes induce ferromagnetic bond disorder.

Large single crystalline samples of frustrated magnets and new instruments at SNS and NIST provide an unprecedented view of dynamic spin correlations in frustrated magnets. Fig. 2 shows data for NiGa₂S₄ and SrHo₂O₄. The former is a spin-1 triangular lattice system where we find dynamic short range order indicating a spin nematic. With increasing $\hbar\omega$ one sees a cross over from periodicity corresponding to the reciprocal lattice parameter \mathbf{a}^* to a periodicity of $\frac{1}{2}\mathbf{a}^*$ indicating competing interactions along \mathbf{a} . Fig. 2 also shows scattering data from SrHo₂O₄ with the same structure as β -CaCr₂O₄ (Fig. 1). A large single crystal was grown by Haifeng Li and Wei Tiang of Ames using the Xenon image furnace at IQM. We find quasi-elastic 1D correlations combined with a flat mode at 3.5 meV both linked to frustration.

The spin-1/2 kagome antiferromagnet has been the subject of intense theoretical and experimental work at IQM [7,11]. Hao and Tchernyshyov have shown that the ground state can be viewed as a collection of fermionic spinons bound into small, heavy singlet pairs. Low-energy excitations in this system correspond to breaking the pairs into individual spinons and the energy of this excitation is $0.06J$ [11].

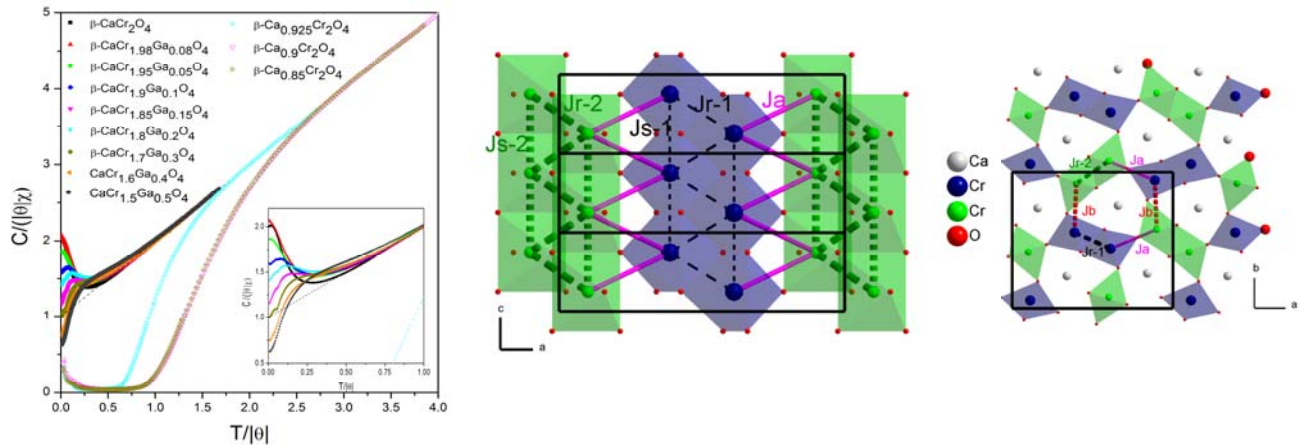


Figure 1. Right images show the structure of β -CaCr₂O₄, a system of corner-linked zig-zag spin-3/2 chains. The susceptibility data (left) show the very different effect of site and bond centered disorder [1].

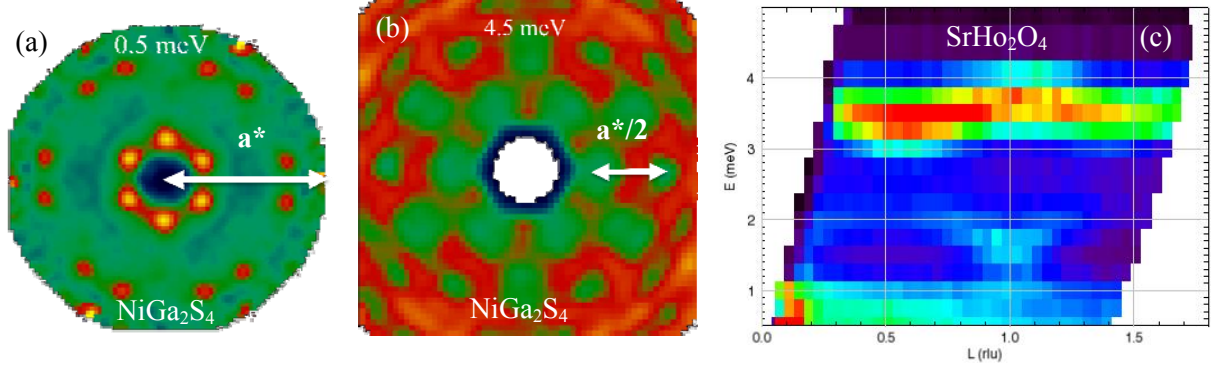


Figure 2. (a)-(b) slices of inelastic magnetic neutron scattering from NiGa_2S_4 at 0.5 meV and 4.5 meV. Inversion symmetry was imposed. The white arrows show that the reciprocal space periodicity halves with increasing energy. (c) Inelastic neutron scattering intensity versus wave vector transfer along the (00L) for SrHo_2O_4 .

For comparison to neutron scattering data they have also calculated the intensity for inelastic neutron scattering from spinon pairs [7]. As indicated in Fig. 3 the result is remarkably similar to the wave vector dependence associated with the singlet to triplet excitation of spin pairs on a kagome lattice.

Neutron scattering has been used to examine the magnetic excitations of iron chalcogenide and iron pnictide superconductors [5,8,12,15,17,19]. IQM published the first evidence for a spin resonance in the excitation spectrum of $\text{FeSe}_{0.4}\text{Te}_{0.6}$, accompanied by an RPA calculation of the corresponding bound state spectrum [12]. Our most recent data show field enhanced fine structure in the spin resonance [8]. Theoretical efforts on pnictide superconductors focus on: (i) the microscopic understanding of new iron-based superconductors [2,9,13,18,20] and (ii) the effort to model their phenomenology, with an eye on supporting work to characterize their important experimental properties [14,16,21].

Towards a microscopic understanding, Tesanovic *et al.* followed their initial work on the “minimal” tight-binding description and the nesting mechanism for SDW and superconductivity [18] with a detailed renormalization group analysis of the interplay between SDW and superconductivity [13]. This has led to a simple physical picture of how the purely electronic interband pairing mechanism operates in an otherwise hostile d-transition metal environment. While the bare interband pairing interaction is smaller than the intraband Coulomb repulsion, eventually, as the SDW instability is cut-off – by either doping or pressure suppressing nesting tendencies – the renormalized pairing interaction flips sign and s^\pm superconductivity is the natural consequence.

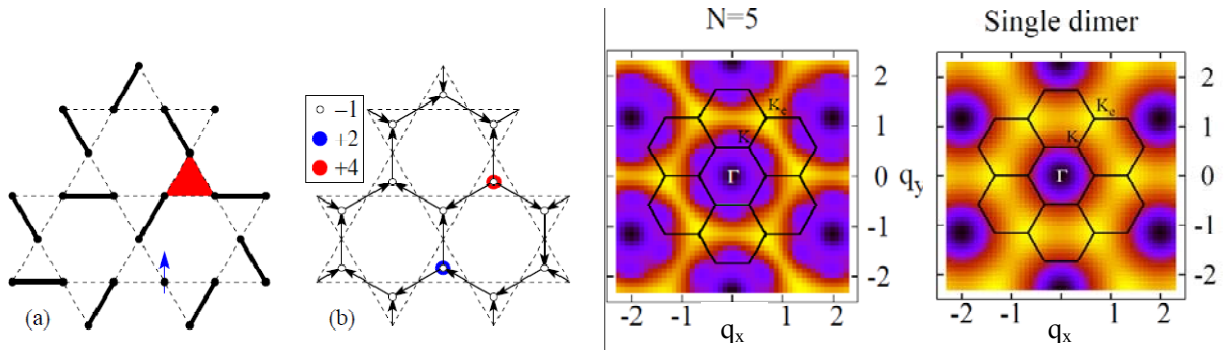


Figure 3. (a) Dimer coverage of the kagome lattice including a defect triangle with no dimers. The corresponding spinon configuration is shown in (b). The $N=5$ image is the calculated structure factor for the spinon and it is compared with the single dimer intensity distribution shown far right [7,11].

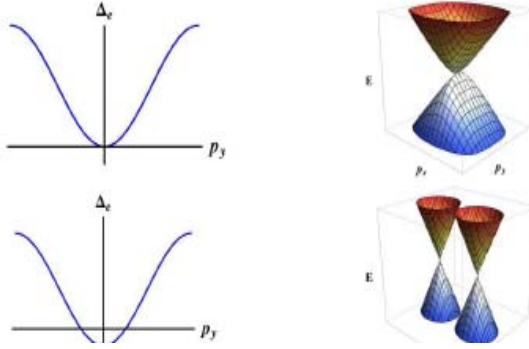


Figure 4. The critical quasiparticle scaling arising from accidental “zero-points” supplants Dirac nodal scaling in many iron-based compounds [1].

On the phenomenological side, experimental properties providing a distinct signature of s^{\pm} superconductivity were determined. This is important as an electronic pairing mechanism hints a substantial increase in T_c may be possible through imaginative chemistry. A time-reversal symmetry breaking was predicted in the phase diagram of iron superconductors, providing an explicit connection between symmetry breaking and the physics behind s^{\pm} [9]. We also explored the unique quasiparticle phenomenology from accidental nodes in the superconducting gap and the effects of fluctuations, a crucial element for applications [1].

Turning to the cuprates, the nature of the essential pseudogap regime continues to be questioned. Armitage et al. used THz time-domain spectroscopy (TTDS) to probe superconducting correlations above T_c in $\text{La}_{2-x}\text{Sr}_x\text{CuO}_4$ thin films with $x=0.06$ to 0.25 [4]. THz spectroscopy can quantify superconducting fluctuations on the relevant time scale. For all samples, the characteristic fluctuation rate increases abruptly above T_c , but is limited when it reaches a scale proportional to temperature. We find that fluctuations in conductivity persist up to - at most - 20 K above T_c , which is in contrast to diamagnetic measurements where the signal persists 100 K above T_c . If the latter effect originates from vortices well above T_c then very unusual correspondences exist between correlations in length probed by magnetic susceptibility and the time correlations measured by TTDS.

TTDS was also used to probe thin films of the pnictide superconductor $\text{BaFe}_{2-2x}\text{Co}_{2x}\text{As}_2$ [3]. Near T_c we find evidence for a coherence peak and qualitative agreement with the weak-coupling Mattis-Bardeen form of the conductivity. Our observation can be contrasted to NMR spin-relaxation measurements, which thus far have not found such a coherence peak. At low temperature, the real part of the THz conductivity is not fully suppressed and the imaginary part of the conductivity is significantly smaller than the Matthis-Bardeen prediction. We interpret these anomalies as consistent with impurity scattering induced pair-breaking as expected for an extended s^{\pm} order parameter.

Future Plans

In frustrated magnetism, Seyed Koohpayeh of JHU has grown large TbMnO_3 crystals to probe magneto-elastic excitations as well as a novel layered frustrated chromium based system. Neutron scattering experiments will be carried out on these and other quantum magnets under development at Princeton. Neutron and THz experiments will explore the relationship between superconductivity and magnetism in Ce based 115 d-wave superconductors. New instrumentation and new ideas also lead us to re-examine magnetic excitation in superconducting UPt_3 and UNi_2Al_3 . We continue to explore the effects of high fields on the spin resonance in $\text{FeSe}_{0.4}\text{Te}_{0.6}$ through experiments and theory. Theoretical work is underway to understand detailed measurements of spin fluctuations in frustrated systems from MACS and CNCS.

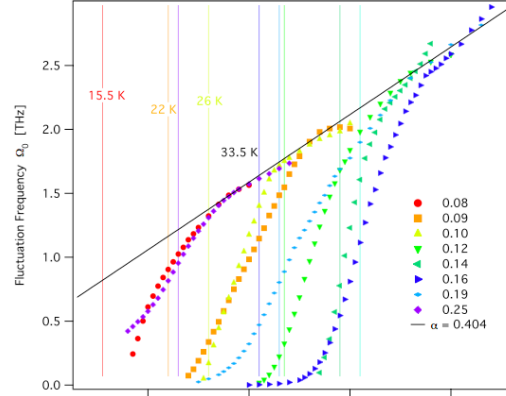


Figure 5. The superconducting fluctuation rate Ω vs. T for $\text{La}_{2-x}\text{Sr}_x\text{CuO}_4$. Vertical lines indicate T_c for each sample. Ω approaches a limiting linear temperature dependence [4].

Publications (FY2008-present)

1. "Robust accidental nodes and zeroes and critical quasiparticle scaling in iron-based multiband superconductors", V. Stanev, B. S. Alexandrov, P. Nikolic, and Z. Tesanovic, arxiv.org/abs/1006.0447, submitted to Phys. Rev. Lett. (2010).
2. "D - 2 \rightarrow ∞ theory of superconducting fluctuations in magnetic field and its application to iron-pnictides", J. M. Murray & Z. Tesanovic, arxiv.org/abs/1004.5277, submitted to Phys. Rev. Lett. (2010).
3. "Observation of coherence peak by THz spectroscopy in BaCo_{2x}Fe_{2-2x}As₂", R. Valdes-Aguilar, L.S. Bilbro, S. Lee, C.-B. Eom, and N. P. Armitage, submitted to Phys. Rev. Lett. (2010).
4. "Probing the extent and character of superconducting fluctuations in LSCO by THz spectroscopy", L.S. Bilbro, R. Valdes-Aguilar, I. Bozovic, and N. P. Armitage, submitted to Nature Physics (2010).
5. "Control of Tetrahedral Coordination and Superconductivity in FeSe_{0.5}Te_{0.5} Thin Films", S. X. Huang, C. L. Chien, V. Thampy, and C. Broholm, Phys. Rev. Lett. **104**, 217002 (2010)
6. "The Divergent effects of static disorder and hole doping in geometrically frustrated β -CaCr₂O₄", S. E. Dutton, R. J. Cava, and C. Broholm, <http://arxiv.org/abs/1004.1390>, J. Solid State Chem. (2010).
7. "Structure factor of low-energy spin excitations in a S = 1/2 kagome antiferromagnet", Z. Hao and O. Tchernyshyov, <http://arxiv.org/abs/1004.2293>, submitted to Phys. Rev. B. (2010).
8. "A triplet resonance in superconducting FeSeTe", W. Bao, A. T. Savici, G. A. Granroth, C. Broholm. K. Habicht, Y. Qiu, J. Hu, T. Liu, and Z. Q. Mao, submitted to Phys. Rev. Lett. (2010).
9. "Three-band superconductivity and time-reversal breaking order parameter", V. Stanev and Z. Tesanovic, Phys. Rev. B **81**, 134522 (2010).
10. "Progress and perspectives in the electron-doped cuprates", N. P. Armitage, P. Fournier, and R. L. Greene, Reviews of Modern Physics (2010).
11. "Fermionic spin excitations in two and three-dimensional antiferromagnets", Z. Hao and O. Tchernyshyov, Phys. Rev. Lett. **103**, 187203 (2009).
12. "Spin Gap and Resonance at the Nesting Wave vector in Superconducting FeSe_{0.40}Te_{0.60}", Yiming Qiu, Yang Zhao, Wei Bao, C. Broholm, V. Stanev, Z. Tesanovic, Y.C. Gasparovic, S. Chang, Jin Hu, Bin Qian, Minghu Fang, and Zhiqiang Mao, Phys. Rev. Lett. **103**, 067008 (2009).
13. "Valley density-wave and multiband superconductivity in Fe pnictides", V. Cvetkovic and Z. Tesanovic, Phys. Rev. B **80**, 024512 (2009).
14. "Are Iron Pnictides New Cuprates?", Z. Tesanovic, Physics 2, 60 (2009).
15. "Itinerant magnetic excitations in antiferromagnetic CaFe₂As₂", S. O. Diallo, V. P. Antropov, T. G. Perring, C. Broholm, J. J. Pulikkotil, N. Ni, S. L. Bud'ko, P. C. Canfield, A. Kreyssig, A. I. Goldman, and R. J. McQueeney, Phys. Rev. Lett. **102**, 187206 (2009).
16. "Determination of Superconducting Gap of SmFeAsO_{1-x}F_x Superconductors by Andreev Reflection Spectroscopy", T. Y. Chen, S. X. Huang, Z. Tesanovic, R. H. Liu, X. H. Chen, and C. L. Chien, Physica C: Superconductivity **469**, 521-528 (2009).
17. "Suppression of antiferromagnetic spin fluctuations in the collapsed tetragonal phase of CaFe₂As₂", D. K. Pratt, Y. Zhao, S. A. J. Kimber, A. Hiess, D. N. Argyriou, C. Broholm, A. Kreyssig, S. Nandi, S. L. Bud'ko, N. Ni, P. C. Canfield, R. J. McQueeney, and A. I. Goldman, (Editors Choice) Phys. Rev. B **79**, 060510(R) (2009).
18. "Multiband magnetism and superconductivity in Fe-based compounds", V. Cvetkovic and Z. Tesanovic, Europhysics Lett. **85**, 37002 (2009).
19. "Anisotropic Three-Dimensional Magnetism in CaFe₂As₂", R. J. McQueeney, S. O. Diallo, V. P. Antropov, G. D. Samolyuk, C. Broholm, N. Ni, S. Nandi, M. Yethiraj, J. L. Zarestky, J. J. Pulikkotil, A. Kreyssig, M. D. Lumsden, B. N. Harmon, P. C. Canfield, A. I. Goldman, Phys. Rev. Lett. **101**, 227205 (2008).
20. "Spin Fluctuation Dynamics and Multiband Superconductivity in Iron Pnictides", V. Stanev, J. Kang, and Z. Tesanovic, Phys. Rev. B **78**, 184509 (2008).
21. "The BCS-like gap in superconductor SmFeAsO_{0.85}F_{0.15}", T. Y. Chen, Z. Tesanovic, R. H. Liu, X. H. Chen, and C. L. Chien, Nature **453**, 1224 (2008).

Complex Electronic Materials

*J. D. Thompson, E. D. Bauer, R. Movshovich, F. Ronning and J. L. Sarrao
Los Alamos National Laboratory, Los Alamos, NM 87545
jdt@lanl.gov*

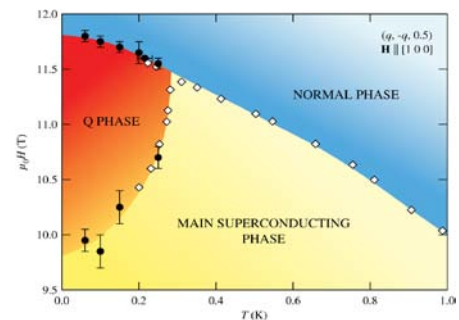
Program scope: Conventional experimental and theoretical approaches to condensed matter are unable to account for the emergence of complex and collective states in complex electronic materials. In these materials, competing interactions nonlinearly couple spin, charge, and lattice degrees-of-freedom to create a near-degeneracy of states and functional responses on multiple length and time scales. Slight changes in sample composition, dimensionality, temperature, pressure/strain or magnetic field tune the delicate balance among competing interactions and induce transitions between broken-symmetry ground states and transitions to complementary uniform states. This project contains three complementary subtasks aimed at exploring and understanding these complex states. One focuses on correlated 4f- and 5f-electron systems as prototypes of complex electronic materials but also studies complementary issues in correlated d-electron materials, such as the recently discovered pnictides and representative intermetallics. This subtask is the subject of this abstract. Of the two other subtasks, one uses photoemission spectroscopy to reveal complex electronic behavior in Pu-based materials and the other emphasizes neutron scattering techniques to develop a fundamental understanding of the role of strain on magnetic/electronic properties of complex oxide films and interfaces. Separate abstracts by John Joyce (Pu materials) and Mike Fitzsimmons (thin films) expand on the scope, progress and future directions of those tasks. The following is specific to the principal subtask of this project.

Complex behaviors are most pronounced near the magnetic/non-magnetic and metal/insulator boundaries in electronically correlated materials and become particularly poorly understood as these boundaries are tuned to absolute zero temperature, i.e., to a quantum-critical point. This subtask focuses on developing an understanding of complex electronic materials and phenomena by discovering new examples of materials that reveal the essential, underlying physics of their complex and collective states. A successful program of discovering new physics through new materials requires integration of materials preparation, in single crystal form where possible, with a necessarily broad suite of materials characterization techniques that probe static and dynamic degrees-of-freedom and their interactions on multiple length and time scales. Our approach is two-fold: one of initial exploratory research on new materials and phenomena and a second of in-depth investigations leading to microscopic understanding of those materials and phenomena. At the exploratory stage, simple structure, transport, magnetic and thermodynamic measurements, often at very low temperatures, high pressures and high magnetic fields, are sufficient to identify new states that deserve more detailed study by various spin and charge spectroscopies, particularly neutron scattering, nuclear quadrupole/magnetic resonance and photoemission. DOE neutron and photon facilities, the Los Alamos N HMFL Pulsed Field Facility and Center for Integrated Nanotechnologies as well as an extensive network of experimental and theoretical collaborators substantially leverage in-house capabilities and are important to the success of this project.

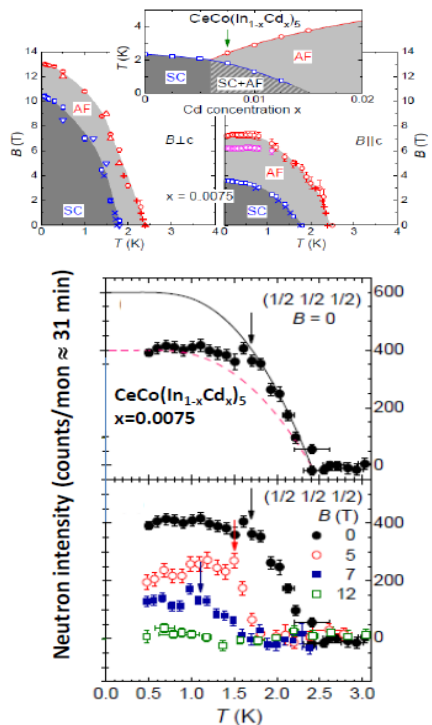
Recent progress: Most attention recently has focused on unconventional superconducting and magnetic states, their coexistence/competition, and relationship to quantum fluctuations expected

as these boundaries are tuned to absolute zero temperature. The family of heavy-fermion compounds CeMIn_5 ($M=\text{Co, Rh, Ir}$), discovered in this project, has proven especially fertile.

Unconventional superconductivity in CeCoIn_5 develops out of a quantum-critical state in which the field-tuned critical point is at or somewhat below the zero-temperature (first-order) upper critical field boundary $H_{c2}(0)$. Exploratory specific heat studies discovered a second-order phase boundary, consistent with the possibility of a Fulde-Ferrel-Larkin-Ovchinnikov phase, that exists only in the low-temperature, high field Arikosov state. Though subsequent NMR measurements showed that this phase also was magnetic, recent neutron-diffraction studies have revealed essential details of this field-induced ‘Q’ phase. In a collaboration with M. Kenzelmann (PSI) and A. Bianchi (Montreal), these experiments find spin-density wave order with small ordered moment ($0.15\mu_B$) and with the same incommensurate propagation vector $Q = (0.44, 0.44, 0.5)$ for magnetic field applied parallel to $[1 -1 0]$ and $[100]$ direction in this tetragonal compound. These results strictly rule out some theoretical scenarios and show that magnetic order is modulated along nodes of the $d_{x^2-y^2}$ superconducting order parameter. Further, these results establish unambiguously that superconductivity is necessary for the existence of this SDW and are consistent with a model in which the onset of magnetic order leads to reconstruction of the superconducting gap and formation of a magnetically induced pair-density wave.



Low-temperature, high-field phase diagram showing the field-induced ‘Q’ phase in the superconducting state of CeCoIn_5 .



Results of neutron diffraction measurements that establish direct coupling of an antiferromagnetic and superconducting orders. Arrows in the lower panel mark T_c .

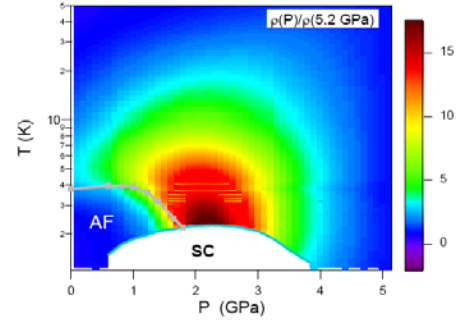
Replacing a small ($\sim 1\%$) number of In atoms with Cd also induces magnetic order in CeCoIn_5 and emphasizes the proximity of its superconductivity to a $T=0$ magnetic/non-magnetic boundary. For a range of Cd concentrations, antiferromagnetism sets in at $T_N > T_c$. NMR studies established the microscopic coexistence of long range magnetic order and unconventional superconductivity for a range of Cd concentrations less than $\sim 1.5\%$; however, these experiments were unable to determine a link between these two orders. In collaboration with Dresden scientists, we have used neutron-diffraction measurements as a function of temperature and magnetic field to discover unequivocal evidence for coupled superconducting and antiferromagnetic order parameters. These results suggest two important conclusions: (1) that low-energy magnetic fluctuations responsible for Cooper pairing are gapped by the onset of superconductivity and likely shifted to higher energies, and (2) that the single 4f-electron states sum simultaneous localized and itinerant characters that are responsible for magnetic order and superconductivity, respectively.

CeRhIn_5 orders in an incommensurate antiferromagnetic structure at atmospheric pressure. Applying pressure initially induces a phase of coexisting magnetic order and

unconventional superconductivity for a range of pressures below $P_1 \sim 1.75$ GPa, which is followed at higher pressures by a solely superconducting phase in which T_c reaches a maximum at a critical pressure $P_2 \sim 2.35$ GPa where $T_N(P)$ extrapolates to zero. Magnetic field induces magnetism that coexists with superconductivity for $P_1 < P < P_2$. Measurements of the electrical resistivity for current flow parallel and perpendicular to the tetragonal c-axis find that the low-temperature resistivity becomes more isotropic near P_2 where there is a quantum-critical, $T = 0$ antiferromagnetic to paramagnetic transition. Further, the residual resistivity at P_2 increases by nearly a factor of 40 compared to its $P = 0$ value, and the temperature dependence of the resistivity is distinctly non-Fermi-liquid, increasing as $T^{0.85}$ over a broad range above T_c . None of these properties is expected at a quantum-critical spin-density wave transition; instead, they are qualitatively consistent with a local (i.e., momentum independent) or Kondo-breakdown type of quantum criticality in which magnetic as well as charge degrees of freedom may be critical. The coincidence of a maximum scattering rate and maximum T_c near P_2 strongly suggests that fluctuations emerging from this momentum-independent criticality are responsible for Cooper-pair formation.

We have prepared and made preliminary studies of the antiferromagnet CePt_2In_7 , which is a new member of the $\text{Ce}_n\text{M}_m\text{In}_{3n+2m}$ family. The $m=1, n=1$ members are the Ce115's that are built structurally from alternating layers of CeIn_3 and MIn_2 ; whereas, the $m=1, n=2$ members (the Ce218's) are more three dimensional, consisting of two adjacent layers of CeIn_3 separated by a single layer of MIn_2 . CePt_2In_7 (Ce127) is structurally the most two-dimensional member of this family, with a single layer of CeIn_3 separated by two layers of PtIn_2 . Its pressure-temperature phase diagram is similar to that of CeRhIn_5 and offers the opportunity to explore systematically the effect of dimensionality on quantum criticality and unconventional superconductivity.

Future plans: In addition to $\text{Ce}_n\text{M}_m\text{In}_{3n+2m}$ and the Pu-based member PuCoGa_5 in which well-defined problems are posed for future study, this subtask also has discovered other families, including $\text{CeM}_4\text{Al}_{15}$, $\text{YbM}_4\text{Al}_{15}$, and $\text{UM}_4\text{Al}_{15}$ ($M = \text{Ru, Os, Co, Rh, Ir, Ni, Pd, Pt}$), ATSi_2 ($A = \text{U, Pu; T = Co, Ni}$) and $\text{R}_3\text{X}_4\text{M}_3$ ($R = \text{Ce, U; X = Sb, Bi; M = Pt, Pd, Au}$), in which competing interactions can be tuned by chemistry. Most interesting members of these families will be studied in more detail using capabilities available to us now and that we are developing as well as through our collaborators. As a counterpoint to the much studied Fe-pnictides, we have discovered superconductivity in Ni-based crystals BaNi_2As_2 , SrNi_2As_2 , SrNi_2P_2 , and CaNi_2As_2 . Our study of these much lower T_c conventional superconductors shows that certain trends of T_c in the iron-pnictides are a monotonically increasing function of T_c of the nickel-arsenide and nickel-phosphide analogs. This correlation suggests that phononic pairing may play a role in the Fe-based superconductors as well, but T_c is boosted by strong electronic correlations/magnetism. Similarities and differences, eg., the presence or not of magnetism, will continue to be explored. The competition between Kondo and RKKY interactions in heavy-fermion systems is, in general, a form of frustration, but some of these systems crystallize in structures that also frustrate the RKKY interaction. Geometric frustration alone can produce physical properties that mimic those due to competing Kondo and RKKY interactions, but the possible role of geometric



Normalized residual resistivity illustrating coincidence of the highest T_c and highest scattering rate near P_2 .

frustration in heavy-fermion materials has been explored little, if at all. We will begin to explore ways to identify what role, if any, these special crystal structures affect the heavy-fermion state.

Publications from this subtask: Only more significant publications during 2008 to present are listed from among approximately 125 since 2007.

- M. Kenzelmann et al., “Coupled superconducting and magnetic order in CeCoIn₅,” *Science* **321**, 1652 (2008).
- A. D. Bianchi et al., “Superconducting vortices in CeCoIn₅ - towards the Pauli-limiting field”, *Science* **319**, 177 (2008).
- Yi-feng Yang et al., “Scaling the Kondo lattice,” *Nature* **454**, 611 (2008).
- T. Park et al., “Isotropic quantum scattering and unconventional superconductivity,” *Nature* **456**, 366 (2008).
- T. Park et al., “Electronic duality in strongly correlated matter,” *Proc. Nat. Acad. Sci.* **105**, 6825 (2008).
- S. Nair et al., “Magnetism and superconductivity driven by identical 4f states in a heavy-fermion metal,” *Proc. Nat. Acad. Sci.* (in press).
- M. Kenzelmann et al., “Evidence for magnetically driven superconducting Q phase in CeCoIn₅,” *Phys. Rev. Lett.* **104**, 127001 (2010).
- D. Talbayev et al., “Hybridization and superconducting gaps in the heavy-fermion superconductor PuCoGa₅ probed via dynamics of photoinduced quasiparticles,” *Phys. Rev. Lett.* (in press).
- E. E. M. Chia et al., “Ultrafast pump-probe study of phase separation and competing orders in the underdoped (Ba,K)Fe₂As₂ superconductors,” *Phys. Rev. Lett.* **104**, 027003 (2010).
- N. Kurita et al., “Low-temperature magnetothermal transport investigation of a Ni-based superconductor BaNi₂As₂: evidence for fully gapped superconductivity,” *Phys. Rev. Lett.* **102**, 147004 (2009).
- S.-H. Baek et al., “NMR investigation of superconductivity and antiferromagnetism in CaFe₂As₂ under pressure,” *Phys. Rev. Lett.* **102**, 227601 (2009).
- W. Bao et al., “Tunable ($\delta\pi, \delta\pi$)-type antiferromagnetic order in α -Fe(Te,Se) superconductors,” *Phys. Rev. Lett.* **102**, 247001 (2009).
- Y.-f. Yang et al., “Magnetic excitations in the Kondo liquid: superconductivity and hidden magnetic quantum critical fluctuations,” *Phys. Rev. Lett.* **103** 197004 (2009).
- J. Spehling et al “Field-induced coupled superconductivity and spin density wave order in the heavy fermion compound CeCoIn₅,” *Phys. Rev. Lett.* **103**, 237003 (2009).
- T. Park, E. D. Bauer and J. D. Thompson, “Probing the nodal gap in the pressure-induced heavy-fermion superconductor CeRhIn₅,” *Phys. Rev. Lett.* **101**, 177002 (2008).
- W.-K. Park et al., “Andreev reflection study of the heavy-fermion superconductor CeCoIn₅: detecting order parameter symmetry,” *Phys. Rev. Lett.* **100**, 177001 (2008).
- S. Nair et al., “A precursor state to superconductivity in CeIrIn₅,” *Phys. Rev. Lett.* **100**, 137003 (2008).
- L. Mendonca Ferreira et al., “Tuning the pressure-induced superconducting phase in doped CeRhIn₅,” *Phys. Rev. Lett.* **101**, 0175005 (2008).
- Y. Tokiwa et al., “Anisotropic effect of Cd and Hg doping on the Pauli limited superconductor CeCoIn₅,” *Phys. Rev. Lett.* **101**, 037001 (2008).
- J. G. Donath et al., “Dimensional crossover of quantum critical behavior in CeCoIn₅,” *Phys. Rev. Lett.* **100**, 136401 (2008).
- Y. Qiu et al., “Crystal structure and antiferromagnetic order in NdFeAsO_{1-x}F_x (x=0 and 0.2) superconducting compounds from neutron diffraction measurements,” *Phys. Rev. Lett.* **101**, 257002 (2008).
- Q. Huang et al, “Neutron-diffraction measurements of magnetic order and a structural transition in the parent BaFe₂As₂ compound of FeAs-based high-temperature superconductors,” *Phys. Rev. Lett.* **101**, 257003 (2008).
- T. M. McQueen et al., “Successive orbital ordering transitions in NaVO₂,” *Phys. Rev. Lett.*, **101**, 166402 (2008).

USING NEUTRON AS A PROBE TO STUDY MAGNETIC EXCITATIONS IN STRONGLY CORRELATED ELECTRON MATERIALS

Pengcheng Dai (daip@ornl.gov)
 Department of Physics and Astronomy
 The University of Tennessee, Knoxville, Tennessee 37996
 and
 Oak Ridge National Laboratory, Oak Ridge, Tennessee 37831

Research Scope

Understanding the interplay between magnetism and superconductivity continues to be a “hot” topic in modern condensed matter physics. The discovery of high-temperature superconductivity in iron-based materials in 2008 provided an unique opportunity to compare and contrast these materials with traditional high- T_c copper oxide superconductors. Neutron scattering plays an important role in determining the dynamical spin properties in these materials. Over the past several years, we have carried out systematic neutron scattering studies of spin dynamics in FeAs-based superconductors and their parent materials. In the following, I summarize several key progresses we made over the past two years, and discuss our future plans.

Recent Progress

The discovery of antiferromagnetic order in the parent compounds of FeAs-based superconductors. Since the discovery of long-range antiferromagnetic (AF) order in the parent compounds of high-transition temperature (high- T_c) copper oxides, there have been tremendous efforts to understand the role of magnetism in the superconducting mechanism because superconductivity occurs when mobile ‘electrons’ or ‘holes’ are doped into the AF parent compounds. Much like high- T_c copper oxides, superconductivity in the newly discovered the rare-earth (R) iron-based oxide systems [RFeAs] are derived from either electron or hole doping of their nonsuperconducting parent compounds. The parent (non-superconducting) LaOFeAs material is metallic but shows anomalies near 150 K in both resistivity and dc magnetic susceptibility. While optical conductivity and theoretical calculations suggest that LaOFeAs exhibits a spin-density-wave (SDW) instability that is suppressed by doping electrons to form superconductivity, there has been no direct evidence of SDW order. Here we use neutron scattering to demonstrate that LaOFeAs undergoes an abrupt structural distortion below ~ 150 K, changing the symmetry from tetragonal (space group $P4/nmm$) to monoclinic (space group $P112/n$) at low temperatures, and then followed by the development of long range SDW-type AF order at ~ 137 K with a small moment but

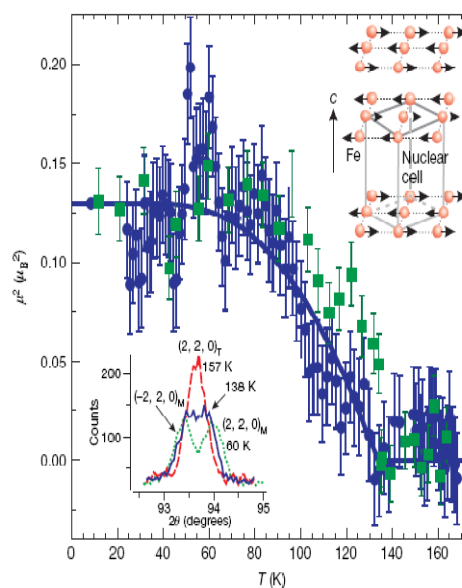


Fig. 1 Observed magnetic structure and order parameter for LaFeAsO.

simple magnetic structure. Doping the system with fluorine suppresses both the magnetic order and structural distortion in favor of superconductivity. Therefore, much like high- T_c copper oxides, the superconducting regime in these Fe-based materials occurs in close proximity to a long-range ordered AF ground state. [Summary paper: *Nature* **453**, 899 (2008). This paper was cited 510 times according to Nature web site since its publication.]

Electronic phase diagram of $CeFeAsO_{1-x}F_x$. Recently, high-transition-temperature (high- T_c) superconductivity was discovered in the iron pnictide $RFeAsO_{1-x}F_x$ (R, rare-earth metal) family of materials. We use neutron scattering to study the structural and magnetic phase transitions in $CeFeAsO_{1-x}F_x$ as the system is tuned from a semimetal to a high- T_c superconductor through fluorine (F) doping, x . In the undoped state, $CeFeAsO$ develops a structural lattice distortion followed by a collinear antiferromagnetic order with decreasing temperature. With increasing fluorine doping, the structural phase transition decreases gradually and vanishes within the superconductivity dome near $x=0.10$, whereas the antiferromagnetic order is suppressed before the appearance of superconductivity for $x>0.06$, resulting in an electronic phase diagram remarkably similar to that of the high- T_c copper oxides. Comparison of the structural evolution of $CeFeAsO_{1-x}F_x$ with other Fe-based superconductors suggests that the structural perfection of the Fe-As tetrahedron is important for the high- T_c superconductivity in these Fe pnictides. [Summary paper: *Nature Materials* **7**, 953 (2008). This paper was cited more than 150 times.]

Future Plans

We will build our future work based on the extensive experiences we have obtained on Fe-based superconductors. In particular, we will continue to focus on the evolution of spin dynamical properties of these materials and hope to establish an overall picture of the spin dynamical behavior and determine its relationship with superconductivity.

Publications (FY08-FY10)

1. “Crystalline Electric Field as a Probe for Long-Range Antiferromagnetic Order and Superconducting State of $CeFeAsO_{1-x}F_x$ ”; Songxue Chi, D. T. Adroja, T. Guidi, R. Bewley, Shiliang Li, Jun Zhao, J. W. Lynn, C. M. Brown, Y. Qiu, G. F. Chen, J. L. Lou, N. L. Wang, and Pengcheng Dai; *Phys. Rev. Lett.* **101**, 217002 (2008).
2. “Structural and magnetic phase diagram of $CeFeAsO_{1-x}F_x$ and its relationship to high-temperature superconductivity”, Jun Zhao, Q. Huang, Clarina de la Cruz, Shiliang Li, J. W. Lynn, Y. Chen, M. A. Green, G. F. Chen, G. Li, Z. Li, J. L.

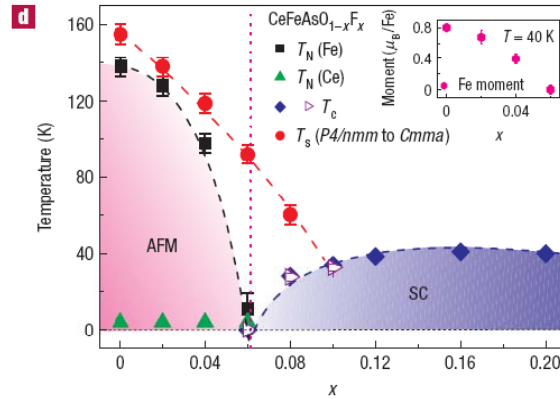


Fig. 2 Electronic phase diagram of $CeFeAsOF$ determined from our neutron diffraction experiments.

- Luo, N. L. Wang, and Pengcheng Dai, *Nature Materials* 7, 953 (2008) and news and view *Nature Materials* 7, 927 (2008) .
3. “Low energy spin waves and magnetic interactions in SrFe₂As₂”, Jun Zhao, Dao-Xin Yao, Shiliang Li, Tao Hong, Y. Chen, S. Chang, W. Ratcliff II, J. W. Lynn, H. A. Mook, G. F. Chen, J. L. Luo, N. L. Wang, E. W. Carlson, Jiangping Hu, Pengcheng Dai, *Phys. Rev. Lett.* 101, 167203 (2008).
 4. “Spin and Lattice Structure of Single Crystal SrFe₂As₂”, Jun Zhao, W. Ratcliff II, J. W. Lynn, G. F. Chen, J. L. Luo, N. L. Wang, Jiangping Hu, and Pengcheng Dai, *Phys. Rev. B* 78, 14504(R) (2008).
 5. “Lattice and Magnetic structures of PrFeAsO, PrFeAsO_{0.85}F_{0.15} and PrFeAsO_{0.85}”, Jun Zhao, Q. Huang, Clarina de la Cruz, J. W. Lynn, M. D. Lumsden, Z. A. Ren, Jie Yang, Xiaolin Shen, Xiaoli Dong, Zhongxian Zhao, and Pengcheng Dai, *Phys. Rev. B* 78, 132504 (2008).
 6. “Doping evolution of antiferromagnetic order and structural distortion in LaFeAsO_{1-x}F_x”, Q. Huang, Jun Zhao, J. W. Lynn, G. F. Chen, J. L. Luo, N. L. Wang, and Pengcheng Dai, *Phys. Rev. B.* 78, 054529 (2008).
 7. “Magnetic order of the iron spins in NdFeAsO”, Ying Chen, J. W. Lynn, J. Li, G. Li, G. F. Chen, J. L. Luo, N. L. Wang, Pengcheng Dai, C. dela Cruz, and H. A. Mook, *Phys. Rev. B* 78, 064515 (2008).
 8. “Impact of oxygen annealing on the superconducting heat capacity and magnetic resonance in Pr_{0.88}LaCe_{0.12}CuO₄”, Shiliang Li, Songxue Chi, Jun Zhao, H.-H. Wen, M. B. Stone, J. W. Lynn, and Pengcheng Dai, *Phys. Rev. B* 78, 014520 (2008).
 9. “Magnetic Order close to superconductivity in the Iron-based layered La(O_{1-x}F_x)FeAs systems”, Clarina de la Cruz, Q. Huang, J. W. Lynn, Jiying Li, W. Ratcliff II, J. L. Zarestky, H. A. Mook, G. F. Chen, J. L. Luo, N. L. Wang, Pengcheng Dai, *Nature* 453, 899-902 (2008).
 10. “Lattice Distortion and Magnetic Quantum Phase Transition in CeFeAs_{1-x}P_xO”, Clarina de la Cruz, W. Z. Hu, Shiliang Li, Q. Huang, J. W. Lynn, M. A. Green, G. F. Chen, N. L. Wang, H. A. Mook, Qimiao Si, and Pengcheng Dai, *Phys. Rev. Lett.* 104, 017204 (2010).
 11. “Low-energy Ce spin excitations in CeFeAsO and CeFeAsO_{0.84}F_{0.16}”, Shiliang Li, Dao-xin Yao, Yi-ming Qiu, Hye Jung Kang, E. W. Carlson, Jiang-ping Hu, Gen-fu Chen, Nan-lin Wang, and Pengcheng Dai, *Frontiers of Physics in China*, doi:10.1007/s11467-009-0077-8 .
 12. “Electronic Self-Organization in the Single-Layer Manganite Pr_{1-x}Ca_{1+x}MnO₄”, F. Ye, Songxue Chi, J. A. Fernandez-Baca, A. Moreo, E. Dagotto, J. W. Lynn, R. Mathieu, Y. Kaneko, Y. Tokura, and Pengcheng Dai, *Phys. Rev. Lett.* 103, 167202 (2009).
 13. “Annealing effect on the electron-doped superconductor Pr_{0.88}LaCe_{0.12}CuO₄”, Yong-Lei Wang, Yan Huang, Lei Shan, S. L. Li, Pengcheng Dai, Cong Ren, and Hai-Hu Wen, *Phys. Rev. B* 80, 094513 (2009).
 14. “Transition from Three-Dimensional Anisotropic Spin Excitations to Two-Dimensional Spin Excitations by Electron Doping the FeAs-Based BaFe_{1.96}Ni_{0.04}As₂ Superconductor” Leland W. Harriger, Astrid Schneidewind, Shiliang Li, Jun Zhao, Zhengcai Li, Wei Lu, Xiaoli Dong, Fang Zhou,

- Zhongxian Zhao, Jiangping Hu, and Pengcheng Dai, *Phys. Rev. Lett.* **103**, 087005 (2009).
15. "Superconducting state coexisting with a phase-separated static magnetic order in (Ba,K)Fe₂As₂, (Sr,Na)Fe₂As₂, and CaFe₂As₂" T. Goko, A. A. Aczel, E. Baggio-Saitovitch, S. L. Bud'ko, P. C. Canfield, J. P. Carlo, G. F. Chen, Pengcheng Dai, A. C. Hamann, W. Z. Hu, H. Kageyama, G. M. Luke, J. L. Luo, B. Nachumi, N. Ni, D. Reznik, D. R. Sanchez-Candela, A. T. Savici, K. J. Sikes, N. L. Wang, C. R. Wiebe, T. J. Williams, T. Yamamoto, W. Yu, and Y. J. Uemura, *Phys. Rev. B* **80**, 024508 (2009).
 16. "Spin waves and magnetic exchange interactions in CaFe₂As₂" Jun Zhao, D. T. Adroja, Dao-Xin Yao, R. Bewley, Shiliang Li, X. F. Wang, G. Wu, X. H. Chen, Jiangping Hu & Pengcheng Dai, *Nature Physics* **5**, 555-560 (2009).
 17. "Structural and magnetic phase transitions in NaFeAs" Shiliang Li, Clarina de la Cruz, Q. Huang, G. F. Chen, T.-L. Xia, J. L. Luo, N. L. Wang, and Pengcheng Dai, *Phys. Rev. B* **80**, 020504(R) (2009).
 18. "Spin gap and magnetic resonance in superconducting BaFe_{1.9}Ni_{0.1}As₂" Shiliang Li, Ying Chen, Sung Chang, Jeffrey W. Lynn, Linjun Li, Yongkang Luo, Guanghan Cao, Zhu'an Xu, and Pengcheng Dai, *Phys. Rev. B* **79**, 174527 (2009).
 19. "Neutron studies of the iron-based family of high TC magnetic superconductors" J. W. Lynn and Pengcheng Dai, *Physica C* **469**, 469-476 (2009).
 20. "Inelastic Neutron-Scattering Measurements of a Three-Dimensional Spin Resonance in the FeAs-Based BaFe_{1.9}Ni_{0.1}As₂ Superconductor", Songxue Chi, Astrid Schneidewind, Jun Zhao, Leland W. Harriger, Linjun Li, Yongkang Luo, Guanghan Cao, Zhu'an Xu, Micheal Loewenhaupt, Jiangping Hu, and Pengcheng Dai, *Phys. Rev. Lett.* **102**, 107006 (2009).
 21. "Static Magnetic Order and Superfluid Density of RFeAs(O,F) (R=La; Nd; Ce) and LaFePO Studied by Muon Spin Relaxation: Unusual Similarities with the Behavior of Cuprate Superconductors", J. P. Carlo, Y. J. Uemura, T. Goko, G. J. MacDougall, J. A. Rodriguez, W. Yu, G. M. Luke, Pengcheng Dai, N. Shannon, S. Miyasaka, S. Suzuki, S. Tajima, G. F. Chen, W. Z. Hu, J. L. Luo, and N. L. Wang, *Phys. Rev. Lett.* **102**, 087001 (2009).
 22. "First-order magnetic and structural phase transitions in Fe_{1+y}Se_xTe_{1-x}", Shiliang Li, Clarina de la Cruz, Q. Huang, Y. Chen, J. W. Lynn, Jiangping Hu, Yi-Lin Huang, Fong-Chi Hsu, Kuo-Wei Yeh, Maw-Kuen Wu, and Pengcheng Dai, *Phys. Rev. B* **79**, 054503 (2009).
 23. "Magnetic form factor of SrFe₂As₂: Neutron diffraction measurements". W. Ratcliff, II, P. A. Kienzle, Jeffrey W. Lynn, Shiliang Li, Pengcheng Dai, G. F. Chen, and N. L. Wang, *Phys. Rev. B* **81**, 140502(R) (2010).
 24. "Neutron spin resonance as a probe of the superconducting energy gap of BaFe_{1.9}Ni_{0.1}As₂ superconductors". Jun Zhao, Louis-Pierre Regnault, Chenglin Zhang, Miaoying Wang, Zhengcai Li, Fang Zhou, Zhongxian Zhao, Chen Fang, Jiangping Hu, and Pengcheng Dai, *Phys. Rev. B* **81**, 180505(R) (2010).
 25. "Electron-doping evolution of the low-energy spin excitations in the iron arsenide superconductor BaFe_{2-x}Ni_xAs₂", Miaoyin Wang *et al.*, *Phys. Rev. B* **81**, 174524 (2010).

Session II

Superconductivity (II)

Electronic Structure and Physical Properties of Iron-Based Superconductors – Results from Theory and Open Questions

David J. Singh

*Materials Science and Technology Division
Oak Ridge National Laboratory*

The discovery of high temperature superconductivity in doped LaFeAsO by Kamihara and co-workers provided the second class of high T_c materials, the other being the cuprate family discovered in 1986 by Bednorz and Mueller. This discovery was revolutionary in that many of the properties of the iron based superconductors are radically different from those of the cuprates, apparently requiring a new and broader understanding of the physics of high temperature superconductivity. The purpose of this talk is to discuss the chemistry and physics of the new superconductors in relation to cuprates. So far, many puzzles remain. The materials appear to be much more band-like and show much stronger signatures of metallic (Fermi surface related) physics than cuprates, with correspondingly weaker signatures of on-site Hubbard correlations. The superconducting pairing is discussed in terms of spin fluctuations based on the electronic structure, and some of the many open questions are laid out.

This work was supported by the Department of Energy, Materials Sciences and Engineering Division.

Correlations and Competition Between the Lattice, Electrons, and Magnetism

R. J. McQueeney (mcqueeney@ameslab.gov), V. P. Antropov, A. I. Goldman, B. N. Harmon,
A. Kreyssig, D. Vaknin, J. L. Zarestky

Ames Laboratory and Dept. of Physics and Astronomy, Iowa State University, Ames, IA 50011

Program Scope

The properties of modern novel materials, such as high-temperature superconductors, charge/orbital ordering systems, and multiferroics, are all sensitively controlled by correlations and competition among the lattice, electronic, and magnetic degrees of freedom. A complete understanding of the interrelations between these different subsystems and the necessary conditions for enhancing or tailoring desirable physical properties has been identified as a Grand Challenge to the scientific community. Neutron and x-ray scattering are powerful probes that directly investigate the structural, electronic, and magnetic aspects of complex ground states, phase transitions, and corresponding excitations. Any one of the many different scattering techniques alone can reveal detailed information about the underlying physics. Within this FWP, the varied expertise of the PIs in different scattering methods is employed in a synergistic approach and systems are studied using a wide range of neutron and x-ray techniques. The experimental program is supported by a closely coupled effort in *ab initio* band structure calculations, theoretical modeling, and scattering simulations. The emphasis of close coupling between different scattering techniques and theory is the unique approach of this FWP.

Recent Progress

Iron pnictide superconductors

We have made a tremendous impact the study of high-temperature superconductivity (SC) in the iron arsenide compounds where the interplay between SC, magnetism, and structure has become the major scientific theme. The parent compounds, $A\text{EFe}_2\text{As}_2$ ($A\text{E} = \text{Ba}, \text{Sr}, \text{Ca}$), manifest strong coupling between magnetism and structure illustrated by the observation of a simultaneous transition from a paramagnetic, tetragonal (T) phase to an antiferromagnetic (AFM) ordered, orthorhombic (O) phase. Chemical doping or applied pressure reduces both the AFM ordering and structural transition temperatures and SC appears. While reduction of the AFM and T-O transition temperatures is necessary for SC to occur, our studies show that the transitions need not be completely suppressed, and SC and long-range AFM order can coexist in “underdoped” (UD) compositions. Perhaps most striking is the observation that both the static magnetic order and lattice distortion for electron-doped BaFe_2As_2 are significantly suppressed below T_C . Even beyond their intrinsic interest as a new class of high temperature SC, they provide a nearly ideal family of compounds to explore the fundamental relationships between lattice, electronic and magnetic degrees of freedom. Some of our major results are listed below:

- Diffraction studies observed coupled first-order magnetic and structural transitions in $A\text{EFe}_2\text{As}_2$ parent compounds, revealing strong magnetoelastic coupling.
- Diffraction studies discovered a collapsed tetragonal (cT) phase in CaFe_2As_2 under modest hydrostatic pressure. In addition to the astonishing change in the c -axis lattice parameter ($\sim 10\%$), the cT phase is also suffers a complete loss of magnetic moment. The results highlight the extreme sensitivity of magnetism to local chemical environments and bonding.
- Measurements of the magnetic excitations and *ab initio* calculations depict CaFe_2As_2 as an itinerant magnet with frustrated magnetism consistent with large magnetoelastic coupling.

- The structural evolution of BaFe_2As_2 under pressure shares many features with chemical substitution, suggesting that SC results from fine tuning of the electronic band structure.
- Strong suppression of both AFM order and orthorhombic distortion are observed below T_C for several compositions of $\text{Ba}(\text{Fe}_{1-x}\text{Co}_x)_2\text{As}_2$, highlighting the competition between AFM ordering and SC occurs in the midst of strong magnetoelastic coupling.
- The magnetic resonance in the AFM ordered SC state in underdoped $\text{Ba}(\text{Fe}_{0.953}\text{Co}_{0.047})_2\text{As}_2$ has substantial c-axis dispersion.
- The comparison of *ab initio* calculations of phonon spectra with inelastic x-ray and neutron scattering measurements is consistent with a strong influence of magnetism on As vibrations.

Verwey transitions

The charge ordered (CO) ground state plays an important role many transition metal oxides as it often competes with other phases, such as SC in the cuprates and colossal magnetoresistive phases in the manganites. The driving force of CO remains a long-standing problem of great interest, and we have focused on the role that magnetism plays in CO (Verwey) transitions. We summarize some of our most important findings below:

- INS measurements of the magnetic exchange energies indicate that magnetism, not the Coulomb interaction, drives the CO transition in $\text{La}_{1/3}\text{Sr}_{2/3}\text{FeO}_3$.
- Spin waves are strongly softened and damped in the AFM ordered mixed valent phase of YBaFe_2O_5 ($T_V < T < T_N$), suggesting competition between strong AFM superexchange between localized Fe e_g -electrons and ferromagnetic double exchange (DE) due to itinerant t_{2g} minority spin electrons associated with Fe^{2+} ions. Hopping conductivity in the AFM state is enabled by local spin flips, leading to severe spin wave damping. In manganites, strong DE between itinerant e_g electrons results in a ferromagnetic metallic ground state.
- Optical spin waves Fe_3O_4 propagating on the mixed valent B site sublattice are shifted upwards in energy above T_V due to the occurrence of B - B ferromagnetic DE. For fast electron hopping in the band limit, cubic symmetry demands that the average DE should uniformly affect all B - B pairs. Rather, we find only spin waves of a specific symmetry are affected by DE, implying electron hopping is restricted by short-ranged charge correlations. The results are evidence that intersite Coulomb interactions among $\text{Fe}^{2+}/\text{Fe}^{3+}$ ions play a role in driving the Verwey transition in Fe_3O_4 .

Multiferroic oxides

Multiferroic compounds, exhibiting both ferroelectric and magnetic effects within the same phase, have attracted considerable attention due to the possibility of controlling electric polarization by an applied magnetic field or, conversely, magnetic order through an applied electric field. In hexagonal HoMnO_3 , it has been proposed that the application of an electric field changes the AFM order of Ho^{3+} to ferromagnetic order. X-ray resonant magnetic scattering and x-ray magnetic circular dichroism studies of HoMnO_3 determined the Ho^{3+} order in zero field where coupling to the Mn^{3+} ions results in spin reorientation transitions at 40 and 5 K. We found no dependence of the Ho ordering after applying electric fields up to 1×10^7 V/m and conclude that Ho is not responsible for the ferromagnetic response in an applied electric field.

The lithium-orthophosphate compounds, LiMPO_4 ($M = \text{Mn, Fe, Co, Ni}$), display a strong magnetoelectric (ME) effect. Detailed INS spectra of LiMPO_4 yield exchange couplings and single-ion anisotropies for each system. For LiNiPO_4 , we found an anomalous spin wave dispersion with a shallow minimum at the modulation vector of an incommensurate (IC) phase appearing above T_N , demonstrating that competing nearest- and next-nearest-neighbor exchange

interactions lead to the IC magnetic structure. The set of exchange parameters were subsequently used to explain the field dependence of the magnetic properties, including the ME effect. The Fe substitution for Ni beyond 20% modifies the exchange parameters and suppresses the IC phase.

Future Plans

Iron pnictide superconductors

Our studies in the Co-doped system have revealed that the interplay between magnetism, SC, and the lattice has two major components; 1) the competition between spin-density-wave and SC gaps, and 2) the coupling of spin fluctuations and lattice distortions, possibly occurring via the nematic degrees of freedom. Our understanding of the Co-doped BaFe_2As_2 system also provides us with a starting point to investigate the relative importance of these interactions in other systems, specifically the $R\text{FeAsO}$ (where single-crystal samples are now available) and hole-doped $A\text{Fe}_2\text{As}_2$ compounds. In addition, we wish to establish the nature of the magnetic excitations across the phase diagram and determine what role the various interactions play in the approach to SC. A central goal is to determine the nature of the excitations in underdoped compositions, i.e. whether they are predominantly spin-wave like or of a different nature, such as Stoner excitations or longitudinal excitations predicted by our *ab initio* calculations of the dynamical susceptibility. Such a distinction, if possible, presents stringent limitations on theories of spin fluctuation-induced SC that can appear in a system with long-range AFM order. The tunability of the electron-doped systems will also allow us to study how the spin resonance evolves from underdoped compositions with strong AFM order and weak SC ($T_N/T_C \gg 1$) to the optimally doped compounds with an absence of AFM order.

Verwey transitions

The CO phase in $RE\text{BaFe}_2\text{O}_5$ compounds has been described as alternating $\text{Fe}^{2+}/\text{Fe}^{3+}$ stripes, similar to the charge stripes observed in high- T_C cuprate SC. Heat capacity and other bulk measurements indicate another phase transition just prior to the Verwey transition, between $T_V < T < T^*$, whose microscopic details are unknown. Preliminary studies show additional crystallographic and magnetic superlattice peaks in this intermediate phase that are consistent with checkerboard charge ordering between $T_V < T < T^*$, suggesting a novel stripe-to-checkerboard CO transition.

In $RE_{1/3}\text{Sr}_{2/3}\text{FeO}_3$, the crystalline distortions due to the smaller RE ions increase the charge-transfer gap and should promote stronger Coulomb interactions that further stabilize the CO. Unexpectedly, it is rather seen that CO is destabilized with decreasing RE ion size. This observation supports implies that the CO is suppressed in the RE series due changes in the magnetism. We plan to measure the magnetic exchange interaction in several $RE_{1/3}\text{Sr}_{2/3}\text{FeO}_3$ compounds using INS to confirm this hypothesis.

Multiferroic compounds

To better understand the ME effect, we propose to study systematically the effect of magnetic field on the behavior of the model system LiMPO_4 compounds. For systems that display weak magnetic anisotropy, a spin-flop transition is expected whereas for stronger anisotropy the systems exhibit metamagnetic phases. Preliminary elastic neutron scattering results under applied magnetic field revealed an unusual continuous spin flop-transition in LiMnPO_4 . We propose to systematically study the transition and determine whether intermediate states during the transition indeed exist and what structures they adopt. We also propose to study the spin-dynamics of the flopped phase and correlate the results with our results and model in the absence of applied magnetic field.

Publications (FY2007-2009)

1. *Electronic Structure, Noncollinear Magnetism, and X-Ray Magnetic Circular Dichroism in the Mn_3ZnC Perovskite*
V.N. Antonov, B.N. Harmon, A.N. Yaresko, and A.P. Shpak
Phys. Rev. B, **75**, 165114 (2007).
2. *X-Ray Magnetic Circular Dichroism in GdN: First-Principles Calculations*
V.N. Antonov, B.N. Harmon, A.N. Yaresko, and A.P. Shpak
Phys. Rev. B, **75**, 184422 (2007).
3. *X-Ray Magnetic Circular Dichroism in UGe_2 : First Principles Calculations*
V.N. Antonov, B.N. Harmon, and A.N. Yaresko
J. Phys. Cond. Matter, **19** 186222 (2007).
4. *Effects of Microalloying with 3d Transition Metals on Glass Formation in AlYFe Alloys*
K.S. Bondi, A.K. Gangopadhyay, Z. Marine, T.H. Kim, A. Mukhopadhyay, A.I. Goldman, W.E. Buhro, and K.F. Kelton
J. Non-Cryst. Solids, **353**, 4723 (2007).
5. *Damping of Antiferromagnetic Spin Waves by Valence Fluctuations in the Double-Layer Perovskite $YBaFe_2O_5$*
S. Chang, P. Karen, M.P. Hehlen, F. Trouw, and R.J. McQueeney
Phys. Rev. Lett., **99**, 037202 (2007).
6. *What Have We Been Doing?*
B. N. Harmon
J. Phase Equilibria and Diffusion, **28**, 139 (2007).
7. *Magnetic Phase Diagram of Ce_2Fe_{17}*
Y. Janssen, S. Chang, A. Kreyssig, A. Kracher, Y. Mozharivskiy, S. Misra, and P.C. Canfield
Phys. Rev. B **76**, 054420 (2007).
8. *X-Ray Resonant Magnetic Scattering Study of Spontaneous Ferrimagnetism*
J.W. Kim, A. Kreyssig, P. Ryan, E. Mun, P.C. Canfield, and A.I. Goldman
Appl. Phys. Lett, **90**, 202501 (2007).
9. *Structural Studies of a Ti-Zr-Ni Quasicrystal Forming Liquid*
T.H. Kim, G.W. Lee, A.K. Gangopadhyay, R.W. Hyers, J.R. Rogers, A.I. Goldman, and K.F. Kelton
J. Phys.: Condens. Matter **19**, 455212 (2007).
10. *Non-Resonant and Resonant X-Ray Scattering Studies on Multiferroic $TbMn_2O_5$*
J. Koo, C. Song, S. Ji, J.-S. Lee, J. Park, T.-H. Jang, C.-H. Yang, J.-H. Park, Y.H. Jeong, K.-B. Lee, T.Y. Koo, Y.J. Park, J.-Y. Kim, D. Wermeille, A.I. Goldman, G. Srajer, S. Park, and S.-W. Cheong
Phys. Rev. Lett. **99**, 197601 (2007).
11. *Crystallographic Phase Transition Within the Magnetically Ordered State of Ce_2Fe_{17}*
A. Kreyssig, S. Chang, Y. Janssen, J.-W. Kim, S. Nandi, J.-Q Yan, L. Tan, R.J. McQueeney, P.C. Canfield, and A. I. Goldman
Phys. Rev. B **76**, 054421 (2007).
12. *Temperature-Dependent XMCD in Er_2Fe_{17}*
Y. Lee, B.N. Harmon, A.I. Goldman, and J.C. Lang
J. Appl. Phys. **101**, 09G525 (2007).
13. *$LiNi_{0.66}Fe_{0.34}PO_4$*
G. Liang, R.E. Benson, J. Li, D. Vaknin, and L.M. Daniels
Acta Cryst. **E63**, i73, (2007).
14. *Zener Double Exchange from Charge Fluctuations in Magnetite*
R.J. McQueeney, M. Yethiraj, S. Chang, W. Montfroofij, T. Perring, P. Metcalf, and J.M. Honig
Phys. Rev. Lett. **99**, 246401 (2007)

15. *Stabilization of Charge Ordering in $La_{1/3}Sr_{2/3}FeO_{3-\delta}$ by Magnetic Exchange*
R.J. McQueeney, J. Ma, S. Chang, J.-Q. Yan, M. Hehlen, and F. Trouw
Phys. Rev. Lett. **98**, 126402 (2007).
16. *Surface Effects on the Orbital Order in the Single Layered Manganite $La_{0.5}Sr_{1.5}MnO_4Y$*
Wakabayashi, M.H. Upton, S. Grenier, J.P. Hill, C.S. Nelson, J.-W. Kim, P.J. Ryan, A.I. Goldman, H. Zheng, and J.F. Mitchell
Nat. Mater. **6**, 972 (2007).
17. *Structural Transition of Ferromagnetic Ni_2MnGa Nanoparticles*
Y.D. Wang, Y. Ren, Z.H. Nie, D.M. Liu, L. Zuo, H. Choo, H. Li, P.K. Liaw, J.Q. Yan, R.J. McQueeney, J.W. Richardson, and A. Huq
J. Appl. Phys. **101**, 065530 (2007).
18. *Orbital Ordering and Orbital Flipping in RVO_3 Perovskites*
J.-Q. Yan, J.-S. Zhou, J.B. Goodenough, Y. Ren, J.G. Cheng, S. Chang, J. Zarestky, O. Garlea, A. Liobet, H.D. Zhou, Y. Sui, W.H. Su, and R.J. McQueeney
Phys. Rev. Lett. **99**, 197201 (2007).
19. *Phonon Density of States of $LaFeAsO_{1-x}F_x$*
A.D. Christianson, M.D. Lumsden, O. Delaire, M.B. Stone, D.L. Abernathy, M.A. McGuire, A. Safa-Sefat, R. Jin, B.C. Sales, D. Mandrus, E.D. Mun, P.C. Canfield, J.Y.Y. Lin, M. Lucas, M. Kresch, J.B. Keith, B. Fultz, E.A. Goremychkin, and R.J. McQueeney
Phys. Rev. Lett. **101**, 157004 (2008).
20. *Magnetic Order Close to Superconductivity in the Iron-Based Layered $LaO_{1-x}F_xFeAs$ Systems*
C. de la Cruz, Q. Huang, J.W. Lynn, J. Li, W. Ratcliff II, J.L. Zarestky, H.A. Mook, G.F. Chen, J.L. Luo, N.L. Wang, and P. Dai
Nature, **453** 899-902 (2008).
21. *The Triple-Axis Spectrometers at the High Flux Isotope Reactor*
J.A. Fernandez-Baca, M.D. Lumsden, B. Winn, J.L. Zarestky, and A. Zheludev
Neutron News **19-2**, 18 (2008).
22. *Lattice and Magnetic Instabilities in $CaFe_2As_2$: A Single Crystal Neutron Diffraction Study*
A.I. Goldman, D.N. Argyriou, B. Ouladdiaf, T. Chatterji, A. Kreyssig, S. Nandi, N. Ni, S.L. Bud'ko, P.C. Canfield, and R. J. McQueeney
Phys. Rev. B **78**, 100506 (2008).
23. *Colossal Positive Magnetoresistance in a Doped Nearly Magnetic Semiconductor*
R. Hu, K.J. Thomas, Y. Lee, T. Vogt, E.S. Choi, V.F. Mitrovic, R.P. Hermann, F. Grandjean, P.C. Canfield, J.W. Kim, A.I. Goldman, and C. Petrovic
Phys. Rev. B **77**, 085212 (2008).
24. *Structural Study of Supercooled Liquid Silicon*
T.H. Kim, K.F. Kelton, and A.I. Goldman
Philos. Mag. **88**, 171 (2008).
25. *Pressure-Induced Volume-Collapsed Tetragonal Phase of $CaFe_2As_2$ as Seen Via Neutron Scattering*
A. Kreyssig, M.A. Green, Y. Lee, G.D. Samolyuk, P. Zajdel, J.W. Lynn, S.L. Bud'ko, M.S. Torikachvili, N. Ni, S. Nandi, J. Leao, S.J. Poulton, D.N. Argyriou, B.N. Harmon, P.C. Canfield, R.J. McQueeney, and A.I. Goldman
Phys. Rev. B **78**, 184517 (2008).
26. *Local Structure of Equilibrium and Supercooled $Ti-Zr-Ni$ Liquids*
G.W. Lee, A.K. Gangopadhyay, R.W. Hyers, T.J. Rathz, J.R. Rogers, D.S. Robinson, A.I. Goldman, and K.F. Kelton
Phys. Rev. B, **77**, 184102 (2008).
27. *Lithium Ion Conductivity in Single Crystal $LiFePO_4$*
J. Li, W. Yao, S. Martin, and D. Vaknin
Solid State Ionics **179**, 2016 (2008).

28. *Anisotropy in the Magnetic Properties and Electronic Structure of Single-Crystal LiFePO₄*
G. Liang, K. Park, J. Li, R.E. Benson, D. Vaknin, J.T. Markert, and M.C. Croft
Phys. Rev. B **77**, 064414 (2008).
29. *Fermi-Surface-Induced Lattice Modulation and Charge-Density Wave in Optimally Doped YBa₂Cu₃O_{7-x}*
X. Liu, Z. Islam, S.K. Sinha, S.C. Moss, R.J. McQueeney, J.C. Lang, and U. Welp
Phys. Rev. B **78**, 134526 (2008).
30. *Anisotropic Three-Dimensional Magnetic Interactions in CaFe₂As₂*
R.J. McQueeney, S. Omar-Diallo, V.P. Antropov, G.D. Samolyuk, C. Broholm, N. Ni, S. Nandi, M. Yethiraj, J.L. Zarestky, J. Joseph-Pulikkotil, A. Kreyssig, M.D. Lumsden, B.N. Harmon, P.C. Canfield, and A.I. Goldman
Phys. Rev. Lett. **101**, 227205 (2008).
31. *Determination of the Exchange Anisotropy in Perovskite Antiferromagnets Using Powder Inelastic Neutron Scattering*
R.J. McQueeney, J.-Q. Yan, S. Chang, and J. Ma
Phys. Rev. B **78**, 184417 (2008).
32. *Magnetic Structure of Dy³⁺ in Hexagonal Multiferroic DyMnO₃*
S. Nandi, A. Kreyssig, J.Q. Yan, M.D. Vannette, J.C. Lang, L. Tan, J.W. Kim, R. Prozorov, T.A. Lograsso, R.J. McQueeney, and A.I. Goldman
Phys. Rev. B **78**, 075118 (2008).
33. *The Nature of Ho Magnetism in Multiferroic HoMnO₃*
S. Nandi, A. Kreyssig, L. Tan, J.W. Kim, J.Q. Yan, R.J. McQueeney, and A.I. Goldman
Phys. Rev. Lett. **100**, 217201 (2008).
34. *First-Order Structural Phase Transition in CaFe₂As₂*
N. Ni, S. Nandi, A. Kreyssig, A.I. Goldman, E.D. Mun, S.L. Bud'ko, and P.C. Canfield
Phys. Rev. B **78**, 014523 (2008).
35. *Anisotropic Thermodynamic and Transport Properties of Single-Crystalline Ba_{1-x}K_xFe₂As₂ (x=0 and 0.45)*
N. Ni, S.L. Bud'ko, A. Kreyssig, S. Nandi, G.E. Rustan, A.I. Goldman, S. Gupta, J.D. Corbett, A. Kracher, and P.C. Canfield
Phys. Rev. B **78**, 014507 (2008).
36. *Single-Crystal Growth and Physical Properties of the Layered Arsenide BaRh₂As₂*
Y. Singh, Y. Lee, S. Nandi, A. Kreyssig, A. Ellern, S. Das, R. Nath, B.N. Harmon, A.I. Goldman, and D.C. Johnston
Phys. Rev. B **78**, 104512 (2008).
37. *Observation of a Spin-Flop Transition in Gd₅Ge₄ by Resonant Magnetic X-Ray Scattering*
L. Tan, A. Kreyssig, S. Nandi, S. Jia, A.I. Goldman, R.J. McQueeney, P.C. Canfield, Y. Lee, B. Harmon, T.A. Lograsso, D.L. Schlagel, V.K. Pecharsky, K.A. Gschneidner, Jr., Z. Islam, and J.C. Lang
Phys. Rev. B **77**, 064425 (2008).
38. *Spin Dynamics in the Magnetoelectric Effect LiCoPO₄ Compound*
W. Tian, J. Li, J.W. Lynn, J.L. Zarestky, and D. Vaknin
Phys. Rev. B **78**, 184429 (2008).
39. *Structural Transition and Anisotropic Properties of Single Crystalline SrFe₂As₂*
J.-Q. Yan, A. Kreyssig, S. Nandi, N. Ni, S.L. Bud'ko, A. Kracher, R.J. McQueeney, R.W. McCallum, T.A. Lograsso, A.I. Goldman, and P.C. Canfield
Phys. Rev. B **78**, 024516 (2008).
40. *Structural Phase Transition in Ba(Fe_{0.973}Cr_{0.027})₂As₂ Single Crystals*
S.L. Bud'ko, S. Nandi, N. Ni, A. Thaler, A. Kreyssig, A. Kracher, J.Q. Yan, A.I. Goldman, and P.C. Canfield
Phys. Rev. B **80**, 014522 (2009).

41. *Structural, Magnetic, and Superconducting Phase Transitions in CaFe₂As₂ under Ambient and Applied Pressure*
P.C. Canfield, S.L. Bud'ko, N. Ni, A. Kreyssig, A.I. Goldman, R.J. McQueeney, M.S. Torikachvili, D.N. Argyriou, G. Luke, and W. Yu
Physica C **469**, 404 (2009).
42. *Absence of Structural Correlations of Magnetic Defects in the Heavy-Fermion Compound LiV₂O₄*
S. Das, A. Kreyssig, S. Nandi, A.I. Goldman, and D.C. Johnston
Phys. Rev. B **80**, 104401 (2009).
43. *Vortex Imaging in Co-Doped BaFe₂As₂*
M.R. Eskildsen, L.Y. Vinnikov, I.S. Veshchunov, T.M. Artemova, T.D. Blasius, J.M. Densmore, C.D. Dewhurst, N. Ni, A. Kreyssig, S.L. Bud'ko, P.C. Canfield, and A.I. Goldman
Physica C **469**, 529 (2009).
44. *Vortices in Superconducting Ba(Fe_{0.93}Co_{0.07})₂As₂ Studied via Small-Angle Neutron Scattering and Bitter Decoration*
M.R. Eskildsen, L.Y. Vinnikov, T.D. Blasius, I.S. Veshchunov, T.M. Artemova, J.M. Densmore, C.D. Dewhurst, N. Ni, A. Kreyssig, S.L. Bud'ko, P.C. Canfield, and A.I. Goldman
Phys. Rev. B **79**, 100501(R) (2009).
45. *Comment on 'Dipolar Excitations at the L-III X-Ray Absorption Edges of the Heavy Rare-Earth Metals'*
A.I. Goldman, B.N. Harmon, Y.B. Lee, and A. Kreyssig
Phys. Rev. Lett. **102** (12), (2009).
46. *Lattice Collapse and Quenching of Magnetism in CaFe₂As₂ under Pressure: A Single Crystal Neutron and X-Ray Diffraction Investigation*
A.I. Goldman, A. Kreyssig, K. Prokes, D.K. Pratt, D.N. Argyriou, J.W. Lynn, S. Nandi, S.A.J. Kimber, Y. Chen, Y.B. Lee, G. Samolyuk, J.B. Leão, S.J. Poulton, S.L. Bud'ko, N. Ni, P.C. Canfield, B.N. Harmon, and R.J. McQueeney
Phys. Rev. B **79**, 024513 (2009).
47. *Unconventional London Penetration Depth in Single-Crystal Ba(Fe_{0.93}Co_{0.07})₂As₂ Superconductors*
R.T. Gordon, N. Ni, C. Martin, M.A. Tanatar, M.D. Vannette, H. Kim, G.D. Samolyuk, J. Schmalian, S. Nandi, A. Kreyssig, A.I. Goldman, J.Q. Yan, S.L. Bud'ko, P.C. Canfield, and R. Prozorov
Phys. Rev. Lett. **102**, 127004 (2009).
48. *Influence of Magnetism on Phonons in CaFe₂As₂*
S.E. Hahn, Y. Lee, N. Ni, A. Alatas, B.M. Leu, D.Y. Chung, I.S. Todorov, E.E. Alp, M.G. Kanatzidis, P.C. Canfield, A.I. Goldman, R.J. McQueeney, and B.N. Harmon
Phys. Rev. B **79**, 220511(R) (2009).
49. *Experimental and Ab Initio Structural Studies of Liquid Zr₂Ni*
S.G. Hao, M.J. Kramer, C.Z. Wang, K.M. Ho, S. Nandi, A. Kreyssig, A.I. Goldman, V. Wessels, K.K. Sahu, K.F. Kelton, R.W. Hyers, S.M. Canepari, and J.R. Rogers
Phys. Rev. B **79**, 104206 (2009).
50. *Editorial on Exascale Computing*
B. N. Harmon
J. Phase Equilib. Diffus. **30**, 305 (2009).
51. *Anomalous Spin Waves and the Commensurate-Incommensurate Magnetic Phase Transition in LiNiPO₄*
T.B.S. Jensen, J. Li, N.B. Christensen, M. Kenzelmann, H.M. Ronnow, C. Niedermeyer, Scheffer, N.H. Andersen, K. Lefmann, J.L. Zarestky, and D. Vaknin
Phys. Rev B **79**, 092413 (2009).
52. *Field-Induced Magnetic Phases and Electric Polarization in LiNiPO₄*
T.B.S. Jensen, N.B. Christensen, M. Kenzelmann, H.M. Ronnow, C. Niedermeyer, N.H. Andersen, K. Lefmann, Scheffer, M. v. Zimmermann, J. Li, J.L. Zarestky, and D. Vaknin
Phys. Rev. B **79**, 092412 (2009).

53. *Similarities Between Structural Distortions under Pressure and Chemical Doping in Superconducting BaFe₂As₂*
S.A.J. Kimber, A. Kreyssig, Y-Z. Zhang, H.O. Jeschke, R. Valenti, F. Yokaichiya, D.N. Argyriou, E. Colombier, J.-Q. Yan, T.C. Hansen, T. Chatterji, R.J. McQueeney, P.C. Canfield, and A.I. Goldman
Nat. Mater. **8**, 471 (2009).
54. *Probing Fractal Magnetic Domains on Multiple Length Scales in Nd₂Fe₁₄B*
A. Kreyssig, R. Prozorov, C.D. Dewhurst, P.C. Canfield, R.W. McCallum, and A.I. Goldman
Phys. Rev. Lett. **102**, 047204 (2009).
55. *Magnetic and Lattice Coupling in Single-Crystal SrFe₂As₂: A Neutron Scattering Study*
H. Li, W. Tian, J.L. Zarestky, A. Kreyssig, N. Ni, S.L. Budko, P.C. Canfield, A.I. Goldman, R.J. McQueeney, and D. Vaknin
Phys. Rev. B **80**, 054407 (2009).
56. *Tweaking the Spin-Wave Dispersion and the Incommensurate Phase in LiNiPO₄ by Iron Substitution*
J. Li, T.B.S. Jensen, N.H. Andersen, J.L. Zarestky, R.W. McCallum, J.W. Lynn, and D. Vaknin
Phys. Rev. B **79**, 174435 (2009).
57. *Antiferromagnetism in the Magnetoelectric Effect Single Crystal LiMnPO₄*
J. Li, W. Tian, Y. Chen, J.L. Zarestky, J.W. Lynn, and D. Vaknin
Phys. Rev. B **79**, 144410 (2009).
58. *Nonexponential London Penetration Depth of FeAs-Based Superconducting RFeAsO_{0.9}F_{0.1} (R = La, Nd) Single Crystals*
C. Martin, M.E. Tillman, H. Kim, M.A. Tanatar, S.K. Kim, A. Kreyssig, R.T. Gordon, M.D. Vannette, S. Nandi, V.G. Kogan, S.L. Bud'ko, P.C. Canfield, A.I. Goldman, and R. Prozorov
Phys. Rev. Lett. **102**, 247002 (2009).
59. *Enhanced Ordering Temperatures in Antiferromagnetic Manganite Superlattices*
S.J. May, P.J. Ryan, J.L. Robertson, J.-W. Kim, T.S. Santos, E. Karapetrova, J.L. Zarestky, X. Zhai, S.G.E. te Velthuis, J.N. Eckstein, S.D. Bader, and A. Bhattacharya
Nat. Mater. **8**, 892 (2009).
60. *In Situ High Energy X-Ray Synchrotron Diffraction Study of the Synthesis and Stoichiometry of LaFeAsO and LaFeAsO_{1-x}F_y*
R.W. McCallum, J.Q. Yan, G.E. Rustan, E.D. Mun, Y. Singh, S. Das, R. Nath, S.L. Bud'ko, K.W. Dennis, D.C. Johnston, P.C. Canfield, M.J. Kramer, A. Kreyssig, T.A. Lograsso, and A.I. Goldman
J. Appl. Phys. **105**, 123912 (2009).
61. *Magnetic Ordering in EuRh₂As₂ Studied by X-ray Resonant Magnetic Scattering*
S.Nandi, A. Kreyssig, Y. Lee, Y. Singh, J.W. Kim, D.C. Johnston, B.N. Harmon, and A.I. Goldman
Phys. Rev. B **79**, 100407R (2009).
62. *Single-Crystal Growth, Crystallography, Magnetic Susceptibility, Heat Capacity, and Thermal Expansion of the Antiferromagnetic S=1 Chain Compound CaV₂O₄*
A. Niazi, S.L. Bud'ko, D.L. Schlagel, J.Q. Yan, T.A. Lograsso, A. Kreyssig, S. Das, S. Nandi, A.I. Goldman, A. Honecker, R.W. McCallum, M. Reehuis, O. Pieper, B. Lake, and D.C. Johnston
Phys. Rev. B **79**, 104432 (2009).
63. *Itinerant Magnetic Excitations in Antiferromagnetic CaFe₂As₂*
S. Omar-Diallo, V.P. Antropov, T.G. Perring, C. Broholm, J. Joseph-Pulikkotil, N. Ni, S.L. Bud'ko, P.C. Canfield, A. Kreyssig, A.I. Goldman, and R.J. McQueeney
Phys. Rev. Lett. **102**, 187206 (2009).
64. *Suppression of Antiferromagnetic Spin Fluctuations in the Collapsed Tetragonal Phase of CaFe₂As₂*
D.K. Pratt, Y. Zhao, S.A.J. Kimber, A. Hiess, D.N. Argyriou, C. Broholm, A. Kreyssig, S. Nandi, S.L. Bud'ko, N. Ni, P.C. Canfield, R.J. McQueeney, and A.I. Goldman
Phys. Rev. B **79**, 060510 (2009).

65. Competition and Coexistence of Antiferromagnetism and Superconductivity in Underdoped $\text{Ba}(\text{Fe}_{0.953}\text{Co}_{0.047})_2\text{As}_2$ Compound Using X-Ray and Neutron Scattering Techniques
D.K. Pratt, W. Tian, A. Kreyssig, J.L. Zarestky, S. Nandi, N. Ni, S.L. Bud'ko, P.C. Canfield, A.I. Goldman, and R.J. McQueeney
Phys. Rev. Lett. **103**, 087001 (2009).
66. *Intrinsic Pinning on Structural Domains in Underdoped Single Crystals of $\text{Ba}(\text{Fe}_{1-x}\text{Co}_x)_2\text{As}_2$*
R. Prozorov, M.A. Tanatar, N. Ni, A. Kreyssig, S. Nandi, S.L. Bud'ko, A.I. Goldman, and P.C. Canfield
Phys. Rev. B **80**, 174517 (2009).
67. *Magnetic Order in BaMn_2As_2 from Neutron Diffraction Measurements*
Y. Singh, M.A. Green, Q. Huang, A. Kreyssig, R.J. McQueeney, D.C. Johnston, and A.I. Goldman
Phys. Rev. B **80**, 100403(R) (2009).
68. *Direct Imaging of the Structural Domains in the Iron Pnictides $A\text{Fe}_2\text{As}_2$ ($A = \text{Ca}, \text{Sr}, \text{Ba}$)*
M.A. Tanatar, A. Kreyssig, S. Nandi, N. Ni, S.L. Bud'ko, P.C. Canfield, A.I. Goldman, and R. Prozorov
Phys. Rev. B **79**, 180508(R) (2009).
69. *Single-Crystal Neutron Diffraction Study of Short-Range Magnetic Correlations in Tb_5Ge_4*
W. Tian, A. Kreyssig, J.L. Zarestky, L. Tan, S. Nandi, A.I. Goldman, T.A. Lograsso, D.L. Schlagel, K.A. Gschneidner, V.K. Pecharsky, and R.J. McQueeney
Phys. Rev. B **80**, 134422 (2009).
70. *Flux Growth at Ambient Pressure of Millimeter-Sized Single Crystals of LaFeAsO , $\text{LaFeAsO}_{1-x}\text{F}_x$, and $\text{LaFe}_{1-x}\text{Co}_x\text{AsO}$*
J.-Q. Yan, S. Nandi, J.L. Zarestky, W. Tian, A. Kreyssig, B. Jensen, A. Kracher, K.W. Dennis, R.J. McQueeney, A.I. Goldman, R.W. McCallum, and T.A. Lograsso
Appl. Phys. Lett. **95**, 222504 (2009).
71. *Anisotropy of Antiferromagnetic 180° Domains in Magnetoelectric LiMPO_4 ($M = \text{Fe}, \text{Co}, \text{Ni}$)*
A.S. Zimmermann, B.B. Van Aken, H. Schmid, J.-P. Rivera, J. Li, D. Vaknin, and M. Fiebig
The Eur. Phys. J. B **71**, 355-360 (2009).

Orbital Correlations, Frustration, and Nanoscale Correlations in Transition Metal Compounds

S. Rosenkranz (srosenkranz@anl.gov), R. Osborn, E.A. Goremychkin, O. Chmaiszen
Materials Science Division, Argonne National Laboratory, Argonne, IL 60439

H. Claus, D.Y. Chung, M.G. Kanatzidis, J.F. Mitchell, M.R. Norman, J.C. Campuzano
Argonne National Laboratory, Argonne, IL 60439

A. D. Christianson, M. D. Lumsden, D.L. Abernathy
Neutron Sciences Division, Oak Ridge National Laboratory

T. Guidi, R.I. Bewley, P. Manuel, L.C. Chapon
ISIS Facility, Rutherford Appleton Laboratory, Chilton, UK.

D. Reznik,
University of Colorado, Boulder, CO.

Research Scope

Many emerging phenomena, and in particular the often spectacular response to externally applied fields, are intimately linked to the existence of short-range correlations in the form of stripes, ladders, checkerboards, or phase separation. Such nanoscale disorder results from the delicate balance of spin, orbital, charge, and strain degrees of freedoms giving rise to competing ground states with incompatible order. Nowhere is this more evident than in transition metal oxides and related compounds whose properties include colossal magnetoresistance, relaxor ferroelectricity, negative thermal expansion, quantum spin liquids, high temperature superconductivity, and more. Understanding the ways in which the spin, charge, orbital and strain degrees of freedom in these systems respond and self-organize on a variety of length scales, and the relation of this self-organization to changes in electronic excitations and properties is a key challenge in condensed matter physics. An important step towards obtaining this understanding is to investigate the nature of the various ground states involved, how the competition between the various underlying interactions affects the static and dynamic correlations, and how the various short-range ordering motifs observed in different systems relate to their bulk properties. In our research program, we utilize a variety of scattering techniques, both elastic and inelastic, neutron and x-ray, to elucidate the correlations in a variety of systems on short and long time- and length-scales.

Recent Progress

Iron Arsenide Superconductors: One of the most striking recent examples of emergent phenomena arising from phase competition are the iron pnictide and chalcogenide superconductors. The superconducting phase occurs when spin-density wave order has been suppressed by electron- or hole-doping. Our inelastic neutron scattering measurements on polycrystalline samples of the hole-doped $\text{Ba}_{1-x}\text{K}_x\text{Fe}_2\text{As}_2$, with $x = 0.4$, provided the first phase-sensitive evidence that the symmetry of the superconducting order parameter in these systems is unconventional, with a change in the sign of energy gap on the disconnected hole and electron Fermi surfaces [Nature **456**, 930 (2008)]. Upon further doping, we find that the resonant excitation becomes incommensurate in momentum space beyond $x = 0.5$, consistent with expected changes in the Fermi surface volumes. This confirms our interpretation of the resonance as a coherent enhancement of the band susceptibility. However, the scaling of the

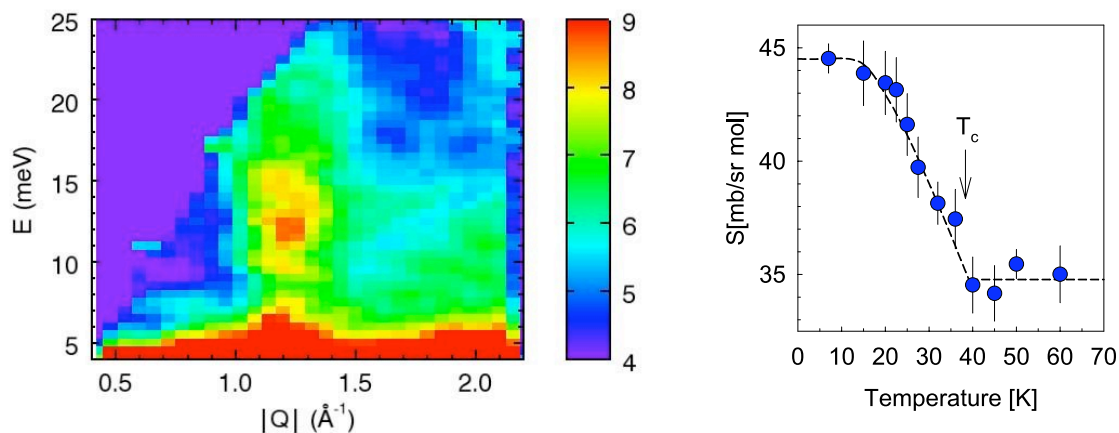


Figure 1: The left panel shows the resonant excitation at 14meV and a wavevector corresponding to the anti-ferromagnetic ordering wavevector of the parent compound observed for the 40% doped $\text{Ba}_{1-x}\text{K}_x\text{Fe}_2\text{As}_2$ sample. The temperature dependence of the integrated intensity of this excitation, shown on the right, clearly shows that this excitation appears at T_c . Above T_c , there is intensity due to short-range antiferromagnetic fluctuations.

resonance energy with T_c breaks down, either from a weakening of electron correlations or from disorder.

Because of the volatility of potassium, $\text{Ba}_{1-x}\text{K}_x\text{Fe}_2\text{As}_2$ is more challenging to synthesize than the more often studied cobalt or nickel-doped BaFe_2As_2 superconductors, but there are a number of advantages. First, there is no disorder in the superconducting Fe_2As_2 layers, and it allows the phase diagram to be studied over a wider range of chemical potentials. The group led by Mercuri Kanatzidis has refined the synthesis of these compounds to improve their homogeneity, and we have revised the phase diagram with neutron powder diffraction showing that the phase coexistence region is smaller than previously reported.

We have also studied the magnetic structure of the recently synthesized novel compound CaFe_4As_3 . Long-range magnetic order with an incommensurate modulation is observed below 85K. Below 25K, a first-order phase transition to a commensurate structure is observed. A Landau analysis is in good agreement with the observed thermodynamic properties and explains the observed drop in resistivity at the lock-in transition.

Bilayer Manganites: In our ongoing investigations of the spin, orbital, and lattice correlations in bilayer manganites $\text{La}_{2-2x}\text{Sr}_{1-2x}\text{Mn}_2\text{O}_7$, we are investigating the connection between short-range lattice correlations, characterized by single crystal diffuse scattering, and electronic properties and phonon anomalies. Utilizing resonant inelastic x-ray scattering (RIXS) on the 50% doped sample, we observe an electronic excitation at around 2eV, whose dispersion provides direct evidence of the non-local character of this excitation. The variation of the intensity with temperature between the various charge, orbital, and magnetically ordered phases can be explained with a model involving intersite d - d excitations as was first proposed for perovskite manganites. In the 50% doped sample, we have observed anomalies in the phonon dispersion at the charge ordering wavevector, using both neutron and x-ray inelastic scattering.

Charge-Density-Wave Compounds: The phonon anomalies in the charge-ordered manganites, along with an interest in phase competition in doped CDW compounds, provided the stimulus to revisit the soft-mode behavior of the classic CDW compounds, NbSe_2 and TiSe_2 . Previous inelastic neutron data were of insufficient quality because of resolution and/or sample quality, but the new generation of synchrotron x-ray spectrometers allow us to overcome these

limitations. A complete softening of the phonon modes at the CDW transition temperature were observed in both compounds. However, the range of wavevectors over which the phonons are overdamped was significantly larger in NbSe₂, whose CDW is incommensurate. This is consistent with theoretical predictions that the CDW is not driven by Fermi surface nesting, but by a broad enhancement of the electron-phonon coupling.

Cobaltites: In our investigations of the spin correlations in the cobalt perovskites La_{1-x}Sr_xCoO₃, we previously observed the existence of competing ferromagnetic and incommensurate correlations in the spin-glass phase at low doping. Utilizing spin-polarized measurements, we find that the incommensurate correlations are also magnetic in origin and that they are destroyed by an external magnetic field applied perpendicular to the short-range ordering wave vector, inducing long-range ferromagnetic order. However, short-range ferromagnetic correlations coexisting with long-range ferromagnetic order are observed even for fields up to 7 T. At higher doping, well within the ferromagnetically ordered phase, we have performed first experiments to determine the spin wave excitations throughout the whole Brillouin zone, in order to determine the influence of strong correlations. Utilizing our asynchronous rotation method on ARCS at SNS, we were able to reconstruct a large volume of S(Q,ω), thus providing measurements of the full phonon and spin-wave dispersions in a single measurement.

Future Plans

Iron Arsenides: In the iron arsenides, we plan to follow up our initial INS studies on powder samples with single crystal measurements on Ba_{1-x}K_xFe₂As₂. These are critical to determine the exact dispersion relations as the resonance becomes incommensurate and for establishing the morphology of the superconducting gaps and how they relate to the multiple *d*-electron Fermi surfaces. Because high quality K-doped crystals can only be grown with masses of 10-20 mg, we are co-aligning hundreds of crystals each experiment. We have successfully assembled composite crystals with an in-plane mosaic of only a couple degrees for *x*=0.4 (150 crystals, 1.5g) and *x*=0.5 (600 crystals, 7g) and plan to further assemble *x*=0.7.

Diffuse scattering will be important in understanding the nature of the phase separation reported by some groups and will also be used to investigate the existence of short-range orbital correlations in the vicinity of the orthorhombic to tetragonal phase transition. We will also utilize neutron scattering to study structural and magnetic properties of novel iron arsenide compounds as they are discovered and become available through the efforts of the MSD Emerging Materials Group.

Bilayer Manganites: We will continue our investigations on the origin of the short-range lattice correlations in 40-60% doped bilayer manganites and their relation to electronic properties and phonon dynamics. We will expand our investigations of the lattice dynamics and study the various different orbitally and charged ordered states observed at 50-60% doping utilizing

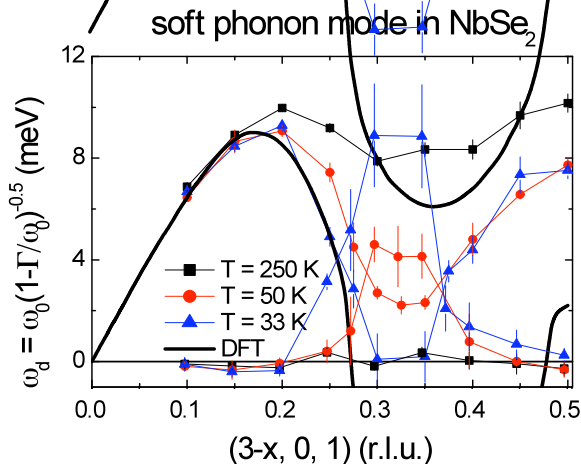


Figure 2: Extended breakdown of the acoustic phonon observed for NbSe₂.

inelastic neutron scattering, in order to investigate possible phonon anomalies associated with the short-range structural order. For these measurements we will further develop and utilize the event-mode based data acquisition strategy at SNS. The results obtained will be compared to angle resolved photoemission study in order to correlate features in the electronic excitations with the structural and phonon anomalies. Of great interest is whether various ordering wavevectors observed with scattering are related to nesting vectors observed in photoemission, how they relate to anomalies observed in phonon dispersions and linewidths and possibly kinks observed in the electronic dispersions.

Charge-Density-Wave Compounds: We plan to investigate the suppression of charge order through the intercalation *e.g.*, of Cu in TiSe₂ and how short-range order affects the lattice dynamics and electronic properties, as a comparison to the manganites.

Publications

1. *d-d Excitations in Bilayer Manganites Probed by Resonant Inelastic X-ray Scattering*, F. Weber, S. Rosenkranz, J.-P. Castellán, R. Osborn, J.F. Mitchell, H. Zheng, D. Casa, J.H. Kim, T. Gog, Phys. Rev. B, unpublished.
2. *Incommensurate spin-density wave and magnetic lock-in transition in CaFe₄As₃*, P. Manuel, L.C. Chapon, I.S. Todorov, D.Y. Chung, J.-P. Castellán, S. Rosenkranz, R. Osborn, P. Toledano, M.G. Kanatzidis, Phys. Rev. B **81**, 184402 (2010).
3. *Extended X-ray Absorption Fine Structure spectroscopy in Co_{0.013}NbSe₂*, F. Weber, J.-P. Castellán, S. Rosenkranz, R. Osborn, D. Rosenmann, M. Iavarone, J. Phys.: Conf Ser. **200**, 012224 (2010).
4. *Observation of a d-wave nodal liquid in highly underdoped Bi₂Sr₂CaCu₂O_{8+d}*, U. Chatterjee, M. Shi, D. Ai, J. Zhao, A. Kanigel, S. Rosenkranz, H. Raffy, Z.Z. Li, K. Kadowaki, D.G. Hinks, Z.J. Xu, J.S. Wen, G. Gu, C.T. Lin, H. Claus, M. R. Norman, M. Randeria, and J.C. Campuzano, Nature Physics **6**, 99 (2010).
5. *Spectroscopic evidence for preformed Cooper pairs in the pseudogap phase of cuprates*, M. Shi, A. Bendounan, E. Razzoli, S. Rosenkranz, M.R. Norman, J.C. Campuzano, J. Chang, M. Mansson, Y. Sassa, T. Claesson, O. Tjernberg, L. Patthey, N. Momono, M. Oda, M. Ido, S. Guerrero, C. Mudry, and J. Mesot, Europhysics Letters **88**, 27008 (2009).
6. *Inelastic neutron scattering studies of the spin and lattice dynamics in iron arsenide compounds*, R. Osborn, S. Rosenkranz, E. A. Goremychkin, A.D. Christianson, Physica C **469**, 498 (2009).
7. *Neutron scattering study of the competing magnetic correlations in La_{0.85}Co_{0.15}O₃*, D. Phelan, D. Louca, S. N. Ancona, S. Rosenkranz, H. Zheng, J. F. Mitchell, Phys. Rev. B **79**, 094420 (2009).
8. *Unconventional Superconductivity in Ba_{0.6}K_{0.4}Fe₂As₂ from inelastic neutron scattering*, A.D. Christianson, E.A. Goremychkin, R. Osborn, S. Rosenkranz, M.D. Lumsden, C.D. Malliakas, I.S. Todorov, H. Claus, D.Y. Chung, M.G. Kanatzidis, R.I. Bewley, T. Guidi, Nature **456**, 930 (2008).
10. *Anomalous dispersion in the autocorrelation of angle-resolved photoemission spectra of high-temperature Bi₂Sr₂CaCu₂O_{8+δ} superconductors*, U. Chatterjee, M. Shi, A. Kaminski, A. Kanigel, H.M. Fretwell, K. Terashima, T. Takahashi, S. Rosenkranz, Z.Z. Li, H. Raffy, A. Santander-Syro, K. Kadowaki, M. Randeria, M.R. Norman, and J.C. Campuzano, Phys. Rev. B **76**, 012504 (2007).
11. *Dynamic Spin-Response Functions of the High-Temperature Bi₂Sr₂CaCu₂O_{8+δ} Superconductor from angle-resolved photoemission spectra*, U. Chatterjee, D.K. Morr, M.R. Norman, M. Randeria, A. Kanigel, M. Shi, E. Rossi, A. Kaminski, H.M. Fretwell, S. Rosenkranz, K. Kadowaki, and J.C. Campuzano, Phys. Rev. B **75**, 172504 (2007).
12. *Reentrant Orbital Order and the True Ground State of LaSr₂Mn₂O₇*, Qing'An Li, K.E. Grey, H. Zheng, H. Claus, S. Rosenkranz, S. N. Ancona, R. Osborn, J.F. Mitchell, Y. Chen, and J.W. Lynn, Phys. Rev. Lett. **98**, 167201 (2007).
13. *Microscopic annealing process and its impact on superconductivity in T'-structure electron-doped copper oxides* H.-J. Kang, P. Dai, B.J. Campbell, P.J. Chupas, S. Rosenkranz, P.L. Lee, Q. Huang, S. Li, S. Komiya, and Y. Ando, Nature Materials **6**, 224 (2007).

Neutron Scattering Studies of High-Temperature Superconductors and Related Systems

John M. Tranquada, Genda Gu, Markus Hücker, Guangyong Xu, and Igor Zaliznyak
jtran@bnl.gov, ggu@bnl.gov, huecker@bnl.gov, gxu@bnl.gov, zaliznyak@bnl.gov
Condensed Matter Physics & Materials Science Department
Brookhaven National Laboratory, Upton, NY 11973-5000

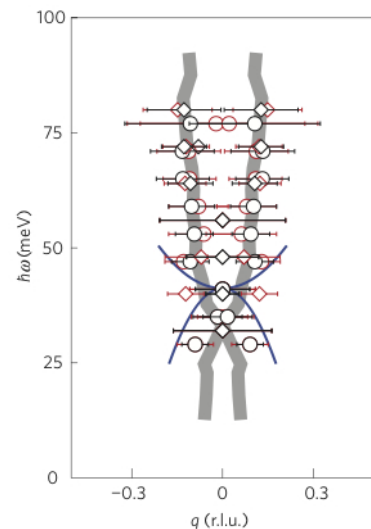
Program Scope

This program is organized around the goal of decoding the mechanism(s) responsible for high-temperature superconductivity, with particular focus on the copper oxides, as well as new systems, such as the iron-based superconductors. The main experimental tool is neutron scattering, with experiments performed at the best facilities in the U.S. and abroad. Problems addressed include: doping of correlated insulators, self-organized spin and charge inhomogeneities (such as stripes), electron-phonon coupling, spin dynamics, quantum magnetism in low-dimensional systems, and the impact of disorder. Growth of suitable single-crystal samples is an essential part of the program, with complementary characterizations performed in collaboration with other Brookhaven groups, especially at the National Synchrotron Light Source. This program has close ties to HYSPEC, an inelastic spectrometer with polarization analysis under construction at the Spallation Neutron Source (SNS); it is also involved with the US-Japan cold-neutron triple-axis spectrometer at the High Flux Isotope Reactor (HFIR), as part of the US-Japan Cooperative Program on Neutron Scattering. The BNL-NIST Alliance involves collaborative efforts at the National Institute of Standards and Technology's Center for Neutron Research.

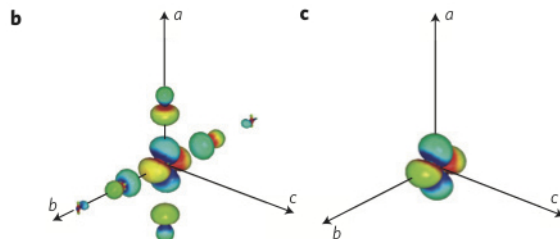
Recent Progress

Here we present selected highlights; further research results are listed in the publications.

Spin fluctuations in optimally-doped $\text{Bi}_2\text{Sr}_2\text{CaCu}_2\text{O}_{8+\delta}$: Having grown Bi2212 crystals of record size [7], we took them to the MAPS spectrometer at ISIS to map out the spin fluctuations; the magnetic character of the excitations was confirmed with polarized neutrons on IN22 at the ILL. The effective dispersions obtained at 10 K (black symbols), well below the superconducting transition temperature, T_c , of 91 K, and at 100 K (red symbols) are shown in the figure at right [14]. The thick gray [thin blue] lines indicate the dispersion reported for $\text{YBa}_2\text{Cu}_3\text{O}_{6+x}$ with $x = 0.5$ by C. Stock *et al.*, PRB (2005) [$x = 0.95$, by D. Reznik *et al.*, PRL (2004)]. The stiffness of the excitations is closer to that of underdoped YBCO, while the “resonance” energy is closer to that of optimally-doped YBCO. Measurements of the momentum-integrated dynamic spin susceptibility indicate that there is relatively little redistribution of weight on warming through T_c . This result is contrary to predictions of models that assume the spin susceptibility comes from the mobile electrons, as the entire energy range studied should be drastically impacted by the opening of the superconducting gap below T_c . Instead, our results support the idea that the dominant contribution to the spin excitations comes from local moments on Cu sites, as a consequence of Coulomb interactions.

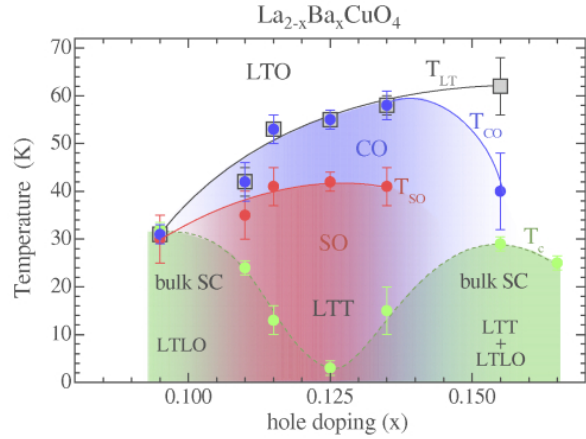


An improved determination of the magnetic form factor for Cu in copper oxides: In order to determine the absolute strength of spin fluctuations in magnetic compounds, it is necessary to know the magnetic form factor. In studies of cuprate superconductors, it has been common to use the form factor obtained from the unpaired spin density of a Cu ion (far right). Electronic structure calculations show that the actual spin density has significant weight on neighboring O atoms (near right), but it is impossible to see this contribution in measurements on antiferromagnetic cuprates with CuO_2 planes, because the net moment on an O site must be zero due to symmetry. Fortunately, this symmetry is broken in the case of spin fluctuations. Taking advantage of this fact,

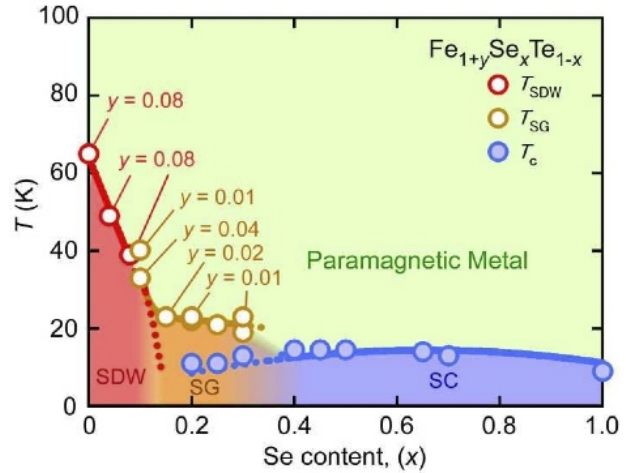


the nature of the form factor has been tested by measuring and analyzing the full spin fluctuation spectrum of the 1D antiferromagnet Sr_2CuO_3 [15], using exact theoretical results for the dynamical spin susceptibility. The analysis demonstrates that there is a large covalency between Cu and O orbitals in cuprates, which has a substantial impact on the form factor, and thus on conclusions regarding the magnitude of spin fluctuations.

Stripes and superconductivity in $\text{La}_{2-x}\text{Ba}_x\text{CuO}_4$: The phase diagram (right) has been determined from a combination of neutron diffraction, x-ray diffraction, and magnetic susceptibility [8] measurements on crystals grown in our lab (Hücker *et al.*, arXiv:1005.5191v1). While the bulk T_c is strongly depressed at $x = 1/8$, where stripe order is maximized, we have also found evidence there for 2D superconductivity setting in at 40 K, together with spin order [1, 11]. To explain the apparent frustration of the interlayer Josephson coupling, a theory of pair-density-wave order has been developed [2,16]. Related behavior is under investigation for $x = 0.095$ in high magnetic fields. The phase diagram indicates that the onset of charge stripe order is generally limited by a structural transition to a phase with an anisotropy in the CuO_2 planes that can orient and pin the stripes; however, this is not universally true. Using high-energy x-ray diffraction to follow stripe order to high pressure, we have found that charge order survives even at pressures where the average anisotropy is completely suppressed [17].



Crystals across the phase diagram for $\text{Fe}_{1+y}\text{Se}_x\text{Te}_{1-x}$: Large crystals have been grown for a broad range of x , as indicated by the circles (except for $x=1$) in the phase diagram at right (N. Katayama *et al.*, arXiv:1003.4525v1). We have been characterizing the spin correlations and dynamics in these crystals both on our own [31,32] (Z.J. Xu *et al.*, arXiv:1005.4856) and in collaboration with Seunghun Lee's group [34]. We have explored the nature of the spin correlations in the spin-glass regime ($0.1 < x < 0.3$), and the change in the spin correlations between the spin-glass regime and the region of bulk superconductivity ($x > 0.3$). Collaborating with photoemission and theory groups, we have proposed that spin and orbital excitations are coupled in the superconducting regime [34].



Future Plans

Underdoped $\text{Bi}_2\text{Sr}_2\text{CaCu}_2\text{O}_{8+\delta}$: To make contact with ARPES and STM studies, we need to prepare crystals of underdoped $\text{Bi}_2\text{Sr}_2\text{CaCu}_2\text{O}_{8+\delta}$ of suitable size for inelastic neutron scattering studies of the spin excitations. This is a challenge, as it requires removing oxygen from as-grown crystals in a homogeneous manner.

Stripes and superconductivity in $\text{La}_{2-x}\text{Ba}_x\text{CuO}_4$: We will study the impact of Zn substitution on the stripe order and superconductivity in this system. Transport studies will complement the diffraction work.

Role of local moments and orbital correlations in Fe-based superconductors: We have begun to explore the nature of the magnetism in Fe_{1+y}Te as a function of temperature using the ARCS spectrometer at the SNS. Initial analysis indicates that the results cannot be explained by Fermi-surface nesting. We also plan to explore the role of orbital occupancy correlations in $\text{Fe}_{1+y}\text{Se}_x\text{Te}_{1-x}$.

High-pressure crystal growth: We are in the process of acquiring a hot isostatic press capable of greater than 1000 bar oxygen partial pressure. We will explore the use of this system to grow oxide crystals that are not stable at oxygen pressures of 11 bar and lower. This system will also provide new options for changing the oxygen content of existing crystals.

Selected DOE-Sponsored Publications, 2007-2010

Cuprates

1. *Two-Dimensional Superconducting Fluctuations in Stripe-Ordered $La_{1.875}Ba_{0.125}CuO_4$* , Li, Q., Hücker, M., Gu, G. D., Tselvelik, A. M. and Tranquada, J. M., *Phys. Rev. Lett.* **99**, 067001 (2007).
2. *Dynamical Layer Decoupling in a Stripe-Ordered High- T_c Superconductor*, Berg, E., Fradkin, E., Kim, E. A., Kivelson, S. A., Oganessian, V., Tranquada, J. M. and Zhang, S. C., *Phys. Rev. Lett.* **99**, 127003 (2007).
3. *Neutron Scattering Studies of Antiferromagnetic Correlations in Cuprates*, Tranquada, J. M., In: *Handbook of High-Temperature Superconductivity: Theory and Experiment*, edited by Schrieffer, J. R. and Brooks, J. S. (Springer, New York, 2007), pp. 257-298.
4. *Disappearance of Antiferromagnetic Spin Excitations in Overdoped $La_{2-x}Sr_xCuO_4$* . Wakimoto, S., Yamada, K., Tranquada, J. M., Frost, C. D., Birgeneau, R. J. and Zhang, H., *Phys. Rev. Lett.* **98**, 247003 (2007).
5. *High-energy magnetic excitations from dynamic stripes in $La_{1.875}Ba_{0.125}CuO_4$* , Xu, G., Tranquada, J. M., Perring, T. G., Gu, G. D., Fujita, M. and Yamada, K. *Phys. Rev. B* **76**, 014508 (2007).
6. *Temperature dependence of the bond-stretching phonon anomaly in $YBa_2Cu_3O_{6.95}$* , Reznik, D., Pintschovius, L., Tranquada, J. M., Arai, M., Endoh, Y., Masui, T. and Tajima, S., *Phys. Rev. B* **78**, 094507 (2008).
7. *Large Bi-2212 single crystal growth by the floating-zone technique*, Wen, J. S., Xu, Z. J., Xu, G. Y., Hücker, M., Tranquada, J. M. and Gu, G. D., *J. Cryst. Growth* **310**, 1401-1404 (2008).
8. *Spin Susceptibility of Underdoped Cuprate Superconductors: Insights from a Stripe-Ordered Crystal*, M. Hücker, G. D. Gu, and J. M. Tranquada, *Phys. Rev. B* **78**, 214507 (2008).
9. *Electronic interlayer coupling in the low-temperature tetragonal phase of $La_{1.79}Eu_{0.2}Sr_{0.01}CuO_4$* , M. Hücker, *Phys. Rev. B* **79**, 104523 (2009).
10. *Magnetic Dispersion of the Diagonal Incommensurate Phase in Lightly Doped $La_{2-x}Sr_xCuO_4$* , M. Matsuda, M. Fujita, S. Wakimoto, J. A. Fernandez-Baca, J. M. Tranquada, and K. Yamada, *Phys. Rev. Lett.* **101**, 197001 (2008).
11. *Evidence for unusual superconducting correlations coexisting with stripe order in $La_{1.875}Ba_{0.125}CuO_4$* , J. M. Tranquada, G. D. Gu, M. Hücker, Q. Jie, H.-J. Kang, R. Klingeler, Q. Li, N. Tristan, J. S. Wen, G. Y. Xu, Z. J. Xu, J. Zhou, and M. v. Zimmermann, *Phys. Rev. B* **78**, 174529 (2008).
12. *Magnetic field induced enhancement of spin-order peak intensity in $La_{1.875}Ba_{0.125}CuO_4$* , J. Wen, Z. Xu, G. Xu, J. M. Tranquada, G. Gu, S. Chang, and H. J. Kang, *Phys. Rev. B* **78**, 212506 (2008).
13. *A clamp-type pressure cell for high energy x-ray diffraction*, Zimmermann, M. v., Nowak, R., Gu, G. D., Mennerich, C., Klauss, H. H. and Hücker, M., *Rev. Sci. Instrum.* **79**, 033906 (2008).
14. *Testing the itinerancy of spin dynamics in superconducting $Bi_2Sr_2CaCu_2O_{8+\delta}$* , G. Xu, G. D. Gu, M. Hücker, B. Fauqué, T. G. Perring, L. P. Regnault, and J. M. Tranquada, *Nat. Phys.* **5**, 642-646 (2009).
15. *Effect of covalent bonding on magnetism and the missing neutron intensity in copper oxide compounds*, A. C. Walters, T. G. Perring, J.-S. Caux, A. T. Savici, G. D. Gu, C.-C. Lee, W. Ku, and I. A. Zaliznyak, *Nat. Phys.* **5**, 867-872 (2009).
16. *Striped superconductors: how spin, charge and superconducting orders intertwine in the cuprates*, Erez Berg, Eduardo Fradkin, Steven A. Kivelson, and J. M. Tranquada, *New J. Phys.* **11**, 115004 (2009).
17. *Spontaneous Symmetry Breaking by Charge Stripes in the High Pressure Phase of Superconducting $La_{1.875}Ba_{0.125}CuO_4$* , M. Hücker, M. v. Zimmermann, M. Debessai, J. S. Schilling, J. M. Tranquada, and G. D. Gu, *Phys. Rev. Lett.* **104**, 057004 (2010).
18. *Incommensurate spin correlations induced by magnetic Fe ions substituted into overdoped $Bi_{1.75}Pb_{0.35}Sr_{1.90}CuO_{6+\delta}$* , H. Hiraka, Y. Hayashi, S. Wakimoto, M. Takeda, K. Kakurai, T. Adachi, Y. Koike, I. Yamada, M. Miyazaki, M. Hiraishi, S. Takeshita, A. Kohda, R. Kadono, J. M. Tranquada, and K. Yamada, *Phys. Rev. B* **81**, 144501 (2010).

Other Oxides

19. *Robust charge stripe order under high electric fields in $Nd_{1.67}Sr_{0.33}NiO_4$* , Hücker, M., v. Zimmermann, M. and Gu, G. D., *Phys. Rev. B* **75**, 041103 (2007).
20. *Stripeless incommensurate magnetism in strongly correlated oxide $La_{1.5}Sr_{0.5}CoO_4$* , Savici, A. T., Zaliznyak, I. A., Gu, G. D. and Erwin, R., *Phys. Rev. B* **75**, 184443 (2007).
21. *Mesoscopic phase coherence in a quantum spin fluid*, Xu, G. Y., Broholm, C., Soh, Y. A., Aeppli, G., DiTusa, J. F., Chen, Y., Kenzelmann, M., Frost, C. D., Ito, T., Oka, K. and Takagi, H., *Science* **317**, 1049 (2007).
22. *Luttinger liquid coupled to quantum spins: Flow equation approach to the Kondo necklace model*, Essler, F. H. L., Kuzmenko, T. and Zaliznyak, I. A., *Phys. Rev. B* **76**, 115108 (2007).
23. *Spin Structures and Spin Wave Excitations*, Zaliznyak, I. A., In: *Handbook for Magnetism and Advanced*

- Magnetic Materials*, edited by Kronmuller, H. and Parkin, S. (John Wiley & Sons, UK, 2007), Vol. 3, Chap. 1.
24. *Temperature evolution of the magnetic excitations in charge ordered $La_{5/3}Sr_{1/3}NiO_4$* , Freeman, P. G., Boothroyd, A. T., Ewings, R. A., Hücker, M., Prabhakaran, D., Enderle, M. and Tranquada, J. M., *J. Phys.: Condens. Matter* **20**, 104229 (2008).
 25. *Phase instability induced by polar nanoregions in a relaxor ferroelectric system*, Xu, G. Y., Wen, J. S., Stock, C. and Gehring, P. M., *Nat. Mater.* **7**, 562-566 (2008).
 26. *Doping-dependent charge and spin superstructures in layered cobalt perovskites*, N. Sakiyama, I. A. Zaliznyak, S.-H. Lee, Y. Mitsui, and H. Yoshizawa, *Phys. Rev. B* **78**, 180406 (2008).
 27. *Effect of local dipole moments on the structure and lattice dynamics of $K_{0.98}Li_{0.02}TaO_3$* , J. Wen, G. Xu, C. Stock, P. M. Gehring, Z. Zhong, L. A. Boatner, E. L. Venturini, and G. A. Samara, *Phys. Rev. B* **78**, 144202 (2008).
 28. *Magnetic-field control of charge structures in the magnetically disordered phase of multiferroic $LuFe_2O_4$* , J. Wen, G. Xu, G. Gu, and S. M. Shapiro, *Phys. Rev. B* **80**, 020403(R) (2009).
 29. *Robust charge and magnetic orders under electric field and current in multiferroic $LuFe_2O_4$* , Jinsheng Wen, Guangyong Xu, Genda Gu, and S. M. Shapiro, *Phys. Rev. B* **81**, 144121 (2010).
 30. *Competing Orders in PZN-xPT and PMN-xPT Relaxor Ferroelectrics*, Guangyong Xu, *J. Phys. Soc. Jpn.* **79**, 011011 (2010).

Fe-based superconductors

31. *Short-range incommensurate magnetic order near the superconducting phase boundary in $Fe_{1+x}Te_{1-x}Se_x$* , J. Wen, G. Xu, Z. J. Xu, Zhi-Wei Lin, Q. Li, W. Ratcliff, G. D. Gu and J. M. Tranquada, *Phys. Rev. B* **80**, 104506 (2009).
32. *Effect of magnetic field on the spin resonance in $FeTe_{0.5}Se_{0.5}$ as seen via inelastic neutron scattering*, Jinsheng Wen, Guangyong Xu, Zhijun Xu, Zhi Wei Lin, Qiang Li, Ying Chen, Songxue Chi, Genda Gu, and J. M. Tranquada, *Phys. Rev. B* **81**, 100513 (2010)
33. *Superconductivity in epitaxial thin films of $Fe_{1.08}Te:O_x$* , Weidong Si, Qing Jie, Lijun Wu, Juan Zhou, Genda Gu, P. D. Johnson, and Qiang Li, *Phys. Rev. B* **81**, 092506 (2010).
34. *Coupling of spin and orbital excitations in the iron-based superconductor $FeSe_{0.5}Te_{0.5}$* , S.-H. Lee, Guangyong Xu, W. Ku, J. S. Wen, C. C. Lee, N. Katayama, Z. J. Xu, S. Ji, Z. W. Lin, G. D. Gu, H.-B. Yang, P. D. Johnson, Z.-H. Pan, T. Valla, M. Fujita, T. J. Sato, S. Chang, K. Yamada, J. M. Tranquada, *Phys. Rev. B* (accepted).

Other studies of Gu's superconductor crystals

35. *High-Energy Kink Observed in the Electron Dispersion of High-Temperature Cuprate Superconductors*, Valla, T., Kidd, T. E., Yin, W. G., Gu, G. D., Johnson, P. D., Pan, Z. H. and Fedorov, A. V., *Phys. Rev. Lett.* **98**, 167003 (2007).
36. *Magnetic field dependence of charge stripe order in $La_{2-x}Ba_xCuO_4$ ($x \sim 1/8$)*, Kim, J., Kagedan, A., Gu, G. D., Nelson, C. S. and Kim, Y.-J., *Phys. Rev. B* **77**, 180513 (2008).
37. *Electronic origin of the inhomogeneous pairing interaction in the high- T_c superconductor $Bi_2Sr_2CaCu_2O_{8+\delta}$* , Pasupathy, A. N., Pushp, A., Gomes, K. K., Parker, C. V., Wen, J. S., Xu, Z. J., Gu, G. D., Ono, S., Ando, Y. and Yazdani, A., *Science* **320**, 196-201 (2008).
38. *Extending Universal Nodal Excitations Optimizes Superconductivity in $Bi_2Sr_2CaCu_2O_{8+\delta}$* , A. Pushp, C. V. Parker, A. N. Pasupathy, K. K. Gomes, S. Ono, J. S. Wen, Z. J. Xu, G. D. Gu, and A. Yazdani, *Science* **324**, 1689-1693 (2009).
39. *Imaging Nanoscale Fermi-Surface Variations in an Inhomogeneous Superconductor*, W. D. Wise, K. Chatterjee, M. C. Boyer, T. Kondo, T. Takeuchi, H. Ikuta, Z. Xu, J. Wen, G. D. Gu, Y. Wang, and E. W. Hudson, *Nat. Phys.* **5**, 213-216 (2009).
40. *Emergence of preformed Cooper pairs from the doped Mott insulating state in $Bi_2Sr_2CaCu_2O_{8+\delta}$* , H.-B. Yang, J. D. Rameau, P. D. Johnson, T. Valla, A. Tsvelik, and G. D. Gu, *Nature* **456**, 77-80 (2008).
41. *Diamagnetism and Cooper pairing above T_c in cuprates*, Lu Li, Yayu Wang, Seiki Komiyama, Shimpei Ono, Yoichi Ando, G. D. Gu, and N. P. Ong, *Phys. Rev. B* **81**, 054510 (2010).
42. *Coupling of low-energy electrons in the optimally doped $Bi_2Sr_2CaCu_2O_{8+\delta}$ superconductor to an optical phonon mode*, J. D. Rameau, H.-B. Yang, G. D. Gu, and P. D. Johnson, *Phys. Rev. B* **80**, 184513 (2009).
43. *Quantitative Raman measurement of the evolution of the Cooper-pair density with doping in $Bi_2Sr_2CaCu_2O_{8+\delta}$ superconductors*, S. Blanc, Y. Gallais, A. Sacuto, M. Cazayous, M. A. Méasson, G. D. Gu, J. S. Wen, and Z. J. Xu, *Phys. Rev. B* **80**, 140502 (2009).
44. *Electronic correlations and unusual superconducting response in the optical properties of the iron chalcogenide $FeTe_{0.55}Se_{0.45}$* , C. C. Homes, A. Akrap, J. S. Wen, Z. J. Xu, Z. W. Lin, Q. Li, and G. D. Gu, *Phys. Rev. B* **81**, 180508 (2010).

Session III

Interfaces and Nanoconfinement

Fluid Interface Reactions, Structures and Transport (FIRST) Energy Frontier Research Center

**David J. Wesolowski, Director
Oak Ridge National Laboratory**

The Fluid Interface Reactions, Structures and Transport (FIRST) Energy Frontier Research Center addresses fundamental gaps in our current understanding of fluid/solid interfacial systems of high importance to future energy technologies, including electrical energy storage and heterogeneous catalysis for solar energy and solar fuels production.

- *How does the interfacial region differ in structure, dynamics and reactivity from the bulk properties of the fluid and solid phases?*
- *How do these altered properties couple with complex interfacial textures to influence chemical reactions, ionic and molecular transport and charge transfer within and across the interface?*
- *How can we control and manipulate interfacial phenomena by informed selection of fluid- and solid-phase components, interfacial geometries, field gradients, temperature, pressure and other environmental parameters?*

These questions permeate the fundamental science needed to solve our nation's long-term energy production, storage and utilization needs, as described in the DOE/BES Basic Research Needs and Grand Challenge reports. The interaction of fluids with solid substrates controls many chemical processes encountered in nature and industry. However, the atomic/nanoscale reactivity, structures and transport properties of the fluid-solid interface (FSI) are poorly understood for the vast majority of fluid and substrate combinations, particularly at environmental extremes (e.g., high surface charge density, extreme chemical non-equilibrium, high ion/electron fluxes, etc.). This lack of fundamental molecular-level understanding of interfacial phenomena has often lead to Edisonian approaches to the resolution of challenges related to advanced energy technologies, including solar energy utilization, batteries, supercapacitors, heterogeneous catalysis, and chemical separations. To address these challenges, we must replace continuum solvent descriptions and hypothetical interfacial structures, with *quantitative, fully dynamic, and chemically realistic descriptions of the interactions of electrons, atoms, ions and molecules that give rise to macroscopic fluid/solid interfacial properties.*

The goal of the FIRST Center is to develop quantitative and predictive models of the unique nanoscale environment at the interface between fluids and solids in order to achieve transformative advances in electrical energy storage and catalysis for energy applications. A wide range of neutron scattering approaches are being employed in order to provide unique, molecular-to nano-scale information on interracial structure and dynamics. These scattering studies can be powerfully coupled with quantum and classical molecular dynamics simulations to not only aid in the interpretation of scattering studies, but to help develop and validate molecular models over wide time and length scales. These approaches are combined with a wide array of experimental and analytical studies to provide a complete picture of ion and solvent transport and reactivity at key interfaces typical of batteries, supercapacitors and catalytic surfaces in contact with dense fluid phases.

Neutron and X-Ray Scattering Studies of the Liquid-Liquid Transition in Supercooled Confined Water and the Dynamics of Biomolecular Assemblies

PI: Sow-Hsin Chen (sowhsin@mit.edu)

*Department of Nuclear Science and Engineering,
Massachusetts Institute of Technology, Cambridge, MA 02139*

Research Scope

During the past several years, we have extensively studied the thermodynamical and dynamical properties of supercooled confined water using elastic, quasi-elastic (QENS), and inelastic (INS) neutron scattering techniques. By confining water in 1-D nano-porous silica material MCM-41-S, 2-D surfaces of the biomolecules, or 3-D interconnected pores of an aged cement paste, we can suppress the temperature of the homogenous nucleation process down to at least 150K. We were thus able to study the anomalous properties of deeply supercooled water in the “no-man’s land”.

We discovered the existence of the density minimum of water (D_2O) at 210K besides the well-known density maximum at 284K. We observed a fragile-to-strong dynamic crossover at $T_L=225K$ for the first time. We detected the appearance of boson peaks and the breakdown of the Stokes-Einstein relation at and below the T_L . We extended this method to study the fragile-to-strong dynamic crossover and dynamic heterogeneity phenomenon in the hydration water of an aged cement paste. We did a series of measurements of the density of confined water as a function of temperatures along various isobars, i.e. to determine the equation of state of the confined water.

We also extended these methods to explore the slow dynamics of hydration water of the biopolymers and its relation to the so-called glass transition of the biopolymers. Using Inelastic X-ray scattering (IXS), we studied the phonon dispersion relation and damping in globular proteins and the relations between phonon-like collective motions in these supramolecular systems and their biological functions for the first time. We used molecular dynamics (MD) simulations to discover the logarithmic beta relaxation of globular proteins, and also verified the simulation results with QENS recently. We extensively measured the relaxational dynamics of lysozyme hydration water using QENS at low-temperatures and high-pressures, and discussed its consequence on the role of hydration water in controlling the biological functions of the proteins at extreme conditions.

Recent Progress

1. The first detection of the intra-protein phonon-like excitation in lysozyme and BSA

D. Liu et al, “Studies of Phononlike Low-Energy Excitations of Protein Molecules by Inelastic X-Ray Scattering”, *Phys. Rev. Lett.* **101** 135501 (2008).

MD simulations and neutron scattering experiments have shown that many hydrated globular proteins exhibit a universal dynamic transition at $T_D = 220$ K, below which the biological activity of a protein sharply diminishes. We studied the phonon-like low-energy excitations of two structurally very different proteins, lysozyme and bovine serum albumin, using inelastic x-ray scattering above and below T_D . We found that the excitation energies of the high-Q phonons show a marked softening above T_D . This suggests that the large amplitude motions of wavelengths corresponding to this specific Q range are intimately correlated with the increase of biological activities of the proteins.

2. *Discovery of the logarithmic relaxation of protein single-particle dynamics* [9, 17]

MD simulations reveal a distinct feature in the decay of globular protein self-intermediate scattering functions (SISF). Instead of the classic stretched exponential decay usually seen in simple glass-forming liquids, protein SISF display a characteristic logarithmic decay in the intermediate time range from 1 ps to 10 ns. We demonstrate here that this exotic relaxation is universal: it does not depend on the globular protein under consideration (lysozyme or ribonuclease), nor on its physical state (powder, crystal or solution). We analyze this logarithmic β -relaxation from 220 K to 340 K, fitting the protein correlators with the predictions of the mode coupling theory (MCT) for systems close to a higher-order singularity. Very recently, we used the new high-resolution backscattering instrument (BASIS) at SNS to study the QENS of hydrated lysozyme and have experimentally verified the predictions of MD simulations.

3. *Discovery of a liquid-liquid tricritical point in low-temperature confined water* [19]

Many of the anomalous properties of water are amplified in the deeply supercooled region. We have recently done a neutron scattering measurement of the density of heavy water confined in a nanoporous silica matrix (≈ 15 Å pore size), in a Temperature-Pressure range inaccessible for the bulk (between 300 K and 130 K and from 1 bar to 2900 bar), namely, the equation of state $\rho(T,P)$. A sudden change of slope in the otherwise continuous density profile is observed below a certain pressure P_c ; however, this feature is absent above P_c . Instead, a hysteresis phenomenon in the density profiles between the warming and cooling scans becomes prominent above P_c . Hence, the data can be interpreted as a line of a apparent 2nd-order phase transition at low pressures evolving in to a line of 1st-order phase transition at high pressures. If so, the existence of a “tricritical point” at $P_c \sim 1500$ bar, $T_c \sim 210$ K becomes a possible scenario to explain the exceptionally rich phase behavior of low-temperature confined water. (See Fig 1 and 2)

Future Plans

1. Equation of state measurement of confined water in a hydrophobic substrate CMK-1 by elastic neutron diffraction using triple-axis spectrometer
2. Temperature and pressure dependence of the relaxational dynamics of confined water in hydrophobic CMK-1 porous carbon material
3. Further experimental study and theoretical justification of the logarithmic time dependence of beta-relaxation in other interesting globular proteins.
4. Further measurements of the intra-protein phonons in other interesting globular proteins and investigation of the biological significance of the intra-protein phonons.

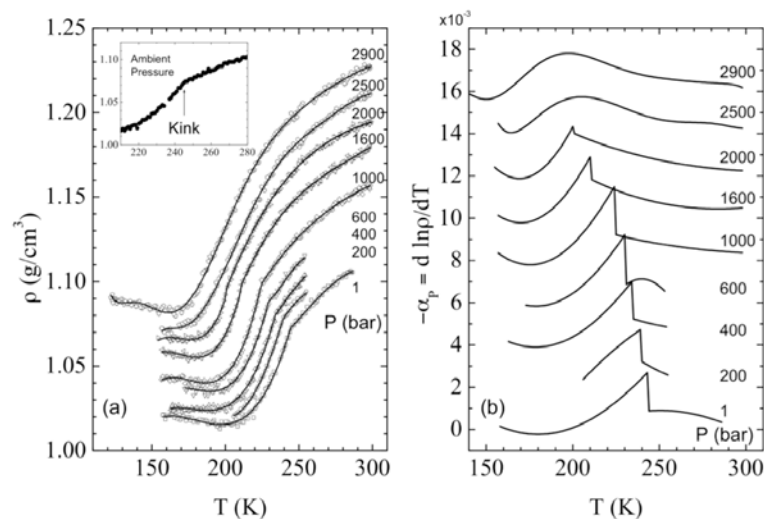


Fig 1. (a) Measured isobaric density profiles of confined heavy water by cooling scans. A well-defined “kink” in the density profile can be observed from ambient pressure to ≈ 1600 bar. The inset zooms in the region of the “kink” at ambient pressure. (b) The isobaric thermal expansion coefficient α_p evaluated from the fitted density curves. The data are shifted by 0.002 between adjacent pressures for clarity. The sudden jump (discontinuity) in α_p below ≈ 1600 bar directly coming from the “kink” in the density profile is the signature of a 2nd-order phase transition by definition. If so, above 2000 bar, the absence of the “kink” in the density profile and the disappearance of the discontinuity in α_p imply the endpoint of the 2nd-order transition line.

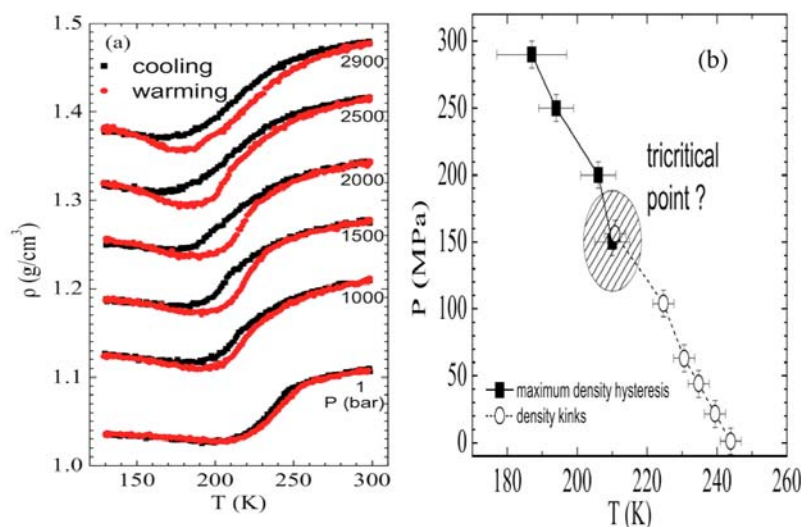


Fig 2. (a) Measured isobaric density profiles of confined heavy water by both warming and cooling scans. A hysteresis phenomenon becomes prominent at ≈ 1500 bar and above, which is a direct evidence of the phase separation when a 1st-order phase transition line is crossed. (b) P-T phase diagram of the confined heavy water. The empty circles, connected by the dotted line (a possible 2nd-order transition line), are determined from the position of the “kinks” in the density profiles. The filled squares, connected by the solid line (a possible 1st-order transition line), are determined from the position of the maximum density hysteresis. Therefore, the shadow area connecting the 2nd-order and 1st-order lines is where one may find a “tricritical point”.

Publications (FY09 – FY10)

1. Yang Zhang, Marco Lagi, Dazhi Liu, Francesco Mallamace, Emiliano Fratini, Piero Baglioni, Eugene Mamontov, Mark Hagen, and S.-H. Chen, “Observation of high-temperature dynamic crossover in protein hydration water and its relation to reversible denaturation of lysozyme”, *J. Chem. Phys.* **130** 135101 (2009)
2. X.-Q. Chu, A. Faraone, C. Kim, E. Fratini, P. Baglioni, J. B. Leao and S.-H. Chen “Proteins remain soft at lower temperatures under pressure” *J. Phys. Chem B* **113** 5001 (2009)
3. Y. Zhang, M. Lagi, E. Fratini, P. Baglioni, E. Mamontov and S.-H. Chen “Dynamic susceptibility of supercooled water and its relation to the dynamic crossover phenomenon”, *Phys. Rev. E* **79**, 040201(R) (2009)
4. A. Faraone, Y. Zhang, K.-H. Liu, C.-Y. Mou, and S.-H. Chen “Single particle dynamics of water confined in a hydrophobically modified MCM-41-S nanoporous matrix” *J. Chem. Phys.* **130**, 134512 (2009)

5. Y. Zhang, K.-H. Liu, M. Lagi, D. Liu, K. Littrell, C.-Y. Mou, and S.-H. Chen “Absence of the Density Minimum of Supercooled Water in Hydrophobic Confinement” *J. Phys. Chem B* **113** 5007 (2009)
6. S.-H. Chen, F. Mallamace, X. Q. Chu, C. Kim, M. Lagi, A. Faraone, E. Fratini, P. Baglioni “Neutron Scattering Studies of Dynamic Crossover Phenomena in a Coupled System of Biopolymer and Its Hydration Water” to appear in *The Journal of Physics: Conference Series* (2009)
7. S.-H. Chen, Y. Zhang, M. Lagi, S.-H. Chong, P. Baglioni and F. Mallamace, “Evidence of Dynamic Crossover Phenomena in Water and Other Glass-Forming Liquids: Experiments, MD Simulations and Theory”, *J. Phys.: Condens. Matter* **21** (2009) 504102
8. S-H Chong, S-H Chen and F Mallamace “A possible scenario for the fragile-to-strong dynamic crossover predicted by the extended mode-coupling theory for glass transition”, *J. Phys.: Condens. Matter* **21** (2009) 504101
9. M. Lagi, P. Baglioni and S.-H. Chen “Logarithmic relaxation of protein single-particle dynamics” *Phys. Rev. Lett.* **103**, 108102 (2009)
10. S.-H. Chen, Y. Zhang, M. Lagi, X.Q. Chu, L. Liu, A. Faraone, E. Fratini, P. Baglioni “The Dynamic Response Function $\chi_r(Q,t)$ of Confined Supercooled Water and its Relation to the Dynamic Crossover Phenomenon”, *Zeit. Fur Chemie*, **224**, 109, (2009)
11. Mallamace, C. Branca, C. Corsaro, N. Leone, J. Spooren, H. E. Stanley and S.-H. Chen “Dynamical Crossover and Breakdown of the Stokes-Einstein Relation in Confined Water and in Methanol-Diluted Bulk Water”, *J. of Phys. Chem. B* **114**, 1870-1878 (2010)
12. P. Gallo, M. Rovere and S.-H. Chen, “Dynamic Crossover in Supercooled Confined Water: Understanding Bulk Properties through Confinement”, *J. Phys. Chem. Lett.*, **1**, 729 (2010)
13. Cheng-Si Tsao, Yi-Ren Tzeng, Ming-Sheng Yu, Cheng-Yu Wang, Huan-Hsiung Tseng, Tsui-Yun Chung, Hsiu-Chu Wu, Takahiro Yamamoto, Katsumi Kaneko and Sow-Hsin Chen, “Effect of Catalyst Size on Hydrogen Storage Capacity of Pt-Impregnated Active Carbon via Spillover”, *J. Phys. Chem. Lett.*, **1** (7), 1060 (2010)
14. C.-T. Tsao, Y. Liu, M. Li, Y. Zhang, J. B. Leao, H.-W. Chang, M.-S. Yu and S.-H. Chen, “Neutron Scattering Methodology for Absolute Measurement of Room-Temperature Hydrogen Storage Capacity and Evidence for Spillover Effect in a Pt-Doped Activated Carbon”, *J. Phys. Chem. Lett.* **1**, 1569-1573 (2010).
15. C.-T. Tsao, Y. Liu, M. Li, Y. Zhang, J. B. Leao, W.-S. Chiang, T.-Y. Chung, Y.-R. Tzeng, M.-S. Yu and S.-H. Chen, “Probing the Room-temperature Spatial Distribution of Hydrogen in Nanoporous Carbon by use of Small-angle Neutron Scattering”, submitted to *J. Phys. Chem. C* (2010).
16. S.-H. Chen, M. Lagi, X.-Q. Chu, Y. Zhang, C. Kim, A. Faraone, E. Fratini and P. Baglioni, “Dynamics of a globular protein and its hydration water studied by neutron scattering and MD simulations”, A feature article in *Spectroscopy: Biomedical Applications* **24** (No. 1,2), 1-24 (2010).
17. X.-Q. Chu, M. Lagi, E. Mamontov, E. Fratini, P. Baglioni and S.-H. Chen, “Experimental evidence of logarithmic relaxation in single-particle dynamics of hydrated protein molecules”, *Soft Matter*, DOI: 10.1039/c002602f (2010).
18. F. Mallamace C. Branca C. Corsaro N. Leone J. Spooren S.-H. Chen H. E. Stanley “Experimental evidence for fragile-to-strong crossover in general glass-forming liquids”, submitted to *PNAS* (2010)
19. Y. Zhang, A. Faraone, W. A. Kamitakahara, K.-H. Liu, C.-Y. Mou, J. B. Leao, S. Chang and S.-H. Chen, “Unusual Phase Behavior of Nanoconfined Water: New Insights” to be published (2010)

Neutron Scattering Studies of Classical and Quantum Fluids in Porous Media

Henry R. Glyde (glyde@udel.edu)

Department of Physics and Astronomy, University of Delaware, Newark, DE 19716

Research Scope

Bose-Einstein Condensation (BEC) and fundamental excitations such as phonons in liquid, solid and amorphous helium are uniquely measured using neutrons. Of central interest is the dependence of superfluidity on BEC and the modes, e.g. the phonon-roton (P-R) mode in liquid ^4He . This interplay between superflow, BEC and the excitations is profoundly modified if helium is confined in porous media which introduces nanoscale disorder or is confined to a surface (2D). Helium in porous media is an example of Bosons in disorder and has many analogies with Bosons in disorder in other fields (e.g. Cooper pairs in high temperature superconductors). Typically, superfluidity is measured by placing the sample in a torsional oscillator. BEC and the modes are determined in neutron scattering measurements. The discovery of BEC in trapped Bose gases of alkali atoms in 1995 (a finite sized system in an external potential often with disorder) and the observation of an apparent superfluid fraction in solid helium in 2004 have stimulated dynamic new interest and energy into this field.

Using neutrons, we are measuring BEC and atomic momentum distributions in bulk liquid helium (as a function of pressure up to solidification) in solid helium, in liquid helium confined in porous media and confined to 2D. These measurements are typically done at the ISIS Facility, Rutherford Appleton Lab. Our first measurement at SNS was completed on May 31, 2010. The measurements of the P-R and other low energy modes are done chiefly at the Institut Laue Langevin (ILL), Grenoble. Our recent measurements at ILL have focused on liquid helium confined in porous media where we observe a disorder induced localized BEC or Bose Glass phase of BEC lying between the superfluid and normal phase (see Fig. 1). We have also recently created completely amorphous solid helium in porous media. Amorphous regions in solid helium are a candidate for the superflow in the solid helium. Monte Carlo calculations predict both superflow and BEC in amorphous solid helium. Some of these topics are sketched below.

Recent Progress

Localized BEC in disorder and a BEC glass phase: The goal of this ongoing program is to reveal and understand the interplay between BEC, the P-R modes and superfluidity in liquid helium in disorder. In bulk liquid ^4He , the onset of BEC, well defined P-R modes and superfluidity are all at the same temperature, denoted T_λ . The three phenomena are all confined to the superfluid phase. BEC and well defined P-R modes are not observed above T_λ . When liquid helium is confined in porous media, the onset of superfluidity is suppressed to a lower temperature, denoted T_c (see Fig. 1 LHS or the Yamamoto $\rho_s(T)$ line in Fig 1 RHS) with $T_c \leq T_\lambda$. This suppression of the transition temperature T_c below T_λ has been demonstrated in several porous media using torsional oscillator measurements. In porous media the liquid phase is also extended to higher pressure, up to 38 bars in Fig. 1. Confinement of liquid helium in porous media also introduces static disorder. Our recent neutron scattering measurements show that there are well defined P-R

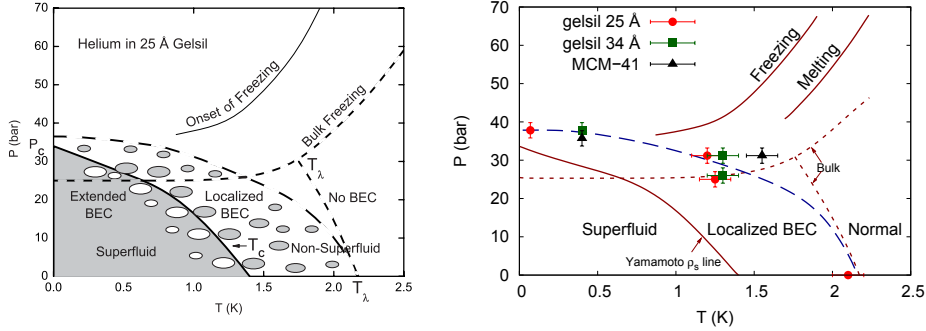


Figure 1: LHS: Schematic phase diagram of ^4He in 25 Å gelsil. The superfluid phase observed by Yamamoto et al. Phys Rev Lett 93, 075302 (2004) is depicted by the solid region bounded by a solid line (T_c). The localized BEC or Bose glass phase containing islands of BEC surrounding the superfluid phase is indicated by dark patches and is bounded by a long dashed line. The short dashed lines are the phase boundaries in bulk ^4He . The solid lines at higher pressure mark the onset of freezing and melting of helium. RHS: Well defined phonon-rotor (P-R) modes are observed at pressures and temperatures up to but not above the points with error bars joined by a long dashed line in 25 Å and 34 Å gelsils and in MCM-41. The long dashed line marks the boundary of the Bose glass phase as on the LHS.

modes and BEC in confined liquid at temperatures above T_c . However, this BEC above T_c is localized into patches separated by regions with no BEC. The BEC above T_c is broken up into separated islands of BEC by disorder. The localized BEC phase lies between the superfluid and the normal liquid phase as shown in the LHS of Fig. 1.

In the localized BEC phase there is no phase coherence across the sample. As temperature is lowered the number and size of the patches of BEC grow until there is a percolation path connecting the patches. At T_c there is percolation and extended BEC with phase coherence across the sample and the onset of superflow. The existence of localized BEC above T_c is similar to the apparent existence of patches of energy gap and Cooper pairs at temperatures above T_c in some high temperature superconductors. The two phenomena appear to be similar with the onset of superflow (superconductivity) occurring when there is a percolation path of BEC (energy gap).

Supersolids and Bose-Einstein Condensation: In 2004, Kim and Chan reported a superfluid fraction, ρ_S/ρ , in solid helium below a critical temperature $T_c \simeq 200$ mK - remarkably extending superflow to solids. Fig. ?? (LHS) shows the supersolid phase. An apparent superfluid fraction has been confirmed in several laboratories. It appears to be associated with defects such as dislocations, grain boundaries, vacancies, amorphous regions in the solid or is a surface effect. The observation of BEC below T_c would be an unambiguous verification that the apparent ρ_S/ρ is indeed superflow. In our first measurement (2007), we found the BEC condensate fraction n_0 to be zero within 1 % at $T = 80$ mK. In a second measurement (2009), we investigated a sample having a large surface area (see Fig. 2 RHS) where large ρ_S/ρ values were reported. We found $n_0 = 0.0 \pm 0.3$ % at 65 mK. Thus we have not observed BEC and are not able to confirm that the NCRI observed below T_c is superflow at this time.

Supersolids and amorphous solid helium: As noted, a superfluid fraction in solid helium has been reported. It is attributed to defects in the solid, for example amorphous regions. Path integral Monte Carlo (PIMC) calculations predict that amorphous solid helium supports observable values of both ρ_S/ρ and n_0 , e.g. $\rho_S/\rho \simeq 5$ -50 % and $n_0 \simeq 0.5$ %. We have measured the static structure factor, $S(Q)$, of solid helium confined in the porous media MCM-41 of pore diameter 47 ± 1.5 Å.

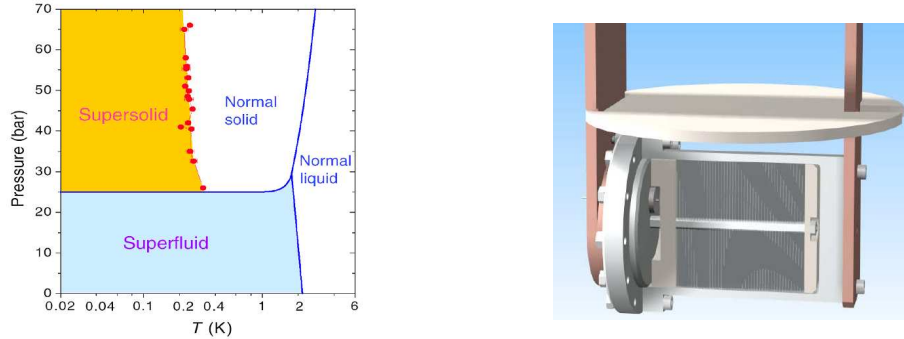


Figure 2: **LHS:** Phase diagram of bulk ^4He showing the “supersolid” region. **RHS:** Sample cell used in our neutron scattering measurements of the condensate fraction containing 95 parallel aluminium sheets to create a large surface area.

The $S(Q)$ shows an entirely amorphous solid. No Bragg peaks are observed and the $S(Q)$ of the solid differs little from that of the liquid. Thus solid helium in small pore media (diameter $d \leq 50 \text{ \AA}$) is entirely amorphous. Our measurements show that amorphous solid helium can be created and it remains a challenge to find a media in which to test the role of amorphous solid helium in superflow.

One and two dimensional solid helium adsorbed on nanotubes: In 2005 we showed that ^4He adsorbed on the surface of carbon nanotube bundles formed 1D and 2D quantum solids (Pearce et al, Phys. Rev. Lett. 95, 185302 (2005)). More recently, we have investigated the dynamics of these 1D and 2D quantum solids using inelastic neutron scattering on IN6 at ILL. The vibrational density of states (DOS) of the 1D solid shows a gap smeared by disorder. The RMS vibrational amplitude in the 1D solid along the nanotube is $\langle u^2 \rangle = 0.28 \text{ \AA}$ giving a Lindemann ratio of $\gamma = (\langle u^2 \rangle)^{-1/2}/R = 0.15$, less than the bulk value. The DOS of the 2D solid shows a clear gap at $\omega \simeq 0.75 \text{ meV}$ indicating a commensurate phase that differs markedly from the commensurate phase on a flat surface. The 1D and 2D DOS are reasonably well fitted with models that reflect the gap and dimensions of the solids.

Future Plans

We have begun a neutron scattering program at SNS (S.O. Diallo, R. T. Azuah and HRG). The initial program will be measurements of BEC and the atomic momentum distribution in bulk liquid ^4He as a function of pressure up to the solidification pressure on ARCS. Current Monte Carlo calculations predict different BEC condensate fractions. We plan to extend the measurements of BEC into solid helium. Observation of BEC in solid helium remains a key ingredient in verifying that superflow in solids exists. Measurements of the phonon density of states of solid helium (above and below T_c) on CNCS related to supersolid behavior are also planned (with H. Lauter).

We plan to continue measurements of the excitations and structure of liquid and solid helium in porous media at ILL. The aim is to continue to explore “Bosons in Disorder” and amorphous solid helium.

Publications (FY07-FY09)

1. *Amorphous solid helium in porous media*
J. Bossy, T. Hansen, and H. R. Glyde
Phys. Rev. B **81**, 184537 (2010) (Editor's suggestion).
2. *Dynamics of one dimensional and two dimensional helium adsorbed on carbon nanotubes*
S. O. Diallo, B. Fåk, M. A. Adams, O. E. Vilches, M. R. Johnson, H. Schober, and H. R. Glyde
Eur. Phys. Lett. **88**, 56005 (2009).
3. *Limits on Bose-Einstein condensation in confined solid ^4He*
S. O. Diallo, R. T. Azuah, O. Kirichek, J. W. Taylor and H. R. Glyde
Phys. Rev. B **80**, 060504(R) (2009).
4. *Superfluidity and BEC in optical lattices and porous media: A path integral Monte Carlo study*
A. A. Shams and H. R. Glyde
Phys. Rev B **79**, 214508 (2009).
5. *Excitations of nanoscale quantum liquids under pressure and the Bose glass phase*
J. Bossy, J. V. Pearce, H. Schober, and H. R. Glyde
Phys. Rev. B **78**, 224507 (2008).
6. *Bose-Einstein coherence in two-dimensional superfluid ^4He*
S. O. Diallo, J. V. Pearce, R. T. Azuah, J. W. Taylor and H. R. Glyde
Phys. Rev. B **78**, 024512 (2008).
7. *Phonon-roton modes and localized Bose-Einstein condensation in liquid helium under pressure in nanoporous media*
J. Bossy, J. V. Pearce, H. Schober, and H. R. Glyde
Phys. Rev. Lett. **101**, 025301 (2008).
8. *Phonon-roton excitations and quantum phase transitions in liquid ^4He in nanoporous media*
H. R. Glyde, J. V. Pearce, J. Bossy, and H. Schober
Recent Progress in Many Body Theories, Vol. 14, Eds. G. E. Astrakharchik, J. Boronat and F. Mazzanti, (World Scientific, Singapore, 2008) p. 411.
9. *Condensate depletion in two-species Bose gases: A variational quantum Monte Carlo study*
A. R. Sakhel, J. L. DuBois, and H. R. Glyde
Phys. Rev. A **77**, 043627 (2008).
10. *Bose-Einstein condensation in solid ^4He*
S. O. Diallo, J. V. Pearce, R. T. Azuah, O. Kirichek, J. W. Taylor and H. R. Glyde
Phys. Rev. Lett. **98**, 205301 (2007).
11. *Boson localization and excitations of liquid ^4He confined in gelsil*
F. Albergamo, J. Bossy, H. Schober, and H. R. Glyde
Phys. Rev. B **76**, 064503 (2007).
12. *Dynamics of quantum liquids in nanoporous media*
H. R. Glyde
Eur. Phys. J. ST **141**, 75 (2007)
13. *Quantum momentum distributions*
B. Withers and H. R. Glyde
J. Low Temp. Phys. **147**, 633 (2007).

FROM FUNDAMENTAL UNDERSTANDING TO PREDICTING NEW NANOMATERIALS FOR HIGH-CAPACITY HYDROGEN STORAGE

GRANT NUMBER: DE-FG02-08ER46522, REPORT DURATION: 04/30/2009 – 04/30/2010

PIs: **Taner Yildirim^{1,2} and Jack E. Fischer¹**

¹Department of Materials Science and Eng., University of Pennsylvania, Philadelphia, PA 19104

²National Institute of Standards and Technology, NCNR, Gaithersburg, MD 20899

Email: taner@seas.upenn.edu

PROGRAM SCOPE:

The main scope of this BES proposal is to focus on achieving fundamental understanding of the chemical and structural interactions governing the storage and release of hydrogen in a wide spectrum of candidate materials. The goals are

- To provide fundamental understanding of how candidate materials (MOF's, alanates, destabilized chemical hydrides, etc) interact with H₂ chemically, structurally and energetically; and
- To provide timely feedback and guidance from theory to de novo materials design and targeted synthesis throughout the DOE programs.

We are currently working on many research avenues along the lines discussed in our original proposal. Below we briefly discuss some selected studies which have been recently completed or are about to be finished. In addition to hydrogen storage, we are also working on closely related problems such as application of neutron scattering to solve carbon-capture problem. Below we will present a brief review of these studies.

RESEARCH ACCOMPLISHMENTS:

1. Novel Graphene-Oxide-Framework Materials and their Gas Adsorption Properties

This is a very recent work and it fits into the *Novel Materials "Outside the Box"* category as described in our original proposal. Even though there has been extensive research on gas adsorption properties of various carbon materials based on activated carbon, nanotubes, and graphite/graphene, there has been little work done on the gas adsorption properties of graphite oxide (GO). In this study, we show that one-and-a-half-century-old graphite oxide can be easily turned into a potentially useful gas storage material. This work was first presented at the APS 2010 March Meeting and has received enormous interest as evidenced by the media coverage (two examples from *Scientific American* and *Physics World* given below):

Graphene used to make a hydrogen molecule "parking garage"

<http://www.scientificamerican.com/blog/post.cfm?id=graphene-used-to-make-a-hydrogen-mo-2010-03-19>

Graphene-oxide framework packs in hydrogen

<http://physicsworld.com/cws/article/news/42171>

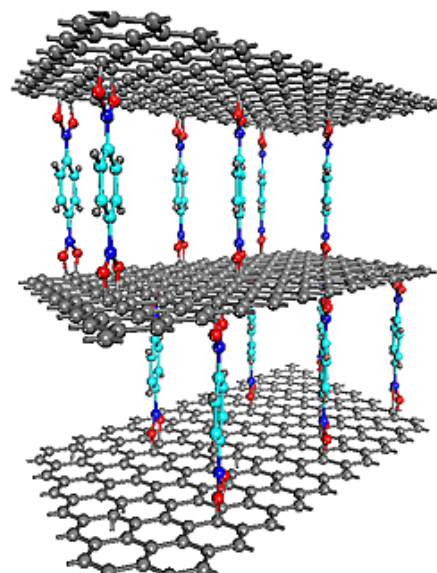


Figure 1. An idealized view of graphene-oxide framework (GOF) material proposed in this study.

2. Hybrid Materials with Ammonia Borane (AB) and Their Hydrogen Release Properties.

In this work, we report synthesis, detailed structural and properties characterization of two new boron-containing materials via the combination of ammonia borane (AB) and light weight borohydrides, i.e. LiBH_4 and $\text{Ca}(\text{BH}_4)_2$, aiming to explore new high H content compounds with potential applications for hydrogen storage. These materials have completely novel structures and very high hydrogen contents. Our findings are useful as general guidelines and inspiration for the design and synthesis of novel materials for hydrogen storage.

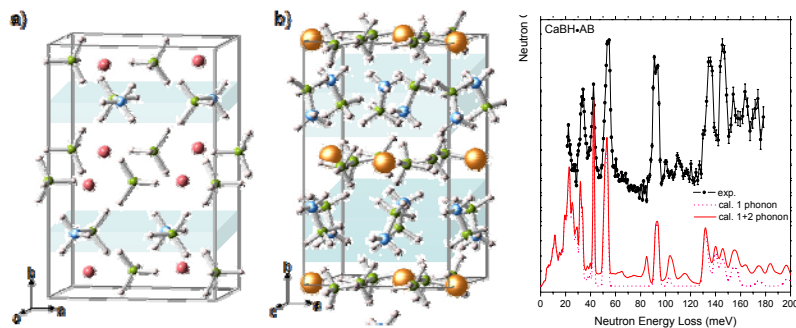
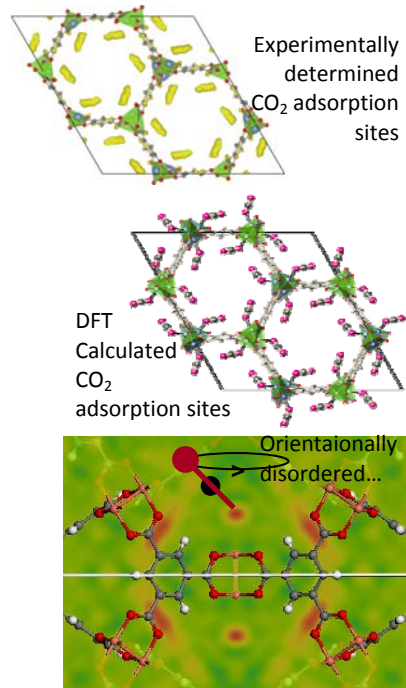


Figure 5. Crystal structure of $\text{LiBH}\cdot\text{AB}$ (a) and $\text{CaBH}\cdot\text{AB}$ (b). Li, Ca, B, N, and H atoms are represented by pink, orange, green, blue, and white spheres, respectively. Light blue rectangles emphasize the alternating AB and borohydride layers in the structure.

3. Adsorption Sites and Binding Nature of CO_2 in Prototypical Metal-Organic Frameworks: A Combined Neutron Diffraction and First-Principles Study

In order to demonstrate that neutron scattering can be effectively used not only in hydrogen storage research but also in other related fields, we are also working on a related topic, namely the carbon capture by MOFs. Our goal is to use our expertise and experience gained in application of neutron scattering methods to hydrogen storage research in solving the carbon capture problem.

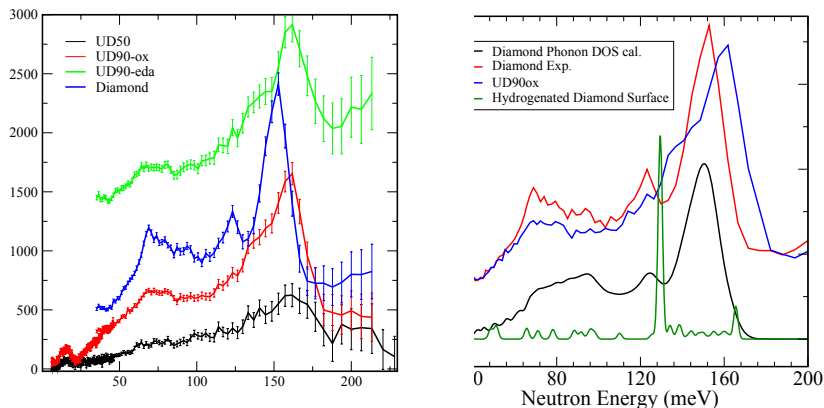
Here we report a detailed study of CO_2 adsorption in two important prototypical MOF compounds containing coordinatively unsaturated metal centers (Mg-MOF-74 and HKUST-1). The major CO_2 adsorption sites in both MOFs were clearly identified through neutron diffraction measurements (see Figure), and the open metal ions were found to be the primary binding sites. The relatively strong metal- CO_2 interaction was attributed to the enhanced electrostatic interaction due to charge overlap between the open metal and one of the oxygen atoms of the CO_2 molecule. Vibrational mode analysis of the adsorbed CO_2 , based on first-principles calculations, further reveals the presence of several very low energy modes and shows that the adsorbed CO_2 molecule is strongly attached to the metal sites through one of its oxygen atoms while the rest of the molecule is relatively free. This high orientational disorder is the reason for the apparent large O-C-O bond bending angle obtained from Rietveld refinement of the diffraction data.



4. Nano-diamond and its functionalized derivatives

This is a new collaborative research with Prof. Yury Gogotsi at Drexel University in Philadelphia. Our goal is to use combined inelastic neutron scattering and first-principles methods to understand the local structure of nano-diamond and its functionalized derivatives. We also use PGAA to extract information about analytical chemistry of the nano-diamond materials. We are interested in understanding the structure of nano-diamond and how we can functionalize it with different molecules such as ethylenediamine (EDA) and increase its surface area by thermal treatment and/or oxidation. We have done some preliminary measurements on several samples which are shown in Figure below.

In the right panel, we compare the observed spectrum with our initial first-principles phonon calculation. The calculated spectrum for diamond (black curve) is in excellent agreement with the spectrum from diamond-powder sample (red curve). Overlaying the spectra from the diamond (red) and UD90x (blue - oxidized nano-diamond) samples clearly indicate the excess phonon modes around 135 meV. In order to get some insight into these modes, we have done a very simple calculation using a diamond slab with some terminating hydrogen atoms on the surface. The very sharp peak near 130 meV is the phonon modes associated with these surface terminating hydrogen molecules (green). Interestingly this sharp feature has about the right energy for the extra modes that we see in UD90x sample, suggesting that during the oxidation we introduce many surface terminating hydrogen atoms on nano-diamond samples. Our PGAA results also support this finding.



PLANNED ACTIVITIES FOR THE NEXT YEAR:

Based on the current results discussed above, we will continue to use the combined first-principles computation, neutron scattering, and synthesis approaches to solve the outstanding problems in hydrogen storage field. In particular, we will focus on (a) Graphene-oxide-framework (GOF) materials, (b) hybrid AB-complex MOF systems, (c) Paddle-Wheel MOFs with open metal sites such as M=Cr, Mo, W, Rh, and (d) Nano-diamond and its functionalized derivatives.

PUBLICATIONS (DE-FG02-08ER46522, Duration : 04/30/2009 – 04/30/2010)

1. "Novel Graphene-Oxide-Framework (GOF) Materials", Jacob Burress, G. Srinivas, Jason M. Simmons, Jamie Ford, Wei Zhou, Taner Yildirim (Submitted., 2010).
2. "A New Family of Metal Borohydride Ammonia Borane Complex", Hui Wu, Wei Zhou, Frederick E. Pinkerton, Martin S. Meyer, Gadipelli Srinivas, Taner Yildirim, T. J. Udovic, J. Rush, *J. Mater. Chem.* (in press, 2010).
3. "Adsorption Sites and Binding Nature of CO₂ in Prototypical Metal-Organic Frameworks: A Combined Neutron Diffraction and First-Principles Study", Hui Wu, Jason M. Simmons, Gadipelli Srinivas, Wei Zhou, and Taner Yildirim, *J. Phys. Chem. Letters*. (in press, 2010).
4. "Metal-Organic Frameworks with Exceptionally High Methane Uptake: Where and How is Methane Stored?", H. Wu, J. M. Simmons, Y. Liu, C. M. Brown, X.-S. Wang, S. Ma, V. K. Peterson, P. D. Southon, C. J. Kepert, H.-C. Zhou, T. Yildirim, and W. Zhou, *Chem. Eur. J.*, 16, 5205–5214 (2010).
5. "Metal Amidoboranes", Hui Wu, Wei Zhou, and Taner Yildirim, in "Boron Hydrides, High Potential Hydrogen Storage Materials", edited by Umit B. Demirci and Philippe Miele, Nova Publishers (2010).
6. "Crystal chemistry and dehydrogenation/rehydrogenation properties of perovskite hydrides RbMgH₃ and RbCaH₃", H. Wu, W. Zhou, T. J. Udovic, J. J. Rush, and T. Yildirim, *J. Phys. Chem. C*, 113, 15091 (2009).
7. "Importance of pore size in high-pressure hydrogen storage by porous carbons", Yury Gogotsi, Cristelle Portet, Sebastian Osswald, Jason M. Simmons, Taner Yildirim, Giovanna Laudisio, John E. Fischer, *Int. J. Hydrogen Energy* (2009), doi:10.1016/j.ijhydene.2009.05.073

PUBLICATIONS (DE-FG02-08ER46522, Duration: 08/15/2008 – 04/30/2009)

8. "High-Capacity Methane Storage in Metal-Organic Frameworks M₂(dhtp): The Important Role of Open Metal Sites", Hui Wu, Wei Zhou, and Taner Yildirim, *J. Am. Chem. Soc.* **131**, 4995 (03/10/2009).
9. "Hydrogen adsorption in HKUST-1: a combined inelastic neutron scattering and first-principles study", C. M. Brown, Y. Liu, T. Yildirim, V. K. Peterson and C. J. Kepert, *Nanotechnology* **20**, 204025 (2009).
10. "Size effects on the hydrogen storage properties of nanoscaffolded Li₃BN₂H₈", H. Wu, W. Zhou, K. Wang, T. J. Udovic, J. J. Rush, T. Yildirim, L. A. Bendersky, A. F. Gross, S. L. Van Atta, J. J. Vajo, F. E. Pinkerton and M. S. Meyer, *Nanotechnology* **20**, 204002 (2009).

11. "Methane Sorption in Nanoporous Metal-Organic Frameworks and First-Order Phase Transition of Confined Methane", W. Hui, W. Zhou, and T. Yildirim, *J. Phys. Chem* **113**, 3029 (2009).
12. "Enhanced H₂ Adsorption in Isostructural Metal-Organic-Frameworks with Open Metal Sites: *Strong Dependence of the Binding Strength on Metal Ions*", W. Zhou, H. Wu, and T. Yildirim, *J. Am. Chem. Soc.* **130**, 15268 (2008).
13. "Alkali and Alkaline-Earth Metal Amidoboranes: Structure, Crystal Chemistry, and Hydrogen Storage Properties", H. Wu, W. Zhou, and T. Yildirim, *J. Am. Chem. Soc.* **130**, 14834 (2008).

PUBLICATIONS (DE-FG02-98ER45701, Duration : 08/15/2008 – 2007)

14. "Origin of the exceptional negative thermal expansion in metal-organic frameworks-5 Zn₄O(1,4-benzenedicarboxylate)(3)", W. Zhou, H. Wu, T. Yildirim, *Phys. Rev. B* **78**, 054114 (2008).
15. "Quasi-Free Methyl Rotation in Zeolitic Imidazolate Framework-8", W. Zhou, H. Wu, T. J. Udovic, J. J. Rush, and T. Yildirim, *J. Phys. Chem. A* **112**, 12602 (2008).
16. "Structural variations and hydrogen storage properties of Ca₅Si₃ with Cr₅B₃-type structure", W. Hui, W. Zhou, T. J. Udovic, J. J. Rush, T. Yildirim, *Chem. Phys. Lett.* **460**, 432 (2008).
17. "Nature and tunability of enhanced hydrogen binding in metal-organic frameworks with exposed transition metal sites", W. Zhou and T. Yildirim, *J. Phys. Chem. C* **112**, 8132 (2008).
18. "Metal-organic frameworks based on double-bond-coupled di-isophthalate linkers with high hydrogen and methane uptakes", X. S. Wang, S. Q. Ma, K. Rauch, J. M. Simmons, D. Q. Yuan, X. P. Wang, T. Yildirim, W. C. Cole, J. J. Lopez, A. de Meijere, H. C. Zhou, *Chem. Mater.* **20**, 3145 (2008).
19. "Metal-Organic Framework from an Anthracene Derivative Containing Nanoscopic Cages Exhibiting High Methane Uptake", Shengqian Ma, Daofeng Sun, Jason M. Simmons, Christopher D. Collier, Daqiang Yuan, and Hong-Cai Zhou, *J. Am. Chem. Soc.* **130**, 1012 (2008).
20. "Structures and Crystal Chemistry of Li₂BNH₆ and Li₄BN₃H₁₀", Hui Wu, Wei Zhou, Terrence J. Udovic, John J. Rush, and Taner Yildirim, *Chem. Mater.* **20**, 1245 (2008).
21. "Crystal Chemistry of Perovskite-Type Hydride NaMgH₃: Implications for Hydrogen Storage", Hui Wu, Wei Zhou, Terrence J. Udovic, John J. Rush, and Taner Yildirim, *Chem. Mater.* **20**, 2335 (2008).
22. "Functionalization of carbon-based nanostructures with light transition-metal atoms for hydrogen storage", E. Durgun, S. Ciraci, and T. Yildirim, *Phys. Rev. B* **77**, 085405 (2008).
23. "Neutron vibrational spectroscopy of the Pr₂Fe₁₇-based hydrides", T. J. Udovic, W. Zhou, W. Wu, C. M. Brown, J. J. Rush, T. Yildirim, E. Mamontov, O. Isnard, *J. Alloys and Comp.* **446**, 504 (2007).
24. "Neutron vibrational spectroscopy and first-principles calculations of the ternary hydrides Li₄Si₂H(D) and Li₄Ge₂H(D): Electronic structure and lattice dynamics", H. Wu, W. Zhou, T. J. Udovic, J. J. Rush, T. Yildirim, M. R. Hartman, R. C. Bowman, and J. J. Vago, *Phys. Rev. B* **76**, 224301 (2007).
25. "Hydrogen and Methane Adsorption in Metal-Organic Frameworks: a High-Pressure Volumetric Study", Wei Zhou, Hui Wu, M. R. Hartman, Taner Yildirim, *J. Chem. Phys. C*, **111**, 16131 (2007).
26. "Hydrogen Storage in a Prototypical Zeolitic Imidazolate Framework-8", Hui Wu, Wei Zhou, and Taner Yildirim, *JACS* **129**, 5314 (2007).
27. "Vibrational properties of TiH_n complexes adsorbed on carbon nanostructures", Jorge Íñiguez, Wei Zhou and Taner Yildirim, *Chem. Phys. Lett.*, **444**, 140 (2007)
28. "Hydrogen-related catalytic effects of Ti and other light transition metals on NaAlH₄ surfaces", J. Iniguez and T. Yildirim, *J. Phys. Condes. Matter* **19**, 176007 (2007).
29. "Hydrogen absorption properties of metal-ethylene complexes", W. Zhou, T. Yildirim, E. Durgun, S. Ciraci, *Phy. Rev. B* **76**, 085434 (2007).
30. "Structure and interstitial deuterium sites of beta-phase ZrNi deuteride", H. Wu, W. Zhou, T. J. Udovic, J. J. Rush, T. Yildirim, Q. Huang, and R. C. Bowman, *Phys. Rev. B* **75**, 064105 (2007).
31. "Structure and Vibrational Spectra of Calcium Hydride and deuteride", H. Wu, W. Zhou, T. J. Udovic, J. J. Rush, T. Yildirim, *J. Alloys Comp.* **436**, 51 (2007).

Session IV

Magnetism

Material Synthesis and Spectroscopy/Diffraction Studies of Multiferroics: Towards Enhanced T_c and Spin/Lattice Coupling (DE-FG02-07ER46382)

Principal Investigator: S-W. Cheong (Department of Physics and Astronomy, Rutgers U., 136 Frelinghuysen Rd., Piscataway, NJ 08854, sangc@physics.rutgers.edu)

Co-PIs: V. Kiryukhin, A. Sirenko, T. Zhou.

Program Scope

Multiferroics belong to a novel class of oxides, whose magnetization, electrical polarizations and strain are closely coupled and can influence each other. Recent excitement in multiferroics stems from the discoveries of giant magnetoelectric cross-coupling effects such as flipping ferroelectric polarization or huge change of dielectric constant with applied magnetic fields. These giant magnetoelectric effects present well recognized possibilities for device applications. However, the spin-lattice coupling, which is the ultimate driving force for the novel effects in multiferroics, is still relatively weak in these newly discovered compounds. In addition, the critical temperature T_c below which couplings of various degrees of freedom take place is still well below room temperature. To discover new multiferroics with enhanced spin-lattice coupling and T_c , it is imperative to identify the connection between macroscopic multiferroicity, microscopic spin-orbital coupling, and the related atomic displacements. To connect the dots and start a virtuous cycle between synthesis of better multiferroics and clear understandings of physical mechanisms in these materials, experimental studies, particularly synchrotron radiation-based x-ray and far-infrared (IR) optical spectroscopy, and neutron scattering have to play a leading role.

Our program with a team from Rutgers University (RU) and New Jersey Institute of Technology (NJIT) includes extensive experiments for the fundamental studies of material synthesis, crystalline structures, magnons, and lattice excitations in multiferroic compounds. The main goal of this Project is to form a positive feedback loop between materials synthesis, spectroscopy/diffraction investigation and physical understanding of the spin-lattice coupling mechanism in multiferroic materials. The obtained insight will be used in the search for multiferroics with increased electric/magnetic polarization, higher T_c , and enhanced coupling effects.

Recent Progress

Our successful collaborative research on multiferroics among PI/coPIs has resulted in a number of important publications [1-16]. We have recently focused on two important multiferroic systems; the chain magnet of $\text{Ca}_3\text{CoMnO}_6$ and orthorhombic HoMnO_3 . Significant cross-coupling effects between magnetism and ferroelectricity have been discovered in the so-called magnetism-driven ferroelectrics. In most of these magnetism-driven ferroelectrics, cycloidal spiral magnetic order with swirling spins induces a uniform ferroelectric polarization through antisymmetric exchange-striction, which stems from the so-called Dzyaloshinski-Moriya interaction. Due to the limited magnitude of Dzyaloshinski-Moriya interaction, the cross-coupling effects in multiferroics with antisymmetric exchange-striction are not expected to be large, which is consistent with experimental results. It turns out that symmetric exchange-striction can also result in magnetism-driven ferroelectricity. Heisenberg-type exchange interaction is responsible for the symmetric exchange-striction, and thus the multiferroic cross-coupling effects in symmetric exchange-strictive systems can be, in principle, large. This

symmetric exchange-strictive effect has been found only in a very limited number of compounds. The best examples include quasi-one-dimensional $\text{Ca}_3\text{CoMnO}_6$ and orthorhombic perovskite HoMnO_3 where up-up-down-down spin order occurs. We have discovered the symmetric exchange-strictive multiferroicity in $\text{Ca}_3\text{CoMnO}_6$, where up-up-down-down spin order, combined with alternating ionic order, results in multiferroicity (see Fig. 1). In addition, we have, for the first time, succeeded in the single crystal growth of $\text{Ca}_3\text{CoMnO}_6$.

Orthorhombic HoMnO_3 with the so-called E-type magnetic order is a three-dimensional system where up-up-down-down spin order, combined with alternating oxygen cage rotation, results in symmetric exchange-strictive multiferroicity. The multiferroic behavior in o- HoMnO_3 has been theoretically proposed. A hint of the multiferroicity in o- HoMnO_3 has been observed in polycrystalline specimens. Since the orthorhombic phase tends to be stable under high pressure, no growth of single crystals with any significant size has been reported. In general, it is difficult to observe intrinsic dielectric properties such as intrinsic polarization in polycrystalline specimens with random orientation of grains and also a large number of grain boundaries. Very recently, we were, for the first time, able to growth single crystals of o- HoMnO_3 . We consider our research accomplishment on $\text{Ca}_3\text{CoMnO}_6$ and o- HoMnO_3 a great success that has already had a significant impact in the research community. The above findings have produced several intriguing spinoffs which are currently being pursued by our group (some of them are described below).

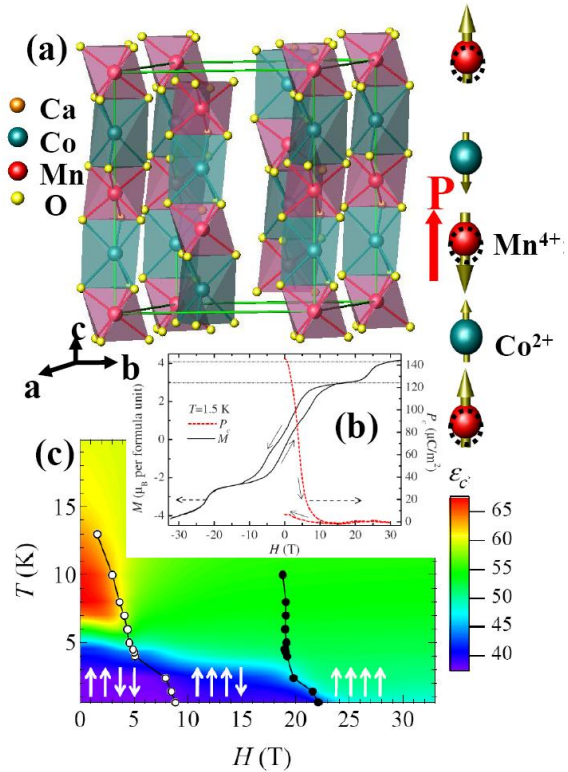


Fig. 1a) Crystallographic structure of the $\text{Ca}_3\text{CoMnO}_6$ chain magnet. The green box represents the crystallographic unit cell. The right-hand-side cartoon shows an Ising chain with the up-up-down-down spin order and alternating ionic order, in which electric polarization is induced through symmetric exchange-striction. b) Magnetization M and c -axis electric polarization P_c as functions of the field H applied along the c axis at 1.5 K and 1.4 K, respectively. Notice the marked hysteresis of both M and P_c among field up and down sweeps. c) Contour plot displaying the behavior of ϵ_c in the T - H plane. Circles indicate magnetic transitions. Spin configurations are shown with arrows. Open and close circles correspond to the maximums in the derivative of ϵ_c with respect to the field, which are associated with the field-induced transitions.

In 2008, we have discovered ferroelectricity in the Ising chain magnet $\text{Ca}_3(\text{Co,Mn})_2\text{O}_6$, which turns out to be the first unquestionable example of symmetric-exchange-striction-driven multiferroics. One of the follow-up projects on $\text{Ca}_3(\text{Co,Mn})_2\text{O}_6$ involves investigation of effects of an applied magnetic field. Using bulk property

measurements in ultra-high magnetic fields, combined with neutron scattering in an applied field, we have found that a new collinear magnetic state with symmetry incompatible with ferroelectricity is realized. As a consequence, very strong magnetoelectric effects occur. Magnetic phase diagrams were constructed. These results provide important information to obtain theoretical models for the magnetoelectric effects. This work has already attracted attention from condensed matter theorists interested in the fundamental physics of magnetism. In particular, our discussions with a group led by P. Chandra (Rutgers) have helped identify this material as an intriguing compound for studies of temperature-dependent spin state of Co^{2+} ion.

Another important and surprising new observation in the $\text{Ca}_3(\text{Co,Mn})_2\text{O}_6$ system resulted from studies of effects of disorder. We found that the long-range magnetic order is only realized in samples with some degree of magnetic-site disorder. In contrast, the stoichiometric $\text{Ca}_3\text{CoMnO}_6$ exhibits a short-range-ordered (SRO) incommensurate magnetic state, even though this compound exhibits a virtually perfect magnetic-site order (see Fig. 2). The incommensurate SRO is only observed in a narrow vicinity of this composition. We argue that a new type of “order-by-static-disorder” phenomenon is realized in $\text{Ca}_3(\text{Co,Mn})_2\text{O}_6$, and expect that this result will also attract attention in the theoretical community.

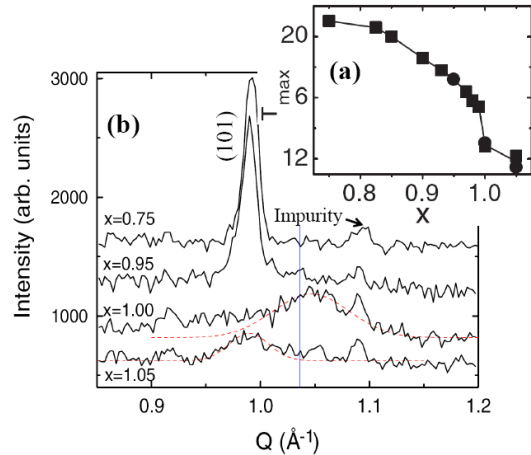


Fig. 2a) Mn-concentration dependence of T_{max} , where temperature-dependent magnetic susceptibility of zero-field-cooled $\text{Ca}_3\text{Co}_{2-x}\text{Mn}_x\text{O}_6$ exhibits a broad peak. b) Neutron powder diffraction patterns in the vicinity of the (101) magnetic peak at 1.4 K for various values of x . Vertical solid line shows the Q of the magnetic peak of a single-crystalline specimen with x near 1. Dashed lines are drawn for the guide of eyes. These results demonstrate that magnetic order is short-ranged at the commensurate concentration of $x=1$, but becomes, surprisingly, long-ranged when x becomes smaller than 1.

Future Plans

Further studies of $\text{Ca}_3(\text{Co,Mn})_2\text{O}_6$ will be carried out. Effects of magnetic frustration, as well as the associated magnetoelectric freezing, will be investigated using various bulk-property measurement techniques, neutron and x-ray scattering. Magnetoelectric coupling will be further studied in magnetic fields. Particular emphasis will be put on the effects of disorder and the newly-discovered “order-by-static-disorder” effect. Magnetic phase diagrams will be established for samples with varying degree of disorder.

We will perform comprehensive experiments on $o\text{-HoMnO}_3$, the crystals of which we have, for the first time, succeeded to grow (see Fig. 3). Neutron scattering and far-IR spectroscopic ellipsometry studies of the $o\text{-HoMnO}_3$ single crystals will be carried out. Effects of an applied magnetic field will be investigated. These results will be combined with the results of measurements of bulk magnetic and ferroelectric properties in zero and applied magnetic field. These studies will provide crucial input for understanding the multiferroic properties of this material.

We will also study various bulk multiferroic single crystals using far-IR spectroscopic ellipsometry. Materials to be investigated include $\text{Ca}_3(\text{Co},\text{Mn})_2\text{O}_6$, $\text{RE}\text{Mn}_2\text{O}_5$ (RE=rare earthes), iron garnets, and nano-checkerboard films with different compositions. In RE-iron garnets we will focus on the hybrid modes that appear due to the close proximity of the magnon and ligand field energies. The control of the light polarization in the ellipsometric measurements will allow a unique separation of the electric- and magnetic dipole activity for the hybrid modes. We want to also perform Raman measurements on these compounds under different polarization configurations, so that the Raman results can compliment the ellipsometer results, and give us better understanding of the nature of these hybrid modes.

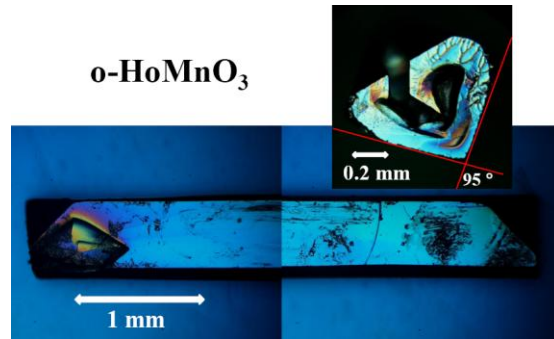


Fig. 3 Optical microscope image of a crystal of o-HoMnO₃ crystal, exhibiting the unique E-type magnetic order. We succeeded in the crystal growth for the first time. Inset shows one cross-sectional side, and the 95 angle in the inset reflects the nature of a single orthorhombic domain and also the lattice constant difference between a and b (a=5.2689, b=5.8450, c=7.3698).

References (publications in 2007-)

- [1] "Coupling between magnon and ligand-field excitations in magnetoelectric Tb₃Fe₅O₁₂ garnet", T. D. Kang *et al.*, Phys. Rev. B, BS11295, submitted in May 2010.
- [2] "Phase coexistence and magnetocaloric effect in La₅O_{8-γ}PryCa₃O₈MnO₃ (γ=0.275)", M. H. Phan *et al.*, Phys. Rev. B **81**, 094413 (2010).
- [3] "Local spin-coupled distortions in multiferroic hexagonal HoMnO₃", T. A. Tyson *et al.*, Phys. Rev. B **81**, 054101 (2010).
- [4] "Spin-state crossover in multiferroic Ca₃Co_{2-x}Mn_xO₆", R. Flint *et al.*, Phys. Rev. B **81**, 092402 (2010).
- [5] "Polar atomic displacements in multiferroics observed via anomalous x-ray diffraction", C. Azimonte *et al.*, Phys. Rev. B **81**, 012103 (2010).
- [6] "Order by static disorder in the Ising chain magnet Ca₃Co_{2-x}Mn_xO₆", V. Kiryukhin *et al.*, Phys. Rev. Lett. **102**, 187202 (2009).
- [7] "3:1 magnetization plateau and suppression of ferroelectric polarization in an Ising chain multiferroic", Y. J. Jo *et al.*, Phys. Rev. B. **79**, 012407 (2009).
- [8] "Electronic Origin of Giant Magnetic Anisotropy in Multiferroic LuFe₂O₄", K.-T. Ko *et al.*, PRL **103**, 207202 (2009).
- [9] "Enhanced magnetic refrigeration capacity in phase separated manganites", A. L. Lima Sharma *et al.*, Appl. Phys. Lett. **95**, 092506 (2009).
- [10] "Magnetic excitations and optical transitions in the multiferroic spin-1/2 system LiCu₂O₂", D. Hübner *et al.*, Phys. Rev. B **80**, 100402R (2009).
- [11] "Local structure of multiferroic RMn₂O₅: Important role of the R site", T.A.Tyson *et al.*, Jurnal of Magnetism and Magnetic Materials **321**, 1714 (2009).
- [12] "Spin freezing and dynamics in Ca₃Co_{2-x}Mn_xO₆ (x≈0.95) investigated with implanted muons: Disorder in the anisotropic next-nearest-neighbor Ising model", T. Lancaster *et al.*, Phys. Rev. B **80**, 020409R (2009).
- [13] "Femtosecond laser excitation of coherent optical phonons in ferroelectric LuMnO₃", Shi-Tao Lou *et al.*, Phys. Rev. B **79**, 214301 (2009).
- [14] "Epitaxial checkerboard arrangement of nanorods in ZnMnGaO₄ films studied by x-ray diffraction", S. M. O'Malley *et al.*, Phys. Rev. B **78**, 165424 (2008).
- [15] "Ferroelectricity in an Ising Chain Magnet", Y. J. Choi *et al.*, Phys. Rev. Lett. **100**, 047601 (2008).
- [16] "Highly Aligned Epitaxial Nanorods with a Checkerboard Pattern in Oxide Films", S. Park *et al.*, Nano Letters **8**, 720-724 (2008).

Magnetic Behavior in Constrained Geometries

S.G.E. te Velthuis (tevelthuis@anl.gov), Axel Hoffmann, J.S. Jiang, Goran Karapetrov
Materials Science Division, Argonne National Laboratory, Argonne, IL 60439

Cristina Visani, Norbert Nemes, Jacobo Santamaria
Facultad de Fisica, Universidad Complutense, 28040, Madrid, Spain

Maria Iavarone
Department of Physics, Temple University, Philadelphia, PA 19122-6082

Research Scope

The properties of materials in constrained geometries, such as thin films and multilayers, can be profoundly modified by strain, surface effects, finite size effects, chemical intermixing, and proximity to another material with inherently different properties. These modifications can be of great interest because of the new phenomena that can result. In all cases, understanding the macroscopic phenomena and relating them to the physical properties requires a detailed knowledge of the magnetic, electronic, and chemical structure within the layers and especially close to these interfaces. Our program involves investigating a variety of problems associated with magnetic thin films, such as the competition between exchange coupling and anisotropy and interactions between ferromagnetic/superconducting materials. Primarily using polarized neutron reflectivity (PNR), the depth-dependent magnetization vector and lateral domain structure is probed, providing the magnetic characterization needed to address the underlying questions.

Recent Progress

Ferromagnetic/superconducting complex oxide superlattices :

Interplay between ferromagnetic order and superconducting order leads to a wealth of physical phenomena [A. Buzdin, Rev. Mod. Phys. 77 (2005) 935]. In collaboration with Axel Hoffmann and the group of Jacobo Santamaria, we studied trilayers consisting of ferromagnetic $\text{La}_{0.7}\text{Ca}_{0.3}\text{MnO}_3$ (LCMO) spaced by superconducting $\text{YBa}_2\text{Cu}_3\text{O}_7$ (YBCO). In these trilayers a large magnetoresistance (MR) effect was observed during the superconducting transition of YBCO. Our PNR experiments, conducted on ASTERIX at the Lujan Neutron Scattering Center, conclusively correlated the peaks in the resistance to an antiparallel alignment between magnetizations M of the two LCMO layers. It is believed that this magnetoresistance phenomenon originates in the spin dependent transport of quasiparticles transmitted from the ferromagnetic electrodes into the superconductor. The antiparallel alignment of the M of the two layers occurs as a result of separate coercivities. Higher resolution PNR measurements revealed that besides an inhomogeneous magnetization profile over the depth of the layers, the top layer M is significantly less than that of the bottom layer. This difference is seen for a series of samples with varying YBCO layer thickness, including 40 unit cells where the MR effect has disappeared. Recent experiments have explained this last phenomena. For thicker YBCO the easy axis is not along the (100) direction, but along (110), which results in a significant rotation of M during reversal. In fact, the rotation of the two layers coincides and therefore antiparallel alignment of the two layers does not occur and therefore the large MR is not observed. Our latest PNR experiments are helping us understand the angular dependent resistance measurements that show both bi-quadratic and unidirectional contributions.

Ferromagnetic/superconducting domain interactions:

Recent explorations of the magnetic interaction between a superconductor (SC) and a ferromagnet (FM) have led to the discovery of intriguing phenomena, like domain-wall (DW) superconductivity in FM/SC bilayers. Interestingly, DW could be used to spatially confine the superconductivity by rearranging the magnetic domain structure in the ferromagnet [A. Belkin et al, Appl. Phys. Lett. 93 (2008) 072510]. Most of the proposed scenarios assume the FM magnetization is not affected by the appearance of superconductivity because the energy scale associated with magnetization is normally much larger than that of superconductivity. However, to rearrange magnetic domain structure costs much less energy than to suppress the magnetization, but it may have significant effect on the transport results. In a collaboration with Maria Iavarone and Goran Karapetrov we have probed the magnetic domains using neutron scattering. In PNR experiments on Py/MoGe and Py/Nb films, conducted on ASTERIX at the Lujan Neutron Scattering Center, we observed off-specular Bragg reflections from the out-of-plane magnetization component of stripe domains inside the 1 micron thick Py layer. In the Py/Nb film a change in period of the stripe domains was observed after crossing the superconducting transition of the Nb film, evidencing that domain-wall superconductivity can modify the FM magnetization as well, despite the differences in energy scales associated with the two phenomena.

Exchange-Spring magnets:

To understand the enhanced maximum density of the magnetic energy in Fe/CoSm spring magnets with graded interfaces, we have determined the depth profile of the magnetic structure. This project is a collaboration with J.S. Jiang. The existence of a large chemically intermixed region between the Fe layer and the CoSm layer has been confirmed. Along the descending branch of the major hysteresis loop, large spin-flip (SF) neutron reflectivity was observed at the reversal field of the Fe layer (Fig. 2a). The PNR data, acquired using the Magnetism Reflectometer at the Spallation Neutron Source, have been analyzed with the aid of micromagnetic simulations using a one-dimension spin-chain model. The depth profiles of the micromagnetic parameters (Fig. 2b) and the magnetization vector (Fig. 2c) have been determined. Our results indicate that the magnetization twist localizes inside the Fe layer and the intermixed region, as predicted by J.S. Jiang *et al.* [Appl. Phys. Lett. **85**, 5293 (2004)]. Interestingly, the rotation rate of the magnetization vector peaks inside the intermixed region due to a combined effect of weak magnetic anisotropy and small exchange stiffness of the graded Fe/CoSm interface. Further, we performed PNR studies along recoil loops starting from fields where the CoSm layer reverses. The results show that at these fields the average magnetization of both the Fe and the CoSm layers are greatly reduced from the saturation values, signifying the formation of magnetic domains in both layers. This agrees with a distribution of magnetic anisotropy inside the CoSm layer, which has been invoked to explain the recoil loop openness by Y. Choi *et al.* [Appl. Phys. Lett. **91**, 022502 (2007)]. It is worth noting that at low fields along the recoil loops, not only the Fe layer rotates backwards, but also some CoSm grains switch back

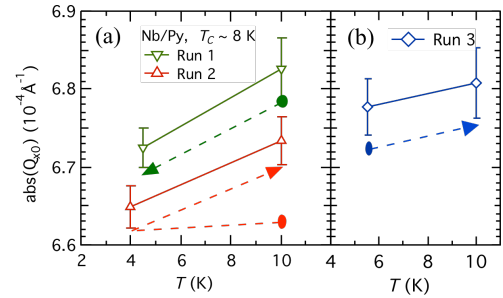


FIG. 1. The 1st order Bragg peak position changes when T crosses T_C ($T_C \sim 8$ K) for runs with initial magnetic states prepared above T_C (a) and below T_C (b). The solid circle labels the temperature at which the initial magnetic state was prepared for each run. Dashed lines shows the temperature history.

to the original direction, in agreement with previous micromagnetic simulations by Y. Choi *et al.* [Appl. Phys. Lett. **91**, 022502 (2007)]. Overall, the graded interface between the Fe and the CoSm layers absorbs a large portion of the magnetization twist so that the magnetization direction of the CoSm layer remains intact at low fields.

Future Plans

While in the past, films and multilayers were typically created using metals, with the recent advances in film growth, it is now possible also to produce high quality superlattices consisting of complex oxide materials. This capability is providing a promising class of new materials exhibiting a wide range of interesting phenomena. Due to the diverse physical properties that these oxides can have, some of which can be varied by doping, the versatility in their applications is large. Unlike metallic systems, the chemical or electronic composition of complex oxides can change close to the interface, thereby dramatically influencing the physical properties. In order to determine whether or not these variations are inherent to the complex oxide materials used or simply growth-related, it is important to do detailed measurements of the magnetic, electronic and chemical properties close to these interfaces. We will continue and expand our studies of complex oxide superlattices. New topics we are planning to address are 1) The influence of engineered interfaces on the electronic reconstruction in $\text{La}_{0.67}\text{Sr}_{0.33}\text{MnO}_3/\text{SrTiO}_3$ superlattices and 2) Phase separation caused by the competition between the ferromagnetism and charge-orbital ordering in $\text{La}_{0.5}\text{Sr}_{0.5}\text{MnO}_3/\text{Pr}_{0.5}\text{Ca}_{0.5}\text{MnO}_3$ superlattices.

Our work on F/S interactions will be expanded to include other systems, such as Nb/CuNi/Nb trilayers, where due to the weak ferromagnetism of CuNi, the energy scales for the ferromagnetic and superconducting order are close, enabling a larger influence on the ferromagnetism by the onset of superconductivity.

Publications (2007-2010)

1. *Spin dependent magnetoresistance at ferromagnet/superconductor/ferromagnet $\text{La}_{0.7}\text{Ca}_{0.3}\text{MnO}_3/\text{YBa}_2\text{Cu}_3\text{O}_{7-d}/\text{La}_{0.7}\text{Ca}_{0.3}\text{MnO}_3$ trilayers*
C. Visani, V. Peña, J. Garcia-Barriocanal, D. Arias, Z. Sefrioui, C. Leon, J. Santamaria, N.M. Nemes, M. Garcia-Hernandez, J.L. Martinez, S.G.E. te Velthuis, A. Hoffmann, Phys. Rev. B **75**, 054501 (2007)
2. *Surface spin-flop transition in a uniaxial antiferromagnetic Fe/Cr superlattice induced by a magnetic field of arbitrary direction*
M.G. Pini, A. Rettori, P. Betti, J.S. Jiang, Y. Ji, S.G.E. te Velthuis, G.P. Felcher, S.D. Bader

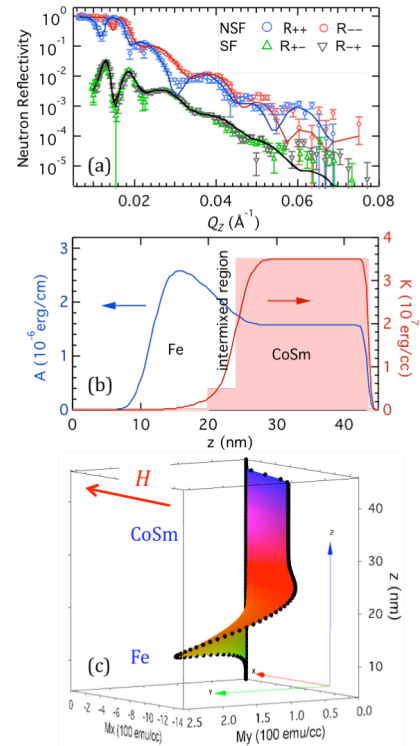


FIG. 2. (a) PNR data taken at $+0.39$ T after saturation in a -1.15 T field. Spin-flip data are divided by a factor of 10 for clarity. With the aid of micromagnetic simulations, the depth profiles of the exchange stiffness and the uniaxial anisotropy (b) and the magnetization vector (c) have been determined from fitting the PNR data.

- J. Phys.: Condens. Matter **19**, 136001 (2007), **Erratum:** *ibid.*, 479003 (2007)
3. *Spin Structure of Exchange-Biased NiFe/FeMn/NiFe trilayers*
A.M. Alsmadi, S.G.E. te Velthuis, G.P. Felcher, and C.G. Kim,
J. of Appl. Phys. **101**, 09E522(3) (2007)
 4. *Magnetoresistance in $La_{0.7}Ca_{0.3}MnO_3$ - $YBa_2Cu_3O_7$ F/S/F trilayers*
V. Peña, C. Visani, F. Bruno, J Garcia-Barriocanal, D. Arias, A. Rivera, Z. Sefrioui, C. Leon, S.G.E. te Velthuis, A. Hoffmann, N. Nemes, M. Garcia-Hernandez, J. L. Martinez, and J. Santamaria,
Journal of Magnetism and Magnetic Materials 316, e745 (2007)
 5. *Spin dependent transport at oxide $La_{0.7}Ca_{0.3}MnO_3$ / $YBa_2Cu_3O_7$ ferromagnet/superconductor interfaces*
V. Peña, N. Nemes, C. Visani, F. Y. Bruno, D. Arias, Z. Sefrioui, C. Leon, S.G.E. te Velthuis, A. Hoffmann, M. Garcia-Hernandez, J. L. Martinez, and J. Santamaria,
Journal of the European Ceramic Society 27, 3967 (2007)
 6. *Field cooling dependence of the anisotropy in exchange biased FeF_2 /Co films*
A.M. Alsmadi, S.G. E. te Velthuis, Z. J. Weber, U. Welp, H. Shi and D. Lederman,
J. of Appl. Phys. **103**, 07C114 (2008)
 7. *Magnetically asymmetric interfaces in a $(LaMnO_3)/(SrMnO_3)$ superlattice due to structural asymmetries*
S. J. May, A. B. Shah, S. G. E. te Velthuis, M. R. Fitzsimmons, J. M. Zuo, X. Zhai, J. N. Eckstein, S. D. Bader, and A. Bhattacharya, Phys. Rev. B **77**, 174409 (2008)
 8. *Metal-Insulator transition and its relation to magnetic structure in $(LaMnO_3)_{2n}/(SrMnO_3)_n$ superlattices*
A. Bhattacharya, S. May, S. G. E. te Velthuis, M. Warusawithana, X. Zhai, Bin Jiang, J.-M. Zou, M. R. Fitzsimmons, S. D. Bader, J. N. Eckstein, Phys. Rev. Lett. **100**, 257203 (2008)
 9. *Origin of the inverse spin-switch behavior in manganites/cuprate/manganite trilayers*
N.M. Nemes, M. Garcia-Hernandez, S.G.E. te Velthuis, A. Hoffmann, C. Visani, J. Garcia-Barriocanal, V. Peña, D. Arias, Z. Sefrioui, C. Leon, J. Santamaria, Phys. Rev. B **78** 094515 (2008)
 10. *Complementary polarized neutron and resonant x-ray magnetic reflectometry measurements in Fe/Gd heterostructures: Case of inhomogeneous intralayer magnetic structure*
E. Kravtsov, D. Haskel, S.G.E. te Velthuis, J. S. Jiang, and B. Kirby,
Phys. Rev. **B 79**, 134438 (2009)
 11. *X-ray Magnetic Circular Dichroism and Small Angle Neutron Scattering Studies of Thiol Capped Gold Nanoparticles*
J. de la Venta, V. Bouzas, A. Pucci, M. A. Laguna-Marco, D. Haskel, S.G.E. te Velthuis, A. Hoffmann, J. Lal, M. Bleuel, G. Ruggeri, C. de Julián Fernández, M. A. García,
Journal of Nanoscience and Nanotechnology **9**, 6434 (2009)
 12. *Magnetic depth profile of a modulation doped $La_{1-x}Ca_xMnO_3$ exchange-biased system*
A. Hoffmann, S.J. May, S.G.E. te Velthuis, S. Park, M.R. Fitzsimmons, G. Campillo, M.E. Gómez,
Phys. Rev. B **80**, 052403 (2009)
 13. *Enhanced ordering temperatures in antiferromagnetic manganite superlattices*
S.J. May, P.J. Ryan, J.L. Robertson, J.-W. Kim, T.S. Santos, E. Karapetrov, J. L. Zarestky, X. Zhai, S.G.E. te Velthuis, J.N. Eckstein, S.D. Bader, A. Bhattacharya, Nature Materials **8** 892 (2009)
 14. *Magnetic coupling in $La_{0.7}Ca_{0.3}MnO_3$ / $YBa_2Cu_3O_7$ / $La_{0.7}Ca_{0.3}MnO_3$ trilayers*
N.M. Nemes, C. Visani, J. Garcia-Barriocanal, F.Y. Bruno, Z. Sefrioui, D. Arias, C. Leon, M. Garcia-Hernandez, S. G. E. te Velthuis, A. Hoffmann, J. Santamaria,
DIFFUSION IN MATERIALS - DIMAT2008, Book Series: Defect and Diffusion Forum Series, Eds: A. Agüero, J.M Albella, M.P. Hierro, J Phillibert, F.J.P. Trujillo, Vol. 289-292, 303 (2009)
 15. *Directionally controlled superconductivity in ferromagnet/superconductor/ ferromagnet trilayers with biaxial easy axes*
C. Visani, N.M. Nemes, M. Rocci, Z. Sefrioui, C. Leon, S.G.E. te Velthuis, A. Hoffmann, M. R. Fitzsimmons, F. Simon, T. Fehér, M. García-Hernández, J. Santamaria,
Phys. Rev. B **81**, 094512 (2010)

A Global Understanding of Magnetic Phase Separation in Doped Cobaltites

Chris Leighton

Materials Science, University of Minnesota

151 Amundson Hall, 421 Washington Ave SE, Minneapolis, MN 55455

leighton@umn.edu, www.cems.umn.edu/about/people/faculty.php?id=20233

Research Scope

Complex transition metal oxides represent an exciting new frontier in condensed matter physics and materials science, as exemplified by the discoveries of high temperature superconductivity and Colossal MagnetoResistance (CMR). Due to their importance in fundamental science, in addition to their potential applications in energy technologies, these oxides constitute a major part of the DoE BES effort. During the intensive research in this area in the last decade or so it has become increasingly obvious, both from experimental and theoretical perspectives, that magnetic/electronic inhomogeneity (often referred to as magneto-electronic phase separation (MEPS)) plays a vital role in properties such as CMR. The inhomogeneity occurs over a range of length scales, in chemically homogeneous materials, and is now considered a general feature of doped correlated systems with acute competition between multiple available ground states. In the DoE-funded effort in our group we are seeking a complete and quantitative understanding of this magneto-electronic phase separation, combining powerful and direct neutron scattering techniques with a wide range of complementary physical property measurements including various forms of magnetometry, electronic transport, heat capacity, etc. We synthesize materials in both bulk and thin film form, focusing on the doped cobaltites as model systems. These cobaltites span the range from the “simplest” doped perovskites (i.e. $\text{La}_{1-x}\text{Sr}_x\text{CoO}_3$), through the complex narrow bandwidth systems (e.g. $\text{Pr}_{1-x}\text{Ca}_x\text{CoO}_3$) and Ruddlesden-Popper phases (e.g. $\text{La}_{1-x}\text{Sr}_{1+x}\text{CoO}_4$), to heterostructured thin films (e.g. $\text{SrTiO}_3/\text{La}_{1-x}\text{Sr}_x\text{CoO}_3$). Our goal is a detailed, quantitative understanding of the global behavior of the magnetic inhomogeneity, employing neutron scattering techniques such as Neutron Diffraction (ND), Small-Angle Neutron Scattering (SANS), and Polarized Neutron Reflectometry (PNR).

Recent Progress

Continued research on magnetic phase separation in $\text{La}_{1-x}\text{Sr}_x\text{CoO}_3$: The considerable body of work we have performed on this system culminated in our recent publication of a doping fluctuation based model for the nanoscopic MEPS. Combining extensive doping dependent SANS with magnetometry, transport, and heat capacity, on the highest quality single crystals available, we were able to establish the new result that the MEPS in this system is actually confined to a well-defined doping range. Remarkably, this range, in addition to the doping dependence of the SANS intensity, can be reproduced by simple statistical simulations where the local variations in chemistry in these randomly doped systems provides the driving force for the nanoscopic electronic and magnetic inhomogeneity. This picture provides a simple explanation for the occurrence of nanoscale inhomogeneity in this material, the important implication being that the more complex models for electronically-driven phase separation are

not required to understand the experimental observations in this material. We anticipate that the narrow bandwidth cobaltites discussed below will provide a further, more stringent, test of this model. In addition to this work on $\text{La}_{1-x}\text{Sr}_x\text{CoO}_3$ we also recently completed an ND/SANS study of the anomalous magnetism in the related $\text{Pr}_{1-x}\text{Sr}_x\text{CoO}_3$ material. This work concluded that the previously unexplained “double magnetic transition” was in fact due to a coupled structural/magnetocrystalline anisotropy transition, driven in this case by the Pr-O bonding. The work highlights the importance of the significant magnetocrystalline anisotropy in Co-based perovskites, a feature that is often overlooked in favor of the well-known spin-state phenomena.

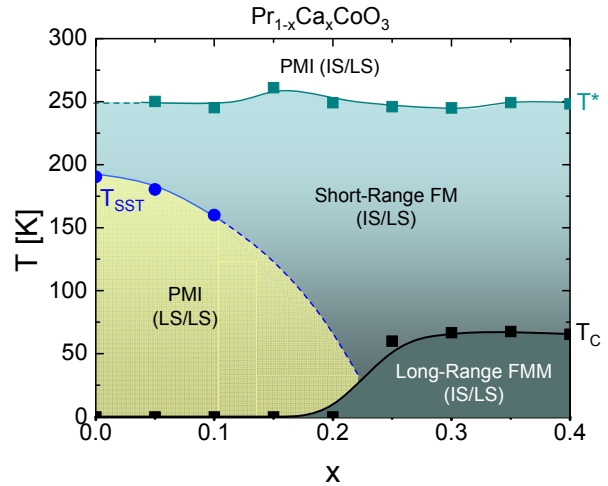


Fig. 1. Magnetic phase diagram of $\text{Pr}_{1-x}\text{Ca}_x\text{CoO}_3$. PMI = paramagnetic insulator, FMM = ferromagnetic metal, T_{SST} = onset spin-state transition temp., T_C = Curie temp. The symbols in brackets indicate the spin state of $\text{Co}^{3+}/\text{Co}^{4+}$ (low spin (LS) or intermediate spin (IS)).

Local magnetism in undoped LaCoO_3 : Much effort, over a period of several decades, has been invested in the thermally-induced spin-state transition in LaCoO_3 , a topic that remains highly controversial. In our recent work we have focused on a very surprising aspect to the behavior of this material that has not received as much attention; the nominally “non-magnetic” low temperature phase in fact displays significant local magnetism, in the form of magnetic excitons. This is a very important observation as these entities likely evolve into the ferromagnetic clusters or droplets underlying the phase separation in the Sr doped case, the nature of this evolution being arguably one of the biggest unsolved issues in the magnetism of this material. In addition to observation of these excitons by muon spin relaxation, and the first demonstration of excited finite spin Co ions trapped at defects in the low temperature limit, we also recently acquired direct neutron scattering evidence for interaction of these excitons over surprisingly large length scales.

Magnetic phase separation in narrow bandwidth cobaltites: As mentioned above, narrow bandwidth cobaltites provide some unique opportunities for understanding the fundamental physics in these systems, particularly with regard to magnetic phase separation and spin-state phenomena. In the $\text{Pr}_{1-x}\text{Ca}_x\text{CoO}_3$ system the smaller average A-site cations result in narrow electronic bandwidth and strongly suppressed ferromagnetic interactions, thus enhancing competition with underlying ground states, at the same time stabilizing the low spin-state of the Co ions. We have recently constructed a magnetic phase diagram of this material (Fig. 1), using magnetometry, transport, heat capacity, ND and SANS. In addition to providing a beautiful example of the widely-anticipated interplay between phase separation and spin-state transitions, this material also exhibits unusual coexistence of long-range and short-range ferromagnetism. The two phases possess very different coercivity and, remarkably, are strongly exchange coupled, providing a very rare example of strong coupling between spatially coexisting order parameters in electronically phase separated systems. This unusual situation

results in the spontaneous formation of a hard/soft ferromagnetic composite, exhibiting prototypical exchange spring magnetism *in the absence of chemical interfaces*.

Cobaltite interfaces and heterostructures:

In addition to extensive work on bulk samples, both poly- and single-crystal, we are also exploring a new frontier in the understanding of magneto-electronic phase separation – the influence of dimensional confinement. Our recent work has in fact established an interfacial form of this magnetic phase separation as the origin of a long-standing problem with thin films of these materials; the degradation in magnetization and conductivity in the very thin film limit. Our results show that the SrTiO₃(001)/La_{1-x}Sr_xCoO₃ interface is susceptible to magnetic phase separation, the key evidence coming from what is, to the best of our knowledge, the first SANS measurements (Fig. 2) that have achieved direct observation of short-range magnetism in complex oxide films as thin as 650 Å. Via a collaboration with the STEM/EELS (Scanning Transmission Electron Microscopy/Electron Energy Loss Spectroscopy) group at ORNL (Fig. 3) we have established that this occurs due to an unexpected depletion in local hole density in the interface region, driven by subtle depth-wise variations in Sr doping and O content. These variations can be understood based on simple thermodynamic and structural arguments, suggesting a potential solution to a long-standing problem in complex oxide heterostructures.

Future Plans

In addition to continuation of the work described above on undoped/lightly doped LaCoO₃, and narrow bandwidth cobaltites, we also plan to study in more detail the magnetocrystalline anisotropy in these materials, an aspect to their magnetic behavior that is emerging as a problem of considerable importance. The interplay between the anisotropy and the well-known oxygen vacancy ordering is of particular interest given some recent observations we have made in thin films. In an effort to further expand our knowledge base on the bulk non-perovskite cobaltites we are also engaged in a collaboration with ANL to grow single crystals of the single- and bi-layer Ruddlesden-Popper phases, which offer the potential to study the influence of dimensionality on the magneto-electronic phase separation.

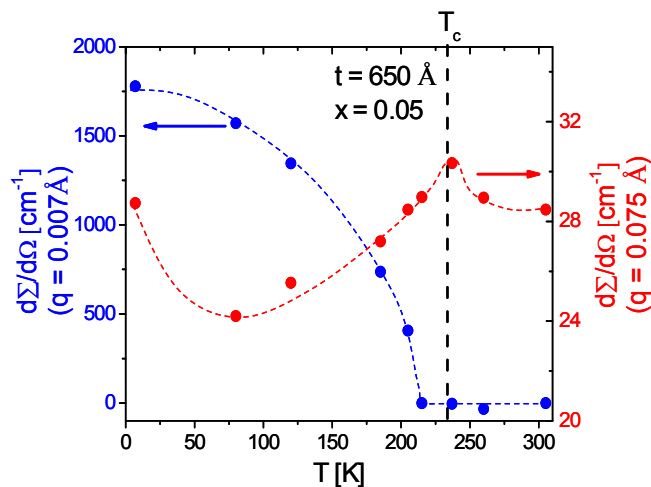


Fig. 2. Temperature dependence of the SANS cross section at $q = 0.007$ (left axis) and 0.075 \AA^{-1} (right axis) for a SrTiO₃(001)/La_{0.5}Sr_{0.5}CoO₃ film with thickness of 650 Å. The films are grown on 1" wafers and are triply stacked.

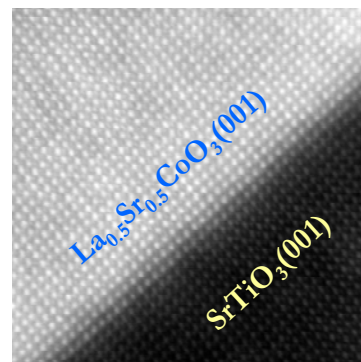


Fig. 3. Atomic resolution STEM image of the interface region in a SrTiO₃(001)/La_{1-x}Sr_xCoO₃ heterostructure.

Publications (2007 - 2010)

1. "Application of aberration corrected scanning transmission electron microscopy and electron energy loss spectroscopy to thin oxide films and interfaces", M. Varela, J. Gazquez, A.R. Lupini, J.T. Luck, M.A. Torija, M. Sharma, C. Leighton, M.G. Biegalski, H.M. Christen, M. Murfitt, N. Dellby, O. Krivanek and S.J. Pennycook, *Int. J. Mat. Res. (Proc. of 7th Int. Workshop on Interfaces)*, **101** 21 (2010)
2. "Low temperature Schottky anomalies in the specific heat of LaCoO_3 : Defect-stabilized finite spin-states", C. He, H. Zheng, J.F. Mitchell, R.J. Cava and C. Leighton, *Appl. Phys. Lett.*, **94** 102514 (2009)
3. "Heat capacity study of magneto-electronic phase separation in $\text{La}_{1-x}\text{Sr}_x\text{CoO}_3$ single crystals", C. He, S. Eisenberg, C. Jan, H. Zheng, J.F. Mitchell and C. Leighton, *Phys. Rev. B.*, **80** 214411 (2009)
4. "Transport signatures of percolation and electronic phase inhomogeneity in $\text{La}_{1-x}\text{Sr}_x\text{CoO}_3$ single crystals", C. He, S. El-Khatib, S. Eisenberg, M. Manno, J.W. Lynn, H. Zheng, J.F. Mitchell and C. Leighton, *Appl. Phys. Lett.* **95** 222511 (2009)
5. "Doping fluctuation-driven magneto-electronic phase separation in $\text{La}_{1-x}\text{Sr}_x\text{CoO}_3$ single crystals", C. He, S. El-Khatib, J. Wu, J.W. Lynn, H. Zheng, J.F. Mitchell and C. Leighton, *Europhys. Lett.* **87** 27006 (2009)
6. "Magnetocaloric effect and refrigerant capacity in charge-ordered manganites", N.S. Bingham, M.-H. Phan, H. Srikanth, M.A. Torija and C. Leighton, *J. Appl. Phys.*, **106** 023909 (2009)
7. "Coupled structural/magnetocrystalline anisotropy transitions in the doped perovskite cobaltite $\text{Pr}_{1-x}\text{Sr}_x\text{CoO}_3$ ", C. Leighton, D.D. Stauffer, Q. Huang, Y. Ren, S. El-Khatib, M.A. Torija, J. Wu, J.W. Lynn, L. Wang, N.A. Frey, H. Srikanth, J.E. Davies, K. Liu and J.F. Mitchell, *Phys. Rev. B.* **79** 214420 (2009)
8. "Low temperature interactions of magnetic excitons in LaCoO_3 ", S.R. Giblin, I. Terry, D. Prabhakaran, A.T. Boothroyd and C. Leighton, *Phys. Rev. B.* **79** 174410 (2009)
9. "Dielectric response to the magnetic defect structure and the spin state transition from a low spin to higher spin state in polycrystalline LaCoO_3 ", R. Schmidt, J. Wu, C. Leighton and I. Terry, *Phys. Rev. B.* **79** 125105 (2009)
10. "Epitaxial $\text{La}_{0.5}\text{Sr}_{0.5}\text{CoO}_3$ thin films: Structure, magnetism and transport", M.A. Torija, M. Sharma, M.R. Fitzsimmons, M. Varela, J. Wu and C. Leighton, *J. Appl. Phys.* **104** 023901 (2008)
11. "Strongly inhomogeneous conduction in cobaltite films: Non-Gaussian resistance noise", V. Orlyanchik, M.B. Weissman, M.A. Torija, M. Sharma and C. Leighton, *Phys. Rev. B.* **78** 094430 (2008)
12. "Spin polarons in $\text{La}_{1-x}\text{Sr}_x\text{CoO}_3$ single crystals", R.X. Smith, M.J.R. Hoch, P.L. Kuhns, W.G. Moulton, A.P. Reyes, G.S. Boebinger, J. Mitchell, and C. Leighton, *Phys. Rev. B* **78** 092201 (2008)
13. "Non-Griffiths-like clustered phase above the Curie temperature of the doped perovskite cobaltite $\text{La}_{1-x}\text{Sr}_x\text{CoO}_3$ ", C. He, M.A. Torija, J. Wu, J.W. Lynn, H. Zheng, J.F. Mitchell and C. Leighton, *Phys. Rev. B.* **76** 014401 (2007)
14. "Direct measurement of the low temperature spin-state transition in LaCoO_3 ", R.F. Klie, J.C. Zheng, Y. Zhu, M. Varela, J. Wu and C. Leighton, *Phys. Rev. Lett.* **99** 047203 (2007)
15. "Disorder and double exchange spin dynamics in $\text{La}_{0.7}\text{Sr}_{0.3}\text{MnO}_3$ and $\text{La}_{0.7}\text{Sr}_{0.3}\text{CoO}_3$ via NMR hyperfine couplings", M.J.R. Hoch, P.L. Kuhns, W.G. Moulton, A.P. Reyes, M.A. Torija, J.F. Mitchell and C. Leighton, *Phys. Rev. B.* **75** 104421 (2007)

A Unified Effort for Crystal Growth, Neutron Scattering, and X-ray Scattering Studies of Novel Correlated Electron Materials

Young Lee
Department of Physics
Massachusetts Institute of Technology
Room 13-2153
77 Massachusetts Ave, Cambridge, MA 02139
Email: younglee@mit.edu

Research scope

Our research activities are focused on understanding the fundamental science of complex electronic and magnetic materials. Much of the research involves performing neutron and x-ray scattering experiments on single crystal samples to investigate the spin, charge, lattice, and orbital correlations which are central to the exotic physics in these systems. We have performed scattering experiments at the High Flux Isotope Reactor at Oak Ridge, the Advanced Photon Source at Argonne, the National Synchrotron Light Source at Brookhaven, and the NIST Center for Neutron Research in Gaithersburg, MD. We have also performed thermodynamic and transport measurements to provide a comprehensive picture of the microscopic behavior. Growing single crystal samples is a crucial aspect of this research. This is especially important in materials which are anisotropic, such as low-dimensional magnets composed of planes or chains.

The idea that the doped copper-oxides may be on the verge of quantum disorder has led to great interest in the possibility of quantum disordered spin ground states (called the spin liquid). It is expected that such systems will have remarkable new properties such as the fractionalization of the spin quantum number. For example, the usual $S=1$ spin wave excitation may be broken up into a pair of $S=1/2$ excitations (called spinons). This phenomenon is well known in one-dimensional spin chains, but has so far been elusive in two-dimensional systems, even though some recent reports are strongly suggestive. One of our ongoing projects involves studying a $S=1/2$ spin-chain system TiOCl based on transition metal ions in the d^1 configuration (in contrast to Cu in the d^9 configuration). Another project involves studying the intriguing triangular lattice compound Na_xCoO_2 , which has both an unusual metallic phase and a superconducting phase, depending on the composition. Since the triangular lattice tends to frustrate spin ordering, this is an especially promising place to look for a spin liquid. Moreover, we have pushed forward in studying $S=1/2$ kagomé lattice systems ($\text{ZnCu}_3(\text{OH})_6\text{Cl}_2$ and $\text{Mg}_x\text{Cu}_{3-x}(\text{OH})_6\text{Cl}_2$) which are even more frustrated.

Recent progress

Pressure-induced transition in spin-Peierls TiOCl In this quantum magnet, the Ti ions are in the d^1 configuration which form $S=1/2$ one-dimensional chains. An important aspect of this system is that adjacent chains are shifted by half of a unit cell along the chain direction. Therefore, the interchain coupling is frustrated, which should yield nearly ideal one-dimensional spin physics down to low temperatures. We have performed x-ray scattering measurements on single crystal samples of TiOCl . A lattice dimerization was observed to occur at a temperature corresponding to the steepest drop in the susceptibility near $T=65$ K, with an incommensurate (nearly dimerized) modulation occurring below $T=92$ K. The dimerization is measured via a weak superlattice peak whose temperature dependence. Moreover, we performed *inelastic* x-ray scattering experiments at the APS to measure the lattice dynamics. The seminal Cross-Fisher theory for the spin-Peierls transition predicts a softening of the phonon mode associated with the transition. We find that the longitudinal acoustic phonon mode becomes strongly overdamped at the zone boundary, with a temperature dependence reminiscent of soft phonon behavior. Our results show good quantitative agreement with the Cross-F

Fisher theory for the phonon dynamics at wave vectors near the zone boundary and temperatures near T_{SP} . This suggests that TiOCl is an ideal spin-Peierls system where the soft-phonon has been observed for the first time.

More recently, we have used synchrotron x-rays to study the insulator-metal phase transition in TiOCl which occurs at high-pressure (~ 12 GPa). We have developed the capability to perform diamond anvil cell measurements at low temperatures using x-ray and optical probes. The ground state of TiOCl was probed using synchrotron x-ray diffraction on a single-crystal sample at $T=6$ K at the APS. We tracked the evolution of the structural superlattice peaks associated with the dimerized ground state as a function of pressure. The dimerization along the b-axis is rapidly suppressed in the vicinity of a first-order structural phase transition at $P_C = 13.1(1)$ GPa, as shown in Figure 1. Surprisingly, the high-pressure phase is characterized by an incommensurate charge density wave perpendicular to the original spin chain direction. This may indicate the presence of a two-dimensional nested Fermi surface at high pressure. At a minimum, these results show that the electronic ground state undergoes a fundamental change in symmetry, indicating a significant change in the principal interactions.

Na-ordering in Na_xCoO_2 We have completed studies of single-crystal Na_xCoO_2 with $0.25 < x < 0.84$ using an electrochemical technique. By carefully mapping the overpotential versus x , we find six distinct stable phases with Na levels corresponding to $x \approx 0.75, 0.71, 0.50, 0.43, 0.33,$ and 0.25 . The composition with $x \approx 0.55$ appears to have a critical Na concentration which separates samples with different magnetic behavior as well as different Na ion diffusion mechanisms. The series of crystals were studied with x-ray diffraction, susceptibility, and transport measurements. The crystal with $x=0.5$ shows a weak ferromagnetic transition below $T=27$ K in addition to the usual transitions at $T=51$ and 88 K. The resistivity of the Curie-Weiss metallic $Na_{0.71}CoO_2$ composition has a very low residual resistivity, which attests to the high homogeneity of the crystals prepared by this improved electrochemical method. These results on the various stable crystal compositions point to the importance of Na ion ordering across the phase diagram.

$S=1/2$ kagomé lattice materials It is believed that a spin-1/2 kagomé lattice (composed of corner sharing triangles) is an ideal system to look for spin liquid physics due to a high degree of spin frustration. Despite intense theoretical interest, experimental studies of the spin-1/2 kagomé lattice have been hampered by the difficulty in synthesizing and characterizing such materials. One of the few known examples of an $S=1/2$ kagome antiferromagnet is the mineral herbertsmithite, the $x = 1$

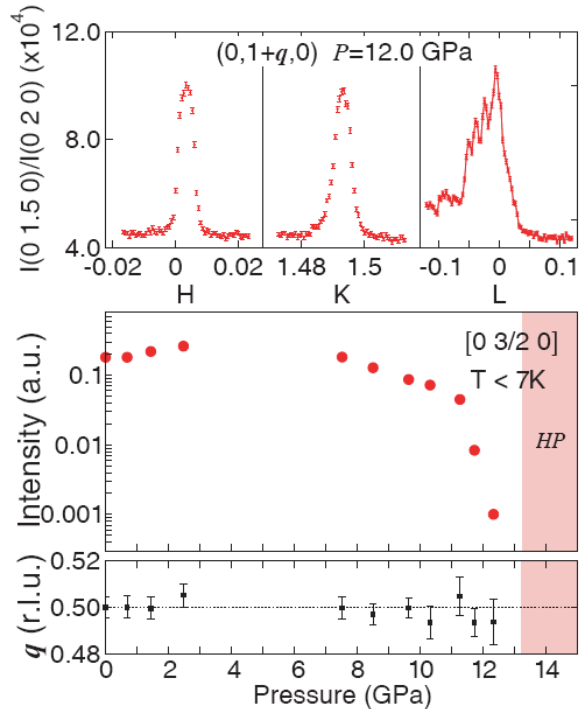


Figure 1. Pressure dependence of a superlattice peak in TiOCl at low temperature measured using synchrotron x-rays with a diamond anvil cell. (top) Representative scans at 12 GPa. (middle) Intensity and (bottom) wave vector of the superlattice peak as a function of pressure. The spin-Peierls dimerization disappears upon entering the pressure-induced metallic state.

end-member of the paratacamite series $\text{Zn}_x\text{Cu}_{4-x}(\text{OH})_6\text{Cl}_2$. It has a perfect 2D kagomé (corner-sharing triangle) lattice of Cu^{2+} ($S=1/2$) ions. However, the chemical similarity between Zn^{2+} and Cu^{2+} combined with the difficulty in differentiating Zn or Cu by x-ray or neutron diffraction techniques has complicated studies of this material, as site mixing of Zn^{2+} and Cu^{2+} in the kagomé planes could also explain some of the observed behaviors. Therefore, we have recently synthesized and characterized a new series of compounds, $\text{Mg}_x\text{Cu}_{4-x}(\text{OH})_6\text{Cl}_2$, which are isostructural with paratacamite. X-ray diffraction studies reveal that, at most, 3% of Cu^{2+} is being replaced by Mg^{2+} . This is significantly less than the 7-10% that has been proposed for $\text{Zn}_x\text{Cu}_{4-x}(\text{OH})_6\text{Cl}_2$ on the basis of neutron diffraction data, and confirms that, at least in $\text{Mg}_x\text{Cu}_{4-x}(\text{OH})_6\text{Cl}_2$, the observed magnetic behavior cannot be due to significant disorder within the kagomé planes.

In addition, we have performed more detailed studies of the $x=1$ end-member $\text{ZnCu}_3(\text{OH})_6\text{Cl}_2$ (herbertsmithite). We find that the magnetic response of this material displays an unusual scaling relation in both the bulk ac susceptibility and the low energy dynamic susceptibility as measured by inelastic neutron scattering. The quantity $\chi''T^\alpha$ with $\alpha = 0.66$ can be expressed as a universal function of H/T or ω/T . In Figure 2, we show $\chi''(\omega)T^{0.66}$ versus ω/T on a log-log scale, where $\chi''(\omega)$ is measured using inelastic neutron scattering. The scaled data collapse fairly well onto a single curve over almost four decades of ω/T . Here we have used the same exponent $\alpha = 0.66$ that was observed in the scaling of the ac susceptibility. The collapse of the $\chi''(\omega)$ data is reminiscent of the behavior observed in certain heavy-fermion metals, including the shape of the functional form of the scaling function. In addition to scenarios based on impurities, the results may indicate that the spin-1/2 kagomé lattice antiferromagnet is near a quantum critical point, or that the ground state of herbertsmithite may behave like a critical spin liquid.

Future Plans

New kagomé materials (single crystals, doping, other spin)

The growth of large single crystals of $\text{Zn}_x\text{Cu}_{4-x}(\text{OH})_6\text{Cl}_2$ will be explored by importing zone furnace techniques under hydrothermal conditions. Our initial results indicate appreciable single crystal sizes (up to ~200 mg) may be obtained. For the neutron scattering studies, deuterated crystals are in the process of being grown. With the deuterated crystals, we will be able to measure the loci of the low-energy inelastic neutron scattering intensity throughout the Brillouin zone. This would enable us to differentiate between competing theories, and should directly address the question of existence of the spin liquid ground state. The development of hydrothermal methods for growing large single crystals will enable new studies of materials beyond the initially targeted herbertsmithite compound $\text{ZnCu}_3(\text{OH})_6\text{Cl}_2$. One straight-forward variant is the $S=1/2$ kagomé compound kapellasite which has the same chemical formula as herbertsmithite but features a very different arrangement of non-magnetic Zn ions. Neutron scattering and thermodynamic

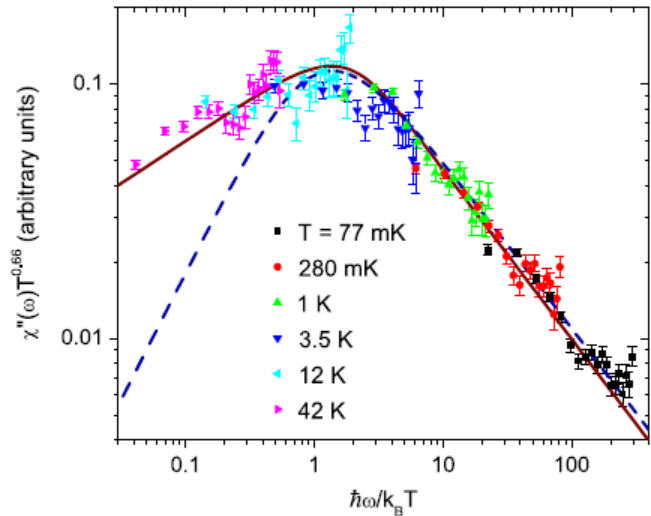


Figure 2. Spin fluctuations in the $S=1/2$ kagome lattice material $\text{ZnCu}_3(\text{OH})_6\text{Cl}_2$. The quantity $\chi''(\omega)T^\alpha$ with $\alpha = 0.66$ plotted against ω/T on a log-log scale, where $\chi''(\omega)$ is measured using inelastic neutron scattering. The data collapse onto a single curve.

measurements on this compound would help determine which of the experimentally observed spin liquid properties are universal. Single crystal growth of clinoatacamite $\text{Cu}_2(\text{OH})_3\text{Cl}$ (with a distorted kagomé-like structure) would be of interest to understand the ordered ground state with neutron scattering (and thereby extract the relevant terms in the spin Hamiltonian) as well as the intriguing transition at intermediate temperature. In addition, we wish to introduce mobile charge carriers into the $S=1/2$ kagomé lattice. Certain theories of the high- T_C superconductors based on the RVB picture predict that the addition of carriers to a spin liquid ground state should lead to superconductivity. Needless to say, this is a very exciting prediction to test. It would also be interesting to synthesize quantum spin systems with small spin-spin couplings, as theories suggest one can drive a zero-temperature quantum phase transition by applying modest magnetic fields. For example, the organic-inorganic hybrid kagomé system $\text{Cu}(1,3\text{-bdc})$, has much smaller magnetic exchange compared to herbertsmithite. Finally, a $S=1$ kagomé lattice system would be of interest to test predictions of a “spin nematic” ground state or an alternate one with topological order.

High pressure measurements We plan to perform scattering experiments on select members of the proposed systems in high pressures. In theories for $S=1/2$ kagomé systems, a singlet ground state with valence bond order is closely competitive with the spin liquid ground state. Valence bond order would cause a static distortion of the crystal structure, so we plan to investigate whether valence bond ordered states are stabilized at any pressure. The soft organic framework of the $\text{Cu}(1,3\text{-bdc})$ kagomé material would be particularly amenable to changes under modest pressures. We also will continue x-ray scattering studies of TiOCl under high pressures to better understand the nature of the insulator to metal transition. Currently, the only high pressure structural data that exist are powder data at room temperature and our single crystal data at $T=6$ K. Future work will explore how the high-pressure charge density wave state evolves with temperature.

Publications resulting from current DOE support

- 7) A. Prodi, J. S. Helton, Yejun Feng, and Y. S. Lee, *Pressure-induced spin-Peierls to incommensurate charge-density-wave transition in the ground state of TiOCl* , Phys. Rev. B 81, 201103(R) (2010).
- 6) S. Chu, T. M. McQueen, R. Chisnell, D. E. Freedman, ‡ P. Muller, Y. S. Lee, and D. G. Nocera, *A Cu^{2+} ($S=1/2$) Kagomé Antiferromagnet: $\text{Mg}_x\text{Cu}_{4-x}(\text{OH})_6\text{Cl}_2$* , J. Am. Chem. Soc. 132, 5570–5571 (2010).
- 5) J.S. Helton, K. Matan, M.P. Shores, E. A. Nytko, B. M. Bartlett, Y. Qiu, D. G. Nocera, and Y. S. Lee, *Dynamic Scaling in the Susceptibility of the Spin- 1/2 Kagome Lattice Antiferromagnet Herbertsmithite*, Phys. Rev. Lett. 104, 147201 (2010).
- 4) K. Matan, J.S. Helton, D. Grohol, D.G. Nocera, S. Wakimoto, K. Kakurai, Y.S. Lee, *Polarized neutron scattering studies of the kagomé lattice antiferromagnet $\text{KFe}_3(\text{OH})_6(\text{SO}_4)_2$* , Physica-B Condensed Matter 404, 2529 (2009).
- 3) D.K. Singh, J.S. Helton, S. Chu, T.H. Han, C.J. Bonnoit, S. Chang, H.J. Kang, J.W. Lynn, and Y.S. Lee, *Spin correlations in the geometrically frustrated pyrochlore $\text{Tb}_2\text{Mo}_2\text{O}_7$* , Phys. Rev. B (Rapid Comm.) 78, 220405(R) (2008).
- 2) E.T. Abel, K. Matan, F.C. Chou, E.D. Isaacs, D.E. Moncton, H. Sinn, A. Alatas, and Y.S. Lee, *X-ray scattering study of the spin-Peierls transition and soft phonon behavior in TiOCl* , Phys. Rev. B 76, 214304 (2007).
- 1) G.J. Shu, A. Prodi, S.Y. Chu, Y.S. Lee, H.S. Sheu, and F.C. Chou, *Searching for stable Na-ordered phases in single crystal samples of Na_xCoO_2* , Phys. Rev. B 76, 184115 (2007).

Session V

Soft Matter

Neutron and X-ray Scattering Studies of Multi-Component Phospholipid Bilayers and Multilayers

Sunil K. Sinha, Yicong Ma, Gang Chen
University of California San Diego

A.N. Parikh
University of California Davis

Zhang Jiang, Mrinmay Mukhopadhyay
Advanced Photon Source, Argonne National Laboratory

David Worcester
University of Missouri-Columbia, MO and CNBT Project,
University of California Irvine, and NCNR, NIST Gaithersburg, MD.

Curt DeCaro and Laurence Lurio
Northern Illinois University, DeKalb, IL

ABSTRACT

Mixed lipid systems are attracting increasing attention because they have the ability to phase separate in ways which may be relevant to a number of important biological processes involving protein interactions with living cells. The prototypical “model” mixed lipid systems are those composed of 1,2-dioleoyl-sn-glycero-3-phosphocholine (DOPC), 1,2-dipalmitoyl-sn-glycero-3-phosphocholine (DPPC), and cholesterol (CH); and also of DOPC and Sphingomyelin (SM) and CH. We have been studying bilayers and multilayers of these systems supported on solid substrates with a combination of neutron diffraction and X-ray reflectivity.

Single bilayers on solid substrates show significant asymmetries between the packing of the proximal and distal leaflets, while the phase separation is hindered compared to bilayers in free giant unilamellar vesicles. Multilayers on the other hand, clearly show the formation of two different d-spacings (corresponding to the bilayer thickness) appearing out of the original set of single (homogeneous phase) diffraction peaks. From the fitting of the Bragg peaks, we find that at the concentration studied, the formation of the larger d-spacing is not a continuous process: the bilayer spacing for the second

phase is discontinuous from that of the homogeneous phase, although there is a temperature dependence of the d-spacing of both phases near the phase transition temperature.

We have also studied the undulation dynamics of the multilayer systems using X-ray Photon Correlation Spectroscopy (XPCS). Together with diffuse scattering measurements, they provide information about the elastic moduli of these membranes.

Structure-Property Relationships of Polymer Brushes in Restricted Geometries and their Utilization as Ultra-low Friction Lubricants

Tonya Kuhl (tlkuhl@ucdavis.edu) and Roland Faller (rfaller@ucdavis.edu)

*Department of Chemical Engineering and Materials Science, University of California at Davis,
One Shields Avenue, Davis, CA 95616*

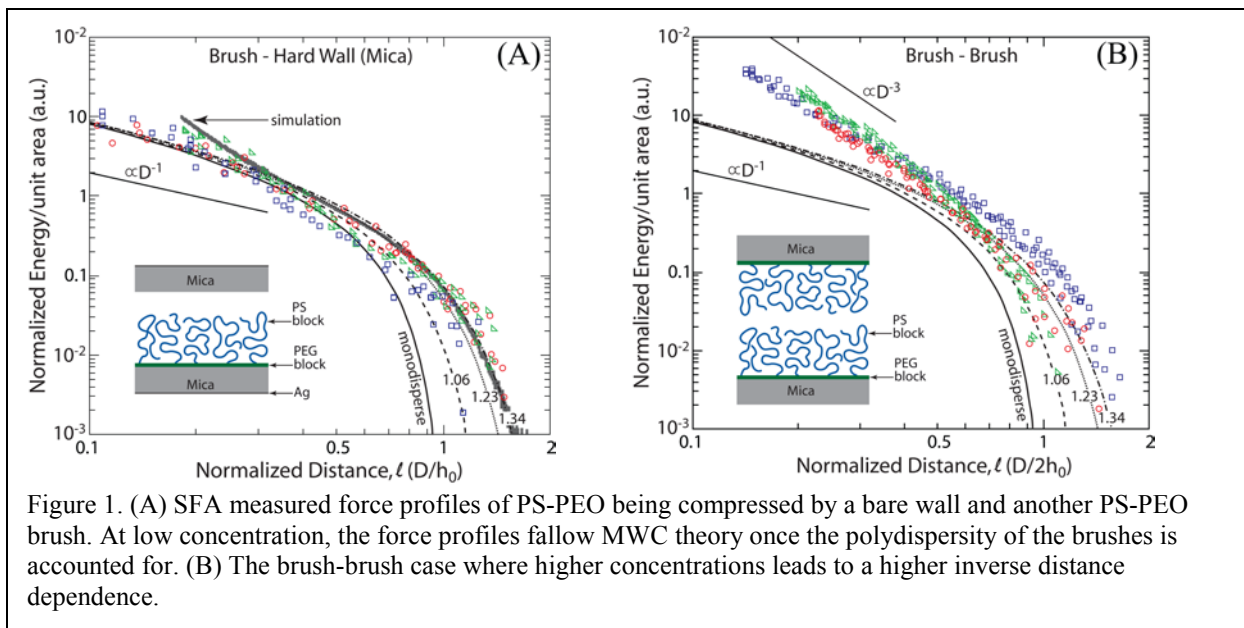
Research Scope

Though polymer films are widely used to modify or tailor the physical, chemical and mechanical properties of interfaces in both solid and liquid systems, the rational design of interface- or surface-active polymer modifiers has been hampered by a lack of information about the behavior and structure-property relationships of this class of molecules. This is especially true for systems in which the role of the polymer is to modify the interaction between two solid surfaces in intimate contact and under load, to cause them to be mechanically coupled (e.g. to promote adhesion and wetting) or to minimize their interaction (e.g. lubrication, colloidal stabilization, etc.). Detailed structural information on these systems has largely been precluded by the many difficulties and challenges associated with direct experimental measurements of polymer structure in these geometries. As a result, many practitioners have been forced to employ indirect measurements or rely wholly on theoretical modeling. This has resulted in an incomplete understanding of the structure-property relationships, which are relied upon for the rational design of improved polymer modifiers.

Over the course of this current research program, we have demonstrated that we can overcome these difficulties using newly developed experimental methods that permit direct measurements of the structure of polymers at the interface between two solid surfaces under confinement (load) and shear and elucidate the fundamental physics behind these phenomena using atomistic and coarse grained simulations of identical systems. As computer based investigations can much more efficiently probe a variety of scenarios and parameter space, by synergistically combining these novel tools, we obtain a higher level of information and predictive capabilities that provide the basis for the rational design of new materials.

Recent Progress

We have expanded our work on polymer brush layers to include polystyrene-polyethylene glycol (PS-PEO) brushes under good solvent conditions as a wide array of MWs and block ratios are available from commercial sources. This allowed a more complete characterization of the impact of polydispersity on measured force profiles and a rigorous testing of theoretical predictions. Surface Force Apparatus (SFA) experiments of force profiles when a PS-PEO brush is compressed by a bare, hard wall or an opposing PS-PEO brush are shown in Figure 1. In the seminal work of Milner, Witten, and Cates (MWC), the equation of state (EOS) used to determine the brush pressure contribution as a function of concentration was $p = \frac{V}{2}\phi^2$, which yields, $E \propto D^{-1}$ dependence. For the past 20 years, MWC theory has been used to compare to, and typically found to match well to, experimentally measured force profiles. However, these comparisons have only been done for relatively low polymer brush grafting densities. A couple of subsequent studies have found a higher inverse distance dependence. No definitive explanation for the deviation was yet been provided in the literature. In addition, our work on



high density PS-P2VP brushes (described below) also clearly show that once the grafting density exceeds a critical concentration, a higher inverse power law for the relationship between force or energy is obtained. We believe this discrepancy is due to the use of an incorrect EOS in the classical MWC theory for higher density brushes. For higher concentrations, we have determined that a modified EOS is more appropriate, $p = \frac{v}{2}\phi^2 + \frac{\omega}{4}\phi^4$. In addition, we have also worked to accurately reflect the impact of chain polydispersity on the resulting measured force profiles and will be accounting for polydispersity in our subsequent simulations over the coming year. The polydispersity of the chains can be sampled well assuming a Flory-Shultz distribution. When polydispersity is properly accounted for, the agreement of brush compression forces at low concentrations to MWC theory is excellent.

Another exciting experimental advancement is our new ability to measure the dynamic shear force and friction coefficients of high density brushes. Preliminary results demonstrate that the friction force is too low to measure until high density brushes are compressed to $\frac{2}{3}$ of their equilibrium extension and the friction force does not become appreciable until the brushes are compressed to less than $\frac{1}{2}$ their equilibrium extension. These studies, in particular, are the first with ultra-high density brushes. In this case, the brushes were ~ 55 times the overlap concentration, $1 \text{ chain}/3.6 \text{ nm}^2$. We are currently working on completing the series of grafting densities to determine if the modified EOS holds at ultra high concentrations and how the frictional force varies as a function of brush grafting density.

On the simulation side we are focusing on two areas. In the first, we are performing and analyzing semi coarse-grained Martini level simulations of single and opposing brushes. Several grafting densities, temperatures and chain lengths are being studied. Figure 2 shows some example results for how the brush height scales with grafting density for short ($N=40$) and longer chains ($N=100$ or 150). In the second area, we are analyzing atomistic simulations performed in the earlier periods and developing a systematically coarse-grained model.

Our atomistic simulations of polystyrene brushes in dry conditions and in toluene showed that single brushes and double layers of opposing brushes are structurally similar. The density

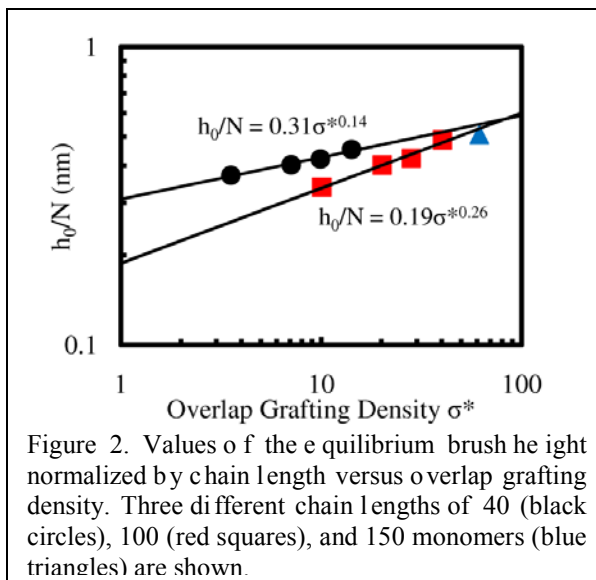
profiles show very pronounced density oscillations up to 1.8 nm regardless of grafting density and solvent conditions. In the absence of a solvent, the chains undergo a transition from an oblate to a spherical shape as the grafting density increases. In good solvent, the chains remain spherical independent of the grafting density. Solvation also increases the extension of the polystyrene chains roughly by a factor 2.5. Toluene forms up to four layers at the base of the grafted chains irrespective of the grafting density.

Simulations of a generic polar polymer brush in a good polar solvent at high grafting densities have been performed using a coarse-grained approach. Chain extension is heavily influenced by temperature, stretching far from the surface at high temperature while adsorbing to a weakly polar surface at low temperature. Increasing grafting density leads to larger chain extension due to excluded volume effects under all conditions, consistent with previous findings. Even at very high grafting densities polymer depletion regions are found near the surface are found in all studies indicating a chain orientation more normal to the surface close to the grafting points. At high grafting densities, a saturation limit is reached with increasing chain length at about half the bulk density. By radial distribution functions we determined that the grafting pattern does not affect the overall brush configuration beyond the direct vicinity of the surface.

Finally, we showed in a joint publication how Molecular simulations and neutron reflectivity are both extremely valuable tools to determine the structure of soft matter at interfaces and under confinement. By combining these two approaches we provide a complete structural and thermodynamic picture of polymer brushes under confinement.

Future Plans

By using a "grafting-from" procedure such as Atom Transfer Radical Polymerization (ATRP), polymer brushes with much higher grafting densities can be obtained compared to conventional "grafted-to" methods such as absorption, spin coating or end-grafting via functional groups. Importantly ATRP formed brushes have been found to have much better lubrication properties compared to brushes formed by "grafted-to" approaches including lower friction coefficients and increased wear resistance. These enhanced properties have been attributed to the extremely high grafting density and strong anchoring of ATRP grown layers. However, the structure of solvated ATRP brushes has not been extensively studied. Most of the current structural information on ATRP films has come from ellipsometry and atomic force microscopy. While these techniques are useful for estimating total thicknesses, they do not provide a detailed structural profile. Our studies will determine the polydispersity of brushes grown via ATRP as well as their compressive loading and frictional properties through physical experiments and simulations. We also continue to measure the density distribution of polymer brushes as a function of confinement in the Neutron Confinement Cell. We have moved to carry out analogous studies as a function of grafting density under good and theta solvent conditions.



On the simulation side we are currently testing different mapping schemes for systematically developing coarse-grained simulations from the existing atomistic data. Initial optimization runs with different selections of superatomic centers are being conducted. This will lead to a systematically coarse-grained model of polystyrene in toluene. We expect this model to be available late 2010. We are studying the influence of the brush geometry on the optimization procedure and therefore will be able to obtain a model which should be useful for both solutions and brushes. With this model we will then perform large scale simulations under various conditions. We will be able for example to systematically study polydispersity.

At the same time we are continuing the studies with the Martini model. Here the focus is shifting to pressure profile measurements both lateral and normal. This will lead to determinations of surface tensions and eventually the force profile between two brushes. We currently develop a scheme which allows us to measure and fix the chemical potential in these simulations as otherwise the comparisons between different brush distances on a force basis is not possible.

Publications (2007-2010)

Ell, J.R., Mulder, D.E., Faller, R., Patten, T.E., Kuhl, T.L. "Structural Determination of High Density, ATRP Grown Polystyrene Brushes by Neutron Reflectivity" *Macromolecules* 42:9523-9527 (2009).

Traskelin, P, Kuhl, T. L., and Faller, R. "Molecular dynamics simulations of polystyrene brushes in toluene solution" *Physical Chemistry Chemical Physics* 11:11324-11332 (2009).

Ian G. Elliott, Dennis E. Mulder, Petra T. Träskelin, John R. Ell, Timothy E. Patten, Tonya L. Kuhl, and Roland Faller, "Confined Polymer Systems: Synergies between Simulations and Neutron Experiments" *Soft Matter* 5(23) 4612-4622 (2009) (DOI 10.1039/b910693f)

Jayeeta Ghosh, Masaomi Hatakeyama, Petra Träskelin, Chenyue Xing and Roland Faller: Molecular Modeling in confined polymer and biomembrane systems Songklanakarin *J Sci Tech* 31(2) 167-173 (2009).

Ell, J. R., Patten, T. E., Mulder, D. J., and Kuhl, T. L. "Modification of Surfaces using Atom Transfer Radical Polymerization" *Polymer Preprints* 2008, 49(2), 197-198.

Cho, J.-H. J., Smith, G. S., Hamilton, W. A., Mulder, D. J., Kuhl, T. L., and Mays, J. "Neuron surface force confinement cell for neutron reflectometry studies of complex fluid under nano-confinement," *Rev. Sci. Instruments* 79:103908 7pgs (2008).

Jayeeta Ghosh and Roland Faller, "Comparing the density of states of binary Lennard Jones glasses in bulk and film" *J Chem Phys* 128(12) 124509 (2008)

Petra T. Träskelin, Florence R. Pon, Qi Sun, and Roland Faller, "Multiscale modeling of polystyrene dynamics in different environments" *Proceedings of ESAT 2008*, Cannes, France, ISBN 2-905267-59-3, pages 593-596.

Laub, C. F. and Kuhl, T.L. "Fitting a free-form scattering length density profile to reflectivity data using temperature-proportional quenching," *J. Chem. Phys.* 125:244702 (8pgs) (2007).

Application of small angle neutron scattering and phase sensitive neutron reflectometry to polymer-based solar cells

Michael E. Mackay

*Materials Science and Engineering Department
University of Delaware, Newark, DE, 19716 USA*

The performance of polymer-based solar cells is dictated by the phase separated morphology of the two components constituting a bulk heterojunction. This is because the exciton lifetime is relatively short and it must reach an interface within a distance of order 5 nm to separate the Coulombically bound particles. Here we use small angle neutron scattering and neutron reflectometry to determine the scatterer size and out of plane concentration profile, respectively, in solar cell mimics and relate this to device performance. Since the system is carbon based for both the polymer (absorber/hole conductor which is a poly(thiophene)) and nanoparticle (electron acceptor which is a C₆₀ fullerene derivative) there is minimal Z-contrast, so, electron and X-ray scattering techniques provide minimal contrast. However, the neutron scattering length density difference between the two components is quite large and is virtually the only useful morphological characterization technique available to distinguish the virgin components. Using the above neutron scattering techniques we find the two components are reasonably well dispersed after initial processing (spin coating), however, the PCBM structure coarsens after annealing simultaneous with improved device performance. Annealing is hypothesized to provide better electron conduction pathways to increase efficiency, however, the coarsening also produces larger gaps between the pathways accounting for a rise in photoluminescence. This demonstrates a delicate balance exists between the two phases and accounts for device performance variations to processing parameter changes.

Neutron Spin Echo studies of Hemoglobin and Myoglobin: Multiscale Internal Dynamics

Jyotsana Lal¹, Peter Fouquet², Marco MacCarini², and Lee Makowski¹

1. Biosciences Division, Argonne National Laboratory, Argonne Illinois 60439
2. Institut Laue-Langevin, Grenoble Cedex 9, France

Neutron spin-echo (NSE) spectroscopy was used to study structural fluctuations that occur in hemoglobin (Hb) and myoglobin (Mb) in solution. Using NSE data to very high momentum transfer, q ($\sim 0.62 \text{ \AA}^{-1}$), the internal dynamics of these proteins were characterized at the level of the dynamical pair correlation function and self-correlation function in the time range of several picoseconds to a few nanoseconds (1). In the same experiment the data transitions from pair correlation to self correlation as the momentum transfer, q , increases. At low q , coherent scattering dominates; at high q , observations are largely due to incoherent scattering. The low q data were interpreted in terms of the effective diffusion coefficient; the high q , in terms of mean square displacements. Comparison of data from the two homologous proteins collected at different temperatures and protein concentrations was used to assess the contributions to the data made by translational and rotational diffusion and internal modes of motion. The temperature dependence of the decay times can be attributed to changes in viscosity and temperature of the solvent as predicted by the Stokes-Einstein relationship. This is true for contributions from both diffusive *and internal* modes of motion indicating an intimate relationship between the internal dynamics of the proteins and the viscosity of the solvent. Our data demonstrate that this motion is highly sensitive to protein concentration, temperature and solvent viscosity, indicating that great care need be exercised in interpreting its effect on protein function.

To demonstrate the capabilities of this approach for functional studies of proteins, we applied it to study the dynamics of Carbonmonoxyhemoglobin (HbCO A) in the presence of an allosteric effector, Inositol Hexaphosphate (IHP) in solution (2). IHP binding resulted in a modest slowing of the average local self motion, but induced a small increase in subunit-subunit correlated motions as anticipated by molecular dynamics simulations.

1. Jyotsana Lal, Peter Fouquet, Marco MacCarini and Lee Makowski “Neutron Spin Echo studies of Hemoglobin and Myoglobin: Multiple Scale Internal Dynamics” *Journal of Molecular Biology*, 397, 423–435, 2010.
2. Jyotsana Lal, Nancy T. Ho, Chien Ho, Peter Fouquet, Marco MacCarini and Lee Makowski “Changes in Dynamics of Carbonmonoxyhemoglobin on Multiple Length Scales on Binding of Effector: Inositol Hexaphosphate in Solution” (to be submitted for publication in *Nature Structural & Molecular Biology*).

Session VI

***Advanced Capabilities
(Sources, Optics,
Instrumentation)***

New Instruments and New Science at SNS and HFIR at Oak Ridge

Stephen Nagler, ORNL

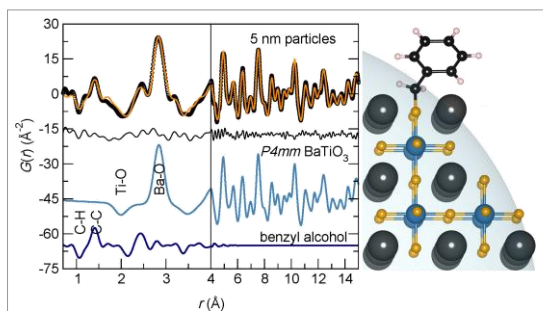
With the transition of the spallation neutron source (SNS) from a multi-year construction project into an operating facility neutron scattering research in the United States has entered a new and exciting era. The SNS is now the world's most intense pulsed neutron source. In this talk I will review the available and planned new neutron scattering instruments at the SNS and highlight some recent examples of science done using the facilities. The advanced new instruments at SNS have wide ranging capabilities. Some of those now in operation or commissioning include two neutron reflectometers, one with polarized neutron capability and a second with horizontal geometry to accommodate liquid surfaces, an extended Q range small angle neutron scattering instrument, a high pressure neutron diffractometer, the VULCAN instrument built for residual stress measurements with a large satellite building to accommodate the study of industrial sized components, and dedicated powder and single crystal diffractometers. Inelastic neutron scattering instruments include the ultra-high resolution backscattering spectrometer BASIS, a cold neutron chopper spectrometer, two thermal chopper spectrometers with complementary characteristics, and a spin-echo spectrometer. If time permits I will also discuss the complementary facilities at HFIR, a high flux continuous neutron source. The new HFIR cold source provides world class flux of cold neutrons, and feeds two excellent small angle scattering instruments now operating in the user program as well as several other instruments that are commissioning or will be operating shortly. The thermal beams include triple axis spectrometers as well as powder and single crystal diffractometers and a dedicated residual stress apparatus. Notably some of the most interesting new science has made use of both continuous and pulsed neutron measurements.

Advanced Capabilities and Enhancements at the Lujan Neutron Scattering Center

Th. Proffen

Lujan Neutron Scattering Center, Los Alamos National Laboratory

The start of the 2010 run cycle at the Lujan Neutron Scattering Center marks the use of the new Mark III spallation target increasing the cold neutron flux significantly. It also marks the complete roll out of the new data acquisition system LDAQ which in addition to greatly improved reliability allows one to use advanced features such as event mode recording enabling new types of science in the near future.



Total scattering study of 5 nm BaTiO₃ nanoparticles: PDF analysis from total scattering data contains information from every pair of atom in the system, making the internal atomic structure of ferroelectric 5 nm BaTiO₃ particles and the structure of the capping ligand (benzyl alcohol) distinguishable. (Page et. al., *Chem. Mat.*, submitted (2010))

The total scattering efforts are centered around the NPDF instrument and an upgrade of the HIPD instrument to complement the total scattering capabilities of the Lujan Center is in the planning stages. Recent efforts of the group focus on the determination of the 'true' structure of nano-particles as demonstrated in a very recent study of BaTiO₃ nanoparticles shown on the left. Later this summer small angle scattering data collected on LQD will be added to the analysis. A recent partnership proposal with sector 11ID-B at the Advanced Photon Source allows NPDF users to collect complementary x-ray total scattering data. Another breakthrough will be the use of the new dilution refrigerator on NPDF with the goal to measure total scattering data below 100mK as part of a user proposal.

Last year the single crystal diffractometer SCD moved from the Intense Pulsed Neutron Source after its closure was successfully installed at the Lujan Center. Other significant instrument improvements include the installation of new Beryllium filters on FDS and the installation of a non-magnetic diffractometer on ASTERIX. The instrument is also well under way towards the spin-echo project (SESAME).

A number of advances have been made in the area of ancillary equipment. A cryo-capability was added to the SMARTS diffractometer allowing one to measure stress/strain in materials at low temperatures e.g. for space applications. HIPPO has added a graphite furnace giving researchers access to neutron powder diffraction at temperatures above 2000°C. On SPEAR the instrument team now uses 'cushioned substrates' to study membranes.

In this presentation an overview of these new and advanced capabilities and the corresponding science opportunities will be given in an effort to form new collaborations and chart a path for future projects.

Neutron Microfocusing Optics and Applications

Gene E. Ice

Rm B256 Bldg 4500S Oak Ridge National Laboratory, Oak Ridge TN 37831-6118

IceGE@ORNL.Gov

Judy W. L. Pang

Rm B262 Bldg 4500S Oak Ridge National Laboratory, Oak Ridge TN 37831-6118

PangJ@ORNL.Gov

Research Scope

The goal of this research is to field high-efficiency achromatic neutron microfocusing optics capable of resolving heterogeneities in materials with 25-50 μm spatial resolution. The program will also demonstrate new applications made possible by combining the unique properties of neutron diffraction with unprecedented neutron spatial resolution and imaging optics based on four-mirror systems. Our approach is based on Kirkpatrick-Baez mirrors widely-used by the X-ray community. The focusing properties of various mirror combinations are studied to understand their theoretical limits using ray-tracing programs. Desirable devices are then fabricated using bent-mirror methods and advanced neutron supermirror surfaces.

At first glance, this project should be trivial. X-ray *nanofocusing* mirrors are now almost routine with bent KB mirror systems below 1000 nm commercially available and with state-of-the-art figured KB mirror systems commercially available with guaranteed 40 nm focusing. However, as described below, neutron microfocusing optics are particularly challenging due to the need to collect the largest-possible divergence onto the sample, and the need for very large mirrors with long working distances. This drives designs toward extremes that are not yet practiced with Kirkpatrick-Baez mirror systems for X-rays. Indeed, the approaches pioneered here are inspiring a new generation of X-ray optics that will push the diffraction limit for achromatic total-external-reflection mirrors beyond the current state-of-the-art.

Recent Progress

We have done extensive ray-tracing of achromatic Kirkpatrick-Baez mirror systems based on neutron supermirrors, and find that under most microfocusing conditions, ideal elliptical mirrors can preserve beam brilliance (phase-space density) within the emittance (product of size and divergence) that can be collected onto the sample. This approach was used for example, to successfully focus neutrons to an $\sim 100 \mu\text{m}$ beam at Chalk river in 2005 with a demonstration of Laue diffraction from small sample volumes.

Based on the success of these experiments, we have recently demonstrated Montel or nested optics (Fig. 1b) for achromatic microfocusing on SNAP^{1,2}. These experiments have focused to $\sim 80 \mu\text{m}$ (Fig. 3,4). Compared to traditional Kirkpatrick-Baez optics, Montel optics, have the advantage of collecting 2-3 x more beam onto the sample for the same spot size and are much more compact. However, Montel optics are complicated by the need to produce a nearly ideal aspherical mirror surface near the edge of one mirror, and by extremely different local mirror curvature at upstream and downstream ends. These two challenges are being overcome with new technical developments as described below.

The performance limits of Montel and KB optics (Fig. 1) were compared in ref 3. This paper was written after first attempts at focusing neutrons with a Montel mirror pair *did not* achieve the desired surface figure and consequently focal spot size.¹ Subsequent measurements although better were still unable to reach the theoretical limits predicted for ideal mirrors.² In reference 3 we re-evaluated the limits to mirror performance to understand by the critical design parameters and the limits to mirror bending schemes. It was recognized that the angle of the

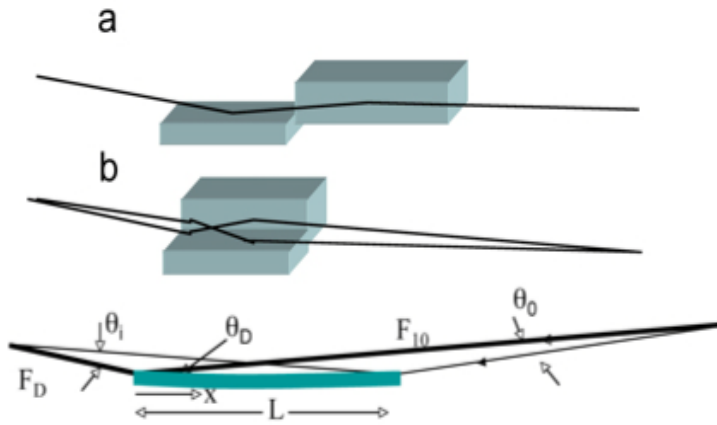


Fig. 1 (a). Standard Kirkpatrick-Baez mirror with sequential elliptical mirrors. (b). Montel mirror pair with parallel reflections of rays. Below- elliptical mirror with various parameters

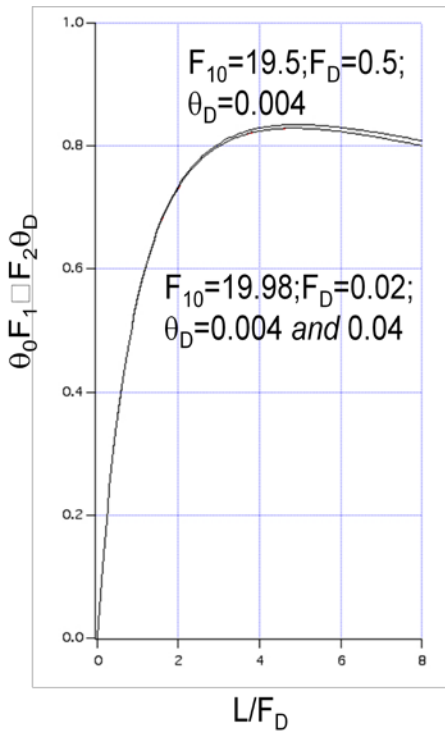


Fig. 2. Figure-of-merit for highest beam intensity as a function of mirror length to clearance ratio $n=L/F_D$. Note that the function is insensitive to the exact mirror parameters.

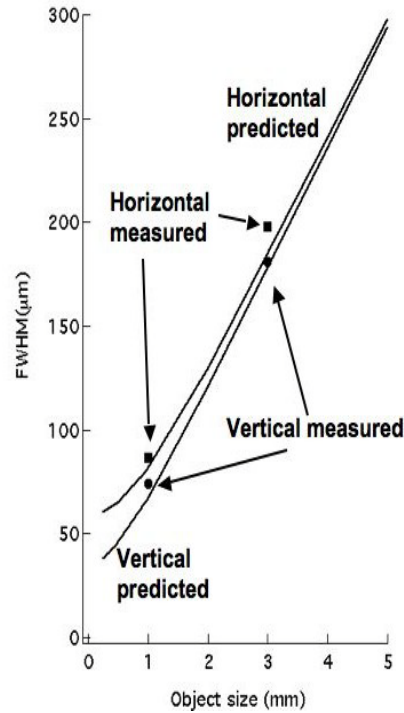


Fig. 3 Nested mirror performance on SNAP for a $n \sim 2.2$ Montel mirror pair.

supermirror (at the downstream edge θ_D) and the ratio, n , of the mirror length, l , to the clearance distance, F_D , largely determine the maximum divergence that can be focused onto the sample (Fig. 2). Based on this understanding, mirror systems with $n \sim 2-3$ are desirable³,

but KB mirror systems with $n > 1$ are impractically large. This understanding justifies the efforts at developing a useful Montel mirror pair and sets our ultimate design goals.

Once the n number of the mirror system is set, the problem becomes how to produce such mirrors. In our first attempts at Montel optics, we concentrated on obtaining mirrors with good surface properties at the mirror edge. We were able to locate some left-over mirrors from a high-energy physics experiment that were polished on 4 sides with very good roughness and figure right up to the mirror edge. These mirrors were slightly thicker than optimum but were otherwise close to ideal in dimensions. Using a special long-trace-profiler optimized for our neutron studies⁴, we optimized the figure of both the vertical and horizontal focusing mirrors. With these mirrors however, we were unable to produce a good figure over the entire mirror surface using a simple unequal bending moment arrangement that had worked well with our first set of sequential KB mirrors.

Modeling of the various bending schemes explained why our initial approach was unsuccessful, and provided new strategies for more precise focusing. In short, the extreme range of local radii from the upstream to the downstream end of a high n elliptical mirror cannot be accurately matched by the linear approximation provided by two unequal bending moments (Fig. 4). A much better approximation is possible with an additional degree of freedom or by optimized mirror shapes (Fig. 4). Using a simple spring to provide an additional degree of freedom we significantly improved the focal spot size. We note that the design principles for these optics are now being adopted by others. For example, IMAGINE a new long-wavelength Laue diffraction beamline on HFIR will use KB optics to focus the beam onto the sample. Ray tracing shows that this approach will produce higher flux density and is far more cost effective than elliptical beam guides.

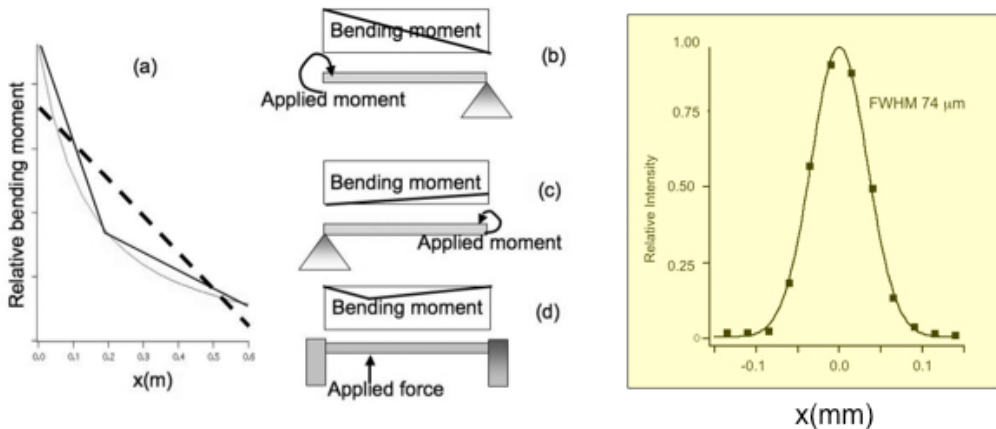


Fig.4. (Left) Schematic showing how the local bending moment changes along an ideal ellipse, and illustrating various approximations to this moment distribution. (Right) Focus on SNAP.

Future Plans

We currently have specially-designed mirrors on order from Swiss neutronics, that should enable near theoretical focusing performance down to 25-50 μm for thermal neutron focusing. The mirrors have a cube-root thickness dependence that will allow for nearly ideal bending to an elliptical shape. In addition, they are surface polished and then cut and edge

polished with the edge having an elliptical profile to nest into the neighbor mirror. We are also designing a more sophisticated bender for standard rectangular mirror blanks that should achieve near ideal performance below 50 μm . This approach has the advantage of slightly-less exotic mirror blanks.

Once the microfocusing mirrors are demonstrated, we will develop a four mirror imaging system based on nested designs and advanced Kirkpatrick-Baez mirrors (AKB). AKB optics are a hybrid of Kirkpatrick-Baez and Wolter type I optics; with AKB optics two elliptical and two hyperbolic mirrors are used to focus the beam. We propose to use nesting to produce a more compact system. As AKB mirror systems are already in use for plasma diagnostics, a nested approach may have implications beyond neutron optics. We also plan to demonstrate special tricks that will enable $\sim 25 \mu\text{m}$ focusing of broad-bandpass long-wavelength neutrons and will demonstrate deflected-beam focusing with an order of magnitude greater flux potential.⁵

Finally, we are also beginning an experimental program based on the ability to resolve small volumes in larger samples. With the imaging optics we are developing, the focal-spot size can be easily configured by adjusting the object size. This allows for various beam sizes and height to width ratios that can be optimized for high-pressure experiments, depth-profiling experiments or 3D spatially resolved experiments.

Publications and Patents (FY07-FY10)

1. Ice G.E., J.-Y Choi, P.Z. Takacs, A Khounsary, Y. Puzyrev, J.J. Molaison, C. A. Tulk, K. H. Andersen and T. Bigault, "Nested Neutron Microfocusing Optics on SNAP", *Applied Physics A*: 99 635 (2010).
2. Ice, G. E., J. W. L. Pang, C. Tulk, J. Molaison, J.-Y. Choi, C. Vaughn, L. Lytle, P. Z. Takacs, K. H. Anderson, T. Bigault, and A. Khounsary, "Design Challenges and Performance of Nested Neutron Mirrors for Microfocusing on SNAP", *J. Appl. Crystallogr.* **42** 1004-1008(2009).
3. Ice, G. E., Rozaliya I. Arabash, and Ali Khounsary, "Nested mirrors for X-rays and Neutrons", in *Proceedings of the SPIE Conference*, San Diego, California (2009).
4. Y. S. Puzyrev, G.E. Ice and P.Z. Takacs, "Long-trace profiler for neutron focusing mirrors", *Nucl. Inst. and Meth. A*: **598** 515-517 (2009).
5. Ice, G. E., U.S. Patent 7,439,492, "Nondispersive neutron focusing method beyond the critical angle of mirrors", October 21, 2008.
6. G.E. Ice, "The Future of Spatially-Resolved Polychromatic Neutron and X-ray Microdiffraction", *Metall. Mater. Trans. A*. **39A** 3058-3064 (2008).

Polarized ^3He in Neutron Scattering

W.M. Snow, IUCF, 2401 Milo B. Sampson Lane, Bloomington, IN 47408; wsnow@indiana.edu

T.R. Gentile, Stop 8461, NIST, Gaithersburg, MD 20899; thomas.gentile@nist.gov

Program scope

The goal of this program is to extend the technique of polarized neutron scattering into new domains by the development and application of polarized ^3He spin filters. We have developed neutron spin filters based on the large spin dependence of the cross section for neutron capture by ^3He , and applied these devices to a small angle neutron scattering spectrometer (SANS), polarized neutron reflectometers, a thermal energy single crystal diffractometer (SCD), and a thermal energy triple-axis instrument. Two optical pumping methods have been employed to construct these spin filters: spin-exchange (SEOP) and metastability exchange (MEOP). We have made progress in both these methods, but our current focus is on SEOP. In this method, alkali vapor is polarized by optical pumping and the polarization is transferred to the ^3He nuclei during collisions.

This program is carried out by a collaboration that includes Indiana University, the National Institute of Standards and Technology (NIST), Hamilton College, and the Univ. of Wisconsin, along with collaborators at the SNS and LENS. In addition, we welcome the opportunity to interact with other laboratories. Our primary current goals include the application of polarized ^3He -based neutron spin filters to a spin echo small angle neutron scattering spectrometer (SESAME) and wide-angle polarization analysis.

Built upon our past research and development, the NCNR has established a spin filter program that now provides spin filters for SANS, reflectometry, and triple-axis spectrometry (TAS). For TAS, published results include studies of the magnetoelectric effect compound LiCoPO_4 , magnetic order in NdFeAsO , BiFeO_3 in an electric field, and electric field controlled magnetism in the multiferroic system $\text{Ni}_3\text{V}_2\text{O}_8$. SANS experiments on magnetic nanoparticles have revealed new features in their core-shell magnetic morphology. Although diffuse reflectometry is quite challenging, experiments have been conducted on spin-valve ellipse arrays and $\text{Ni}_{80}\text{Fe}_{20}$ stripes on a silicon substrate. At the SNS a polarized ^3He analyzer has been employed on the magnetism reflectometer, and several SNS instruments (HYSPEC, TOPAZ, EQ-SANS, and CNCS) and HFIR instruments (the SCD, TAS, and GP-SANS) envision the use of ^3He polarizers and analyzers. The SNS has set up a polarization group which is charged with developing ^3He spin filters for the SNS. The establishment of these ^3He groups at the NCNR and SNS has realized one of the long-term goals of our research and development program. Connections between all of these ^3He spin filter programs is strong, with the interaction contributing to the development of technology and applications at all laboratories.

Recent progress

At the Indiana LENS facility, we have constructed and tested an in-situ SEOP ^3He polarization analyzer for SESAME. Hamilton has developed systems for inverting the ^3He polarization in on-line spin filters using nuclear magnetic resonance (NMR) and measuring the ^3He polarization using electron paramagnetic resonance (EPR), both of which are being

employed at the SNS and NIST. Wisconsin has recently completed a detailed study of the circular dichroism of the alkali vapor, which sheds light on the question as to why SEOP cells require much more laser power than is expected. These studies also provide a quantitative understanding of the practical importance that we have previously reported for spectrally narrowed laser light. A paper with the key results has been submitted to Phys. Rev. Lett. and detailed papers are in progress.

At NIST, we have made substantial progress towards wide-angle polarization analysis, employed a polarized ^3He target and ^3He based polarimetry for a neutron interferometry experiment, contributed to activities at the NCNR and the SNS, and made progress in aspects of continuous optical pumping. The first goal for wide-angle analysis is to develop a general apparatus for demonstration on different instruments, with the constraints and needs of the Multi-Axis Crystal Spectrometer (MACS) as a guide. This scheme requires a large static field solenoid with good off-axis magnetic field homogeneity, a polarizer cell, two analyzer cells that can cover a total angular range of 240 degrees, a shielded radio frequency solenoid so that the polarization in the polarizer cell can be inverted without perturbing the analyzer cell, and an NMR method for monitoring the polarization in each cell. We have demonstrated this complete system on the MACS instrument. A key issue for this development are the analyzer cells, which to date we have not been able to fabricate from our preferred aluminosilicate glass. We have encountered difficulties in obtaining long polarization lifetimes in quartz cells. Although we have now surmounted this problem, we have discovered an unexpected temperature dependence in the relaxation in these cells that limits the achievable polarization. On the short term we are aiming to do our first experiments on MACS with an aluminosilicate cell with reduced angular coverage. On the longer term we are investigating whether we can address the relaxation time issue in quartz or switch to refillable cells to avoid the high temperature issue.

We have collaborated with others at the NCNR in a measurement of the spin dependence of the neutron scattering length for ^3He via neutron interferometry. Small, flat windowed cells were polarized off-line and stored in the highly confined space between the silicon interferometer blades. In addition, we employed a spin filter analyzer cell for highly accurate measurement of the neutron polarization of the NG7 beam.

We have collaborated with the ILL on studies of the effect of high neutron flux on in-situ spin-exchange optical pumping. We had first observed this phenomenon during the course of the NPDGamma experiment on the FP12 fundamental physics beam line at LANSCE. At the PF1b beam line at the ILL the magnitude of the neutron beam induced alkali spin relaxation and its dependence on neutron flux were established. In the second experiment the effect on nitrogen (required in SEOP cells) were studied. For most neutron scattering applications beam-induced relaxation should not be a major issue, but does need to be considered for in-situ SEOP in high flux beams. We have recently tested double cells as a practical solution. In this scheme, which has been extensively used in electron scattering research, polarized gas is exchanged by diffusion between an optically pumping cell and a spin filter cell.

We continue to investigate and test new laser technologies. Our workhorses have been high power diode array lasers that we spectrally narrow using an external cavity, but we have also employed a commercial system consisting of a diode array narrowed with a volume Bragg grating (VBG) and coupled to an optical fiber in a sealed package. Such an arrangement eliminates the need for external spectral narrowing optics and provides greater flexibility in the location of the laser relative to the spin filter. If successful, this system would be particularly useful for continuous optical pumping on neutron beam line. We have also employed "chirped"

VBGs, which yield better performance than our externally narrowed systems with simpler operation and a smaller footprint.

Future plans

We plan to implement our polarized ^3He spin filter as a polarization analyzer for a spin echo small angle neutron scattering spectrometer (SESAME). This development is pursued in collaboration with Roger Pynn, a professor of physics at Indiana University, who has led the development of this new spin echo technique over the last several years. We propose to focus on implementation of ^3He analyzers on SESAME because we feel that this type of spin echo spectroscopy has great potential for scientific impact.

Goals include more extensive development and practice of wide-angle polarization analysis, development of continuous optical pumping, and study of the fundamental issues in the limits of spin-exchange optical pumping. For wide-angle analysis we expect to conduct our first neutron scattering experiment in collaboration with our MACS collaborators soon. We plan to gain as much experience on this instrument before the long NCNR shutdown in 2011. In addition, we will collaborate with the SNS on developing wide-angle analysis for a greater range of instruments. Solving or bypassing the temperature-dependent relaxation observed in quartz cells is of great importance for all future applications of SEOP where direct optical pumping of wide-angle cells is desired. Because we believe that this effect may be due to the known high permeability of quartz, we are renewing our efforts to determine if these cells can be made from aluminosilicate glass and/or whether sodium or sol-gel could be used to coat quartz cells.

Another important activity in this proposal is our continued research on both the atomic physics and surface effects involved in spin exchange optical pumping (SEOP). It is important to note that our current limit of 75% ^3He polarization could be surpassed if we could understand the phenomenon of alkali density dependent relaxation that our collaboration first identified. In addition, we will continue our studies of the excess photon absorption that contributes to the high laser power demand for SEOP. The recent observation of a slow neutron-induced reduction of alkali polarization for cells optically-pumped in-situ and operated as polarizers in very intense neutron beams also emphasizes the importance of a better understanding of the atomic physics processes in these cells. Wisconsin plans studies of excited-state nuclear spin nonconservation, which is relevant to both excess photon absorption and neutron beam induced relaxation.

Hamilton has developed experience with in-situ pumping for small neutron beams. The simplest case of an axial solenoid pumped from the end is already running at the Magnetism Reflectometer at SNS. However, for an axial polarizer the neutron spins must be adiabatically rotated along tens of centimeters of beamline to make the neutron polarization transverse to the beam at the sample. Many of the applicable beamlines have space constraints which make the required rotation difficult to implement. The next generation of polarizers will have magnetic fields transverse to the neutron beam eliminating the need for adiabatic rotation. We intend to develop transverse field polarizers using well-shielded solenoids.

2007 - 2010 Publications

1. W.C. Chen *et al*, *Physica* **397**, 168-171 (2007). "³He neutron spin filters for a thermal neutron triple-axis spectrometer"
2. W.C. Chen, T.R. Gentile, T.G. Walker, and E. Babcock, *Phys. Rev. A* **75**, 013416 (2007). "Spin-exchange optical pumping of ³He with Rb-K mixtures and pure K"
3. T.E. Chupp *et al*, *Nucl. Instrum. Meth. A* **574**, 500-509 (2007). "A large area polarized ³He neutron spin filter"
4. M.R. Fitzsimmons *et al*, *Phys. Rev. B* **76**, 245301 (2007). "Suppression of nuclear polarization near the surface of optically pumped GaAs"
5. P.-N. Seo *et al*, *Phys. Rev. ST Accel. Beam* **11**, 084701 (2008). "High-Efficiency resonant RF spin rotator with broad phase space acceptance for pulsed polarized cold neutron beams"
6. M. Sharma *et al*, *Phys. Rev. Lett.* **101**, 083002 (2008). "Neutron beam effects on spin-exchange-polarized ³He"
7. M.G. Huber *et al*, *Phys. Rev. Lett.* **102**, 200401 (2009). "Precision measurement of the n-³He incoherent scattering length using neutron interferometry"
8. J.W. McIver, R. Erwin, W.C. Chen and T.R. Gentile, *Rev. Sci. Instrum.* **80**, 063905 (2009). "End-compensated magnetostatic cavity for polarized ³He neutron spin filters"
9. I. Cabrera *et al*, *Phys. Rev. Lett.* **103**, 087201 (2009). "Coupled magnetic and ferroelectric domains in multiferroic Ni₃V₂O₈"
10. S. Boag *et al*, *Physica B* **404**, 2659-2662 (2009). "In-situ SEOP polarised ³He neutron spin filter for incident beam polarisation and polarisation analysis on neutron scattering instruments"
11. E. Babcock *et al*, *Physica B* **404**, 2655-2658 (2009). "In-situ SEOP polarizer and initial tests on a high flux neutron beam"
12. W.C. Chen *et al*, *Physica B* **404**, 2663-2666 (2009). "Applications of ³He neutron spin filters at the NCNR"
13. K.L. Krycka *et al*, *Physica B* **404**, 2561-2564 (2009). "Resolving 3D magnetism in nanoparticles using polarization analyzed SANS"
14. E. Babcock *et al*, *Phys. Rev. A* **80**, 033414 (2009). "Effects of high flux neutron beams on ³He cells polarized in-situ with spin-exchange optical pumping"
15. M. Gericke *et al*, *Nucl. Instrum. Meth. A* **611**, 239-243 (2009). "Parity violation in neutron-proton capture: the NPDGamma experiment"
16. M.G. Huber *et al*, *Phys. Rev. Lett.* **103**, 179903 (2009). "Erratum: Precision measurement of the n-³He incoherent scattering length using neutron interferometry [*Phys. Rev. Lett.* **102**, 200401 (2009)]"
17. M.G. Huber *et al*, *Nucl. Instrum. Meth. A* **611**, 235-238 (2009). "Precision measurement of the neutron-³He spin-dependent scattering length using neutron interferometry"
18. K.L. Krycka *et al*, *J. Appl. Phys.* **107**, 09B525 (2010). "Internal magnetic structure of magnetite nanoparticles at low temperature"
19. W.-T. Lee *et al*, accepted by *Journal of Physics: Conference Series (ICNS2009)*. "In-situ polarized ³He-based neutron polarization analyzer for SNS magnetism reflectometer"
20. K.L. Krycka *et al*, *Phys. Rev. Lett.* **104**, 207203 (2010). "Core-shell magnetic morphology of structurally uniform magnetite nanoparticles"
21. William Happer, Yuan-Yu Jau, and Thad G. Walker, *Optically Pumped Atoms*, Wiley 2010.

Inelastic X-ray Scattering at Third Generation Synchrotron Sources: Present Activities and Future Plans

J.P. Hill,

Condensed Matter Physics and Materials Science,

Brookhaven National Laboratory

In this talk, I will briefly discuss present activities utilizing inelastic x-ray scattering to study excitations in hard condensed matter systems. In particular, I will show that at current third generation sources it is now possible to observe all the major elementary excitations in solids, including phonons, magnons, orbital excitations and electronic excitations such as plasmons and charge transfer excitations. I will illustrate this with a few recent examples. The first of these will discuss work studying phonons in $\text{SmFeAs}(\text{O},\text{F})$ which show an anomalous renormalization of certain phonons and for which momentum-dependent measurements of the electron-phonon coupling have been made. The second example will focus on work being performed at the Swiss Light Source in which spin waves in $(\text{La},\text{Sr})\text{CuO}_4$ have been observed. Finally, I will discuss the current state of instrumentation in this country, at the Advanced Photon Source, and plans for new inelastic beamlines at the NSLS-II source currently under construction at Brookhaven National Laboratory.

Poster Sessions

Neutron Scattering Contractors Meeting
U. S. Department of Energy
Office of Basic Energy Sciences

POSTER SESSION I

- 1) Structure/Property Relationships in Complex Oxides
O. Chmaissem, Northern Illinois University
- 2) Single crystal growth and superconductivity of Fe-Te-Se materials
G. D. Gu, Jinsheng Wen, Zhijun Xu, M. Enoki Z. W. Lin, Qiang Li, and J. M. Tranquada, Brookhaven National Laboratory
- 3) Evolution of magnetic order and spin fluctuations in $\text{Fe}(1+y)\text{Te}(1-x)\text{Se}(x)$
Zhijun Xu, Jinshen Wen, Qing Jie, Zhiwei Lin, Qiang Li, Songxue Chi, Deepak Singh, Matt Stone, Genda Gu, Guangyong Xu, Igor Zaliznyak, and John Tranquada, Brookhaven National Laboratory
- 4) THz investigations of Exotic Superconductors
Peter Armitage, Johns Hopkins University
- 5) From Mechanism to Phenomenology in Iron-Based Superconductors
Zlatko Tesanovic, Johns Hopkins University
- 6) Structure factor of low-energy spin excitations in a $S=1/2$ kagome antiferromagnet
Oleg Tchernyshyov, Johns Hopkins University
- 7) Frustrated Magnets and their varied response to impurities
Robert Cava, Princeton University
- 8) Exploring the relationship between magnetism and superconductivity through new materials and neutron scattering
Eric Bauer, Los Alamos National Laboratory
- 9) Neutron diffraction and doping studies of the Q-phase in CeCoIn_5
Roman Movshovich, Los Alamos National Laboratory
- 10) Ni-based pnictide superconductors: pairing mechanisms and trends relative to Fe-based superconductors
Filip Ronning, Los Alamos National Laboratory

- 11) Photoelectron Spectroscopy of Transuranics
John Joyce, Los Alamos National Laboratory
- 12) Structure, magnetism, and superconductivity in CaFe_2As_2
Alan Goldman, Ames Lab
- 13) Structure, magnetism, and superconductivity in electron-doped BaFe_2As_2
Andreas Kreyssig, Ames Lab
- 14) Local structure and superconductivity in Fe pnictides
Keeseong Park and Despina Louca, University of Virginia
- 15) Magneto-elastic effects in hole and electron doped oxides
Juan Yu and Despina Louca, University of Virginia
- 16) Quantum Critical Behavior in $\text{Ce}(\text{Ni}_{0.935}\text{Pd}_{0.065})_2\text{Ge}_2$
Jon Lawrence, University of California, Irvine
- 17) Neutron Scattering Study of Geometrically Frustrated Spinels and Unconventional Superconductors
Seung-hun Lee, U Virginia
- 18) Uncovering a Hidden Bragg-Glass Phase in Edge-Contaminated Vortex Matter using Slicing Neutron Diffraction
Sean Ling, Brown U
- 19) Designer phase transitions in lithium-based spinels
Wouter Montfrooij, University of Missouri, Columbia

POSTER SESSION II

- 20) Polarized ^3He in Neutron Scattering
Thomas Gentile, NIST
- 21) Towards New Extremes in Neutron Diffraction
Malcolm Guthrie, Carnegie Inst of Washington
- 22) Optics for Advanced Neutron Imaging and Scattering
Boris Khaykovich, MIT
- 23) Development of New Methods for Studying Nanostructures using Neutron Scattering
Roger Pynn, Indiana University
- 24) Neutron Imaging at ORNL: Ongoing Efforts and Future Prospect
Hassina Bilheux, Oak Ridge National Laboratory
- 25) Neutron and X-ray Scattering Group: Instrumentation and Outreach
Ray Osborn, Argonne National Laboratory
- 26) High Efficiency Neutron Scattering Capabilities on MACS
Collin Broholm, Johns Hopkins University
- 27) Atomic and Mesoscopic Study of Metallic Glasses
Takeshi Egami, University of Tennessee, Knoxville
- 28) Vibrational Thermodynamics of Materials
Brent Fultz, Caltech
- 29) Self assembly of conjugated polymer networks
Danilo Pozzo, Washington State University
- 30) Novel Molecular Materials for Hydrogen Storage Applications
Maddury Somayazulu, Carnegie Institute of Washington
- 31) Neutron Compton Scattering as a Probe of Hydrogen Bonded (and other) Systems
George Reiter, University of Houston
- 32) Behavior of Lipid Mixtures: From Lipid Rafts to Protein Crystallization
Ursula Perez-Salas, Argonne National Laboratory

- 33) Unusual phase behavior of nano-confined water: new insights
Yang Zhang and Sow-Hsin Chen, MIT
- 34) Neutron and X-Ray Studies of Spin and Charge Manipulation in Magnetic Nanostructures
Sunil Sinha and Eric Fullerton, University of California, San Diego
- 35) Control of Structure-Property Relationships in Complex Oxides by Designed Strain
Michael Fitzsimmons, Los Alamos National Laboratory
- 36) CNMS interactions and opportunities for neutron scattering sciences
Michael Simonson, Center for Nanophase Materials Sciences, Oak Ridge National Lab
- 37) Characterizing High Density Polymer Monolayers Formed Using Non-traditional In Situ Chemistries
Dale Huber, CINT, Sandia National Laboratory
- 38) New Crystal Growth Capabilities at Hopkins,
Seyed M. Koohpayeh, Johns Hopkins University

Poster Abstracts

Structure/Property Relationships in Complex Oxides

O. Chmaissem (chmaissem@anl.gov), B. Dabrowski (dabrowski@anl.gov)
Materials Science Division, Argonne National Laboratory, Argonne, IL 60439
Physics Department, Northern Illinois University, DeKalb, IL 60115

R. Osborn (rosborn@anl.gov)
Materials Science Division, Argonne National Laboratory, Argonne, IL 60439

Research Scope

Despite considerable progress made during the last decade, the successful application of colossal magnetoresistance manganites (CMR) faces serious challenges largely because of the high magnetic fields needed to suppress the metal to insulator transition that takes place when the material becomes phase separated or charge ordered. Key questions have been investigated and tremendous experimental and theoretical advances have been made toward expressing the CMR behavior in terms of internal parameters that include spin interactions, electron-phonon and superexchange antiferromagnetic couplings, charge distributions, and structural order and disorder. The physics of three-dimensional perovskite-based (ABO_3) manganites is relatively well understood; however, much less is known when the materials are designed to exhibit A- or B-site layer ordering. To this end, we recently initiated a detailed study of the effects of A-site layering in $La_{1-x}Ba_{1+x}Mn_2O_6$ ($x \sim 0$) and the consequent reduced dimensionality on the magnetic and transport properties of the ordered materials. Our work revealed the presence of multiple magnetic ground states and a strong phase separation that result in fragile charge and orbital ordering that can be melted by the application of relatively low magnetic fields.

On the other hand, the timely development of practical thermoelectric devices for the direct conversion of surplus heat into electricity requires stable, inexpensive and environmentally friendly materials with large figure of merit $ZT = \sigma\alpha^2 T / \kappa > 2$, where α is thermopower, σ is electrical conductivity, κ is thermal conductivity and T is temperature. Based on the linear response theory, it has been proposed that high temperature thermopower can be achieved in strongly correlated transition metal (TM) oxides following the extended Heikes formulation $\alpha = -(k_B/e) \{ \ln[g_3/g_4] + \ln[x/(x-1)] \}$, where x is the concentration of TM^{4+} ions, and g_3 and g_4 are additional spin and orbital degeneracy terms corresponding to TM^{3+} and TM^{4+} , respectively. New compounds with the concomitant in-depth measurements of their structural, electronic and heat transport, and thermopower properties will provide a basis for understanding the competing roles of interactions. In a first step, enhanced thermopower properties are searched for in promising mixed-valent perovskite candidates based on $TM = Mn^{4+/3+}$, $Co^{3+/4+}$ and $Ti^{4+/3+}$.

Recent Progress

Competing Magnetic Ground States in A-Site Layer Ordered Manganites: We have investigated the formation of an unusually large and complex charge ordered superstructure arising from the ordering of the A-site cations in layered $La_{1-x}Ba_{1+x}Mn_2O_6$ materials with reduced quenched disorder. In these materials, two-dimensional Mn-O sheets are asymmetrically sandwiched between adjacent and alternating A^{3+} and Ba^{2+} layers, thus, giving rise to magnetic and transport properties that are significantly different from those of their three-dimensional A-site disordered $A_{0.5}Ba_{0.5}MnO_3$ counterparts. Neutron and x-ray diffraction experiments enabled the construction of temperature-composition and temperature-magnetic field phase diagrams demonstrating that structural disorder (deliberate disorder introduced on the otherwise perfectly ordered layers) can be tuned to bring the system closer to a multicritical point where at least three magnetic phases meet,

Fig. 1. For the right composition and temperature, we observe a strong competition between the magnetically different states that start to separate as a function of decreasing temperature and eventually these states freeze in their respective domains; thus giving rise to spin glass clusters. For $\text{LaBaMn}_2\text{O}_6$, phase separation and structural phase transitions (responsible for the CMR properties) can be suppressed under the application of low magnetic fields of no more than 1-2 Tesla (Fig. 2) which is a huge improvement of at least an order of magnitude compared with the large fields of 10-60 Tesla required to suppress charge ordering, structural transitions, and phase separation in the disordered counterparts. In $\text{La}_{0.96}\text{Ba}_{1.04}\text{Mn}_2\text{O}_6$, charge ordering partially yields in favor of an A-type orbital ordered state that can also be suppressed by relatively low critical magnetic fields. In contradiction with theory, our work suggests that quenched disorder is not the primary reason for phase separation and magnetoresistance but rather it can be used as a tuning tool in the vicinity of the multicritical point. Additionally, our work show that hole-doping introduced by the small and deliberate disorder leads to electronic phase separation.

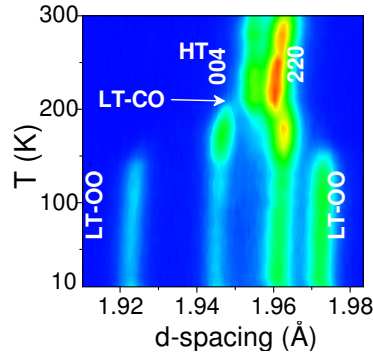


Fig. 1. $\text{La}_{0.96}\text{Ba}_{1.04}\text{Mn}_2\text{O}_6$: Synchrotron data showing the coexistence of three magnetic ground states at a multicritical point below ~ 200 K. The phases are: high temperature ferromagnetic (HT-FM), low temperature charge ordered (LT-CO) and low temperature orbital ordered (LT-OO).

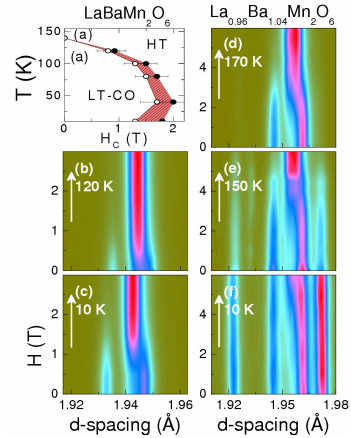


Fig. 2. Synchrotron x-ray data showing the melting of the LT-CO and LT-OO phases under the application of low magnetic fields. Temperature-magnetic field phase diagram for $\text{LaBaMn}_2\text{O}_6$ is shown in (a).

Thermopower Properties of Metastable Perovskite Manganites: Recent reports of attractive thermoelectric properties in rare earth substituted $\text{CaMn}^{4+}\text{O}_3$ perovskites prompted us to investigate the properties of similar lightly electron doped $\text{SrMn}^{4+}\text{O}_3$ materials. Both the Mn or Sr site substituted compounds behave in a similar manner; *i.e.*, resistivity and thermopower decrease rapidly due to the introduction of itinerant charges for equivalent substitution level. Notably, all substitutions significantly reduce thermal conductivity to 1–3 W/K.m. The largest value of $ZT=0.015$ at 400 K was found for 5-10% Mo substituted materials. Measurements at 400 and 1000 K showed that the theoretical Heikes formulation describes relatively well the observed charge doping dependence of thermopower. However, instead of the predicted increase ($x \sim 1$, $g_3/g_4=10/4$, $-(k_B/e)\{\ln[g_3/g_4]\}=-79 \mu\text{V/K}$) these manganites exhibit a reduced absolute magnitude of thermopower. Because of that and complicated synthesis conditions we conclude that these materials are not ideal for future investigations.

Thermopower Properties of Cobaltates: Rare Earths $\text{RCo}^{3+}\text{O}_3$ perovskites are, on the other hand, known to exhibit low spin ground states of $g_3=1$. Transition temperatures to intermediate and high spin states - possessing a higher degree of degeneracy - increase with a decrease in the ionic size of R and reach 800 K for Y. Sr and Ca hole-doped cobaltites are proposed as some of the most attractive compounds for enhanced thermopower because all the Co^{4+} spin states have high degeneracy ($x \sim 0$, $g_3/g_4 < 1$). Our synthesis study has found a very limited solubility range of Sr and Ca for small size R ions. We have observed the largest value of $ZT=0.04$ at 400 K for 10-15% Ca substituted $\text{NdCo}^{3+}\text{O}_3$ compounds. The dependence of thermopower on charge doping and temperature (a maximum at 200-300 K) does not follow the extended Heikes formulation and appears to indicate that Co^{3+} and Co^{4+} exist in several spin states. Several options are presently pursued to further enhance the thermopower properties of cobaltites by stabilizing the low spin Co^{3+}

state at room temperature through substitutions on the Co-site and by tuning the doping at lower levels for smaller rare earth sizes.

Thermopower Properties of Titanates: Electron doped $\text{SrTi}^{4+}\text{O}_3$ perovskites are expected to provide a clear-cut enhancement of thermopower by $-154 \mu\text{V/K}$ since both degeneracy terms are well defined as $g_3 = 6$ and $g_4 = 1$. To date among all investigated compositions, we have observed the largest $ZT \sim 0.3$ values for 3-8% Nb substituted materials at 800 K. The thermopower increases with temperature and achieves fully saturated values at ~ 700 K, Fig. 3. The dependence of thermopower on electron doping for these compounds is very well satisfied; however, no additional enhancement due to spin and orbital degeneracy terms has been observed. The origin of this behavior requires further study.

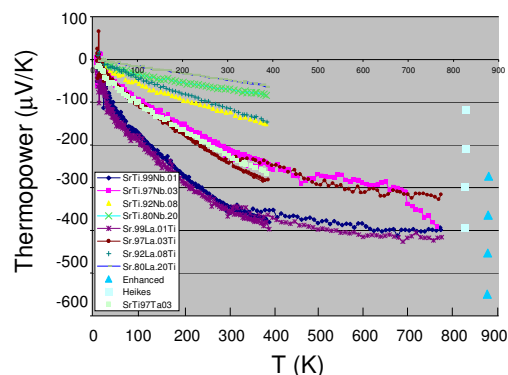


Fig. 3 Thermopower properties of B-site substituted SrTiO_3 . Largest ZT and thermopower values achieved with Nb substitutions.

Future Plans

Structure-Property Relationships in Cobaltates: In many ways, strongly correlated electron cobaltates exhibit properties that are reminiscent of the manganites. However, much more complex properties are being identified owing to the fact that the oxidation state of the cobalt ions often behave in unpredictable ways depending on the exact chemical composition of the investigated material and the complexity of the Co local environment. Hence, Co^{3+} and Co^{4+} ions with high, intermediate and low spin states are often produced offering an additional degree of freedom to be accounted for when designing new materials with tunable magnetic properties.

The recently discovered $R\text{BaCo}_2\text{O}_{5+d}$ family (R = rare earth) stands out as one of the most fascinating cobaltate systems because of its layered structure and the many possibilities it offers for diverse chemical substitutions at the R , Ba and/or Co sites. In turn, the substituting elements may have various oxidation states and therefore could act as a controlling parameter for injecting or removing charges from the system without having to severely modify the structure of the material and the local oxygen environment around the Co ions. On the other hand, the materials' magnetic properties can also be carefully tuned by the insertion/removal of excess oxygen into/from the structure. In this case, the extra oxygen atoms would modify the structure and the coordination number between the Co ions and their first neighbors. In either case, whether opting for the excess oxygen or the chemical substitution synthesis routes, both methods are expected to lead to a series of phase transitions, structural distortions, deliberate order or disorder on one or more of the layers, and superstructures. In turn, any one of these "side effects" would heavily influence the spin state of the Co ions and produce different magnetic and transport properties.

Enhancing the Thermopower Properties of TM Oxides: Taking into account the decreased electrical conductivity in our polycrystalline samples, the ZT values found to date should be considered as the lower estimates of realistic values. Further attempts to enhance thermopower by optimizing charge doping, improving electrical conductivity and decreasing phonon thermal conductivity should produce considerably increased ZT . Once the most promising compounds are identified we will follow with in-depth investigations of their structural and lattice dynamical properties. This task will involve *in situ* neutron experiments under a wide range of temperatures and oxygen pressures. Investigation of phonon dispersion by inelastic neutron scattering will guide our understanding of the reduction of phonon thermal conductivity by targeted chemical

substitutions. Another avenue for the increase of thermopower and the reduction of phonon conductivity will be explored in naturally layered structures based on transition metal oxides. In all of these compounds attempts will be made to reduce phonon thermal conductivity through formation of point and extended defects to scatter phonons at various length scales.

Publications (FY07-FY09)

1. *Element-specific probe of Ru magnetism and local structure in $RuSr_2Eu_{1.5}Ce_{0.5}Cu_2O_{10}$*
N. M. Souza-Neto, D. Haskel, J. C. Lang, O. Chmaissem and B. Dabrowski and I. Felner
Phys. Rev. B 80, 140414(R) (2009)
2. *Crystal structure and magnetic properties of high-oxygen pressure annealed $Sr_{1-x}La_xCo_{0.5}Fe_{0.5}O_{3-\delta}$ ($0 \leq x \leq 0.5$)*
K. Świerczek, B. Dabrowski, L. Suesscun and S. Kolesnik
Journal of Solid State Chemistry 182, 280–288 (2009)
3. *Synthesis and structural characterization of $La_xSr_{1-x}MnO_{2.6+\delta}$ ($0.1 \leq x \leq 0.4$) compounds displaying compressed octahedral coordination of $Mn^{(4.5x)+}$*
L. Suesscun, B. Dabrowski, S. Remsen and J. Mais
Journal of Solid State Chemistry 182, 187–195 (2009)
4. *Structural and physical properties of $SrMn_{1-x}Ru_xO_3$ perovskites*
S. Kolesnik, B. Dabrowski and O. Chmaissem
Phys. Rev. B 78, 214425 (2008)
5. *Universal doping dependence of the ground-state staggered magnetization of cuprate superconductors*
R. Ofer, A. Keren, O. Chmaissem and A. Amato
Phys. Rev. B 78, 140508(R) (2008)
6. *Competing interactions and complex magnetism at $SrRuO_3/SrMnO_3$ interfaces*
Y. Choi, Y. C. Tseng, D. Haskel, D. E. Brown, D. Danaher and O. Chmaissem
Applied Physics Letters 93, 192509 (2008)
7. *Net Mn moment due to canted spins at $SrRuO_3/SrMnO_3$ interfaces*
Y. Choi, Y. Z. Yoo, O. Chmaissem, A. Ullah, S. Kolesnik, C. W. Kimball, D. Haskel, J. S. Jiang and S. D. Bader
Journal of Applied Physics 103, 07B517 (2008)
8. *Formation of Co^{3+} octahedra and tetrahedra in $YBaCo_4O_{8.1}$*
O. Chmaissem, H. Zheng, A. Huq, P.W. Stephens and J.F. Mitchell
Journal of Solid State Chemistry 181, 664–672 (2008) *Rapid Communication*
9. *Structural, magnetic and electronic properties of $LaNi_{0.5}Fe_{0.5}O_3$ in the temperature range 5–1000 K*
M. Gateshki, L. Suesscun, I. S. Kolesnik, J. Mais, K. Świerczek, S. Short and B. Dabrowski
Journal of Solid State Chemistry 181, 1833–1839 (2008)
10. *Magnetic properties of $RuSr_2GdCu_2O_8$ using the temperature dependence of the Mössbauer spectrum*
D. Coffey, M. DeMarco, B. Dabrowski, S. Kolesnik, S. Toorongian and M. Haka
Phys. Rev. B 77, 214412 (2008)
11. *Pressure effects on magnetic and structural properties of pure and substituted $SrRuO_3$*
J. Pietos, B. Dabrowski, A. Wisniewski, R. Puzniak, R. Kiyonagi, T. Maxwell and J.D. Jorgensen
Phys. Rev. B 77, 104410 (2008)
12. *$Sr_{4+n}Mn^{3+}_4Mn^{4+}_nO_{10+3n}$: a new homologous series of oxygen-vacancy-ordered perovskites built from $Mn^{3+}O_5$ pyramids and $Mn^{4+}O_6$ octahedra*
L. Suesscun and B. Dabrowski
Acta Cryst. B64, 177–186 (2008)
13. *Oxygen Ordered Phases in $La_xSr_{1-x}MnO_y$ ($0 \leq x \leq 0.2$, $2.5 \leq y \leq 3$): An In situ Neutron Powder Diffraction Study*
L. Suesscun, B. Dabrowski, J. Mais, S. Remsen, J.W. Richardson Jr., E.R. Maxey and J.D. Jorgensen
Chem. Mater 20, 1636–1645 (2008)
14. *Structural, transport, and magnetic properties of the cation-ordered cobalt perovskite $Ho_{1/3}Sr_{2/3}CoO_{3-\delta}$*
A. Baszczuk, S. Kolesnik, B. Dabrowski, O. Chmaissem and J. Mais
Phys. Rev. B 76, 134407 (2007)
15. *Ferromagnetic Mn moments at $SrRuO_3/SrMnO_3$ interfaces*
Y. Choi, Y. Z. Yoo, O. Chmaissem, A. Ullah, S. Kolesnik, C. W. Kimball, D. Haskel, J. S. Jiang and S. D. Bader
Applied Physics Letters 91, 022503 (2007)
16. *Crystal structures, charge and oxygen-vacancy ordering in oxygen deficient perovskites $SrMnO_x$ ($x < 2.7$)*
L. Suesscun, O. Chmaissem, J. Mais, B. Dabrowski and J.D. Jorgensen
Journal of Solid State Chemistry 180, 1698–1707 (2007)

Atomic and Mesoscopic Study of Metallic Glasses

T. Egami (egami@utk.edu), J. R. Morris, E. P. George

Materials Science and Technology Division, Oak Ridge National Laboratory

D. M. Nicholson

Computer Science Division, Oak Ridge National Laboratory

Research Scope:

The purpose of our project is to address some of the most fundamental unsolved scientific questions in the field of liquids and glasses using theory, computer simulation and experiment, including neutron scattering. The questions addressed are, why the viscosity of a liquid changes as much as 15 orders of magnitude over a relatively small temperature range without significant changes in the structure, what is the exact nature of the glass transition, the phenomenon of a liquid becoming a glass, and what is the atomistic mechanism of deformation in metallic glasses. While the recent development of bulk metallic glasses (BMG) has drastically improved the prospect of application of metallic glasses as a structural material, the science of these materials, in particular at the atomistic and mesoscopic level, is quite immature. We plan to resolve these complex and difficult questions through integrated and concerted efforts by a team of top researchers with various expertise using most advanced tools of investigation, including large scale computer simulation and spallation neutron sources. Our ultimate goal is to establish general principles that could guide the effort for further alloy development and improvement.

Recent Progress:

A. Atomic Dynamics in Liquids and Glasses

The normal modes of atomic dynamics in solids, crystalline or amorphous, can readily be calculated by diagonalizing the dynamical matrix, $\{M_{ij} = d^2E/dr_i dr_j\}$. In liquids, however, the dynamical matrix itself is strongly time-dependent, so that the diagonalization does not provide the normal modes. We discovered that the atomic dynamics in the liquid is extremely localized as described below. To express the local dynamics, we devised the method of the dynamic pair-density function (DPDF) [1]. The DPDF, $\rho(r, E)$, describes the atomic dynamics in real space, and captures local dynamics very effectively. Fig. 1 shows the DPDF of a metallic glass $Zr_{50}Cu_{40}Al_{10}$ obtained with MARI of ISIS. The dynamical structure factor, $S(Q, E)$, was obtained by inelastic neutron scattering and the $Q \rightarrow r$ Fourier-transformation was made to obtain the DPDF.

We simulated the atomic dynamics in the liquid state of iron by molecular dynamics. As shown in Fig. 2 we found most of the high frequency dynamics is *strongly localized* to the nearest neighbors, and only the low-frequency vibrations are delocalized. We recently have carried out the pulsed neutron DPDF measurement of liquid Sn using the ARCS of

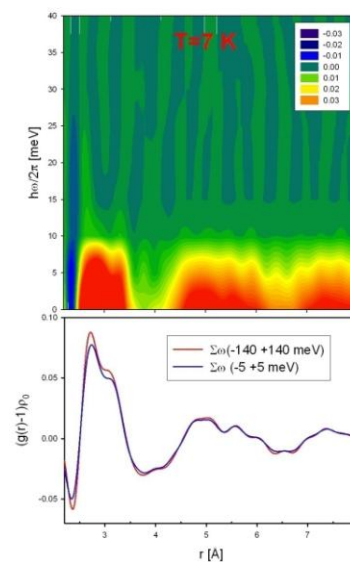


Fig. 1 DPDF of a metallic glass $Zr_{50}Cu_{40}Al_{10}$ obtained with MARI of ISIS.

the SNS. The results are being analyzed and compared to the results of first-principles molecular dynamics simulation. Such dynamics of the nearest neighbor atoms can be well expressed in terms of the dynamics of the atomic-level-stresses [2], and strong localization of the vibrational modes to the nearest neighbors justify the view that the dynamics of the atomic-level-stresses are the normal modes in the liquid state [3]. Indeed the simulation shows that the fluctuations in the atomic-level-stresses satisfy the equipartition theorem as shown in Fig. 3, as expected for the normal modes [4, publ. 2]. The equipartition theorem provides the basis for statistical mechanics in the liquid state [2, publ. 30].

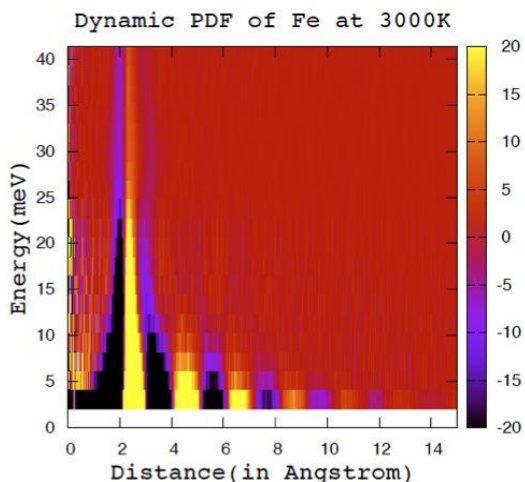


Fig. 2 DPDF of liquid iron at 3000K.

B. Mechanical Failure and Glass Transition

The microscopic mechanism of mechanical failure in metallic glasses has been a mystery for a long time. Recently we achieved a major breakthrough by showing that mechanical failure is the stress-induced glass transition, and that a simple scaling law exists to describe the interplay between temperature and stress (Fig. 4) [publ. 29]. This conclusion was obtained by computer simulation of $Zr_{50}Cu_{40}Al_{10}$ glass in the steady state flow. The scaling law suggests that the applied stress reduces the barrier in the local potential energy landscape, thus promotes local atomic mobility and induces glass transition.

In order to verify this prediction we recently carried out the inelastic neutron scattering measurement with ARCS of the SNS to measure the excitation under stress on a $Zr_{50}Cu_{40}Al_{10}$ metallic glass. Indeed the stress was found to soften the local atomic dynamics. The results are being analyzed. We will also carry out the inelastic x-ray scattering experiment at the APS to determine the anisotropic DPDF.

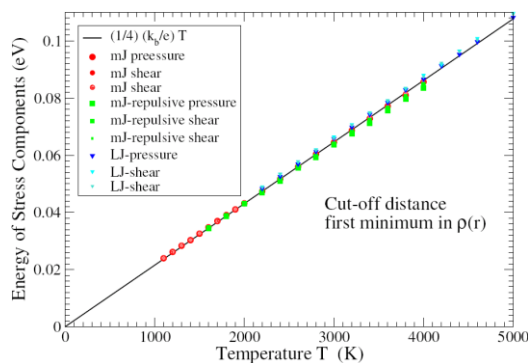


Fig. 3 The self-energy of the fluctuation of atomic-level-stress is equal to $kT/4$ [5].

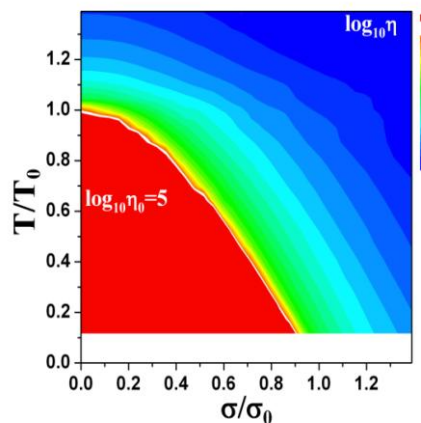


Fig. 4 Equal viscosity lines as a function of normalized temperature and stress. Note that they are self-similar, resulting in a simple scaling law [publ. 29].

Future Directions

A. Specific Heat at Glass Transition

We just discovered a rather tantalizing law that the jump in the specific heat at the glass transition is equal to $3/2k$, and verified with experimental data and simulation. This discovery became possible only because the development of bulk metallic glasses allowed accurate measurements of the specific heat jump. We are now generalizing this idea to different classes of glasses. Generally it is equal to $3/2nk$, where n is the number of atoms in the motional unit.

B. Effect of Stress on Energy Landscape

The implication of the scaling law described above will be investigated to develop the theory of the stress effect on the local energy landscape. This theory will extend our statistical mechanics theory [publ. 30] to the kinetic theory of the excited states. This will be done by calculating the local elastic energy to deform the cage around an atom. This extension will enable calculation of kinetic properties, such as viscosity, internal friction and two-level tunneling probabilities.

References:

1. W. Dmowski, S. B. Vakhrushev, I.-K. Jeong, M. P. Hehlen, F. Trouw and T. Egami, *Phys. Rev. Lett.*, **100**, 137602 (2008).
2. T. Egami, K. Maeda, and V. Vitek, *Phil. Mag. A* **41**, 883 (1980).
3. T. Egami and D. Srolovitz, *J. Phys. F* **12**, 2141 (1982).
4. S.-P. Chen, T. Egami and V. Vitek, *Phys. Rev. B* **37**, 2440 (1988).

Publications FY2008-10

1. *Topological Fluctuations in a Connectivity Network of a Simple Atomic Liquid*, V. A. Levashov, T. Egami, R. S. Aga and J. R. Morris, “*Phys. Rev. E*, **78**, 041202 (2008).
2. *Equipartition Theorem and the Dynamics of Liquids*, V. A. Levashov, R. S. Aga, J. R. Morris, and T. Egami, *Phys. Rev. B* **78**, 064205-1 (2008).
3. *Geometrical Frustration and Glass Formation*, T. Egami, V. Levashov, R. Aga and J. R. Morris, “*Met. Trans. A*, **39**, 1786 (2008).
4. *Shear Fracture of Bulk Metallic Glasses with Controlled Applied Normal Stresses*, C. H. Hsueh, H. Bei, C. T. Liu, P. F. Becher, and E. P. George, *Scripta Mater.* **59**, 111 (2008).
5. *Phase Stability and Transformations in the $Zr_2Ni_xCu_{1-x}$ System*, M. J. Kramer, M. Xu, Y. Y. Ye, D. J. Sordelet, and J. R. Morris, *Met. Trans. A* **39A**, 1847 (2008).
6. *Transitions from the Oscillatory to Smooth Fracture Propagation in Brittle Metallic Glasses*, Y. Braiman and T. Egami, *Phys. Rev. E*, **77**, 065101R (2008).
7. *Composition Effects on Glass Forming Ability and its Indicator γ* , Z. P. Lu, C. T. Liu, Y. Wu, H. Tan, Y. Li, and G. L. Chen, *Intermetallics* **16**, 410 (2008).
8. *Oxygen Effects on Plastic Deformation of a Zr-Based Bulk Metallic Glass*, Z. P. Lu, H. Bei, Y. Wu, E. P. George, C. T. Liu, and G. L. Chen, *Appl. Phys. Lett.* **92** 011915 (2008).
9. *Many-Body Effects in BCC Metals: An Embedded Atom Model Extension of the Modified Johnson Pair Potential for Iron*, J. R. Morris, R. S. Aga, V. Levashov, and T. Egami, *Phys. Rev. B*, **77**, 174201 (2008).
10. *Temperature-Dependent Mechanisms of Homogeneous Crystal Nucleation in Quenched Lennard-Jones Liquids*, L. J. Peng, J. R. Morris and Y. C. Lo, *Phys. Rev. B* **78**, 012201 (2008).

11. *Flow Serration in a Zr-based Bulk Metallic Glass in Compression at Low Strain Rates*, S. X. Song, H. Bei, J. Wadsworth, and T. G. Nieh, *Intermetallics*, **16**, 813 (2008).
12. *Heterogeneous Nucleation in a Glass-Forming Alloy*, J. J. Wall, C. T. Liu, W. K. Rhim, J. J. Z. Li, P. K. Liaw, H. Choo, and W. L. Johnson, *Appl. Phys. Lett.* **92**, 244106 (2008).
13. *Size-Dependent Plasticity and Fracture of a Metallic Glass in Compression*, S. Xie and E. P. George, *Intermetallics* **16**, 485 (2008).
14. *Modeling: The Role of Atomistic Simulations*, R. S. Aga and J. R. Morris, p. 57 in *Bulk Metallic Glasses*, ed. M. K. Miller and P. Liaw, Springer-Verlag, Berlin, 2008.
15. *Atomistic Theory of Metallic Liquids and Glasses*, T. Egami, p. 27 in *Bulk Metallic Glasses*, ed. M. K. Miller and P. Liaw, Springer-Verlag, Berlin, 2008.
16. *Evaluation of Glass-Forming Ability*, Z. P. Liu, Y. Liu, and C. T. Liu, p. 87 in *Bulk Metallic Glasses*, ed. M. K. Miller and P. K. Liaw, Springer-Verlag, Berlin, 2008.
17. *Hardness and Shear Band Evolution in Bulk Metallic Glasses After Plastic Deformation and Annealing*, S. Xie and E. P. George, *Acta Mater.* **56**, 5202-5213 (2008).
18. *Structural Anisotropy in Metallic Glasses Induced by Mechanical Deformation*, W. Dmowski and T. Egami, *Adv. Eng. Mater.* **10**, 1003 (2008).
19. *Nanoscale Oscillatory Fracture Propagation in Metallic Glasses*, Y. Braiman and T. Egami, *Physica A*, **388**, 1978 (2009).
20. *Enhanced Plasticity in a Zr-based Bulk Metallic Glass Composite with in situ Formed Intermetallic Phases*, G. Chen, H. Bei, Y. Cao, A. Gali, C. T. Liu, and E. P. George, *Appl. Phys. Lett.* **95**, 081908 (2009).
21. *The role of the electronic structure on the relationship between crystallinity of CoFe and its tunneling magnetoresistance*, Li Gao, Xin Jiang, D. M. C. Nicholson, Teya Topuria, and Stuart S. P. Parkin, *App. Phys. Lett.* **95**, 012508 (2009).
22. *Controlled Normal/Shear Loading and Shear Fracture in Bulk Metallic Glasses*, C. H. Hsueh, H. Bei, C. T. Liu, E. P. George, and P. F. Becher, *Intermetallics* **17**, 802-810 (2009).
23. *Alloying Effects of Iridium on Glass Formation and Glass-Forming Ability of the Zr-Cu-Al System*, Z. Y. Liu, Y. Wu, H. X. Li, H. Bei, and Z. P. Lu, *J. Mater. Res.* **24** 1619-1623 (2009).
24. *Simulating the Effect of Poisson Ratio on Metallic Glass Properties*, J. R. Morris, R. S. Aga, T. Egami and V. A. Levashov, *Int. J. of Mod. Phys. B* **23**, 1229 (2009).
25. *In situ observation of thermal expansion of tetragonal C11_b phase in Zr₂Cu_(1-x)Pd_x alloys*, Min Xu, Y. Y. Ye, J. R. Morris, D. J. Sordelet and M. J. Kramer, *Intermetallics* **18**, 8 (2010).
26. *Structural Rejuvenation in a Bulk Metallic Glass Induced by Severe Plastic Deformation*, W. Dmowski, Y. Yokoyama, A. Chuang, Y. Ren, M. Umemoto, K. Tuchiya, A. Inoue, and T. Egami, *Acta Materialia*, **58**, 429 (2010).
27. *Understanding the Properties and Structure of Metallic Glasses at the Atomic Level*, T. Egami, *Journal of Metals*, **62**, 2, 70 (2010).
28. *Kinetics of Volume and Enthalpy Relaxation in Pt₆₀Ni₁₅P₂₅ Bulk Metallic Glass*, M. Kohda, O. Haruyama and T. Egami, *Phys. Rev. B*, **81**, 092203 (2010).
29. *On the Stress-Temperature Scaling for Steady-State Flow in Metallic Glasses*, P. Guan, M.-W. Chen and T. Egami, *Phys. Rev. Lett.*, **104**, 205701 (2010).
30. *Statistical Mechanics of Metallic Glasses and Liquids*, T. Egami, V. A. Levashov, J. R. Morris and O. Haruyama, *Mater. Trans. A*, **41**, 1628 (2010).

Control of Structure-Property Relationships in Complex Oxides by Designed Strain

M.R. Fitzsimmons, J. Olamit¹ and S. Singh
Los Alamos National Laboratory, Los Alamos, NM 87545
fitz@lanl.gov

Program Scope (0.25 FTE and 1 Postdoc): Since the electronic and magnetic properties of complex oxides are closely coupled to their atomic, electronic and orbital structures, these materials can exhibit extraordinary responses, e.g., large changes of resistivity, to small perturbations in their environment.² Changes of pressure, chemistry, temperature, electric and magnetic fields are examples of perturbations that affect complex oxides. In general, the influence of strain and physical confinement can produce novel behavior in many materials, but for complex oxides the behavior can become extreme. A complication that indeed makes these materials complex includes the coupling of strain and atomic (and/or orbital) reconstruction.³ Such coupling is nonlinear, and the influence of nonlinear coupling represents an ongoing challenge to predict.

A specific example of nonlinear behavior is observed in bulk hole-doped manganites in which multiple electronic phases co-exist as a consequence of non-uniform distributions of strain and structural order in what is believed to be chemically homogenous material. Electronic phase co-existence has been reasonably well documented for bulk manganites⁴ and at least once for a (manganite) thin film.⁵ In bulk manganites, the metallic phase is believed to be ferromagnetic, while the charge ordered phase is not ferromagnetic (either paramagnetic or anti-ferromagnetic). Bulk manganites may exhibit both electronic and magnetic phase co-existence. Electronic and magnetic phase co-existence offer intriguing technological opportunities, particularly for thin films.

An example of a successful application of complex oxide behavior in technology is the integration of complex oxide thin films with silicon-based semiconductors in commercial electronic memories.⁶ Yet, it is possible that novel behavior observed in bulk materials is altered or perhaps not observed in thin films. For example, *magnetic* phase co-existence in manganite thin films is controversial.

Thin films differ from bulk materials in one important aspect—films are physically confined in at least one dimension, if not more. Physical confinement is a consequence of surfaces and interfaces. Surfaces and interfaces may have atomic and orbital structures that are not necessarily the same as in the bulk. Also, films are not often self-supporting, consequently, the proximity of a substrate may impart strain on the interface and film that propagates for several nanometers into the film. Since the affected region can be a significant fraction of the film, the properties of the film may be less like the bulk and

¹ Now a NRC postdoc fellow at NIST, Gaithersburg MD.

² N. Mathur and P. Littlewood, *Physics Today* **56**, 25 (2003).

³ K.H. Ahn et al., *Nature* **428**, 401 (2004).

⁴ V. Kiryukhin, *Nature* **386**, 813 (1997).

⁵ M. Fäth et al., *Science* **285**, 1540 (1999).

⁶ R. Ramesh and D.G. Schlom, *MRS Bulletin* **33**, 1006 (2008)

more like those of the surface or interface. Indeed, the importance of strain in thin films and its importance in complex oxides motivate our study. Our interests are two-fold. (1) Using observations of novel behavior in bulk complex oxides as a guide, we wish to understand such behavior in thin complex oxide films. We chose to study thin films of $(\text{La}_x\text{Pr}_{1-x})_y\text{Ca}_{1-y}\text{MnO}_3$ (LPCMO), which in the bulk exhibit electronic and magnetic phase co-existence. Our intention is to identify similar behavior in thin film samples and to study the influence of stress on this behavior. (2) We wish to understand novel behavior that is unique to complex oxide interfaces. The novel behavior we chose to investigate was the emergence of magnetism at the interface between LaAlO_3 (LAO) and SrTiO_2 (STO).

Recent Progress—magnetic phase co-existence in LPCMO films: This part of the project involves (1) development of techniques to apply pure bending stress to thin films and (2) investigation of magnetism in complex oxide thin films. First we discuss our progress on application of stress to our films. We pursued two strategies. The first strategy involved bombarding thin (0.35 mm thick) NdGaO_3 (NGO) substrates with 400 keV neon ion beams. This process is supposed to place damage in the substrate at a prescribed depth that may cause the substrate to bend.⁷ By bending the substrate, a film on the substrate's surface will also bend, and depending upon the side of the sample that faced the ion beam, the film can be placed in a state of tensile or compressive stress. The attraction of this approach is that the stressed-sample can be readily examined with a variety scattering techniques. The process works well for silicon substrates and has been shown to work for STO substrates, but for NGO substrates, we detected *no* measurable bending using five radically different ion beam doses. We conclude ion beam bombardment is not an effective means to apply stress to NGO substrates (or the films grown on them).

The second strategy involved development of a four-point mechanical jig (Figure 1a). The jig was made from aluminum, thus, it is transparent to neutrons. Small windows were machined into the jig to allow restricted access to the sample for x-ray and light beams.

By turning a screw, stress can be applied to the sample. The orientation of the sample with respect to the screw, i.e., film-side up or down, allowed us to apply compressive or tensile stress/strain.

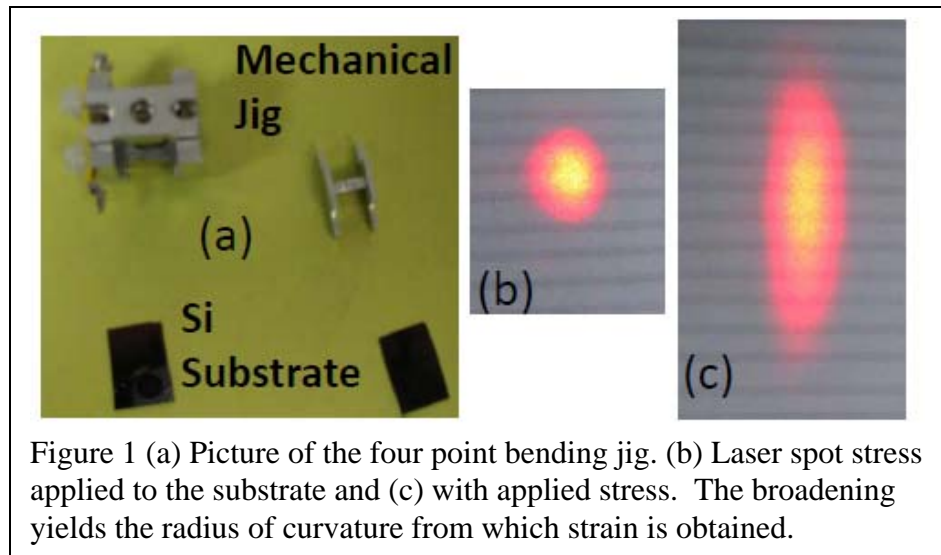


Figure 1 (a) Picture of the four point bending jig. (b) Laser spot stress applied to the substrate and (c) with applied stress. The broadening yields the radius of curvature from which strain is obtained.

⁷ C.A. Volkert, J. of Appl. Phys. **70**, 3521 (1991).

The amount of strain can be obtained from measurement of the broadening of a laser (or neutron) beam (Figure 1b and c). Stress yielding 0.08% strain can be applied to 0.25 mm thick NGO substrates before fracture. The jig can be mounted onto the cold finger of a cryostat, which in turn can be placed between the poles of an electromagnet. We monitored the broadening of the neutron beam from a sample bent in the jig as a function of temperature and found no change, thus, stress applied to the sample at room temperature remains the same at low temperatures. Our apparatus allows us to measure the influence of stress, temperature and field on the magnetic structure (with x-ray or neutron scattering) and properties (including the resistivity) of a sample.

The second part of the manganite study involved looking for magnetic phase co-existence in our LPCMO films. Depending upon the chemical composition of the LPCMO, the sizes of ferromagnetic domains (in bulk LPCMO) can be tailored in the range from hundreds of nm to a few microns. (In the bulk, these domains are surrounded by non-ferromagnetic material.) We examined two film compositions: $\text{La}_{0.27}\text{Pr}_{0.40}\text{Ca}_{0.33}\text{MnO}_3$ and $\text{La}_{1/4}\text{Pr}_{3/8}\text{Ca}_{3/8}\text{MnO}_3$ with neutron reflectometry and small angle neutron scattering. These scattering techniques probe magnetic structures with dimensions ranging from ~ 100 nm to several microns. We observed *no* evidence for magnetic phase co-existence in our thin film samples. An outstanding question is whether the samples exhibit electronic phase co-existence.

Future Progress—magnetic phase coexistence in LPCMO films: In the next few months we will redouble our efforts to find evidence for magnetic phase co-existence in our LPCMO films. These efforts will include: off-specular reflectometry using neutron and resonant soft x-ray beams from, and SANS from a specially prepared 300 nm thick LPCMO film. Critically important, however, will be electrostatic field microscopy or conductive atomic force microscopy of our films at modest temperatures, ~ 80 K. The microscopy measurements are critical because they can show whether our LPCMO films exhibit electronic phase co-existence. In fact, the measurements are presently more pressing than the scattering measurements, since the microscopy results could provide valuable guidance to our scattering experiments. Regrettably, we have been unsuccessful acquiring time at different DOE nanotech user facilities to carry out the research. We will investigate opportunities to pursue the microscopy measurements overseas.

Recent Progress—emergence of magnetism in LAO/STO superlattices: In the bulk, LAO and STO are neither magnetic nor normally thought of as conductors (although evidence for superconductivity in bulk STO was observed many years ago). Recently, several groups have reported novel behavior, including conductivity, superconductivity and magnetism, associated with the interface between LAO and STO. The novel behavior has been attributed alternatively to (1) (avoidance of) a polarization catastrophe,⁸ (2) vacancies, band bending and accumulation of electrons at the interface,⁹ or (3) interdiffusion of La across the interface (creating a mixture of Ti^{3+} and Ti^{4+} at the interface).¹⁰ Accumulation of electrons at the interface, or the presence of Ti^{3+} could produce the previously reported paramagnetic response to field.¹¹ In order to identify the

⁸ N. Nakagawa et al., Nat. Mater., **5** 204 (2006).

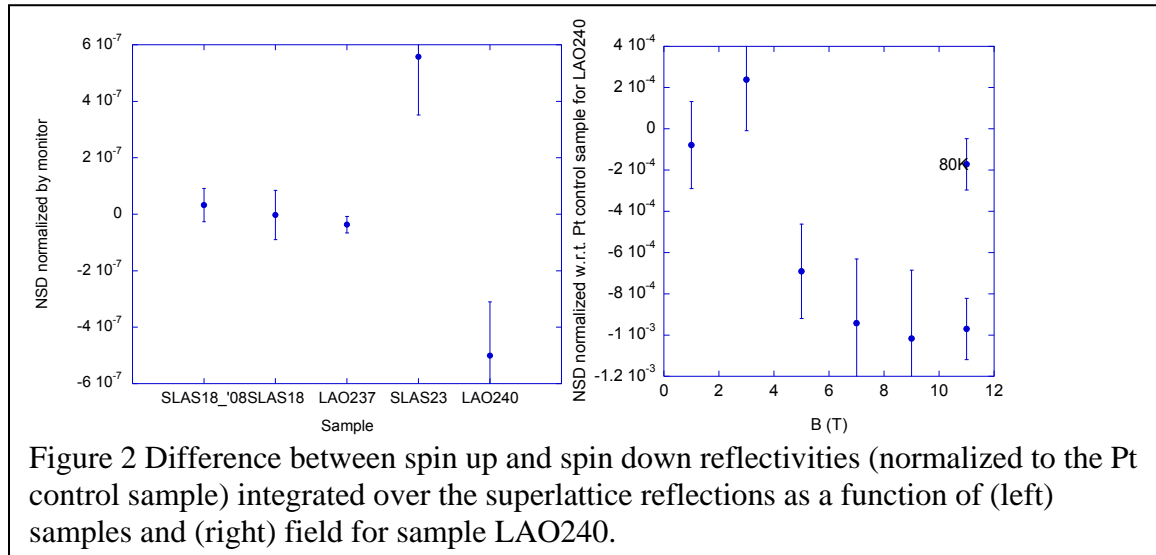
⁹ K. Yoshimatsu et al., Phys. Rev. Lett., **101** 026802 (2008).

¹⁰ P.R. Willmott et al., Phys. Rev. Lett., **99** 155502 (2007).

¹¹ A. Brinkman et al., Nature Materials **6**, 493 (2007).

location of magnetism and quantify its magnitude in the LAO/STO system, we used polarized neutron reflectometry to measure the magnetic depth profile of a LAO/STO superlattice. By measuring the dependence of the Bragg reflection intensity on neutron beam polarization we were able to prove that for two of our five samples magnetism was present in the superlattice (and not the substrate) and to measure its strength as a function of field and temperature. Samples were obtained from two different groups (A. Brinkman, Twente and Santamaria, Spain). Since the magnetization was expected to be very small, we developed a novel way to measure the spin dependence of the Bragg reflection intensity relative to a non-magnetic control sample at the same time. The magnitude of the moment can be inferred from our measurements of the neutron spin difference between the Bragg reflection intensities for up and down neutron beam polarizations (Figure 2). From the fact that some samples show magnetism and others do not, we tentatively conclude paramagnetism is not intrinsic to the LAO/STO interface.

Future Progress—emergence of magnetism in LAO/STO superlattices: We have received neutron beam time to pursue additional measurements on our LAO/STO superlattices. We anticipate the additional measurements will give insight into an origin for magnetism in some of the samples, e.g., is the magnetism affected by field cooling etc. Neutron scattering is uniquely suited to the study of magnetism in LAO/STO interfaces, since the technique can discriminate between magnetism from the periodic array of interfaces and “background” from the sample’s substrate. We will also investigate (with x-ray diffraction and x-ray reflectometry) the orthorhombic to tetragonal phase transition in STO (at ~ 110 K) and its relationship to rumpling of the STO surface. We have some anecdotal evidence which suggests rumpling of the STO surface influences the electronic/magnetic properties of our LAO/STO samples.



Neutron and X-Ray Studies of Spin and Charge Manipulation in Magnetic Nanostructures

Eric E. Fullerton¹ and Sunil Sinha²

¹ Departments of Electrical and Computer Engineering and NanoEngineering
University of California, San Diego
La Jolla, CA 92093
efullerton@ucsd.edu

² Department of Physics
University of California, San Diego
La Jolla, CA 92093
ssinha@physics.ucsd.edu

Program scope: The interrogation and manipulation of electron charge, spin, and magnetization in thin films and magnetic nanostructures is currently one of the frontier areas of research in Condensed Matter Physics and Materials Science [1-3]. These include issues that are directly related to scaling down the dimensions such that finite size, interfacial and collective effects dominate the behavior. Examples include magnetization reversal of single domain and dense arrays of nano-magnets, influence of surfaces on magnetic behavior, and the broad field of spintronics which relies on manipulating the spin rather than the charge of the electron via spin injection, manipulation and detection [2]. Magnetic materials and devices have also played a major role in science and technology for the last half century where hard disk drives dominate information storage [4] and magnetic random access memory (MRAM) is emerging in the memory market [5, 6]. The nano-magnetic systems developed for the data storage industry have sparked new technologies that exploit similar underlying physics. That combined with advances in semiconductor science and technology, that have until recently ignored the spin of the electron, has spurred the field of spintronics, ushering in a range of new magnetic sensors [7], memories [5, 6] and provides a spin-based vision for the electronics of the future. However, many spin-based devices are still in their infancy and a thorough understanding of the underlying materials and electronic properties and their effect on device performance will be essential for all future applications.

A driving force for continued progress is that materials that previously did not exist can now be made in the laboratory, and their properties can be optimized using a suite of incisive analytical and theoretical tools. There is, therefore, a close coupling between state-of-the-art thin film growth and patterning techniques [8] and cutting-edge characterization techniques. The increasing role of interfacial structure and the modification of the physical and magnetic structure at interfaces highlight the importance of structural and magnetic measurements at the atomic scale. The application of synchrotron [9] and neutron techniques [10] to attack this problem provides the opportunity for detailed structural and magnetic description of nano-scale magnetic systems and are crucial ingredients in the understanding of the physical properties.

By combining skills in neutron and synchrotron techniques with sample fabrication, magnetic and transport measurements in films and devices a complete data set is obtained that tests current models of spin and charge manipulation in magnetic nanostructures.

Recent Progress:

Exchange bias: We are addressing the spin structure at antiferromagnetic (AF)-ferromagnetic (FM) interfaces and the interaction across the common interface. We have grown polycrystalline as well as epitaxial AF CoO layers of different orientations on single crystal sapphire substrates

with FM Permalloy layers deposited on top of them in order to study both low-temperature AF-induced uni-directional anisotropy and the high-temperature FM-induced order in the AF layer and its role on uni-axial anisotropy [11, 12]. Neutron specular and off-specular reflectivity measurements have been carried out at room temperature and at low temperatures (below T_N of CoO) in a field-cooled state at the magnetic reflectometer at the Spallation Neutron Source. The results indicate that the FM induced order in the polycrystalline AF CoO layer lies in a thin (~ 1 -nm-thick) layer at the interface which has the majority of its magnetization coupled ferromagnetically to the FM moments in the permalloy and reverses with it in applied fields at low temperatures, while a small fraction is pinned in a direction opposite to the cooling field, implying antiferromagnetic coupling to the permalloy moments. These give rise to the exchange bias. Similar magnetization profiles are seen in the epitaxial CoO layers. We have also analyzed the off-specular resonant magnetic scattering from another exchange bias system (FM Co on AF single crystal FeF_2). This was done in the nominally saturated exchange biased state as a function of temperature and analyzed in terms of a magnetic roughness model for the magnetization at the interface separately for both the Co magnetization and the Fe magnetization due to the uncompensated spins in the FeF_2 . The results show that there is very little magnetic disorder in the Co magnetization and it is temperature independent, while there is a large and systematic increase in the roughness correlation length of the magnetic disorder in the FeF_2 as the temperature is decreased below the Neél Temperature of FeF_2 .

Electric field effects: In this proposal we are exploring the relatively unexplored field of using electric (E) to control the intrinsic magnetic properties (e.g. Curie temperature (T_C), moment density or magnetic anisotropy) in metallic systems. We are employing a number of complementary approaches to address this problem. An example is neutron scattering from CoPd alloy films where an electric field is applied to the film in an electrochemical cell (in collaboration with M. Zhernenkov, M.R. Fitzsimmons, J. Chlistunoff, and J. Majewski of Los Alamos National Laboratory). When a negative potential is applied to a metal (FM, in our case) electrode in an electrochemical cell, the metal surface is charged with excess electrons. The charge is counterbalanced by the cations from the electrolyte solution, which collect predominantly at the electrode surface and form an insulating ionic layer (double layer). This phenomenon results in a high E-field at the interface. We use neutron to probe the interface of the ferromagnetic electrode in the presence of the E-field. Figure 1 shows results obtained at the Asterix reflectometer at LANL. A thin CoO layer formed at the surface was detected in the neutron reflectivity results. In addition we observed a slight reaction between the film and electrolyte near the surface when the electrolyte is first introduced into the cell. This reaction and oxidation should be controllable in the future by depositing a thin insulating layer on the ferromagnetic surface.

However, we were able to see reversible changes in the surface magnetization that is linear with the applied E field (Fig. 1). The fitting procedure for the film in contact with electrolyte consisted of two steps: first we fitted a model to the R^+ and R^- curves directly, then we fine-tuned the magnetization depth profile by optimizing the χ^2 metric for the NSD curves (Fig. 1a). For the reflectivity data taken for $U = -0.02$ V the nuclear and magnetic SLD's of the CoPd layer were equal to those of the virgin sample and the four adjustable parameters were optimized: the thickness of the CoPd layer, the thickness of the layer "3", its nuclear SLD and its roughness. In order to fit the reflectivities taken when a potential was applied to the sample, the CoPd film was divided into two layers (CoPd layer "1" and "2", Fig. 1b) whose overall length and nuclear SLD were constrained to be that found for -0.02 V measurement. The two adjustable parameters we

optimized were the thickness of the layer “2” and its magnetic SLD. We found the best fit to the data when the thickness of the E -field affected layer “2” was 7.2(1) nm. The magnetization of the 7-nm surface region was $904 \pm 5 \text{ emu/cm}^3$ ($\chi_r^2 = 3.1$) and $920 \pm 5 \text{ emu/cm}^3$ ($\chi_r^2 = 2.5$) for applied potentials of -0.15 V and -0.32 V , respectively (see Fig. 1d). For comparison, had the uniform model for $M_0(z)$ been used to fit the data taken for negative applied potentials, the values of χ_r^2 would increase by 48 and 88% for -0.15 and -0.32 V , respectively. The big improvement of χ_r^2 achieved with a non-uniform magnetization depth profile is compelling evidence for the influence of E -field on the near-surface magnetization of the CoPd film. In particular, the magnetization of the surface region increases linearly with increasing magnitude of the negative applied potential (see Fig. 1c). The largest applied potential $U = -0.32 \text{ V}$ corresponds to the electric field of about 10^8 V/m since the typical thickness of the insulating layer is several nm.

Domain Wall Dynamics

Using coherent soft X-rays with photon energies at the M-edge of Dy at the Advanced Light Source, we were able to observe magnetic speckle around the satellite reflections in the antiferromagnetic spiral phase. Due to long-term stability problems, we could not quantitatively observe the time correlation of these speckles, but we were able to show the feasibility of studying slow magnetic dynamics such as domain wall motion in magnetic systems. This is of interest for understanding, for instance, the origins of $1/f$ noise in magnetic tunnel junctions and other magnetic heterostructures potentially useful for spintronics.

Future Plans:

- **Magnetic nano-structured arrays:** We will explore the role of lateral patterning on the magnetic properties of complex heterostructures. These will include high-anisotropy materials proposed for patterned media and selected exchange bias systems. We will determine the magnetic structure of patterned islands and layer-dependent reversal mechanisms.
- **Electric field effects on magnetic nanostructures:** We will continue the study of electric fields to control the intrinsic magnetic properties (e.g. Curie temperature (T_C), moment density or magnetic anisotropy) in metallic systems. We will study both the electric field control of magnetism and anisotropy of FePt and related compounds and the control of T_C in Cu-Ni alloys using both neutron reflectivity and resonant magnetic absorption and scattering.

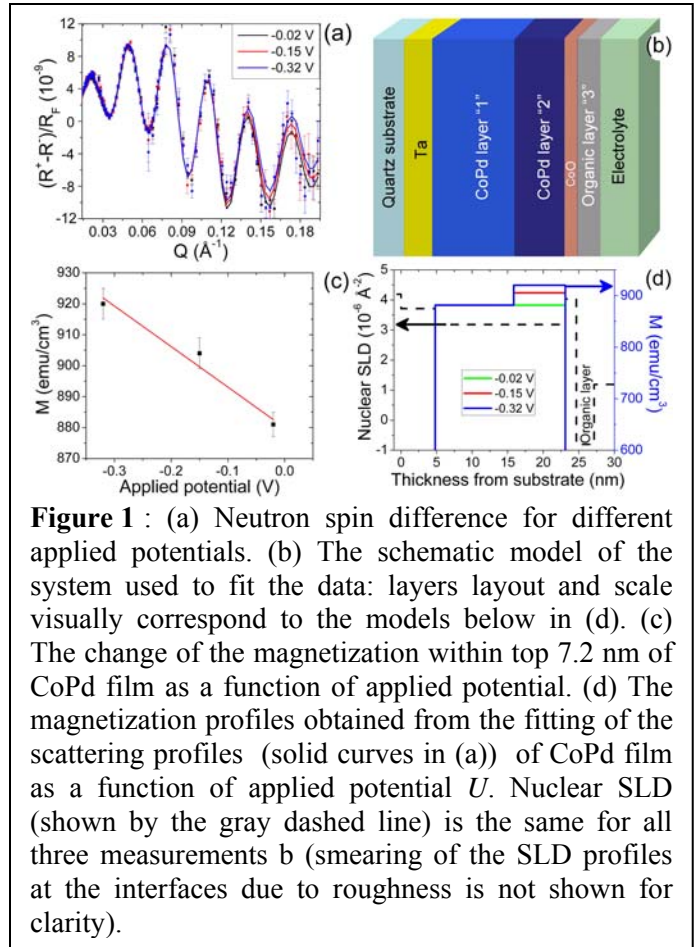


Figure 1 : (a) Neutron spin difference for different applied potentials. (b) The schematic model of the system used to fit the data: layers layout and scale visually correspond to the models below in (d). (c) The change of the magnetization within top 7.2 nm of CoPd film as a function of applied potential. (d) The magnetization profiles obtained from the fitting of the scattering profiles (solid curves in (a)) of CoPd film as a function of applied potential U . Nuclear SLD (shown by the gray dashed line) is the same for all three measurements b (smearing of the SLD profiles at the interfaces due to roughness is not shown for clarity).

- **Spin transfer effects in nanostructures:** We will probe the magnetic properties of candidate high-anisotropy spintronic materials, image domain wall motion in devices and characterize spin-injection from FM leads into non-magnetic material

Each topic has important unanswered scientific questions which impact on a broad range of future nano-technologies. These topics share a common theme that the magnetic properties are dependent on details of the interfaces and lateral structure. We will use the unique capabilities of neutron and synchrotron techniques to probe that magnetism of buried interfaces with high spatial and depth sensitivity. The understanding and control of magnetic properties at the nanoscale and their relationship to new functionality will lead to applications in other areas as well.

1. S.D. Bader, "Colloquium: Opportunities in nanomagnetism" *Rev. Mod. Phys.* **78**, 1-15 (2006).
2. C. Chappert, A. Fert, and F.N.V. Dau, "The emergence of spin electronics in data storage" *Nat. Mat.* **6**, 813 (2007).
3. L.M. Falicov, D.T. Pierce, S.D. Bader, R. Gronsby, K.B. Hathaway, H.J. Hopster, D.N. Lambeth, S.S.P. Parkin, G. Prinz, M. Salamon, I.K. Schuller, and R.H. Victora, "Surface, Interface, and Thin-Film Magnetism" *Journal of Materials Research* **5**, 1299-1340 (1990).
4. A. Moser, K. Takano, D.T. Margulies, M. Albrecht, Y. Sonobe, Y. Ikeda, S.H. Sun, and E.E. Fullerton, "Magnetic recording: advancing into the future" *J. Phys. D-Appl. Phys.* **35**, R157-R167 (2002).
5. B.N. Engel, J. Akerman, B. Butcher, R.W. Dave, M. DeHerrera, M. Durlam, G. Grynkewich, J. Janesky, S.V. Pietambaram, N.D. Rizzo, J.M. Slaughter, K. Smith, J.J. Sun, and S. Tehrani, "A 4-Mb toggle MRAM based on a novel bit and switching method" *IEEE Trans. Magn.* **41**, 132 (2005).
6. W.J. Gallagher and S.S.P. Parkin, "Development of the magnetic tunnel junction MRAM at IBM: From first junctions to a 16-Mb MRAM demonstrator chip" *IBM J. Res. & Dev.* **50**, 5 (2006).
7. J.M. Daughton, "GMR applications" *J. Magn. Magn. Mater.* **192**, 334-342 (1999).
8. J.I. Martin, J. Nogues, K. Liu, J.L. Vicent, and I.K. Schuller, "Ordered magnetic nanostructures: fabrication and properties" *J. Magn. Magn. Mater.* **256**, 449-501 (2003).
9. G. Srajer, L.H. Lewis, S.D. Bader, A.J. Epstein, C.S. Fadley, E.E. Fullerton, A. Hoffmann, J.B. Kortright, K.M. Krishnan, S.A. Majetich, T.S. Rahman, C.A. Ross, M.B. Salamon, I.K. Schuller, T.C. Schulthess, and J.Z. Sun, "Advances in nanomagnetism via X-ray techniques" *J. Magn. Magn. Mater.* **307**, 1-31 (2006).
10. M.R. Fitzsimmons, S.D. Bader, J.A. Borchers, G.P. Felcher, J.K. Furdyna, A. Hoffmann, J.B. Kortright, I.K. Schuller, T.C. Schulthess, S.K. Sinha, M.F. Toney, D. Weller, and S. Wolf, "Neutron scattering studies of nanomagnetism and artificially structured materials" *J. Magn. Magn. Mater.* **271**, 103-146 (2004).
11. S. Roy, C. Sanchez-Hanke, S. Park, M.R. Fitzsimmons, Y.J. Tang, J.I. Hong, D.J. Smith, B.J. Taylor, X. Liu, M.B. Maple, A.E. Berkowitz, C.C. Kao, and S.K. Sinha, "Evidence of modified ferromagnetism at a buried Permalloy/CoO interface at room temperature" *Physical Review B* **75**, 014442 (2007).
12. E. Blackburn, C. Sanchez-Hanke, S. Roy, D.J. Smith, J.I. Hong, K.T. Chan, A.E. Berkowitz, and S.K. Sinha, "Pinned Co moments in a polycrystalline permalloy/CoO exchange-biased bilayer" *Physical Review B* **78**, 180408 (2008).

Vibrational Thermodynamics of Materials

Brent Fultz btf@caltech.edu

California Institute of Technology, W. M. Keck Laboratory, Pasadena CA 91125 USA

Phonon thermodynamics provides the vibrational entropy of materials, which is now known to be important for alloy phase stability and phase transformations. Until recently, however, it was not practical to study vibrational thermodynamics with sufficient accuracy for quantitative predictions, at least not efficiently. For example, heat capacities or phonon frequencies should be accurate to approximately 1% if vibrational entropies of different phases are to be compared quantitatively. Ab-initio tools for calculating phonons in solids have made rapid progress, and we perform such calculations to support our experimental program. The core of our work is measurements of phonon spectra by inelastic neutron scattering, for which impressive new capabilities are now available, such as the ARCS instrument at the SNS. Especially in combination, neutron scattering and computation allow us to discover the reasons for differences in vibrational entropies of materials. In the past decade or so, there has been considerable progress in our understanding of the vibrational entropy of materials, at least at lower temperatures when harmonic models are reliable.

Most of our work is on vibrational entropy at elevated temperatures, an important topic for the synthesis and processing of materials. A “quasiharmonic model” is often used to extend the systematics of harmonic phonons to high temperatures by accounting for the effects of thermal expansion against a bulk modulus. Effects that cannot be accounted for by the quasiharmonic approximation originate from two important effects that are discussed below, and are now at the core of our research

- in all materials there are interactions of thermally-excited phonons with other phonons (phonon-phonon interactions),
- in metals there are interactions of phonons with electronic excitations (electron-phonon interactions, PPI).

1. Adiabatic Electron-Phonon Interactions in Metals

In metals, the electron screening of ion motions governs the restoring forces on the nuclei, and hence phonon frequencies. Electron screening depends on the size and shape of the Fermi surface, which is blurred with temperature for two reasons. The well-known Fermi–Dirac distribution gives a thermal smearing function that is approximately a Gaussian of standard deviation $2k_B T$. Secondly, when the EPI is strong, at higher temperatures there is a proportionate increase in electron scattering by phonons, and a shortening of the electron lifetime. The “adiabatic” EPI occurs when there are simultaneous thermal excitations of both electrons and phonons.

In what is arguably our most important work during the previous budget period, we showed how the adiabatic EPI can cause large, non-harmonic effects on vibrational entropy at surprisingly high temperatures [1, 2]. In our first effort, we measured the phonon DOS for bcc solid solutions of V metal by inelastic neutron scattering [3, 4]. For dissolving 6.25 at.% Pt in V, the vibrational entropy of mixing was $\Delta S_{\text{vib}}^{\text{mix}} = -0.272 k_B/\text{atom}$, exceeding the configurational entropy of mixing, $S_{\text{conf}} = +0.234 k_B/\text{atom}$. For a V-6.25% Pt alloy, the total entropy of mixing is therefore negative(!) We interpreted these results by showing how transition metal solutes alter the electron states at the Fermi level of bcc V. In short, pure V is anomalous with a large electron DOS at the Fermi level, strong electron screening, and soft phonons. Solute atoms such as Ni, Pd, and Pt reduce this

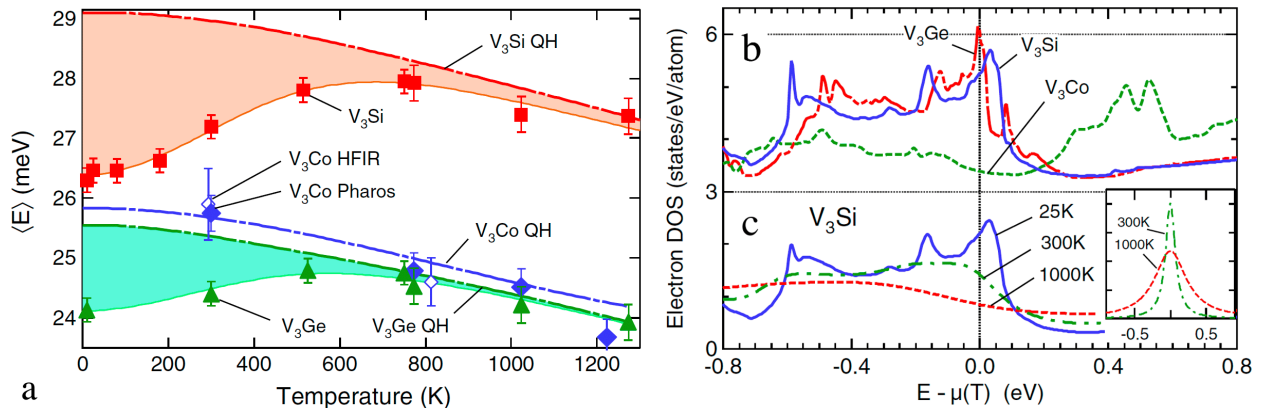


Figure 1. (a) Average phonon energy of A15 compounds of V₃Si, V₃Ge, and V₃Co as functions of temperature (from inelastic neutron scattering measurements). Markers are results from INS measurements, dash-dotted lines correspond to conventional quasiharmonic (QH) behavior. The QH curves were offset vertically to match the experimental data at the highest T measured. After [1]. *(b)* Electronic DOS for A15 V₃Si, V₃Ge, and V₃Co from first-principles VASP calculations. *(c)* Electronic DOS for V₃Si broadened by EPI at 25 K, 300 K, and 1000 K, using electron-phonon coupling parameter $\lambda = 1.0$ at all T. Energies are with respect to the electron chemical potential $\mu(T)$. Inset: broadening function at 300 K and 1000 K.

effect. For pure V, temperature suppresses the adiabatic EPI, and with temperature the *loss* of this source of softening approximately cancels the increased softening from quasiharmonic behavior.

We measured the changes with temperature of phonon DOS curves of three compounds with the A15 structure [1]. The compounds V₃Si and V₃Ge are well-known superconductors (with strong electron-phonon coupling), but V₃Co is not. The compound V₃Co shows a normal quasiharmonic phonon softening with temperature. On the other hand, the phonons in V₃Si actually stiffen with temperature, as summarized in Fig. 1a. At high temperatures when the electron-phonon coupling is suppressed, normal quasiharmonic softening occurs.

The origin of the thermal suppression of the EPI is indicated in Fig. 1c, where the electron DOS at the Fermi level is shown to be strongly temperature-dependent for V₃Si, owing to thermal broadening of the electron DOS from the Fermi distribution function, and from shortened lifetimes of electron states. Figure 1b shows that in contrast, V₃Co does not have much structure of its electron DOS near the Fermi level, and the changes with temperature are small. Phonon DOS curves for V₃Si were calculated with ab-initio methods using VASP (using PAW and GGA), and the small displacement method implemented in PHON. Including the effects of thermal smearing of electron energy levels plus the quasiharmonic effects of volume expansion gave an excellent accounting for the phonon DOS curves measured at high temperature.

2. Anharmonicity and Phonon-Phonon Interactions

Vibrational entropy is fundamentally determined from the volume of phase space in position and momentum coordinates explored by vibrating atoms. The phase space explored by coupled anharmonic oscillators is much less well understood than for harmonic oscillators, and is a subject of modern research on nonlinear phenomena. The usual approach is to treat anharmonic solids by using expressions for harmonic entropy, with phonon energy spectra measured by inelastic scattering experiments. An important question that we are addressing by molecular dynamics methods is, “Is this approach reliable?”

In experimental work, we measured the phonon DOSs of several fcc metals at elevated temperatures. The thermal softening of phonon energies were small, and could be accounted for by simply

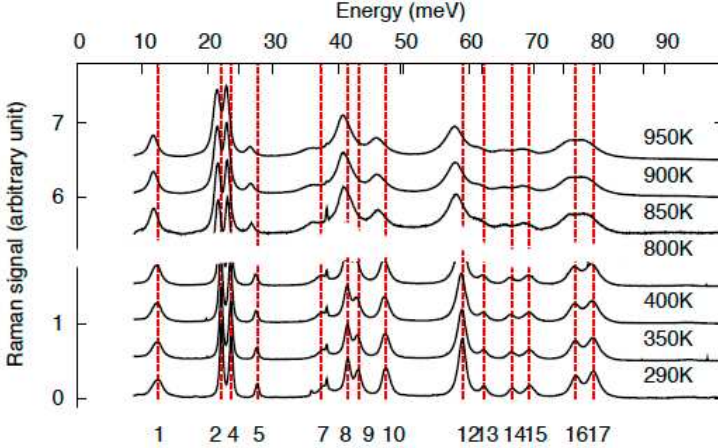


Figure 2. Raman spectra of monoclinic zirconia at temperatures from 295 to 950 K, with laser power at 50mW, exposure time of 60 seconds and at least 20 accumulations of the spectra. Peaks are numbered as proposed assignments. The sharp features near peaks 7 are artifacts.

rescaling the energy axis. The larger effects in the spectra were the thermal broadenings of the DOS, which we accounted for by a damped harmonic oscillator function with the same value of Q for all phonons. This Q was less than 10 for Al metal, for example. Simple approximations were surprisingly successful for fcc metals such as Al, Cu, Ni [5, 6, 7]. We are cautiously optimistic that the phonon anharmonicity in fcc metals may be possible to understand in a general way. Incidentally, from work on bcc Fe, bcc Fe-V and bcc Fe-Cr, we know that bcc metals are more complicated, with a large temperature dependence of the low transverse modes. This work is ongoing, and we are also analyzing neutron scattering data from fcc Pb.

We have begun to study phonon-phonon anharmonicity in oxides, for which we can neglect electron-phonon interactions. Raman spectra of monoclinic zirconia (ZrO_2) and hafnia (HfO_2) were measured at temperatures of up to nearly 1000 K, and some data are presented in Fig. 2. Temperature-dependent Raman peak shifts and broadenings were measured and compared between zirconia and hafnia [9, 10]. Phonon dynamics calculations were performed with both shell model and density functional theory to obtain Raman frequencies, and the total and partial phonon density of states (DOS). These calculations were also used to identify the individual motions of metal and oxygen atoms in the Raman modes. By correlating these motions to the thermal peak shifts and broadenings, it was found that modes involving changes in oxygen-oxygen bond length were the most anharmonic for both zirconia and hafnia. The metal-dominated modes were reasonably quasi-harmonic, and showed less broadening with temperature. Very recently we have measured inelastic neutron scattering spectra on zirconia as a function of temperature, and obtained similar results. The neutron data will allow better assessment of thermodynamic properties and their origin.

3. Ongoing Work

In further work on the adiabatic electron-phonon interaction, we have recently acquired inelastic neutron scattering data at elevated temperature on the compounds $Mg_{0.75}Al_{0.25}B_2$ and MgB_2 , prepared with ^{11}B . The data are still under analysis, but it appears that these compounds are generally quasi-harmonic. There is an unusual thermal behavior in the MgB_2 spectrum around 70 meV, however, that is not observed for $Mg_{0.75}Al_{0.25}B_2$. This is in the energy range of the e_{2g} modes that seem to be responsible for the strong electron-phonon coupling in this material, but the theory for this material is complex.

We also have data under analysis for the compound ScF_3 , which exhibits anomalously large negative thermal expansion.

More Raman work on oxides at elevated temperature is underway.

We have been awarded beamtime on ARCS for a study of Pd and Pt at elevated temperatures. Although Pd and Pt are not superconductors in pure form, they have significant EPIs, with electron mass enhancement factors, λ , of about 0.69 (Pd) and 0.24 (Pt). We will measure phonons in these metals to temperatures as high as 1500 K. We will also assess the importance of phonon-phonon anharmonicity in these metals.

References

1. O. Delaire, M.S. Lucas, J.A. Munoz, M. Kresch, and B. Fultz, "Adiabatic Electron-Phonon Interaction and High-Temperature Thermodynamics of A15 Compounds," *Phys. Rev. Lett.* **101**, 105504 (2008).
2. O. Delaire, M.G. Kresch, J. Munoz, M.S. Lucas, J.Y.Y. Lin, and B. Fultz, "Electron-Phonon Interactions and High-Temperature Thermodynamics of Vanadium and its Alloys", *Phys. Rev. B* **77**, 214112 (2008).
3. O. Delaire, T. Swan-Wood, and B. Fultz, "Negative entropy of mixing for solutions of vanadium-platinum", *Phys. Rev. Lett.* **93**, 185704 (2004).
4. O. Delaire and B. Fultz, "Charge Redistribution and Phonon Entropy of Vanadium Alloys", *Phys. Rev. Lett.* **97**, 245701 (2006).
5. M. Kresch, O. Delaire, R. Stevens, J.Y.Y. Lin, and B. Fultz, "Neutron scattering measurements of phonons in nickel at elevated temperature", *Phys. Rev. B* **75**, 104301 (2007).
6. M. Kresch, M. Lucas, and B. Fultz, "Phonons in aluminum at high temperatures studied by inelastic neutron scattering", *Phys. Rev. B* **77**, 024301 (2008).
7. M.G. Kresch, Ph.D. Thesis in Materials Science, California Institute of Technology, Dec. 5, 2008.
8. Olivier Delaire, "The Phonon Entropy of BCC Transition Metals and Alloys: Effects of Impurities and of a Martensitic Phase Transition" Ph.D. Thesis in Materials Science, California Institute of Technology, May 12, 2006.
9. C.W. Li, M.M. McKerns, and B. Fultz, "Raman spectrometry study of phonon anharmonicity of hafnia at elevated temperatures," *Phys. Rev. B* **80**, 054304 (2009).
10. C.W. Li, M.M. McKerns, and B. Fultz, "Raman spectrometry study of phonon anharmonicity of zirconia at elevated temperatures," *J. Amer. Ceramic Soc.*, submitted.

3.1. PUBLICATIONS NOT CITED ABOVE (2008-2010)

B. Fultz, "Vibrational Thermodynamics of Materials," *Progress in Materials Science* **55**, 247-352 (2010).

The literature on vibrational thermodynamics of materials is reviewed. The emphasis is on metals and alloys, especially on the progress over the last decade in understanding differences in the vibrational entropy of different alloy phases and phase transformations. Includes nearly 400 references.

J.B. Keith, W. Wang, B. Fultz, and J.P. Lewis, "Ab-initio free energy of vacancy formation and mass-action kinetics in vis-active TiO_2 ," *J. Phys: Condens. Matter* **20**, 022202 (2008). (partially supported by BES)

Matthew S. Lucas, M. Kresch, R. Stevens, and B. Fultz "Phonon Partial Densities of States and Entropies of Fe and Cr in bcc Fe-Cr from Inelastic Neutron Scattering" *Phys. Rev. B* **77**, 184303 (2008).

Matthew S. Lucas, "Cluster Expansion Method Applied to Inelastic Scattering Experiments" Ph.D. in Materials Science, July 25, 2008. (partially supported by BES)

Max G. Kresch, "Temperature Dependence of Phonons in Elemental Cubic Metals Studied by Inelastic Scattering of Neutrons and X-Rays" Ph.D. in Materials Science, Nov. 17, 2008.

M.S. Lucas, O. Delaire, M.L. Winterrose, T. Swan-Wood, M. Kresch, I. Halevy, B. Fultz, J. Hu, M. Lerche, M.Y. Hu, M. Somayazulu, "Effects of Vacancies on Phonon Entropy of B2 FeAl, *Phys. Rev. B* **80**, 214303 (2009).

M.S. Lucas, O. Delaire, M.L. Winterrose, T. Swan-Wood, M. Kresch, I. Halevy, B. Fultz, J. Hu, M. Lerche, M.Y. Hu, M. Somayazulu, "Effects of Vacancies on Phonon Entropy of B2 FeAl, *Phys. Rev. B* **80**, 214303 (2009).

M. S. Lucas, J. A. Munoz, L. Mauger, Chen W. Li, A. Sheets, Z. Turgut, J. Horwath, D. L. Abernathy, M. B. Stone, O. Delaire, and Yuming Xiao and B. Fultz "Effects of chemical composition and B2 order on phonons in bcc Fe-Co alloys *J. Appl. Phys.*, in press. (partially supported by BES)

Polarized ^3He in Neutron Scattering

W.M. Snow, IUCF, 2401 Milo B. Sampson Lane, Bloomington, IN 47408; wsnow@indiana.edu

T.R. Gentile, Stop 8461, NIST, Gaithersburg, MD 20899; thomas.gentile@nist.gov

Program scope

The goal of this program is to extend the technique of polarized neutron scattering into new domains by the development and application of polarized ^3He spin filters. We have developed neutron spin filters based on the large spin dependence of the cross section for neutron capture by ^3He , and applied these devices to a small angle neutron scattering spectrometer (SANS), polarized neutron reflectometers, a thermal energy single crystal diffractometer (SCD), and a thermal energy triple-axis instrument. Two optical pumping methods have been employed to construct these spin filters: spin-exchange (SEOP) and metastability exchange (MEOP). We have made progress in both these methods, but our current focus is on SEOP. In this method, alkali vapor is polarized by optical pumping and the polarization is transferred to the ^3He nuclei during collisions.

This program is carried out by a collaboration that includes Indiana University, the National Institute of Standards and Technology (NIST), Hamilton College, and the Univ. of Wisconsin, along with collaborators at the SNS and LENS. In addition, we welcome the opportunity to interact with other laboratories. Our primary current goals include the application of polarized ^3He -based neutron spin filters to a spin echo small angle neutron scattering spectrometer (SESAME) and wide-angle polarization analysis.

Built upon our past research and development, the NCNR has established a spin filter program that now provides spin filters for SANS, reflectometry, and triple-axis spectrometry (TAS). For TAS, published results include studies of the magnetoelectric effect compound LiCoPO_4 , magnetic order in NdFeAsO , BiFeO_3 in an electric field, and electric field controlled magnetism in the multiferroic system $\text{Ni}_3\text{V}_2\text{O}_8$. SANS experiments on magnetic nanoparticles have revealed new features in their core-shell magnetic morphology. Although diffuse reflectometry is quite challenging, experiments have been conducted on spin-valve ellipse arrays and $\text{Ni}_{80}\text{Fe}_{20}$ stripes on a silicon substrate. At the SNS a polarized ^3He analyzer has been employed on the magnetism reflectometer, and several SNS instruments (HYSPEC, TOPAZ, EQ-SANS, and CNCS) and HFIR instruments (the SCD, TAS, and GP-SANS) envision the use of ^3He polarizers and analyzers. The SNS has set up a polarization group which is charged with developing ^3He spin filters for the SNS. The establishment of these ^3He groups at the NCNR and SNS has realized one of the long-term goals of our research and development program. Connections between all of these ^3He spin filter programs is strong, with the interaction contributing to the development of technology and applications at all laboratories.

Towards New Extremes in Neutron Diffraction

M. Guthrie, R. Boehler, X. Chen & D. Mao

EFree Center, Carnegie Institution of Washington, Washington DC 20015.

C. A. Tulk, A.F. Moreira Dos Santos, J. Molaison & N. Pradham

Spallation Neutron Source, Oak Ridge National Laboratory, Oak Ridge, TN 37831.

The Spallation Neutron Source (SNS) at ORNL is now routinely generating the highest fluxes of pulsed neutrons in the world. The brightness of the source offers a great potential for extreme conditions science, as higher flux equates directly to smaller sample volumes and thereby higher pressures and temperatures. Throughout its 1 year commissioning period, the SNAP high-pressure beamline has been extremely successful, proving itself to be a highly versatile instrument not only for characterizing single-crystal samples, but also powdered and even liquid materials. Most importantly, its capacity to collect high quality data from samples 1-2 orders of magnitude smaller than rival facilities has been demonstrated.

The Carnegie Institution is currently working closely with SNS staff towards the technical challenge of realizing the full potential of the SNAP instrument. In particular, new pressure devices are essential to compress volumes of 1 to 0.1mm³ to pressures exceeding 50 GPa. Furthermore, the implementation of single-crystal diamond windows should facilitate simultaneous laser heating to temperatures exceeding 2000K. These sample environment advances will be coupled with continued optimization of the beamline itself, with “synchrotron-like” alignment and collimation procedures becoming indispensable as sample sizes reduce. We will present an up-to-the-minute summary of current capabilities and development activities.

Photoelectron Spectroscopy of Transuranics

J.J. Joyce (jjoyce@lanl.gov), T. Durakiewicz, K.S. Graham
Los Alamos National Laboratory, Los Alamos, NM 87545

Program Scope

In the arena of complex electronic materials, actinides straddle the middle ground between the more itinerant transition metal compounds and the more localized rare-earth materials. There is a transition from Friedel-like bonding of the 5f electrons in the early actinide elements, to localized, rare-earth-like f-electron character in the actinides beyond Pu. The goal of this program is to advance the understanding of actinide (An) materials through focused experiments on select actinide materials and to couple these experiments to innovative theories for electronic structure. The central focus in understanding actinide materials requires a detailed knowledge of the behavior of the 5f electrons. An essential technique to quantifying f-electron characteristics is photoelectron spectroscopy (PES). This program uses a variety of PES techniques to isolate and quantify the role of the 5f electrons in the electronic structure of actinide materials with a strong emphasis on Pu materials. The emphasis on Pu is dictated by the nature of the 5f electrons in the actinide series. Plutonium is the transition point in the element series between localized and itinerant character for the 5f electrons, additionally, there is a wide range of strongly correlated electron properties in Pu compounds including; covalency in the Mott insulator PuO₂, superconductivity at 18.5 K in PuCoGa₅, and magnetic signatures in the properties of PuSb₂. These Pu compounds have interesting counterparts in uranium as well as some rare-earths but the Pu materials often provide the most dramatic manifestations of complex electronic structure. This program is a subtask of the larger and more broad-ranging Complex Electronic Materials program lead by Joe Thompson. The restricted scope of materials and experimental technique provides for a detailed examination of key materials within the larger context of complex electronic materials.

This program draws on the unique transuranic single crystal growth capabilities available at Los Alamos as well as theoretical research on actinides including Pu both within and beyond Los Alamos. The program takes advantage of single crystal samples of both intermetallic Pu compounds as well as Mott insulators. Using a range of PES approaches, including angle-resolved photoelectron spectroscopy (ARPES), resonance photoemission (RESPES), temperature dependent PES and high energy PES, this program provides detailed spectroscopic data necessary for the development and validation of electronic structure models beyond an independent particle approach. Models for these complex materials include the dynamical mean field theory (DMFT) and the hybrid functional model. The transuranic ARPES capability within this program is the only such capability in the world and thus provides unique insight into the electronic structure of transuranic materials. The transuranic ARPES system was commissioned, and is now operational in the past 18 months with first results for PuSb₂, PuCoGa₅ and PuO₂.

Recent Progress

Kink physics and ARPES in AnSb₂: Both USb₂ and PuSb₂ were investigated using ARPES at low temperature. USb₂ is antiferromagnetic at 200 K while PuSb₂ shows a complicated magnetic signature below 30 K. Analysis of the quasiparticle peak near the Fermi energy of USb₂ revealed a kink 21 meV below the Fermi energy indicative of strong electron correlations. The kink represents a change in slope for the energy vs. crystal momentum dispersion relation. The kink is also observed in the linewidth and asymmetry of the quasiparticle peak. This kink observed in USb₂ may provide a tie to the kink observed in the cuprate materials on a larger energy scale and represents the first observation of kink physics in an f-electron material. First ARPES measurements on PuSb₂ provide preliminary evidence of hybridization between the Pu 5f electrons near the Fermi energy as well as crystal momentum (**k**) dependence. Both **k**-dependence and hybridization are issues of contention in Pu materials with a range of computational efforts favoring a more-localized interpretation for the 5f electrons in both delta Pu and Pu compounds.

Dispersion in PuCoGa₅: The original angle-integrated PES research on the 18.5 K superconductor PuCoGa₅ published in 2003 indicated a dual nature to the 5f electrons with some 5f spectral weight localized 1 eV or more below the Fermi energy while a smaller fraction of 5f intensity was near the Fermi energy and presumed itinerant. This interpretation was challenged recently both theoretically and experimentally with a more localized interpretation for the electronic structure of PuCoGa₅. The first results from ARPES on PuCoGa₅ presented in Figure 1 show clear indication of a quasiparticle peak dispersing through the Fermi energy and should provide sufficient evidence for itinerant character of the 5f electron spectral intensity located near the Fermi surface.

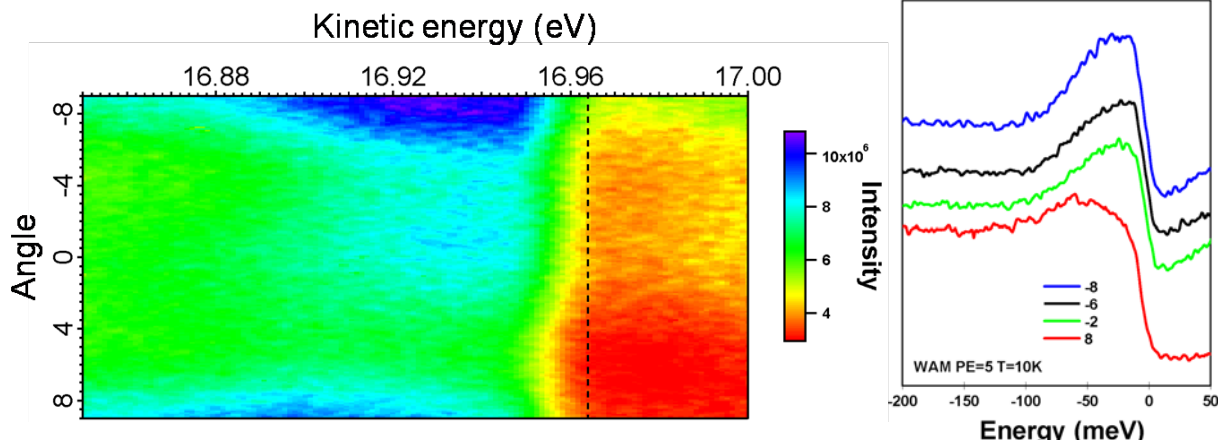


Figure 1: Left frame, kinetic energy vs. crystal momentum for PuCoGa₅ at 10 K. The Fermi level is the dashed black line. Right frame, energy distribution curves (horizontal lines from left frame) show the quasiparticle peak approaching and moving through the Fermi energy from -8 to 8 degrees.

There is an ongoing collaboration to provide DMFT calculations for PuCoGa₅ including energy vs. momentum dependence which could then be directly compared against these ARPES data.

Delta Pu electronic structure: Recent (2010) published results from this program on delta Pu metal provide additional experimental input for continuing collaborations on Pu metal electronic structure which resulted in both DMFT calculations for delta Pu in 2007 and 2008 as well as a first principles calculation with matrix element f-f electron cancellation published in 2008. As there are now a wide range of DMFT calculations (Hubbard I, FLEX, quantum Monte Carlo, one-crossing) and resulting spectral functions for Pu metal and Pu compounds, it is particularly important to provide more detailed experimental constraints for the Pu computational efforts. Photoemission has and will continue to play a central role in providing experimental input used in development and validation of electronic structure models for actinides and Pu.

Actinide oxide ARPES and models: The An oxides are Mott insulators, as such, density functional theory (DFT) fails to predict the insulating character of these materials since DFT does not account for the substantial Coulomb correlation of the 5f electrons. Photoemission was undertaken to quantify the electronic structure of key members of the AnO₂ family of Mott insulators and provide input to new computational schemes to address the Mott insulator problem in actinides. It was first established that single crystal thin films of UO₂ gave the same results as bulk single crystals. Subsequently the large dispersion in the O 2p bands was mapped along with a small (200-400 meV) dispersion in the U 5f levels along with a large energy separation between the 2p and 5f states. This large state separation and the minimal hybridization are consistent with the notion of an ionic solid. Noteworthy is the small 5f dispersion in the U 5f which can not arise from direct f-f overlap as the crystal structure puts too much separation between nearest neighbor uranium's thus the dispersion may well arise from a small amount of hybridization with O 2p which is predicted by the hybrid functional calculation.

Establishing the single crystal thin film capability for the AnO_2 system was essential since there are no bulk single crystals of PuO_2 available for ARPES (mm size) but it is now possible to grow large area single crystal thin films of PuO_2 as well as UO_2 . In figure 2 the PES data is overlaid with the hybrid functional integrated calculations for UO_2 and PuO_2 along with the orbital character breakout. The

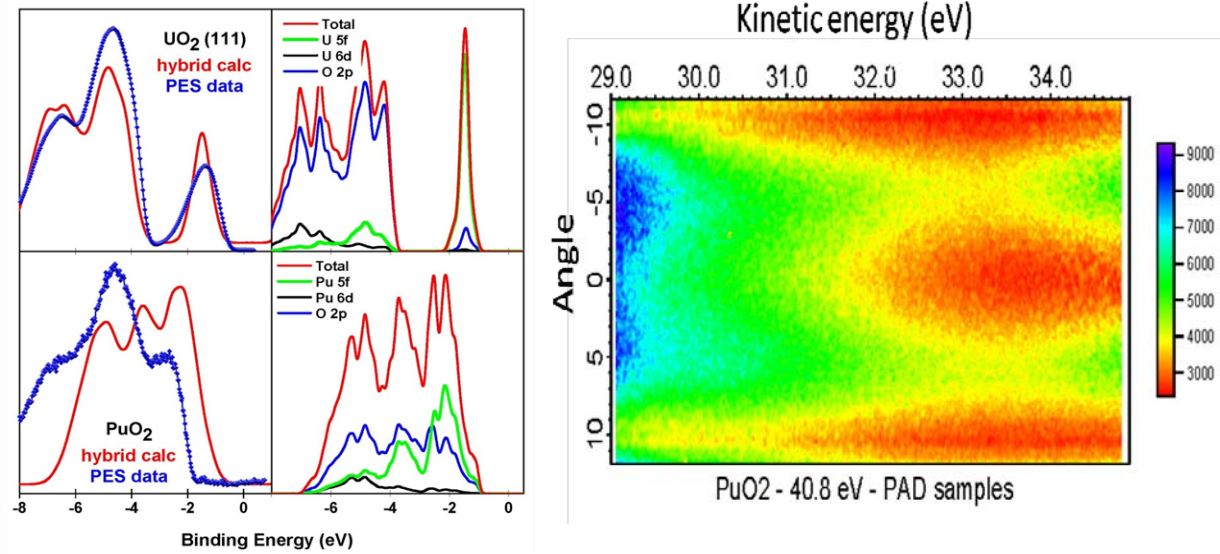


Figure 2: Left quad frame, left side, angle-integrated PES (blue) and hybrid functional calculations (red) capture the separation of O 2p and U 5f and also the hybridization of O 2p and Pu 5f states. Right part of quad frame shows the orbital breakout of the hybrid functional calculations. Right frame shows ARPES for PuO_2 displaying dispersion and intermixing of Pu 5f and O 2p consistent with hybrid functional. The right frame Fermi energy is at 36.6 eV.

agreement between model and experiment is very good and shows the ionic character of UO_2 as well as the change in character moving from UO_2 to PuO_2 . In PuO_2 , the separation between the An 5f states and the O 2p states has gone to zero and there is then strong intermixing between the 5f and 2p states. The angle-integrated PES largely substantiated this model but it was necessary to directly observe the 5f and 2p intermixing in order to validate the model predictions. The ARPES data for PuO_2 in figure 2 provides the direct experimental evidence of this orbital state mixing. The ARPES capability for actinide materials has played a significant role in the development of an effective model for the family of AnO_2 Mott insulators which span the range from ionic to covalent insulators. As a check on the thin film sample integrity, x-ray PES at 1486 eV photon energy was used to demonstrate the Pu 4f and O 1s levels were present in the sample and that the Pu 4f levels showed the characteristic two features for each spin orbit component consistent with previous results for UO_2 .

Future Plans

Having established a transuranic ARPES capability, there are five groups of materials which will require substantial experimental research over the coming years. The first materials category ripe for exploration is the PuMGa_5 ($M=\text{Co, Rh}$) family. With preliminary ARPES on PuCoGa_5 indicating itinerant character of the peak near the Fermi energy, we will need to map out the Fermi surface of PuCoGa_5 both above and below the superconducting transition. Additionally, we will begin a detailed investigation of the 9 K superconductor PuRhGa_5 . Second, the Mott insulators within the actinide oxides will require a sustained effort to both quantify the electronic structure as well as validate theoretical efforts using the hybrid functional approach. The first results for PuO_2 ARPES are encouraging but will necessitate a broader range of ARPES experiments including a range of photon energies. Additionally, research on Pu_2O_3 as the cross-over material will be undertaken using both ARPES and XPS to follow the transition

from ionic to covalent character in the series of the actinide oxides. It may also be possible by use of thin film samples to explore the low temperature characteristics of UO_2 through the antiferromagnetic transition at 31 K. As the third system to explore, we will conduct temperature dependent PES studies of PuTe to compare with the recent dynamical mean field theory predictions of a strong temperature dependence to the three-peak structure near the Fermi energy. PuTe is a starting point for the interesting actinide chalcogenides which, in the Pu monochalcogenides, exhibit an interesting three peak structure associated with the most localized 5f configurations. The fourth group of materials for study is Pu metal, both in the alpha phase and the cubic delta phase stabilized with small additions of trivalent metals. For the Pu metal research we will focus on temperature dependent PES using the new capability of our transuranic endstation, exploring details of electron-phonon coupling. A stretch goal here would be to determine the electronic structure of delta Pu through APRES but we still do not have access to single crystals of delta Pu of sufficient size. The final group of materials for upcoming research would be a family of actinide pnictide compounds which exhibit a range of magnetic ground states.

Publications

1. *5f Electronic Structure and Fermiology of Pu Materials*, J.J. Joyce, T. Durakiewicz, K.S. Graham, E.D. Bauer, D.P. Moore, J.N. Mitchell, J.A. Kennison, T.M. McCleskey, Q. Jia, A.K. Burrell, E. Bauer, R.L. Martin, L.E. Roy, and G.E. Scuseria, *Mat. Res. Soc. Symp. Proc.* *accepted* (2010).
2. *Strong Coupling Approach to Actinide Metals*, C. D. Batista, J. E. Gubernatis, T. Durakiewicz and J. J. Joyce, *Phys. Rev. Lett.* **101**, 016403 (2008).
3. *Observation of a kink in the dispersion of f-electrons*, T. Durakiewicz, P.S. Riseborough, C.G. Olson, J.J. Joyce, E. Bauer, J.L. Sarrao, S. Elgazzar, P. M. Oppeneer, E. Guziewicz, D.P. Moore, M.T. Butterfield, and K.S. Graham, *Euro. Phys. Lett.* **84**, 37003 (2008).
4. *Spectral Properties of δ -Plutonium: Sensitivity to 5f Occupancy*, Jian-Xin Zhu, A.K. McMahan, M.D. Jones, T. Durakiewicz, J.J. Joyce, J.M. Wills, and R.C. Albers, *Phys. Rev. B*, **76**, 245118 (2007).
5. *Controlling Oxidation States in Uranium Oxides Through Crystal Lattice Pinning*, A.K. Burrell, T.M. McCleskey, P. Shukla, H. Wang, T. Durakiewicz, D.P. Moore, C.G. Olson, J.J. Joyce, and Q.X. Jia, *Adv. Mater.* **19**, 3559-3563 (2007).
6. *Quest for Band Renormalization and Self-Energy in Correlated f-Electron Systems*, T. Durakiewicz, P.S. Riseborough, C.D. Batista, Y. Yang, P. M. Oppeneer, J.J. Joyce, E.D. Bauer, and K.S. Graham, *Acta Physica Polonica A* **117**, 264-267 (2010).
7. *Unusual quasiparticle renormalizations from angle resolved photoemission on USb_2* , X. Yang, P.S. Riseborough, T. Durakiewicz, C.G. Olson, J.J. Joyce, E.D. Bauer, J.L. Sarrao, D.P. Moore, K.S. Graham, S. Elgazaar, P. Oppeneer, E. Guziewicz, M.T. Butterfield, *Phil. Mag.* **89** (22-24), 1893-1911 (2009).
8. *Theoretical studies of the Spectral Properties of δ -Plutonium*, Jian-Xin Zhu, A.K. McMahan, M.D. Jones, T. Durakiewicz, J.J. Joyce, J.M. Wills, and R.C. Albers, *Mat. Res. Soc. Symp. Proc.* **1104**, 59-64 (2008).
9. *Dispersion in the Mott insulator UO_2 : A comparison of Photoemission Spectroscopy and screened Density Functional Theory*, L.E. Roy, R.L. Martin, J. Peralta, G.E. Scuseria, T. Durakiewicz, C. G. Olson, J.J. Joyce, E. Guziewicz, *J. of Computational Chemistry*, **29** (13), 2288-2294 (2008).
10. *Localized and Itinerant States in Actinide Materials*, J.J. Joyce, T. Durakiewicz, C.G. Olson, E. Guziewicz, K.S. Graham, D.P. Moore, and L.A. Morales, *Mat. Res. Soc. Symp. Proc.* **986**, pp. 35-40 (2007).
11. *A comparison of bulk-sensitive spectroscopic probes of Yb valence in Kondo systems*, L. Moreschini, C. Dallera, J.J. Joyce, J.L. Sarrao, E.D. Bauer, V. Fritsch, S. Bobev, E. Carpena, G. Monaco, G. Panaccione, P. Lacovig, G. Paolicelli, A. Fondacaro, P. Torelli, and M. Grioni, *Phys. Rev B*, **75**, 035113 (2007).

Investigation of the spin-glass regime between the antiferromagnetic and superconducting phases in $\text{Fe}_{1+y}\text{Se}_x\text{Te}_{1-x}$

N. Katayama¹, S. Ji¹, D. Louca¹, S.-H. Lee¹, M. Fujita², T.J. Sato³, J.S. Wen⁴, Z.J. Xu⁴, G.D. Gu⁴, G. Xu⁴, Z.W. Lin⁴, M. Enoki², S. Chang⁵, K. Yamada² and J.M. Tranquada⁴

1 Department of Physics, University of Virginia, Charlottesville, Virginia 22904, USA

2 Institute for Materials Research, Tohoku University, Sendai 980-8577, Japan

3 ISSP, University of Tokyo, Kashiwa, Chiba 277-8581, Japan

4 Condensed Matter Physics and Materials Science Department,

Brookhaven National Laboratory, Upton, New York 11973, USA

5 NIST Center for Neutron Research, Gaithersburg, Maryland 20899, USA

Research Scope

Following the discovery of superconductivity in Fe-based pnictides, a resurgence of interest in the field of high temperature superconductivity ensued. There has been particular interest in the possible connection between magnetism and superconductivity. In the iron pnictides, an antiferromagnetically ordered phase is in close proximity to optimal superconductivity. In some cases, such as $\text{SmFeAsO}_{1-x}\text{F}_x$ and $\text{Ba}(\text{Fe}_{1-x}\text{Co}_x)_2\text{As}_2$, there is evidence for coexisting antiferromagnetic order and superconductivity. The situation is somewhat different in the chalcogenide system, $\text{Fe}_{1+y}\text{Se}_x\text{Te}_{1-x}$. Here the details are sensitive to the Fe as well as the Se concentration, and we will focus on the situation for minimized excess Fe (i.e. $y \approx 0$). The Néel temperature drops rapidly for $x < \sim 0.1$, but our measurements indicate that bulk superconductivity only appears for $x > \sim 0.4$.

One reason for a difference between the pnictides and chalcogenides concerns the nature of the antiferromagnetic order. To discuss that order, we first have to consider the crystal structure. In the α -PbO structure of $\text{Fe}_{1+y}\text{Se}_x\text{Te}_{1-x}$ (FST), the Fe layers have a square lattice structure; however, the positions of the Se/Te atoms above and below those planes break the translational symmetry. Thus, it is crystallographically appropriate to choose a unit cell with two Fe atoms per layer, such that the lattice parameter is $a \approx 3.8$ Å. We will specify reciprocal lattice vectors, $\mathbf{Q} = (h, k, l)$, in reciprocal lattice units (rlu) of $(2\pi/a, 2\pi/b, 2\pi/c)$. In Fe_{1+y}Te , the long-range SDW state is accompanied by a tetragonal-to-monoclinic (or orthorhombic, depending on y) structural transition. The spin arrangement is ferromagnetic along the b -direction and alternates in a $++--$ fashion along the a -direction, leading to a characteristic wave vector of $(0.5, 0, 0.5)$. For larger y (e.g., $y = 0.14$), the in-plane component of the magnetic wave vector becomes slightly incommensurate. In $\text{Fe}_{1+y}\text{Se}_x\text{Te}_{1-x}$ with $0.25 \leq x \leq 0.33$, static, but short-range, incommensurate magnetic order with $\mathbf{Q}_m = (0.5 - \delta, 0, 0.5)$ is observed. At higher Se concentration, $x > \sim 0.4$, where bulk superconductivity is achieved, a spin resonance at $\hbar\omega \approx 6.5$ meV

appears at incommensurate $Q_c = (0.5 + \delta', 0.5 - \delta', l)$.

The reduction in crystallographic symmetry is important for the magnetic ordering in $Fe_{1+y}Te$. The monoclinic (or orthorhombic) structure provides the magnetic ordering wave vector with a unique orientation within the Fe planes. On the other hand, the short-range magnetic order observed at $x \sim 0.3$ occurs in a tetragonal phase, so that there are two degenerate orientations for Q_m . This suggests that competition among degenerate domains may lead to frustration and keep the ordering short range. A recent study has shown that the crossover to the tetragonal phase occurs between $x = 0.075$ and $x = 0.10$, with long-range magnetic order only for $x \leq 0.075$. Thus, one might expect a transition to short-range SDW order for $x > \sim 0.1$.

Recent Progress

Using bulk magnetization along with elastic and inelastic neutron scattering techniques, we have investigated the phase diagram of $Fe_{1+y}Se_xTe_{1-x}$ and the nature of magnetic correlations in three nonsuperconducting samples of $Fe_{1.01}Se_{0.1}Te_{0.9}$, $Fe_{1.01}Se_{0.15}Te_{0.85}$ and $Fe_{1.02}Se_{0.3}Te_{0.7}$. As shown in Fig.1, the x - T phase diagram is characterized between SDW, SG, SC and paramagnetic metallic phase. A cusp and hysteresis in the temperature dependence of the magnetization for the $x = 0.15$ and 0.3 samples indicates spin-glass (SG) ordering below $T_{sg} = 23$ K. Neutron scattering measurements indicate that the spin-glass behavior is associated with short-range spin density wave (SDW) ordering characterized by a static component and a low-energy dynamic component with a characteristic incommensurate wave vector of $Q_m = (0.46, 0, 0.50)$ and an anisotropy gap of $\Delta \sim 2.5$ meV. Our high Q-resolution data also show that the systems undergo a glassy structural distortion that coincides with the short-range SDW order.

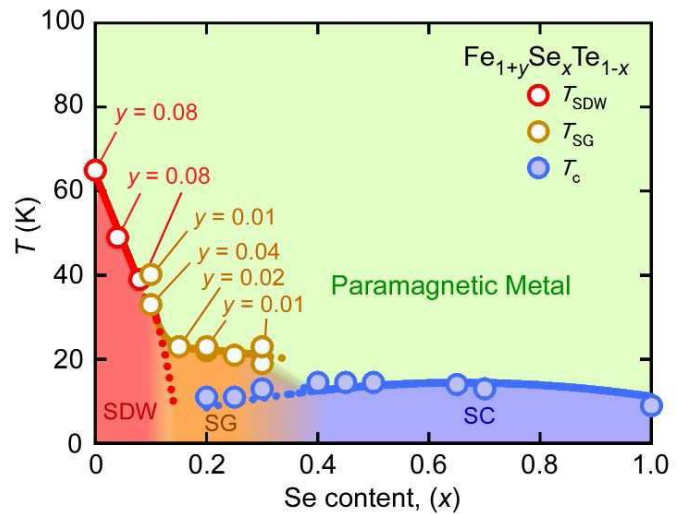


Fig.1 x - T phase diagram of $Fe_{1+y}Se_xTe_{1-x}$

Future Plans

From the high energy excitation study of 11 system, we will understand the nature of the high T_c superconductivity. We will compare $Fe(Se,Te)$ system with $Fe(S,Te)$ system using high quality single crystals.

Publications

- *Investigation of the spin-glass regime between the antiferromagnetic and superconducting phases in $Fe_{1+y}Se_xTe_{1-x}$* , N. Katayama, S. Ji, D. Louca, S.-H. Lee, M. Fujita, T. J. Sato, J. S. Wen, Z. J. Xu, G. D. Gu, G. Xu, Z. W. Lin, M. Enoki, S. Chang, K. Yamada, J. M. Tranquada ; arXiv:1003.4525.
- *Coupling of spin and orbital excitations in an Fe-based superconductor*, S.-H. Lee, Guangyong Xu, W. Ku, J. S. Wen, C. C. Lee, N. Katayama, Z. J. Xu, S. Ji, Z. W. Lin, G. D. Gu, H.-B. Yang, P. D. Johnson, Z.-H. Pan, T. Valla, M. Fujita, T. J. Sato, S. Chang, K. Yamada, J. M. Tranquada, arXiv:0912.3205.

Optics for Advanced Neutron Imaging and Scattering

B. Khaykovich¹

Nuclear Reactor Laboratory, MIT, 77 Massachusetts Ave., Cambridge, MA 02139, USA

M. V. Gubarev²

Marshall Space Flight Center /NASA, Huntsville, AL 35812

Y. Bagdasarova

Department of Physics, MIT, 77 Massachusetts Ave., Cambridge, MA 02139, USA

B. D. Ramsey

Marshall Space Flight Center /NASA, Huntsville, AL 35812

D. E. Moncton³

*Nuclear Reactor Laboratory and Department of Physics, MIT, 77 Massachusetts Ave.,
Cambridge, MA 02139, USA*

I. Program scope

Neutron scattering methods are among the most important tools for studying the structure and dynamics of matter on a wide range of scales from atomic to mesoscopic to macroscopic. The powerful new Spallation Neutron Source (SNS) at Oak Ridge National Laboratory (ORNL) is stimulating new discoveries and creating novel opportunities for research using neutrons. Nevertheless, neutron methods will remain limited, sometimes severely, by available neutron fluxes. The efficient use of existing sources can therefore be as important a path toward more powerful instruments as the development of brighter sources. The tool-box of neutron instrument components is still relatively small, especially compared to that of x-rays, where much brighter and smaller sources are available and the dawn of x-ray lasers is in sight. Manipulating neutron beams is difficult exactly for the same reason that neutrons are so useful for materials science—namely, their weak interaction with matter. Existing neutron components, such as neutron guides and detectors, are constantly improving. However, new techniques for manipulating neutron beams might bring significant, even transformative, improvements of neutron instrumentation, and enable new science. We have initiated a program to develop such a new tool: grazing-incidence mirrors based on full figures of revolution.

In 1952, Hans Wolter described the advantages of glancing-angle mirrors for an x-ray microscope based on the pairing of a con-focal ellipsoid (or a paraboloid when the source is at an infinite distance such as in x-ray telescopes) and hyperboloid. Such mirrors can now be made by a replication technique, which is a mature technology developed for x-ray astronomy applications. This method permits coating the mirrors with a multilayer structure, as done for neutron supermirrors. Two major problems exist with grazing incidence optics. First, collection efficiency is small because of the small critical angle. (The collection area of grazing incidence mirrors is the projection of the mirror surface onto the aperture plane.) Second, grazing incidence mirrors suffer from large aberrations, distorting the image in the focal plane. In our

¹ bkh@mit.edu

² Mikhail.V.Gubarev@nasa.gov

³ dem@mit.edu

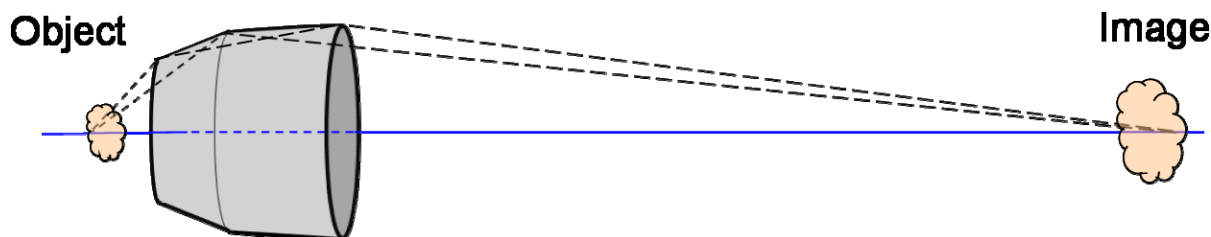


Figure 1. Schematic illustration of a single pair of Wolter mirrors. (The mirrors are confocal hyperboloid and ellipsoid.) In the microscope-like configuration shown here, neutron beam travels from left to right. Magnified image of the object is formed at the focal plane. Only one mirror shell is shown for clarity, but several co-axial shells of the same length should be used to increase collection efficiency.

program we address both issues. First, nesting multiple mirrors increases collection area by placing co-axial mirrors one inside another, as routinely done in x-ray astronomy. A multilayer coating will further increase the critical angle and thus collection efficiency. Second, aberrations are removed by meeting the Abbe sine condition, which requires that all geometrical paths through the optical system produce the same magnification. With grazing incidence optics, the neutrons must undergo two reflections between source and image, which is exactly what occurs in the Wolter design. Eliminating aberrations is important for imaging methods, SANS, and other applications because (i) a true image of an object can be formed and (ii) all the reflected neutrons travel the same distance from source to image, a property important for some time-of-flight applications. (Technically, path length is the same only for neutrons hitting one mirror pair, but in nested configurations the differences are very small). Focusing mirrors are especially important for the SNS instruments, which operate with polychromatic beams.

II. Recent Progress

We developed ray-tracing tools for neutron Wolter optics and demonstrated focusing of a neutron beam by 4 nested Ni mirrors at the MIT Reactor. Figure 1 shows the schematic view of the mirrors. The system is defined by the following initial parameters: the radius at the intersection of two mirrors, the distance from the source focal plane to the intersection, grazing angles at the intersection, magnification and the length of the mirrors. Ray-tracing studies of the mirrors were done using McStas, a standard software package.

Using ray-tracing simulations, the mirrors were optimized for maximum flux at the sample. As an example, we used mirrors with the following characteristics: source-to-sample distances of 10 and 25 m, several magnifications between 0.1 and 1 and critical angle of 21 mrad (corresponding to an $m = 3$ supermirror multilayer coating and 5 meV neutrons). The flux was maximized by changing the mirror intersection radius r_i . We found that the maximal flux density at the sample was about 3 times that of the source for one mirror pair, while a system of 4 nested mirrors collects about 8 times the flux density of the source. Importantly, the image flux grows with r_i until the grazing angle reaches the critical angle; thus, the collection efficiency increases with the critical angle. Therefore, (i) developing supermirror multilayer coating is crucial for successful application of neutron Wolter mirrors, and (ii) for lower-energy neutrons used in many neutron applications, the flux density ratio between the source and the sample will be larger than ten in our examples. In this geometry, maximum flux is achieved at de-magnification

of 0.1; so, a 1 mm sample could be illuminated by a 10 mm source 10 to 25 m away, with the flux density of almost 10 times that of the source.

We made a set of 4 nested ellipsoid-hyperboloid Ni mirrors and studied their performance at the MIT Reactor. The optics have a magnification 4 and the source to detector distance of 3.2 m. A 2 mm diameter Cd aperture was installed as the source of neutrons in one focal plane and the detector captured the image in the second focal plane. The detector is a standard scintillator-based detector with the pixel size of 90 μm . Figure 2 shows the demagnified image of the 2 mm source on the detector 3.2 m away. Calculations confirmed that expected focal spot diameter is 0.5 mm, 4 times smaller than that of the source; corresponding half-power diameter is 0.35 mm. The half-power diameter was measured 0.6 mm. The measured focal spot size is slightly larger than the calculated one due to known distortions of the shells from imperfect mechanical fitting of the mirrors holder during our experiment. Figure 2 shows the result of an experiment when the detector was placed between the optics and the image focal plane. In this case, the optics had two nested mirrors. The image shows two light rings formed by the neutrons that are reflected by each of the two mirrors, confirming that both mirrors contribute to deflecting the beam into the focal spot. Ray-tracing calculations showed that only neutrons below 5 meV can be focused by these Ni mirrors. Coating the optics with supermirror multilayers will significantly increase the energy range of neutrons reflected by the mirrors, and thus available neutron flux.

In conclusion, we produced ray-tracing tools suitable for analyzing and predicting the performance of neutron Wolter mirrors. We also demonstrated the performance of four nested Ni Wolter mirrors of magnification 4 and source-to-image distance of 3.2 m. We showed that the low-energy neutrons from the MIT Reactor can be focused and the focal spot can be detected and measured.

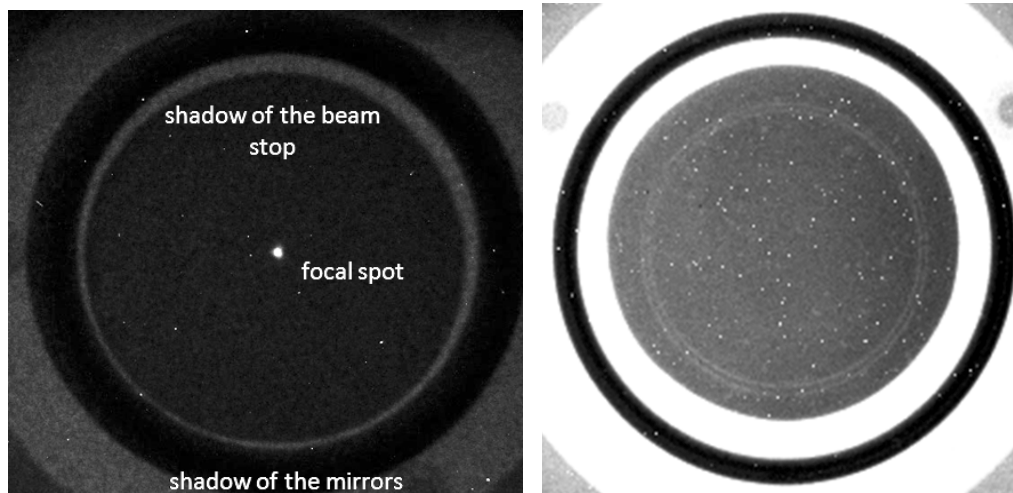


Figure 2. (Left) The image of the focal spot on the neutron detector. The large dark disk around the focal spot is the shadow of the Cadmium beam stop placed at the entrance aperture of the mirrors (25 mm diameter and 2mm thick). The dark ring outside the beam stop is the shadow of the mirrors themselves. (Right) Image of two concentric rings formed by the neutrons reflected by two co-axial nested Wolter mirror pairs. The image is taken when the detector is placed close behind the optics. The darkest outer ring is the shadow of the mirrors. Inside the mirrors there is the gray disk shadow of the beam stop. The two light concentric rings on the background of the beam stop shadow are formed by reflected neutrons. The light background around the mirrors is formed by the neutrons from direct beam.

III. Future plans

A major theme will be to improve collection efficiency. For neutron applications, Wolter mirrors should be either coated with high- m multilayers or nested (or both). A system made of a small number of nested high- m mirrors will collect larger flux than a system made of a large number of Ni mirrors. As we discussed earlier, larger critical angle leads to higher collection efficiency, not easily achievable with nested Ni mirrors. Also, precise alignment of a large number of mirrors is difficult. In addition, neutrons reflected by different nested mirrors will have slightly different path lengths between the source and the image. Therefore, using large number of nested mirrors might decrease the resolution of the TOF methods requiring equal path length.

Therefore, developing a multilayer coating is of utmost importance. The technology for x-ray multilayers, such as W/Si, has been developed already for x-ray astronomy. For neutrons, multilayers such as Ni/Ti, NiC/Ti or possibly even $^{58}\text{Ni}/^{62}\text{Ni}$ will be considered. At the later stage, we will evaluate applying a neutron polarizing supermirror coating, such as Fe/Si multilayer. New multilayers will be made and tested first in the form of flat coupons polished and coated with the same technique as the mandrels which form the mirrors. We will conduct neutron reflectivity, optical and surface studies of the coupons and, later, Wolter mirrors.

Another major theme will be the detailed study of a set of neutron methods to optimize the implementation of Wolter optics. We will optimize optical designs for Wolter mirrors for imaging, considering three configurations: (i) image-forming (objective) lens for absorption imaging, when the mirrors are placed between the sample and detector; (ii) lenses for phase-contrast imaging, placed either between the sample and detector, or between the source and the sample. The sample is illuminated from a small pin-hole and sample-detector distance is as large as possible; (iii) scanning microscope, when the sample is illuminated by a small focal spot. For SANS application, we will simulate a traditional focusing SANS instrument with Wolter mirrors in place of a lens. The chief advantage of such a design is that it is suitable for polychromatic neutron beams at the SNS. Also, double reflection allows collecting larger beam divergence to both enhance the flux and shorten the sample-to-detector distance. However, Wolter mirrors in front of the sample will not illuminate the sample well far from the focal spot. To avoid the problem of illumination, the sample can be placed further away from the mirrors. Also, a sample can be masked in a ring-like shape, adjusting to the illumination pattern behind the mirrors. Finally, we propose a novel optical design concept for a SANS instrument, when the mirrors are between the sample and a detector. Such a design can produce instrument with very high resolution, which does not depend on the size of the sample.

Research supported by the U.S. Department of Energy, Office of Basic Energy Sciences, Division of Materials Sciences and Engineering under Award # DE-FG02-09ER46556.

IV. Publications

B. Khaykovich, M. V. Gubarev, Y. Bagdasarova, B. D. Ramsey, and D. E. Moncton, “From x-ray telescopes to neutron scattering: using axis-symmetric mirrors to focus a neutron beam”. In preparation (2010).

Quantum Critical Behavior in $\text{Ce}(\text{Ni}_{0.935}\text{Pd}_{0.065})_2\text{Ge}_2$

Jon Lawrence

Department of Physics and Astronomy, University of California, Irvine, CA 92697

CuiHuan Wang and Andrew Christianson

Neutron Scattering Science Division, Oak Ridge National Laboratory, Oak Ridge, TN 37831

Eric Bauer

MPA-CMMS, Los Alamos National Laboratory, Los Alamos, NM 87545

Research Scope

In strongly correlated electron systems, a quantum critical point (QCP) can separate an antiferromagnetic (AF) or ferromagnetic (FM) state from a nonmagnetic Fermi liquid state at $T = 0$ K. The nature of this quantum ground state phase transition is one of the biggest open questions in condensed matter physics. In the vicinity of the QCP, the critical fluctuations are of quantum nature and give rise to non-Fermi liquid (NFL) behavior. A spin fluctuation theory has been established to explain the non-Fermi liquid behavior. This theory, implemented through a renormalization-group approach^[1] or through the self-consistent renormalization (SCR) method^[2] has successfully explained various cases of the non-Fermi liquid behavior. However, the experimental results for some systems do not follow this spin fluctuation theory. A locally critical phase transition has been invoked to explain the behavior of these latter systems.^[3] Hence, measurements in other systems are needed to understand the behavior near the QCP.

Heavy Fermion (HF) compounds are very good candidates for studying the QCP. These compounds behave as Fermi Liquids (FL), with large constant values for the specific heat coefficient $\gamma = C/T$ and susceptibility $\chi(0)$, and with the resistivity varying as $\Delta\rho \sim T^2$ at low temperature. When such systems are tuned close to a QCP by adjusting a control parameter such as alloy parameter x , external pressure P , or applied magnetic field H , the AF spin fluctuations affect the thermodynamic behavior and lead to NFL behavior such as $\Delta\rho \sim T^\alpha$ with $\alpha < 2$ and $C/T \sim -\ln T$ at low temperature.

At low temperature, in the interval $1 < T < 4$ K, the tetragonal compound CeNi_2Ge_2 exhibits NFL behavior for the resistivity and specific heat: $\Delta\rho \sim T^{1.28}$ and $C/T \sim \ln T$.^[4] The inelastic neutron scattering shows two low energy features. A broad peak at 4 meV that is only weakly \mathbf{Q} -dependent corresponds to Kondo scattering with $T_K = 46$ K. A peak at 0.7 meV that is highly \mathbf{Q} -dependent and shows a maximum intensity at $\mathbf{Q}_N = (1/2, 1/2, 0)$ corresponds to scattering from antiferromagnetic fluctuations.^[5] Although this compound is clearly close to a QCP, for $T < 0.4$ K the system enters the FL state where C/T saturates to a constant value and $\Delta\rho \sim T^2$.^[4,6] The compound can be brought closer to the QCP by alloying with Pd. According to the phase diagram proposed by Knebel et al^[7] the QCP occurs in $\text{Ce}(\text{Ni}_{2-x}\text{Pd}_x)_2\text{Ge}_2$ when $x = 0.065$. Fukuhara et al^[8] found that when $x = 0.10$, the critical wavevector remains $\mathbf{Q}_N = (1/2, 1/2, 0)$; for larger x it changes to $\mathbf{Q}_N = (1/2, 1/2, 1/6)$.

We have undertaken to study the inelastic neutron scattering of a single crystal of $\text{Ce}(\text{Ni}_{0.935}\text{Pd}_{0.065})_2\text{Ge}_2$. Our goal is to determine key critical exponents for the staggered susceptibility $\chi(\mathbf{Q}_N)$, the inverse coherence length $\kappa(T) \sim 1/\xi$, and the inverse spin fluctuation time $\Gamma(\mathbf{Q}_N) \sim 1/\tau$. We note that the dynamic exponent z , which to our knowledge has never been measured near a QCP, can be obtained from the temperature dependence of κ and $\Gamma(\mathbf{Q}_N)$ through the relation $\Gamma \sim \xi^{-z}$.

Recent Progress:

We successfully grew a large (~ 10 gram) crystal of $\text{Ce}(\text{Ni}_{0.935}\text{Pd}_{0.065})_2\text{Ge}_2$ by the Czochralski method. The crystal was grown with 58-Ni to reduce the incoherent scattering. In Fig. 1 we plot the specific heat coefficient C/T . The data is logarithmic with temperature in the range 1 K to 5 K. When an external field is applied, the data deviates from the $\ln T$ behavior and shows saturation. This is because the magnetic field forces the system to enter the FL state. However, in the inset of Figure 1, the low temperature ($T < 1\text{K}$) data can be seen to fit the form $\gamma(T) = \gamma(0) - a T^{1/2}$ with $\gamma(0) \sim 695 \text{ mJ/mole-K}^2$. The resistivity $\rho(T)$ is roughly linear in temperature over a wide range 1 to 12 K, indicating NFL behavior, but below 0.8 K the resistivity varies as $\rho(T) \sim \rho(0) + AT^{3/2}$ (Fig. 2). Hence, at temperatures higher than 2 K, this alloy exhibits typical NFL behavior, with the resistivity varying as $\rho \sim T$ and the specific heat varying as $C/T \sim \ln T$, but at temperatures below 1 K $\rho \sim T^{3/2}$ and $C/T \sim \gamma(0) - a T^{1/2}$. This is the behavior predicted by SCR theory for a three dimensional antiferromagnet at a QCP.

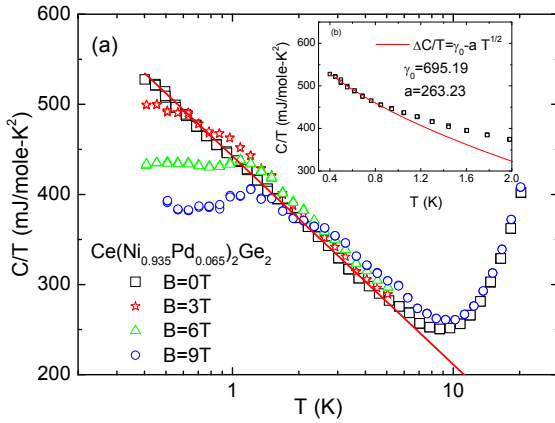


Fig. 1 Specific heat coefficient C/T of $\text{Ce}(\text{Ni}_{0.935}\text{Pd}_{0.065})_2\text{Ge}_2$ in several magnetic fields.

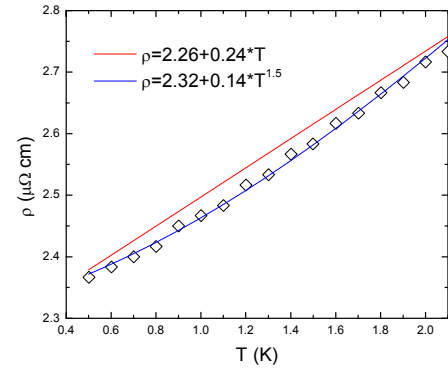


Fig. 2 Low temperature resistivity of $\text{Ce}(\text{Ni}_{0.935}\text{Pd}_{0.065})_2\text{Ge}_2$.

We measured the inelastic scattering of this crystal on three spectrometers: SPINS, MACS, and CNCS, the data being essentially identical in all three cases. A broad peak near 1.5 meV (not shown here) is only weakly \mathbf{Q} -dependent; this peak can be fit by an inelastic Lorentzian with position $E_1 = 1.51 \text{ meV}$ and width $\Gamma_1 = 0.90 \text{ meV}$. As for the 4 meV peak in CeNi_2Ge_2 , we identify this as representing Kondo scattering; equating $E_1 = k_B T_K$, we have $T_K = 17.5 \text{ K}$. We note that T_K appears to be finite at the QCP, consistent with spin fluctuation theory^[1,2] but not with local criticality.^[3]

Near $\mathbf{Q} = (1/2, 1/2, 0)$, extra intensity is observed when $\Delta E < 1 \text{ meV}$ (Fig. 3). As can be seen from Fig. 4, this extra intensity is strongly peaked in the vicinity of $(1/2, 1/2, 0)$. This is the wavevector of the antiferromagnetic fluctuations seen for CeNi_2Ge_2 near 0.7 meV, hence we identify it as the critical wavevector \mathbf{Q}_N for the QCP. We can fit this spectrum to a quasi-elastic Lorentzian with peak width $\Gamma(\mathbf{Q}_N)$ and amplitude $\chi(\mathbf{Q}_N)$; at 0.4 K, we find $\Gamma(\mathbf{Q}_N) = 0.4 \text{ meV}$.

The linewidth $\Gamma(\mathbf{Q}_N)$ is the inverse of the correlation lifetime τ of the critical fluctuations and $\chi(\mathbf{Q}_N)$ is the staggered susceptibility. Their temperature dependence thus manifests critical behavior near the QCP. We have measured the temperature dependence of these quantities. As can be seen in Fig. 5, the data from the three spectrometers is consistent. Both the inverse staggered susceptibility $\chi(\mathbf{Q}_N)^{-1}$ and the inverse correlation time $\Gamma(\mathbf{Q}_N)$ appear to vary as $C + D T^{3/2}$. Such $T^{3/2}$ behavior is expected based on the SCR theory.^[2]

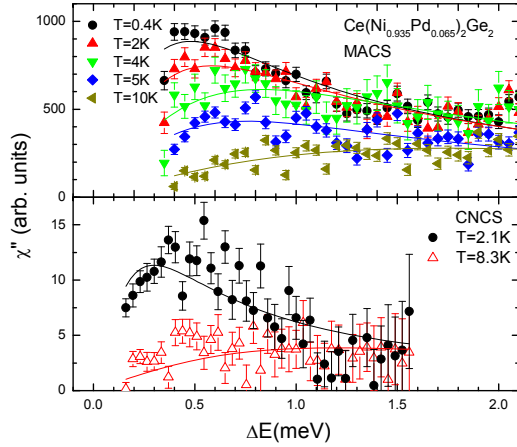


Fig. 3 Inelastic neutron scattering spectra of $\text{Ce}(\text{Ni}_{0.935}\text{Pd}_{0.065})_2\text{Ge}_2$ at the critical wavevector $\mathbf{Q}_N = (1/2, 1/2, 0)$ and at several temperatures. (a) Data taken on MACS; (b) Data taken on CNCS.

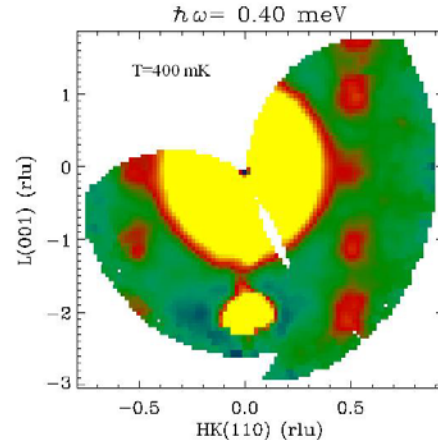


Fig. 4 Scattering from $\text{Ce}(\text{Ni}_{0.935}\text{Pd}_{0.065})_2\text{Ge}_2$ seen on MACS in the (H,H,L) scattering plane at 0.4 K for fixed energy transfer $\Delta E = 0.4$ meV.

While the SCR theory thus appears to do a good job in predicting the exponents of the resistivity, specific heat, staggered susceptibility, and correlation time of this alloy, we need to point out a very serious discrepancy: neither $\chi(\mathbf{Q}_N)$ nor $\tau \sim 1/\Gamma(\mathbf{Q}_N)$ diverges at the QCP. Such a "saturation" of the spin fluctuation lifetime and staggered susceptibility to a finite value has been observed for other HF systems where the QCP is attained by alloying^[8] and may arise from the fact that the QCP occurs in a disordered environment.^[9]

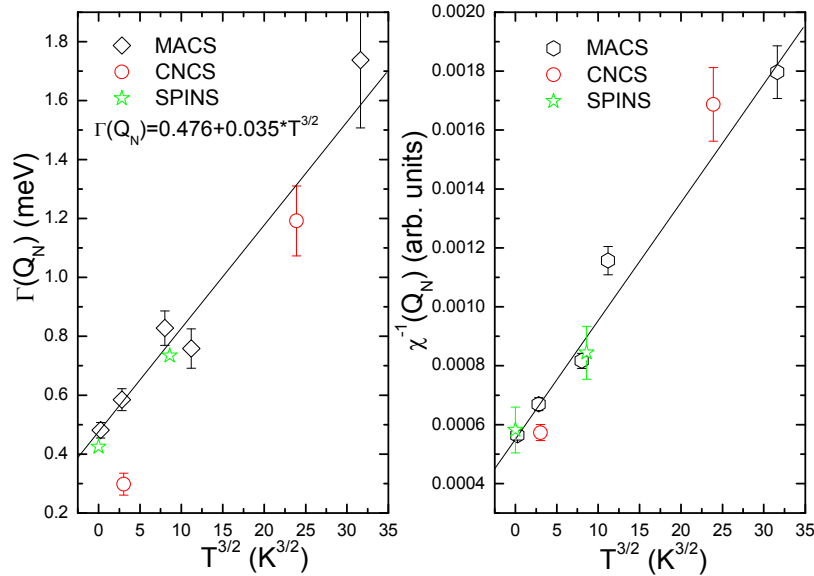


Fig. 5 The inverse staggered susceptibility $\chi''(\mathbf{Q}_N)^{-1}$ and the inverse correlation time $\Gamma(\mathbf{Q}_N)$ of $\text{Ce}(\text{Ni}_{0.935}\text{Pd}_{0.065})_2\text{Ge}_2$ versus temperature, as measured on three spectrometers.

Future Plans:

We plan to re-measure the inelastic scattering in the vicinity of the critical wavevector \mathbf{Q}_N , and analyze the data using the formula $\chi''(\mathbf{Q}, \Delta E) = \{\chi(\mathbf{Q}_N)/[|\mathbf{Q}-\mathbf{Q}_N|^2 + \kappa^2]\} * \{\Gamma_Q \Delta E / [\Delta E^2 + \Gamma_Q^2]\}$. By fixing $\mathbf{Q} = \mathbf{Q}_N$ and measuring on a single spectrometer at a larger number of temperatures than seen in Figs. 3 and 5, we

hope to do a better job of characterizing the temperature dependence of $\chi(\mathbf{Q}_N)$ and $\Gamma(\mathbf{Q}_N)$. To obtain the temperature dependence of the coherence length $\xi \sim 1/\kappa(T)$, we will need to determine the full surface of scattering, i.e. χ'' as a function of both \mathbf{Q} and ΔE in the vicinity of \mathbf{Q}_N . This can be accomplished either by performing a series of angular scans around \mathbf{Q}_N for various fixed energy transfers, or by obtaining energy spectra at a series of \mathbf{Q} in the vicinity of \mathbf{Q}_N . Either MACS or CNCS should be useful for this purpose. Using the relation $\Gamma \sim \xi^{-z}$ we will then determine the dynamic exponent z , which to our knowledge has never been measured near a QCP, as mentioned above.

1. A.J. Millis, Phys. Rev. B **48** (1993) 7183.
2. T. Moriya and T. Takimoto., Journ. Phys. Soc. Japan **64** (1005) 960.
3. Q. Si et al, 2001 Nature **413** (2001) 804.
4. F. Steglich et al, J. Phys. Condens. Matter **8** (1996) 9909.
5. H. Kadowaki et al, Phys. Rev. B **68** (2003) 140402.
6. S. Koerner et al, Journ. Low Temp. Phys. **119** (2000) 147.
7. G. Knebel et al, Phys. Rev. B **59** (1999) 12390.
8. T. Fukuhara et al, Journ. Phys. Soc. Japan **71** (2002) 1360.
9. W. Knafo et al, Phys. Rev. B **70** (2004) 174401.
10. T. Heitmann et al, Phys. Rev. B **81** (2010) 014411.

DOE-funded Publications FY 07-09 and accepted papers:

- Low temperature behavior of the heavy Fermion $\text{Ce}_3\text{Co}_4\text{Sn}_{13}$, A.D. Christianson, J.S. Gardner, H.J. Kang, J.-H. Chung, S. Bobev, J.L. Sarrao and J.M. Lawrence, Journal of Magnetism and Magnetic Materials **310** (2007) 266.
- Crystal field excitations in the singlet ground state compound Pr_3In , A.D. Christianson, J.M. Lawrence, K.C. Littrell, E.A. Goremychkin, A.I. Kolesnikov, J.D. Thompson and J.L. Sarrao, Journal of Applied Physics **101** (2007) 09D505.
- Inelastic magnetic neutron scattering in CePd_3 , J.M. Lawrence, V.R. Fanelli, E.A. Goremychkin, R. Osborn, E.D. Bauer, K.J. McClellan and A.D. Christianson, Physica B **403** (2008) 783.
- Neutron diffraction study of magnetic field induced behavior in the heavy Fermion $\text{Ce}_3\text{Co}_4\text{Sn}_{13}$, A.D. Christianson, E.A. Goremychkin, J.S. Gardner, H.J. Kang, J.-H. Chung, P. Manuel, J.D. Thompson, J.L. Sarrao, and J.M. Lawrence, Physica B **403** (2008) 909.
- Magnetic order in the induced magnetic moment system Pr_3In , V.R. Fanelli, A.D. Christianson, M. Jaime, J.D. Thompson, H.S. Suzuki and J.M. Lawrence, Physics B **403** (2008) 1368.
- Simplifying strong electronic correlations in uranium: Localized uranium heavy Fermion $\text{UM}_2\text{Zn}_{20}$ ($M = \text{Co}, \text{Rh}$) compounds, E.D. Bauer, C. Wang, V.R. Fanelli, J.M. Lawrence, E.A. Goremychkin, N.R. de Souza, F. Ronning, J.D. Thompson, A. Silhanek, V. Vildosola, A.M. Lobos, A.A. Aligia, S. Bobev, and J.L. Sarrao, Physical Review B **101** (2008) 115120.
- Intermediate valence metals, J. M. Lawrence, Modern Physics Letters **22** (2008) 1273.
- Transition from heavy Fermion to mixed valence behavior in $\text{Ce}_{1-x}\text{Y}_x\text{Al}_3$: A quantitative comparison with the Anderson impurity model, E.A. Goremychkin, R. Osborn, I.L. Sashin, P. Riseborough, B.D. Rainford, D.T. Adroja, and J.M. Lawrence, Physical Review Letters **104** (2010) 176402.
- Kondo behavior, ferromagnetic correlations, and crystal fields in the heavy Fermion compounds Ce_3X ($X = \text{In}, \text{Sn}$), C.H. Wang, J.M. Lawrence, A.D. Christianson, E.A. Goremychkin, V.R. Fanelli, K. Gofryk, E.D. Bauer, F. Ronning, J.D. Thompson, N.R. DeSouza, A.I. Kolesnikov, and K.C. Littrell, arXiv:1003.3462 (2010). (Accepted for Physical Review: BQ11114)

Neutron Scattering Study of Geometrically Frustrated Spinels and Unconventional Superconductors

A. Research Scope

Our research is to examine the effects of competing interactions and phases that are ubiquitous in complex materials using neutron scattering. Systems of interest are geometrically frustrated magnets, quantum magnets, and novel superconductors. Geometrically frustrated magnets, where competing interactions arise purely due to topology of the magnetic lattice, provide us a unique opportunity to study the physics of frustration, such as the elementary low lying excitations in the presence of a macroscopic ground state degeneracy and novel mechanism to lift the frustration. The newly discovered Fe-based pnictide superconductors show a number of similarities to and differences from the most well-known unconventional superconducting cuprates. In both systems, the relation between magnetism and superconductivity seems to hold the key to understanding the microscopic mechanisms for the superconductivity. We study how the magnetic ground state evolves as the nature of the charge carrier changes, by performing neutron scattering experiments on an ambipolar cuprate $Y_{1-2}La_2(Ba_{1-x}La_x)_2Cu_3O_y$ (YLBCO), a superconducting Fe pnictide $FeTe_{1-x}Se_x$.

B. Research Highlights

B.1 Geometrically Frustrated Magnets

Microscopic Mechanism of the Spin-Lattice Coupling in a highly frustrated magnet. Cr-based spinel compounds ACr_2O_4 ($A = Mg, Zn, Cd, \text{ and } Hg$) are so far the best model systems for a network of corner-sharing tetrahedrons with isotropic nearest-neighbor antiferromagnetic interactions. The system undergoes a phase transition at a non-zero temperature from a cubic paramagnetic state to a tetragonal (or orthorhombic) Neel state.[R1, R16] The exact nature of the lattice distortion, and the one-to-one-correspondence between the distortion and the magnetic ground state has been a long-standing issue in the field of frustration. We have recently determined the complex crystal and magnetic structures of the tetragonal phase of the geometrically frustrated spinel $ZnCr_2O_4$. [R13] To unveil the mystery, we have performed synchrotron x-ray diffraction measurements on a single crystal, neutron diffraction measurements on a powder sample, and polarized neutron diffraction measurements on a single crystal. Our detailed analysis of the single crystal x-ray data showed that below T_N the symmetry of the crystal structure is lowered from the cubic to the tetragonal with doubled unit cell along a, b and c crystallographic axes forming a complex pattern of Cr-Cr clustering. On the base of structural information, 32 equivalent magnetic structures that reproduce neutron powder diffraction pattern matched with data were determined by the group theoretical analysis. Antiferromagnetic pairs in the obtained magnetic structures do not exactly coincide with the pattern of lattice distortion, which calls for theoretical works that go beyond the nearest neighbor exchange interactions to explain the spin-lattice coupling in this highly frustrated magnet.[R13]

Field-induced quantized magnetization states in highly frustrated spinels. When an external magnetic field is applied in the Neel state of $CdCr_2O_4$ and $HgCr_2O_4$, magnetic field-induced half magnetization plateau states emerge above a critical field and are stable over a wide range

of field. We performed both neutron and synchrotron X-ray diffraction measurements on HgCr_2O_4 under an external magnetic field to understand the plateau states. Our results show that at the field-induced transition crystal structure as well as magnetic structure changes to a structure with $P4_332$ symmetry, suggesting that the structural distortion stabilizes the plateau state. We have recently performed neutron diffraction measurements on CdCr_2O_4 up to 30 T using a newly developed pulsed magnet.[R15] We found that the magnetic structure in the plateau phase also shows $P4_332$ symmetry, indicating that the field-induced spin-lattice coupling mechanism is universal in the Cr-based spinels.

B.2 Quantum Magnetism

Bose-Einstein Condensation of Magnons in $\text{Ba}_3\text{Cr}_2\text{O}_8$. For the past two decades, the field of quantum magnets has provided a number of new exotic collective phenomena. Progress has always been moderated by the availability of suitable spin 1/2 materials with distinct structural motifs. The ubiquitous Cu^{2+} ($3d^9$, $s = 1/2$) ion is often relied upon as the platform for new materials design. Magnetic field-induced quantum phase transitions are a typical example. The field-induced condensation of magnons have been experimentally observed in coupled quantum ($s = 1/2$) dimer systems based on Cu^{2+} ions, such as TiCuCl_3 and $\text{BaCuSi}_2\text{O}_6$, which are adequately described by the Bose-Einstein condensation (BEC) theory.

We have synthesized at our laboratory, in collaboration with Prof. Ueda's group at ISSP, single crystals of a new Cu-less quantum magnet $\text{Ba}_3\text{Cr}_2\text{O}_8$. Combined inelastic neutron scattering and electron spin resonance (ESR) in collaboration with Prof. Nojiri at IMR, Tohoku University allowed us to determine the effective spin-hamiltonian of the new system: the effective spin Hamiltonian has spatially anisotropic exchange interactions due to Jahn-Teller distortion and an intradimer Dzyaloshinsky-Moriya (DM) interaction with a DM vector perpendicular to the crystallographic c -axis.[R9, R11] We have also performed elastic neutron scattering and specific heat measurements under an external magnetic field (H) near the quantum critical point of condensation and found that the H - T phase boundary follows the power-law predicted by the BEC theory.[R11]

Exotic Quantum States in $\text{Cu}_{4-x}\text{Zn}_x(\text{OD})_6\text{Cl}_2$. Over the last two decades or so, frustrated magnets have been studied as excellent systems to look for exotic quantum spin liquid states because of their intrinsic macroscopic ground state degeneracy. Recently $\text{Zn}_x\text{Cu}_{4-x}(\text{OD})_6\text{Cl}_2$ has been proposed as an ideal candidate for the quantum ($S = 1/2$) kagome system where quantum spins form a two-dimensional network of corner-sharing triangles. Our neutron diffraction studies, however, have found that $\text{ZnCu}_3(\text{OD})_6\text{Cl}_2$ with rhombohedral symmetry realizes a perfect kagome lattice but with $\sim 10\%$ nonmagnetic site disorder. Furthermore, when Zn ions are replaced by Cu ions, $\text{Zn}_x\text{Cu}_{4-x}(\text{OD})_6\text{Cl}_2$ with $x < 0.3$, becomes monoclinic $P2_1/n$ due to the Jahn-Teller effects of Cu^{2+} ion. This leads to different bond angles for different Cu-O-Cu superexchange paths in such a way that the kagome lattice is distorted to have nonuniform nearest neighbor interactions and the interplane coupling between the kagome and triangular planes is expected to be weak. Thus $\text{Zn}_x\text{Cu}_{4-x}(\text{OD})_6\text{Cl}_2$ realizes a good two-dimensional quantum spin system for all x but it does have defects with regards to an ideal kagome quantum antiferromagnet: for $x = 1$ the nonmagnetic site disorder while for $x = 0$ the nonuniform coupling constants. Our bulk magnetization, and elastic and inelastic neutron scattering measurements under an external magnetic field on $\text{Cu}_2(\text{OD})_3\text{Cl}$ show that the ordered state below 6.7 K is a canted anti-

erromagnet and consists of large antiferromagnetic *ac*-components and a smaller ferromagnetic *b*-component. By first-principle calculations and linear spin wave analysis, we present a simple spin hamiltonian with non-uniform nearest neighbor exchange interactions resulting in a system of coupled spin trimers with a single-ion anisotropy that can qualitatively reproduce the spin dynamics of $\text{Cu}_2(\text{OD})_3\text{Cl}$. [R5]

B.3 Superconductivity

Incommensurate spin resonance in an iron superconductor. Magnetic excitations and electronic structures hold the key to understanding the microscopic mechanism for the unconventional superconductivity that was recently discovered in iron pnictide superconductors. A spin excitation mode that is highly localized in momentum and energy space, called spin resonance, has been observed to appear in the superconducting phase of a number of the Fe-based superconductors, which is due to nesting of the Fermi surface of the electron states near (0,0), and the hole states near (p,0) – using the chemical unit cell containing one Fe. Our inelastic neutron scattering and photoemission data obtained from a superconducting single crystal of $\text{FeTe}_{0.5}\text{Se}_{0.5}$, and *ab initio* calculations revealed highly anomalous behaviors in the low energy magnetic excitations and electronic Fermi surface. The neutron spin resonance with a characteristic energy of 6.5 meV in the superconducting phase is incommensurate around (p,0). Our photoemission and *ab initio* calculation results are consistent with the neutron data. We are in the process of analyzing the data in a more detail. [R18]

C. Future Plans

We will study unconventional superconducting and their isostructural materials using neutron scattering. The newly discovered Fe-based pnictide superconductors show a number of similarities to and differences from the most well-known unconventional superconducting cuprates. In both systems, the relation between magnetism and superconductivity seems to hold the key to understanding the microscopic mechanisms for the superconductivity. We will focus on two systems: a superconducting Fe pnictide $\text{FeTe}_{1-x}\text{Se}_x$ and nonsuperconducting (La,Ce)MnAsO. Large single crystals of the new Fe-based superconductors are now beginning to be available in the chemical form of $\text{Fe}_{1.01}\text{Te}_{1-x}\text{Se}_x$, which allows us to investigate in detail the relation between magnetism and superconductivity using intensity-limited inelastic neutron scattering techniques. We will study how the magnetic correlations and lattice vibrations change upon doping Se by performing elastic and inelastic neutron scattering experiments on the system with several Se concentrations representing the spin-density-wave, the spin-glass and the superconducting phases. (La,Ce)MnAsO that is non-superconducting but isostructural to the superconducting (La,Ce)FeAsO system will also be studied for this project.

D. Publications (FY05-FY09)

- R1** *Neel to Spin-Glass-like Phase Transition versus Dilution in Geometrically Frustrated $\text{ZnCr}_{2-2x}\text{Ga}_{2x}\text{O}_4$* , S.-H. Lee, W. Ratcliff, Q. Huang, T. H. Kim, S.-W. Cheong, Phys. Rev. B **77**, 014405 (2008).
- R2** *Magnetic excitations and orbital physics in ferrimagnetic spinel, MnB_2O_4 ($B = \text{Mn}, \text{V}$)*, J.-H. Chung, J.-H. Kim, S.-H. Lee, T. J. Sato, T. Katsufuji, Phys. Rev. B **77**, 054412 (2008).
- R3** *Frustrated minority spins in GeNi_2O_4* , M. Matsuda, J.-H. Chung, S. Park, T. J. Sato, K. Matsuda, H. Aruga-Katori, H. Takagi, K. Kakurai, K. Kamazawa, Y. Tsunoda, I. Ka-

- gomiya, C. L. Henley, S.-H. Lee, *Europhys. Lett.* **82**, 37006 (2008).
- R4** *Neutron scattering study of the oxyprictide superconductor $La(O,F)FeAs$* , Y. Qiu, M. Kofu, W. Bao, S.-H. Lee, Q. Huang, T. Yildirim, J. R. D. Copley, J. W. Lynn, T. Wu, G. Wu, X. H. Chen, *Phys. Rev. B* **78**, 052508 (2008).
- R5** *External magnetic field effects on a distorted kagome antiferromagnet*, J.-H. Kim, S. Ji, S.-H. Lee, B. Lake, T. Yildirim, H. Nojiri, K. Habicht, Y. Qiu, K. Kiefer, *Phys. Rev. Lett.* **101**, 107201 (2008).
- R6** *Spin and charge order in single-layered perovskite cobaltates*, N. Sakiyama, Y. Mitsui, H. Yoshizawa, I. A. Zaliznyak, S.-H. Lee, *J. Kor. Phys. Soc.* **53**, 995 (2008).
- R7** *Spiral spin structures and origin of the magneto-electric coupling in YMn_2O_5* , J.-H. Kim, S.-H. Lee, S. I. Park, M. Kenzelmann, J. Schefer, J.-H. Chung, C. F. Majkrzak, M. Takeda, S. Wakimoto, S. Y. Park, S.-W. Cheong, M. Matsuda, H. Kimura, Y. Noda, K. Kakurai, *Phys. Rev. B* **78**, 245115 (2008).
- R8** *Low-energy spin fluctuations in the ground states of electron-doped $Pr_{1-x}LaCe_xCuO_4$ cuprate superconductors*, M. Fujita, M. Matsuda, S.-H. Lee, M. Nakagawa, K. Yamada, *Phys. Rev. Lett.* **101**, 107003 (2008).
- R9** *Weakly coupled $s = 1/2$ quantum spin singlets in $Ba_3Cr_2O_8$* , M. Kofu, J.-H. Kim, S. Ji, S.-H. Lee, H. Ueda, Y. Qiu, H. J. Kang, M. Green, Y. Ueda, *Phys. Rev. Lett.* **102**, 037206 (2009).
- R10** *Hidden quantum spin gap state in the static stripe phase of $La_{2-x}Sr_xCuO_4$* , M. Kofu, S.-H. Lee, M. Fujita, H.-J. Kang, H. Eisaki, K. Yamada, *Phys. Rev. Lett.* **102**, 047001 (2009).
- R11** *Magnetic field-induced phase transitions in a weakly coupled $s = 1/2$ quantum spin dimer system $Ba_3Cr_2O_8$* , M. Kofu, H. Ueda, H. Nojiri, Y. Oshima, T. Zenmoto, K. Rule, S. Gerischer, B. Lake, C. D. Batista, Y. Ueda, S.-H. Lee, *Phys. Rev. Lett.* **102**, 177204 (2009).
- R12** *Neutron scattering investigation of the magnetic order in single crystalline $BaFe_2As_2$* , M. Kofu, Y. Qiu, W. Bao, S.-H. Lee, S. Chang, T. Wu, and X. H. Chen, *New J. Phys.* **11**, 055001 (2009).
- R13** *Spin-lattice order in frustrated $ZnCr_2O_4$* , S. Ji, S.-H. Lee, C. Broholm, O. Tchernyshov, T. Y. Koo, W. Ratcliff, S.-W. Cheong, P. Zachack, *Phys. Rev. Lett.* **103**, 037201 (2009).
- R14** *Glassy spin freezing and gapless spin dynamics in a spatially anisotropic triangular antiferromagnet Ag_2MnO_2* , S. Ji, J.-H. Kim, Y. Qiu, M. Matsuda, H. Yoshida, Z. Hiroi, M. A. Green, T. Ziman, to appear in *Phys. Rev. B*, arXiv:0907.3157 (2009).
- R15** *Universal magnetic structure of the half-magnetization phase in Cr-based spinels*, M. Matsuda, K. Ohoyama, S. Yoshii, H. Nojiri, P. Frings, F. Duc, B. Vignolle, G. L. J. A. Rikken, L.-P. Regnault, S.-H. Lee, H. Ueda, Y. Ueda, submitted to *Phys. Rev. Lett.*, arXiv:0907.4835 (2009).
- R16** *Frustrated magnetism and cooperative phase transitions in spinels*, S.-H. Lee, H. Takagi, D. Louca, M. Matsuda, S. Ji, H. Ueda, Y. Ueda, T. Katsufuji, C. Broholm, an invited review article on spinels, to appear in *J. Phys. Soc. Jpn.* (2009).
- R17** *Lattice vibration modes in $CdCr_2O_4$* , J.-H. Kim, M. Matsuda, S.-H. Lee, H. Ueda, Y. Ueda, J.-H. Chung, S. Tsutsui, A. Baron, in preparation for *Phys. Rev. B*. (2009).
- R18** *Structure of the spin resonance and Fermi surface of an iron superconductor*, S.-H. Lee, G. Xu, W. Ku, J. Wen, N. Katayama, Z. Xu, S. Ji, G. Gu, H. Yang, P. Johnson, M. Fujita, T. J. Sato, S. Chang, K. Yamada, J. M. Tranquada, *Phys. Rev. B*, inpress (2010).
- R19** *Zero-doping state and electron-hole asymmetry in an ambipolar cuprate*, K. Segawa, M. Kofu, S.-H. Lee, I. Tsukada, H. Hiraka, M. Fujita, S. Chang, K. Yamada, Y. Ando, *Nature Physics*, in press (2010).

Neutron Scattering Studies of Vortex Matter in Type-II Superconductors

X. S. Ling (xsling@brown.edu), Helen A. Hanson, Xi Wang, I.K. Dimitrov, J. Shi

Department of Physics, Brown University, Providence RI 02912, USA

B.B. Maranville, C.F. Majkrzak

NIST Center for Neutron Research, Gaithersburg, MD 20899, USA

M. Laver

Paul Scherrer Institut, Villigen PSI, CH 5232 Switzerland

U. Keiderling, M. Russina

Helmholtz Zentrum Berlin für Materialien und Energie GmbH, 14109 Berlin, Germany

Program Scope

The vortex matter in type-II superconductors provide a convenient model system for addressing fundamental questions in condensed matter physics concerning the effects of random pinning and quenched disorder. The classical Larkin-Imry-Ma analyses suggested that in any real physical system with a continuous order parameter, long-range order cannot exist in the presence of random pinning. However, more rigorous theoretical work later by Nattermann, Giamarchi, Le Doussal predicted that a Bragg glass phase, a novel solid matter with topological order, can exist in the vortex states of type-II superconductors (e.g. Nb and YBCO single crystals) with weak random pinning. In addition to addressing the basic issues, the vortex matter physics also provides insights into the useful properties of superconductors, such as critical current.

Since the vortex lines are embedded inside the atomic lattice, neutron scattering is the only experimental technique capable of probing the bulk structural information of the vortex matter. The science goal of this program is to use high-resolution (in q) neutron scattering to directly probe the long-wavelength regime of the structure factor of a single domain of vortex Bragg glass. There has been mounting evidence that a phase transition (e.g. X.S. Ling et al., PRL 86, 712 9 (2001)) into an ordered Bragg glass phase does exist, there has been no direct evidence of the power-law structure factor predicted for weak-pinning type-II superconductors.

Recent Progress

Growth of Bragg Glass: The challenge in the study of the Bragg-glass structure factor is similar to that in studying regular atomic solids. In conventional solid-state structure studies, the first

key task is to grow a single crystal sample. There, one has to overcome the complex effects of phase transition kinetics. In vortex matter, one often finds a similar situation that a single domain vortex lattice of Bragg glass phase is difficult to obtain. We carried out a series of in-situ neutron scattering (using AND/R instrument at NIST) experiments to explore various approaches in obtaining a single domain Bragg glass. In this work, we found the first direct evidence for the “edge-contamination effect” previously implicated in transport and magnetization experiments.

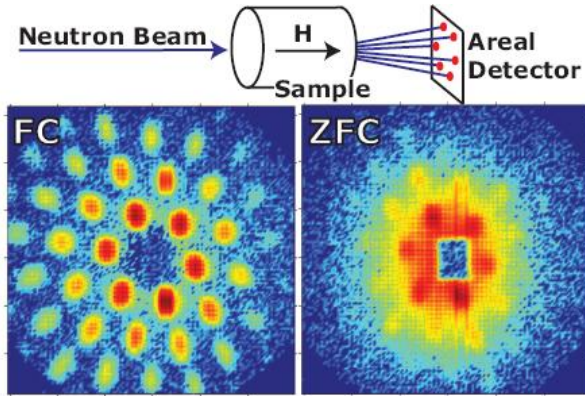


Figure 1: (Above) Scattering geometry for conventional small angle neutron scattering (SANS). (Below) SANS images (summed over the rocking angle) for the ZFC and the FC states at 1.5 K and 0.14 T.

FC SANS image (left) shows well defined Bragg peaks to several orders, indicating that the FC vortex state is clearly ordered. For the ZFC state (right), the Bragg peaks are emerging but there are significant scattering signals between the expected Bragg peaks indicating a spatially inhomogeneous and partially ordered vortex state. The scattering geometry for our SANS experiment is shown in Fig.1(top).

Figure 1 illustrates the anomalous metastability behavior as revealed by using the standard small angle neutron scattering (SANS) technique. The

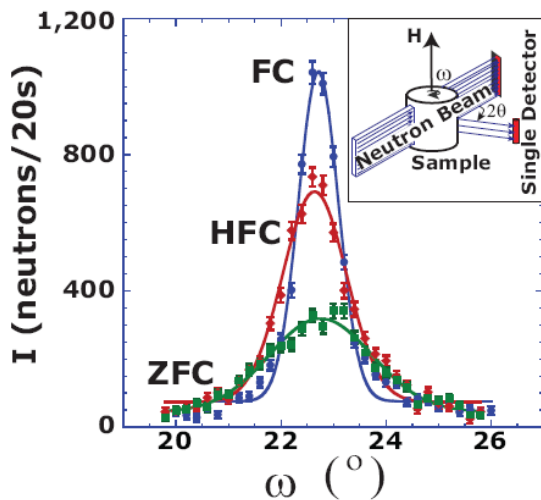


Figure 2: Bragg peaks at $T=3.5$ K and $H=0.14$ T for ZFC(green square), HFC(red diamond) and FC (blue circle) vortex matter. Solid lines are single Gaussian fits (form given in text). (Inset) Scattering geometry.

Our scattering geometry, shown in Fig.2, allows us to investigate the radial and azimuthal widths of the Bragg peak as the sample is scanned by a narrow neutron beam. The azimuthal direction is measured by rotating the sample (and the magnet field) and measuring the scattered neutron

Slicing Neutron Diffraction: To explore the nature of the disorder in the ZFC state, and that in the FC state, we turn to the slicing diffractometer measurements afforded by the AND/R at the NIST.

intensity as a function of rotation angle ω . The AND/R instrument utilizes a thin beam of neutrons, the beam width of 0.5 mm is much smaller than the sample diameter 12.1 mm. This feature allows us to vary the section of the Nb crystal exposed to the neutron beam and measure the vortex structure factor for a particular location (geometry shown in Fig.2). Figure 2 shows rocking curves for different thermal-magnetic history. The FC is cooling the sample in a magnetic field of 0.14 T, the ZFC is cooling the sample in zero magnetic field and then ramping the field to 0.14 T, and the high-field cooled (HFC) is cooling the sample in a field of 0.40 T and then reducing the field to 0.14 T.

In this sample, the ZFC state is drastically more disordered than the FC state, opposite to that found in the previous Nb crystal (X.S. Ling et al., PRL 86, 712 9 (2001)). The broad Bragg peak for the ZFC state in Fig.2 is a direct confirmation of the edge contamination effect. Clearly, the broad Bragg peak in the ZFC state is indicative of a vortex lattice full of edge dislocations and/or broken into many small domains separated by low-angle grain boundaries. The sharp FC peak is not surprising since the measurement is deep inside the Bragg glass phase, no supercooling effect to be expected there.

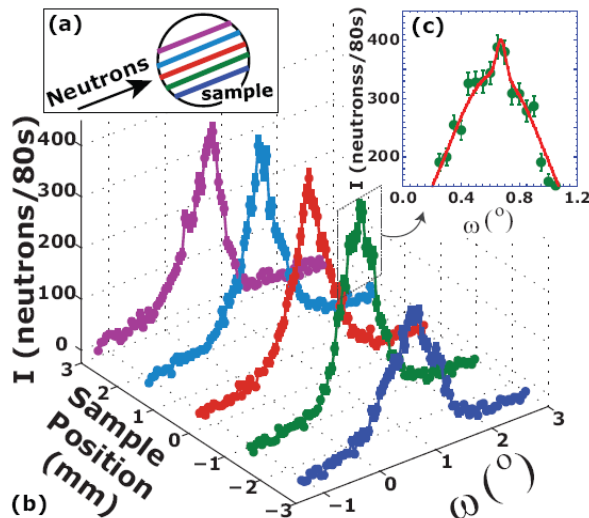


Figure 3: (a) Geometry for scanning neutron diffraction. (b) 3D plot of annealed FC Bragg peaks at $T=4.5$ K and $H=0.14$ T: Intensity versus rocking angle as a function of the sample position relative to the neutron beam. The solid lines are guides for the eyes. (c) A zoomed 2D plot of the peak at -1.4 mm fitted with a double Gaussian, solid red line.

Using AND/R as a scanning diffractometer, we find that the edge effect is still present even after thermally annealing the vortex lattice. As shown in Fig.3, the Bragg peak is broad at the edges of the sample, indicating that the disordered vortex state cannot be annealed further. This fact suggests that the edge vortex matter is possibly a vortex glass. In the middle of the sample, there is a single-domain vortex lattice, or a Bragg glass. When the beam is directed through the center of the sample, the Bragg peak has a characteristic cusp shape, as seen in the center curve. When the neutron beam is a few millimeters away from the center of the sample, a sharp peak poking through a broad base is visible, indicative of a single-domain Bragg glass surrounded by a coexisting disordered phase. This peak can be fitted with a double-Gaussian. The broad Gaussian corresponds to a disordered phase. The narrow Gaussian is evidence of a highly ordered Bragg glass phase. Apparently,

thermal annealing has led to the growth of a single domain of the Bragg glass phase out of a dirty vortex matter induced by edge disorder.

Thermal Annealing of Vortex Matter: We find that it is possible to greatly improve the Bragg glass order by thermally annealing the vortex matter, in both ZFC and FC vortex states, indicating that neither of the ZFC or FC as-prepared states is in equilibrium. The ZFC state has dynamically generated disorder (by “edge contamination”), while the FC state has kinetically frozen-in disorder (by “supercooling”).

The fact that disordered edge vortex matter exists even in the annealed FC state, as shown in Fig.3, is significant. This observation implies that the structural information obtained by standard SANS measurements cannot be directly correlated with dynamical measurements such as magnetization and transport for systems exhibiting edge contamination. The SANS signal is dominated by the central region of the sample, while the latter are determined by supercurrent or magnetic field gradient on the sample surface. Our observation here may also offer a resolution to the longstanding puzzle concerning the appearance or absence of the peak effect. Since the ac magnetic measurement is dominated by the surface current in the sample, the appearance or the absence of the peak effect will depend on the residual short-range order in the edge vortex matter. If the edge vortex matter is strongly disordered by the surface defects, there will be no observable effect from the thermally-induced disordering due to the Bragg glass melting transition in the bulk.

Future Plans

“TISANE” or time-dependent SANS: Presently, our “crystal growth” effort in obtaining a single domain Bragg glass is reminiscent of the primitive crystal growth effort, by trial-and-error. Very little is known about the dynamics of ordering in vortex matter. It has been known for decades that vortex matter system does relax towards equilibrium, as seen in the decay of the Bean critical state. The mechanism by which this “flux creep” phenomenon occurs has been controversial. An interesting idea was proposed by Fisher, Fisher, and Huse in which a nucleation-and-growth of “vortex loops” is responsible for equilibration of vortex matter. TISANE studies of ZFC vortex state can shed light on this issue.

Search for a single domain Bragg glass: We are in the process of carrying out surface treatment (using oxygen plasma) of Nb single crystals to suppress or remove their surface barrier. Hopefully we can use our in-situ slicing diffraction experiment to guide us to the first single-domain Bragg glass on which a definitive structure factor measurement can be made.

Publications:

[1] Helen A. Hanson, Xi Wang, I.K. Dimitrov, J. Shi, X.S. Ling, B.B. Maranville, C.F. Majkrzak, M. Laver, U. Keiderling, M. Russina, submitted to Phys. Rev. Lett. (2010).

Spin Transitions, Phase Competition and Ordering in Perovskite Oxides

Despina Louca
University of Virginia, Dept. of Physics,
Charlottesville, VA 22904
louca@virginia.edu

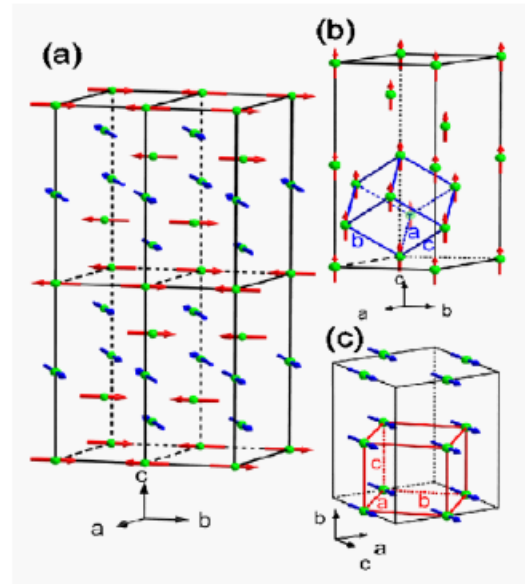
Research Scope:

Spatially inhomogeneous states are ubiquitous in complex transition metal oxides. Such states are the result of competing mechanisms resulting from strong interactions among the viable degrees of freedom. The main goal of our program is to understand the nature, origin and organization of such states, their microscopic interactions and mechanisms that lead to such states, and how they relate to the macroscopic thermodynamic properties. To do so, transition metal oxides such as the magnetoresistive cobalt perovskite, ABO_3 , multiferroic $AMnO_3$ and garnets are used as they exhibit unusual behaviors. Understanding the nature of their ground state may provide us with useful insights regarding the functionality of strongly correlated electron systems.

Recent Progress:

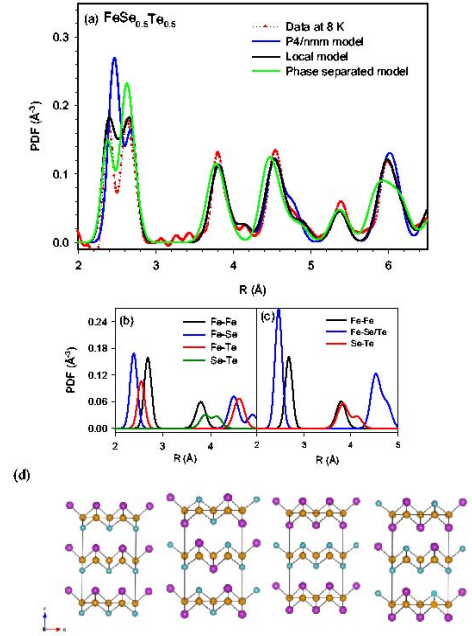
Possible link of a structurally driven spin flip transition and the insulator-metal transition in the perovskite $La_{1-x}Ba_xCoO_3$

The complex nature of the magnetic ground state in $La_{1-x}A_xCoO_3$ ($A = Ca, Sr, Ba$) has been investigated via neutron scattering. It was previously observed that ferromagnetic (FM) as well as antiferromagnetic (AFM) correlations can coexist prior to the insulator-metal transition (IMT). We focused on a unique region in the Ba phase diagram, from $x = 0.17 - 0.22$, in which a commensurate AFM phase appears first with a propagation vector, $k = (0, -0.5, 0.5)$, and the Co moment in the $(001)_R$ plane of the rhombohedral lattice. With increasing x , the AFM component weakens while an FM order appears with the FM Co moment directed along the $(001)_R (= (111)_C)$ axis. By $x = 0.22$, a spin flip to new FM component appears as the crystal fully transforms to an orthorhombic ($Pnma$) structure, with the Co moments pointing along a new direction, $(001)_O (= (110)_C)$. It is the emergence of the magnetic $Pnma$ phase that leads to IMT.



The local atomic structure of superconducting Fe-Se-Te

The isovalent substitution of Te for Se in the superconducting α -FeSe raises T_c where the average chalcogen-Fe bond angle decreases and the chalcogen-Fe distance increases. Locally, however, the Se and Te ions do not share the same site and have two distinct z-coordinates, in contrast to what is presumed in the P4/nmm symmetry. The local bond angle between the chalcogens and Fe increases with the substitution, consistent with the rise in T_c , the Fe-Te bonds become shorter than in the binary FeTe, while the Fe-Se bonds stay the same as in the binary. Ab-initio calculations based on spin density functional theory yielded an optimized structure with distinct z-coordinates for Se and Te, in addition to a stronger hybridization of Te with Fe.



Investigation of the spin-glass regime between the antiferromagnetic and superconducting phases in $Fe_{1+y}Se_xTe_{1-x}$

Using bulk magnetization along with elastic and inelastic neutron scattering techniques, we have investigated the phase diagram of $Fe_{1+y}Se_xTe_{1-x}$ and the nature of magnetic correlations in three nonsuperconducting samples of $Fe_{1.01}Se_{0.1}Te_{0.9}$, $Fe_{1.01}Se_{0.15}Te_{0.85}$ and $Fe_{1.02}Se_{0.3}Te_{0.7}$. A cusp and hysteresis in the temperature dependence of the magnetization for the $x = 0.15$ and 0.3 samples indicates spin-glass (SG) ordering below $T_{sg} = 23$ K. Neutron scattering measurements indicate that the spin-glass behavior is associated with short-range spin density wave (SDW) ordering characterized by a static component and a low-energy dynamic component with a characteristic incommensurate wave vector of $Q_m = (0.46, 0, 0.50)$ and an anisotropy gap of ~ 2.5 meV. Our high Q-resolution data also show that the systems undergo a glassy structural distortion that coincides with the short-range SDW order.

Formation of electric dipoles with no unique polar axis in $Tb_3Fe_5O_{12}$

The results of our investigation using neutron scattering on the ferrimagnetic $Tb_3Fe_5O_{12}$ garnet suggest that the dielectric (ϵ) constant is enhanced by the volume striction induced under field and not by the magnetic transition of the Tb ions. In cooling from high temperatures, we find that the previously suggested phase transition from a cubic to a rhombohedral structure symmetry cannot adequately describe the data in any range, while a tetragonal phase is more appropriate. Simultaneously, pronounced magnetic diffuse scattering is observed at high temperatures that gradually decreases with cooling as the Tb spins take on an ordered structure at about 50 K. At the same time, large oxygen distortions, of the order of $0.1-0.2 \text{ \AA}$, first observed starting at 90 K and up to 550 K, indicate that electric dipoles are indeed present. However, they are not ordered and the lack of a unique polar axis in the hyperkagome structure may be linked to the absence of a polarized phase in this system. If it were present, the system could have a high ferroelectric transition temperature.

Local structure effects of the Ba-122 superconductor

In collaboration with Dr. Yan from Ames Laboratory who provided us with a series of $\text{Ba}(\text{Fe}_{1-x}\text{Co}_x)_2\text{As}_2$ samples, we are currently working on the analysis of this system. We are currently working on a manuscript based on our results on this topic.

Planned activities for next year (key challenges, future issues):

Several topics will be actively pursued for the remaining one year duration of this project:

1. We will continue our work on the FeSe superconductor as this is a hot topic now. We have submitted one paper on the spin dynamics. We are currently analyzing the data that we collected at ISIS on the MARI spectrometer. From this, we want to extract the dynamic PDF from the $S(\mathbf{Q}, \omega)$.
2. We will be investigating the effects of possible ordering of $\text{FeSe}_{0.5}\text{Te}_{0.5}$ by performing long annealing on samples of this composition and nearby. We will characterize the properties to see if annealing has an effect on T_c . If it does, we will perform further neutron experiments to determine the structural differences with ordering.
3. We are currently analyzing the data on Ba-122. This project will be completed soon. Further experiments are planned as well to examine the overdoped regime.
4. We will continue with the powder measurements of $\text{La}_{1-x}\text{Ba}_x\text{CoO}_3$ to resolve the crystal symmetry beyond 22 % of doping.
5. Two papers are currently under preparation regarding $\text{LaCo}_{1-x}\text{Ni}_x\text{O}_3$ and $\text{LaCo}_{1-x}\text{Fe}_x\text{O}_3$.
6. We will investigate one new system that undergoes negative thermal expansion in Ge doped anti-perovskite manganese nitrides.

List of Papers:

1. "Frustrated magnetism and cooperative phase transitions in spinels", S.-H. Lee, H. Takagi, D. Louca, M. Matsuda, S. Ji, H. Ueda, Y. Ueda, T. Katsufuji, J.-H. Chung, S. Park, S.-W. Cheong and C. Broholm, *J. Phys. Soc. Jpn* **79**, 011004 (2010).
2. "The local atomic structure of superconducting Fe-Se-Te", Despina Louca, K. Horigane, A. Llobet, P. Tong, K. Yamada, *Phys. Rev. B* **81**, 134524 (2010).
3. "A neutron scattering study of the competing magnetic correlations in $\text{La}_{0.85}\text{Sr}_{0.15}\text{CoO}_3$ ", D. Phelan, Despina Louca, S. N. Ancona, S. Rosenkranz, and J. F. Mitchell, *Phys. Rev. B* **79**, 094420 (2009).
4. "Uncharacteristic phase separation trends with the tolerance factor in Cobaltites", J. Yu, Despina Louca, D. Phelan, K. Tomiyasu, K. Horigane and K. Yamada, *Phys. Rev. B* **80**, 052402 (2009).
5. "Formation of electric dipoles with no unique polar axis in $\text{Tb}_3\text{Fe}_5\text{O}_{12}$ ", D. Louca, K. Kamazawa and T. Proffen, *Phys. Rev. B* **80**, 214406 (2009).

6. "The crystal structure of superconducting $\text{FeSe}_{1-x}\text{Te}_x$ by pulsed neutron diffraction", M. C. Lehman, A. Llobet, K. Horigane, and D. Louca, to appear in *J. Phys. Chem. Solids* (Conference proceedings) (2009).
7. "A complex magnetic structure in the magnetoresistive $\text{Ba}_{0.82}\text{Ba}_{0.18}\text{CoO}_3$ ", P. Tong, Q. Huang, M. Kofu, M. C. Lehman, J. Yu and D. Louca, to appear in *J. Phys. Chem. Solids* (Conference proceedings) (2009).
8. "Field-induced antiferromagnetism and competition in the metamagnetic state of terbium gallium garnet", K. Kamazawa, Despina Louca, R. Morinaga, T. J. Sato, Q. Huang, J. R. D. Copley, and Y. Qiu, *Phys. Rev. B* **78**, 064412 (2008).
9. "Jahn-Teller spin polarons in perovskite Cobaltites", D. Phelan, J. Yu and Despina Louca, *Phys. Rev. B* **78**, 094108 (2008).
10. "Influence of the ionic size on the evolution of local Jahn-Teller distortions in cobaltites" D. Phelan, Despina Louca, K. Kamazawa, M. F. Hundley, and K. Yamada, *Phys. Rev. B* **76**, 104111 (2007).

Designer phase transitions in lithium-based spinels

DOE Award No. DE-FG02-07ER46381

PI: Wouter Montfrooij

Department of Physics and Astronomy, University of Missouri, Columbia, 65211
573-882-8362, montfrooijw@missouri.edu

Introduction / research scope

When electrons in a metal become correlated with each other, new cooperative behavior can arise. This correlation is magnified when the metal has magnetic ions embedded in it. These atomic magnets try to line up with each other, but in doing so actually create a correlation between the motions of conduction electrons. In turn, these correlated electron motions prevent the magnetic ions from aligning, even at zero Kelvin. When this competition is strongest (at the so-called quantum critical point-QCP) the response of the system can no longer be described using the text book theory for metals. In addition, a range of new phenomena has been seen to emerge in the vicinity of a QCP, such as heavy-fermion superconductivity, coexistence of magnetism and superconductivity and hyper-scaling. The main goal of our research is to try to unravel the details of the feedback mechanism between electron motion and magnetism that lies at the heart of this new physics. We have chosen lithium-based spinel structures as the most promising family of systems to achieve our goal.

Known lithium-based spinels $\text{Li}_x\text{M}_2\text{O}_4$ [M=V, Ti and Mn] show a variety of ground states: heavy-fermion, superconducting, or geometrically frustrated local moment systems. $\text{Li}_x\text{M}_2\text{O}_4$ should be ideal systems for studying QCPs since their properties can easily be fine-tuned, simply by extracting some Li [which can be done without introducing disorder in the immediate surroundings of the magnetic ions]. The premise of the proposal was that since this Li-extraction can be done both in the metallic as well as in insulating compounds, that we can expand the types of quantum phase transitions that can be studied to beyond transitions in magnetic metals.

The project called for developing a better understanding of quantum phase transitions by measuring all aspects of the electronic response of $\text{Li}_x\text{M}_2\text{O}_4$ by means of neutron scattering, giving microscopic information about the behavior of the individual magnetic moments and their interactions, as well as by macroscopic measurements. In addition, the aim was to synthesize new lithium-based spinel compounds by using other transition metals that exhibit both 3^+ and 4^+ valencies. Here we report on the progress towards these goals while already stating that we have not been successful yet in the synthesis of new compounds free from impurity phases.

Progress

1) Magnetism in $\text{Li}_x\text{Mn}_2\text{O}_4$ below 300 K:

We investigated and proved that the magnetic scattering in $\text{Li}_x\text{Mn}_{1.96}\text{Li}_{0.04}\text{O}_4$ ($x=1.0$) -the compound commonly used in lithium batteries- corresponded to the presence of clusters of Mn^{4+} -ions. We verified that our hypothesis was correct. Using Monte Carlo computer simulations we identified that clusters were present in this material, and we were able to determine the morphology of these clusters [1]. We summarize our results in Fig. 1.

Neutron scattering studies of other lithium concentrations showed that clusters were present for all concentrations. The phase diagram for $\text{Li}_x\text{Mn}_{1.96}\text{Li}_{0.04}\text{O}_4$ turns out to be fairly complex [4]. All concentrations display a departure from standard Curie-Weiss behavior below ~ 70 K, the

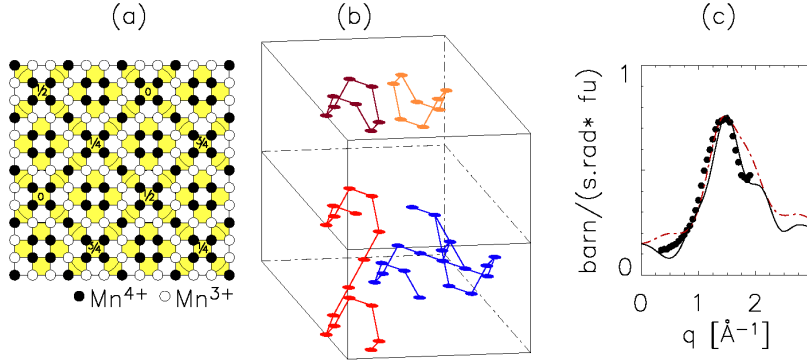


Fig 1: (a) The unit cell for stoichiometric LiMn_2O_4 projected along the c-axis [Rodríguez-Carvajal et al., Phys. Rev. Lett. 81 4660 (1998)]. The Mn^{4+} -ions (open circles) form 8-fold rings. (b) Two unit cells stacked along the c-axis for $\text{LiMn}_{1.96}\text{Li}_{0.04}\text{O}_4$. Two ring clusters from part (a) are shown at the top of the figure. Upon Li substitution on the Mn-sites some Mn^{3+} -ions will become

Mn^{4+} -ions, leading to modified rings [1] and linked rings, two possibilities of which are shown in the bottom half of the figure. (c) These 2-ring clusters give a satisfactory description of the neutron scattering data [1] (solid line, bottom left cluster in part b, or dashed line, bottom right cluster in part b).

temperature identified as the point where the moments within the preformed Mn^{4+} clusters align antiferromagnetically. Depending on the number of Mn^{4+} -ions (that is, depending on the Li-concentration), the clusters form a spin glass and/or long range-order establishes itself. The phase diagram is shown in Fig. 2.

The appearance of long range order, the maximum of the real part of the susceptibility, as well as the sign of the Curie-Weiss temperature all display a marked change at a Li-concentration of $x \sim 0.5$ (see fig. 2). It is this disappearance of long range order, heralded by the onset of ferromagnetic interactions, which originally led us to believe that we would observe quantum critical behavior in this system. Unfortunately, it turns out that a potential quantum critical point is masked by the spin-glass transition.

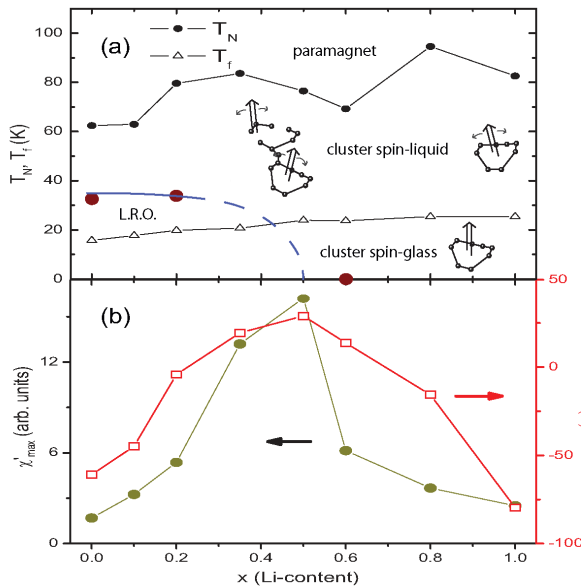


Fig. 2. The phase diagram for $\text{Li}_x\text{Mn}_{1.96}\text{Li}_{0.04}\text{O}_4$ as established from AC-susceptibility measurements (top panel). The change from long-range to short-range order as a function of Li-concentration x is visible in the peak of the magnetic susceptibility (bottom panel, left-hand scale), and it is marked by a change in sign of the Curie-Weiss temperature (bottom panel, right hand scale).

Next we investigated whether the quasi-elastic scattering observed at low temperatures in this compound exhibits E/T-scaling. This E/T-scaling is believed to only occur in quantum critical systems, and hence it should not be manifest in a classical system like LiMn_2O_4 that is far removed from any quantum critical point. Surprisingly, we found [2] (Fig. 3) that the scattering in this system associated with the magnetic clusters did mimic E/T-scaling for all

concentrations x investigated. This unexpected result indicated that the scattering associated with a collection of magnetic clusters might well be the origin of E/T-scaling observed in quantum critical systems, or at least, that these magnetic clusters would play a major role. In fact, the shape of the scaling curves is rather similar to that observed in quantum critical systems, such as quantum critical $\text{CeRu}_{0.5}\text{Fe}_{1.5}\text{Ge}_2$. This is shown in Fig. 4.

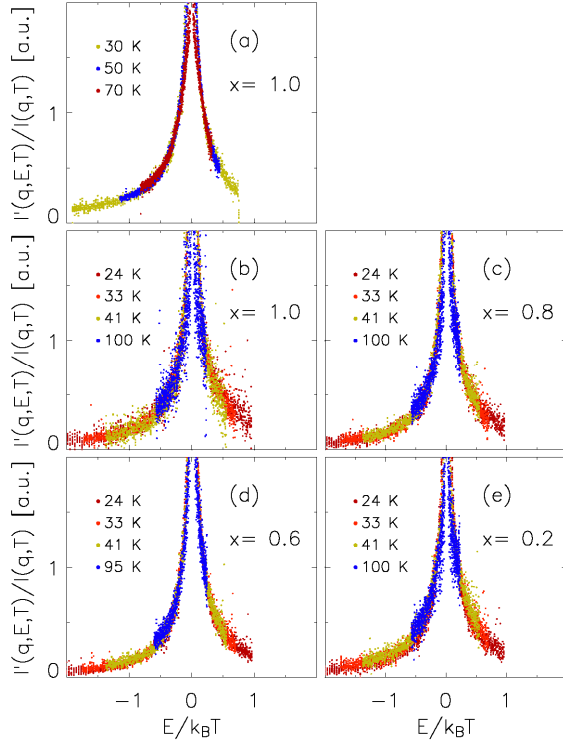


Fig. 4. When the neutron scattering data $I'(q,E,T)$ [corrected for thermal population factors] are plotted on a log-log scale [3], the scattering appears to display dynamical scaling over the full range. The lower curve are the ILL data from Fig. 3a, the middle curve are MURR data shown, and the upper curve are the data for $\text{CeRu}_{0.5}\text{Fe}_{1.5}\text{Ge}_2$ at $q=0.4 \text{ \AA}^{-1}$ [Montfrooij et al., Phys. Rev. Lett. 91, 087202 (2003)] The three curves are offset for plotting clarity.

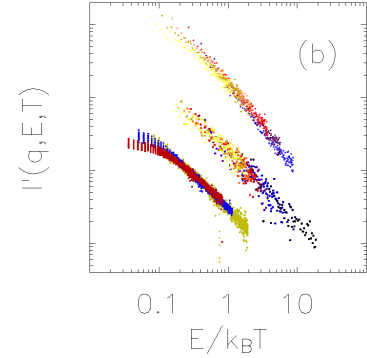
2) Specific heat of a quantum critical system and clusters:

Given the connection between the presence of clusters and the appearance of unusual dynamics, we are investigating to what degree cluster formation also influences macroscopic properties such as the specific heat of a quantum critical system. The premise behind this is straightforward. When a system changes from a 3-D system to some sort of a fractal structure because of Kondo shielding in the presence of a distribution of Kondo temperatures, its response should change accordingly. In particular, when a magnetic cluster becomes isolated from the rest of the system, this cluster will be forced to order magnetically because of finite size effects. Thus, cluster formation would be reflected in the specific heat of the system; whenever a cluster becomes isolated and is forced to order, the loss of entropy will show up in the specific heat, bestowing it with an unusual temperature dependence.

Using the programs we developed to identify the clusters shapes [1] in LiMn_2O_4 , we are carrying out a range of simulations for purely quantum critical systems in which we vary the distribution of shielding temperatures (that is known to lead to the formation of clusters). Our initial results look very promising. As an example we display our findings for the specific heat of a 122-system (such as quantum critical $\text{CeRu}_{0.5}\text{Fe}_{1.5}\text{Ge}_2$) using the Kondo distribution shape from heavily doped quantum critical CeCu_4Pd and whose average shielding temperature coincides with the value inferred from scattering measurements. The next step will be to fine tune this toy-

In summary: $\text{Li}_x\text{Mn}_{1.96}\text{Li}_{0.04}\text{O}_4$ harbors magnetic short-range clusters that remain present even when long range order emerges, and these clusters remain the dominating mechanism in determining the excitations on either side of a phase transition. The dynamics associated with these clusters yield scaling laws that mimic the hyper-scaling laws found in quantum critical systems. It now seems likely that the dynamics of doped quantum critical systems are strongly influenced by the emergence of clusters upon cooling; this finding possibly removes the conflict between theory and experiment.

Fig. 3: (a) ILL data of our pilot experiment [Schimmel et al., Phys. Rev. B 63, 214409 (2001)], parts (b)-(e) correspond to new ILL experiments [3] on $\text{Li}_x\text{Mn}_{1.96}\text{Li}_{0.04}\text{O}_4$. The Li-concentrations x and temperatures are shown in the figure. All curves collapse onto each other, giving the appearance of dynamical scaling.



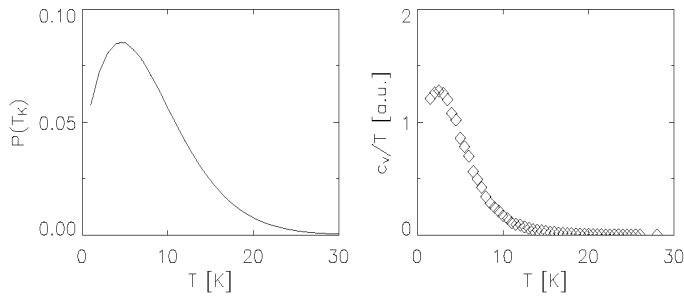


Fig. 5. Shown are the effects of a distribution $P(T_K)$ (left panel) in Kondo-shielding temperatures T_K on the specific heat (right panel). Assigning random Kondo shielding temperatures to magnetic ions in a bcc-lattice results in cluster formation. Assuming that isolated clusters order because of finite size effects yields a specific heat curve that peaks below the average Kondo shielding temperature. Note that even though the specific

heat curve has a similar shape to the magnetic specific heat measured for quantum critical systems, the temperature dependence of c_v/T shown is entirely due to the change in geometry, it is not related to quantum critical physics.

model until we obtain the best agreement possible with the measured magnetic specific heat. The difference between the best agreement and the experimental data should then be a measure of true quantum critical physics, free from geometric effects.

Planned FY2011 program

The focus in FY2011 will be on tying up loose ends and on submitting manuscripts.

A) Completion of computer simulations for specific heat investigation

We will complete the investigation into the unusual low temperature dependence of quantum critical systems and the emergence of magnetic clusters through simulating the specific heats of systems such as UCu_4Pd as a function of Kondo shielding temperatures.

B) Compounds for which data have been collected, but for which analysis is not complete.

- $LiMn_2O_4$: We have all but resolved the magnetic structure of stoichiometric $LiMn_2O_4$.
- Li_xVMO_4 : We have done neutron scattering experiments and taken ac-susceptibility measurements on $M=Ni, Co$ and Fe doped samples to study the interplay of the conduction electrons and the magnetic moments at finite temperature phase transitions. This will shed light upon the role of Fe -doping in relationship to the electronic properties.
- $CeRu_{0.5}Fe_{1.5}Ge_2$: We have performed inelastic neutron scattering experiments scrutinizing the dynamics of the magnetic clusters. The aim was to isolate those parts of the E/T -scaling that are related to the cluster morphology from those parts that are related to quantum mechanical fluctuations. We do not know yet whether we have succeeded in this aim.

Publications acknowledging DOE support

1. J. Gaddy, J. Lamsal, M. Petrovic, W. Montfrooij, A. Schmetts, and T. Vojta, *Magnetic ordering in the spinel compound $Li[Mn_{2-x}Li_x]O_4$ ($x=0, 0.04$)*, J. Appl. Phys. 105, 07D532 (2009).
2. J. Lamsal, J. Gaddy, M. Petrovic, W. Montfrooij, and T. Vojta, *The search for quantum critical scaling in a classical system*, J. Appl. Phys. 105, 07E322 (2009).
3. T. Heitmann, A. Schmetts, J. Gaddy, J. Lamsal, M. Petrovic, T. Vojta, and W. Montfrooij, *Magnetic excitations in the spinel compound $Li_xMn_{1.96}Li_{0.04}O_4$ ($x= 0.2, 0.6, 0.8, 1.0$): how a classical system can mimic quantum critical scaling*, Phys. Rev. B 81, 014411 (2010) [editor's choice]
4. Thomas Heitmann, John Gaddy, Jagat Lamsal, Marcus Petrovic, and Wouter Montfrooij, *AC susceptibility of the quantum point mimicking series $Li_xMn_{1.96}Li_{0.04}O_4$ ($x=0.0, 0.1, 0.2, 0.35, 0.5, 0.6, 0.8, 1.0$)*, J. Appl. Phys. 107, 09E143 (2010).

Peer press: (APS Physics) <http://physics.aps.org/synopsis-for/10.1103/PhysRevB.81.014411>

Neutron and X-ray Scattering Group: Instrumentation and Outreach

R. Osborn (rosborn@anl.gov), S. Rosenkranz, S.G.E. te Velthuis, U. Perez-Salas
Materials Science Division, Argonne National Laboratory, Argonne, IL 60439

D.L. Abernathy, F. Ye

Neutron Scattering Science Division, Oak Ridge National Laboratory, Oak Ridge, TN 37831

Research Scope

The role of the Neutron and X-ray Scattering Group within the Materials Science Division (MSD) is to pursue world-class multidisciplinary research programs that combine neutron and x-ray scattering with materials synthesis, characterization, and theory. Members of the group play lead roles in a variety of scientific programs that couple MSD to state-of-the-art probes of the structure and dynamics of materials at major neutron and x-ray scattering facilities. However, if existing techniques show limitations that hinder our scientific goals, we have a strong tradition of using our scattering expertise to develop ways of overcoming those limitations, designing new instrumentation and novel scattering techniques involving both neutrons and x-rays. Our group is responsible for proposing a novel SNS instrument, *Corelli*, dedicated to measuring single crystal diffuse scattering using cross correlation to combine the high efficiency of time-of-flight Laue diffraction with elastic discrimination. Based on our numerical Monte Carlo simulations, this technique can lead to efficiency gains up to two orders of magnitude as compared to traditional techniques using monochromatic time-of-flight spectrometers. *Corelli* has recently received CD-3 approval and is scheduled for completion in 2013. Group members played leading roles in an international collaboration to develop the Spin-Echo Resolved Grazing Incidence Scattering (SERGIS) technique into a powerful tool for the study of lateral surface inhomogeneity. A prototype instrument was successfully tested at the Institut Laue Langevin, Grenoble, France, and experiments to use the technique to study phase separation in multi-component biomimetic membranes are planned in the next year. We have developed a novel method of measuring inelastic neutron scattering over complete four-dimensional volumes of (\mathbf{Q}, ω) -space that exploits efficiencies offered by the event-mode data acquisition system in use at the SNS. Our group have now successfully tested this technique on the ARCS time-of-flight spectrometer for the measurement of both magnetic and phonon scattering.

These examples represent ways in which the group's scientific program within MSD has stimulated new scattering techniques that make a contribution to the wider neutron scattering community. Another contribution is through sponsoring the two week long *National School of Neutron and X-ray Scattering* at Argonne that has now been running for over ten years. The school accepts 60 graduate students each summer, who hear lectures from leading experts in the field and conduct hands-on experiments on neutron and x-ray scattering instruments. Originally, neutron experiments were performed at IPNS and the x-ray experiments were performed at APS. With the closure of IPNS, we obtained funding for a new arrangement, in which the neutron experiments are performed at the SNS. Two schools have been successfully run in this form, with a third due in June, 2010.

Recent Progress

Corelli: Our proposal to build an instrument at the SNS dedicated to measuring single crystal diffuse scattering arose out of a long-standing interest in materials with competing interactions that exhibit complex disorder, *i.e.*, nanoscale correlations in the form of stripes, checkerboards, phase separation, and other short-range ordering motifs. It is important to discriminate between quasi-static disorder and dynamic fluctuations. *Corelli* achieves this by using a statistical chopper to modulate the incident beam. The scattering function can then be reconstructed in both \mathbf{Q} and ω by cross correlation of the measured signal with the modulation sequence. Monte Carlo simulations show potential gains in efficiency of two orders of magnitude compared to a monochromatic instrument.

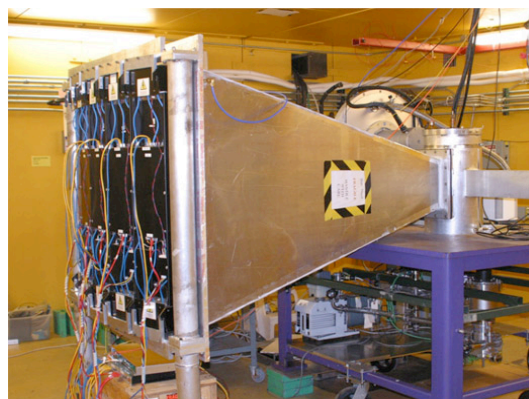


Fig. 1: Installation of *Christina* inside the FP12 cave. The picture shows the secondary flight path (under helium atmosphere) and the back of the five detector modules, each containing 8 linear position sensitive detectors. The statistical chopper is visible behind the detector tank.

Following submission of our proposal to the SNS, *Corelli* received funding as part of the SING-II suite of instruments. The SNS is now responsible for the engineering design, which successfully underwent a CD-3 review in December, 2009. We are conducting tests of the new technique using a prototype instrument, named *Christina*, that was first installed at IPNS and

subsequently transferred to the Manuel Lujan Neutron Scattering Center at Los Alamos. It has been installed on beamline FP12, which has an existing guide with bandwidth chopper as well as a shielded experimental hutch (Fig. 1).

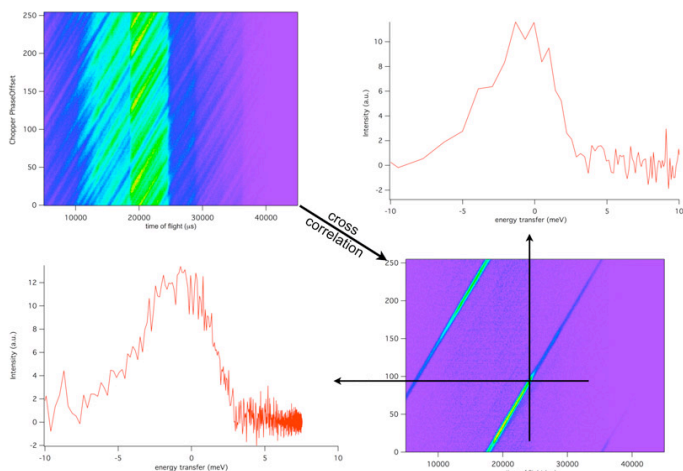


Fig. 2: Raw data (top left) as a function of total time of flight and chopper phase-offset. The bottom right shows the scattering function reconstructed through cross correlating the raw data with the modulation sequence. The panels above and to the side of the of the cross correlated data show cuts either for fixed incident energy (side) or fixed final time of flight (above).

The tests have confirmed the basic operation of statistical chopper and shown that the elastic peak from powders can be successfully extracted from the modulated signal. Figure 2 shows the raw data as a function of total time of flight and chopper phase-offset with the chopper running asynchronously at 3793 RPM.

Inelastic Neutron Scattering from Four-Dimensional $S(\mathbf{Q},\omega)$: The measurement of inelastic neutron scattering from single crystals using time-of-flight spectrometers has become well-established in the new generation of pulsed neutron instruments such as ARCS and SEQUOIA. This technique has provided important data on the magnetic excitations in transition metal magnets, high-temperature superconductors and the recently discovered iron pnictide and chalcogenides superconductors. One of the limitations of the technique is that the data are only measured over paraboloid surfaces that cut through four-dimensional (\mathbf{Q},ω) -space so that it is not possible to reconstruct the scattering at constant \mathbf{Q} or within reciprocal space planes at constant energy. This limitation is not critical when models of the scattering function are well-defined, or for low-dimensional systems with limited \mathbf{Q} -dependence along one or more reciprocal space axes. In other systems, the data can be extremely challenging to interpret.

The enhanced flux and increased detector coverage of the latest spectrometers allows a solution to this problem. If the scattering function is measured as a function of the rotation angle of the crystal about an axis orthogonal to the incident beam, the paraboloid surfaces are rotated through reciprocal space allowing the full four-dimensional $S(\mathbf{Q},\omega)$ to be measured. This method has been tested at ISIS by Toby Perring and collaborators, where it is referred to as *Horace*-mode. A series of scans, in which the sample rotation angle is stepped over a full quadrant, typically takes two days to measure, after which arbitrary planes and cuts through $S(\mathbf{Q},\omega)$ can be visualized. The main drawback of this method is that it is difficult to optimize measurement strategies since the scan results can only be fully assessed when the scan is over.

We have been testing a variant of the technique that exploits specific features of the SNS data acquisition system to allow the complete results to be monitored immediately. The SNS uses event-mode data collection, in which each neutron is recorded as a separate event with its own time-stamp. This means that the sample can be rotated continuously during the measurement as long as the rotation angle is logged and can be correlated to the neutron pulses. The results of the entire angular sweep can be continuously histogrammed into four-dimensional (\mathbf{Q},ω) -space, allowing the experimenter to monitor the results over the entire range of the scan as soon as data collection starts. If preliminary inspection of the data indicates that the experimental conditions are not optimal, or that the rotation angles can be confined to a more limited range, they can be changed at any time without compromising the value of the data already collected.

Tests of this ‘sweep’-mode have now been successfully performed with measurements of magnetic excitations in cobaltites and phonons in a bilayer manganite. These experiments have

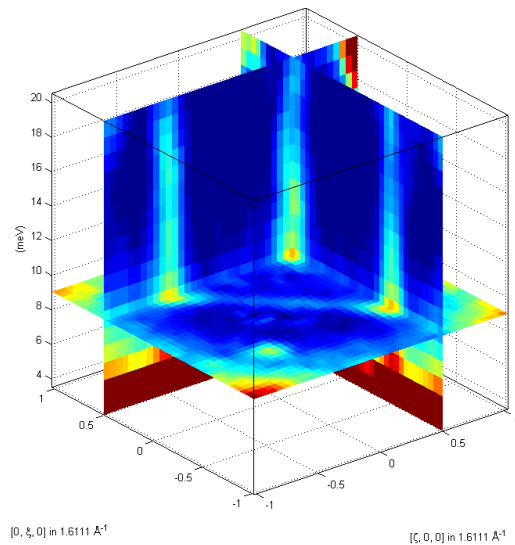


Fig. 3: An example of using the ‘sweep’ mode of measuring $S(\mathbf{Q},\omega)$ in all four-dimensions. The sample is $\text{Ba}_{0.6}\text{K}_{0.4}\text{Fe}_2\text{As}_2$, a 38K superconductor, in which the magnetic scattering is simultaneously observed at four-symmetry-related zone-boundary wavevectors.

resolved a number of technical issues, such as synchronizing pulses with sample environment log files, which will be valuable in other uses of event-mode data under development at SNS.

Future Plans

Corelli: We will continue to provide guidance to the SNS scientists and engineers in finalizing the design of *Corelli*, now that CD3 approval has been obtained. Further tests of the prototype spectrometer, *Christina*, are planned at Los Alamos. Background conditions need to be optimized to allow single crystal diffuse scattering to be measured. Monte Carlo simulations of diffuse scattering in a manganite displaying polaronic disorder have shown that it should be possible to separate the quasi-static Huang scattering from acoustic phonon scattering except very close to the Bragg peaks. This is an especially challenging measurement as both are strongly enhanced in the same regions of reciprocal space. These tests require us to modify the secondary flight path to remove some sources of secondary scattering. We also plan to develop proposals for a more permanent installation as a cold-neutron magnetic diffuse scattering instrument that would complement the capabilities of *Corelli* at the SNS

Inelastic Neutron Scattering from Four-Dimensional $S(\mathbf{Q},\omega)$: We are collaborating with Argonne's Mathematics and Computer Science Division to improve the computational efficiency of histogramming the data in real time during the measurement. The real value of the 'sweep' mode is only realized when the experimenter can efficiently monitor the data as it is being streamed, but this is not possible with current software. We will continue developments so that this method will become part of the standard operation on the chopper spectrometers at SNS.

SERGIS: The type and range of scientific problems that can profitably be addressed with SERGIS are still under investigation, but they include the structure of films with rough surfaces or structural and/or chemical inhomogeneity, *e.g.*, surface landscapes that display islands, facets, self-affine roughness, and capillary waves. We will continue contribute to the development of SERGIS and the complementary Spin Echo Small Angle Neutron Scattering (SESANS) by exploring their applicability to systems of scientific interest to us, *e.g.* biological membranes, and contributing to developing tools for data analysis. Use of existing instruments (OFF-SPEC at ISIS, UK and SESANS at Delft University of Technology, The Netherlands) is envisioned.

Publications (FY07-FY09)

1. *Magnetic compound refractive lens for focusing and polarizing cold neutron beams*
K. C. Littrell, S. te Velthuis, G. Felcher, S. Park, B. Kirby and M. Fitzsimmons
Review of Scientific Instruments **78**, 035101 (2007).
2. *Corelli: Efficient single crystal diffraction with elastic discrimination*
S. Rosenkranz and R. Osborn
PRAMANA - Journal of Physics **71**, 705 (2008).
3. *Complementary polarized neutron and resonant x-ray magnetic reflectometry measurements in Fe/Gd heterostructures: Case of inhomogeneous intralayer magnetic structure*
E. Kravtsov, D. Haskel, S. G. E. te Velthuis, J. S. Jiang and B. J. Kirby
Physical Review B **79**, 134438 (2009).
4. *A spin-echo resolved grazing incidence scattering setup for the neutron interrogation of buried nanostructures*
J. Major, A. Vorobiev, A. Rühm, R. Maier, M. Major, M. Mezger, M. Nülle, H. Dosch, G. P. Felcher, P. Falus, T. Keller and R. Pynn
Review of Scientific Instruments **80**, 123903 (2009).

Behavior of Lipid Mixtures: From Lipid Rafts to Protein Crystallization

U. Perez-Salas (perez-salas@anl.gov) and S. Garg

Materials Science Division, Argonne National Laboratory, Argonne, IL 60439

D. Hanson and P. Laible

BioSciences Division, Argonne National Laboratory, Argonne, IL 60439

P. Bulter

*Center for Neutron Research, National Institute of Standards and Technology,
Gaithersburg, MD 01003*

L. Porcar

Large Scale Structures Group, Institut Laue-Langevin, Grenoble, CEDEX 9, France

Research Scope

Phase competition plays an important role in functionalizing multi-components in biomembranes. In this regard, an important paradigm is known as “lipid rafts”; phase separated domains within the membrane, rich in cholesterol and saturated lipids. Because it is not easy to do quantitative studies of the cell’s membranes *in vivo* due to the cell’s complexity, much work devoted to understanding the actual mechanisms driving lateral organization in membranes has been done on model membrane systems where the putative lipid rafts *in vivo* are modeled using simple binary and/or ternary mixtures of cholesterol, saturated and unsaturated lipids. The greatest insight gained from miscibility studies of ternary mixtures was the discovery of liquid-liquid coexistence regions. Because one of the liquid phases was rich in cholesterol and saturated lipids, it was conjectured that raft formation was thermodynamically inevitable; the liquid character of both phases supported the idea of a fluid membrane coexisting with freely diffusing, liquid raft domains. Moreover, the phase diagrams obtained give quantitative information about the relative amounts of each species present in either of the liquid phases. Important problems remain. A cell is tens of microns in size and can easily be modeled by a model vesicle of the same size. The paradox is that in the model system large rafts are clearly seen, while no such rafts are visible *in vivo*. This could be due to a number of things. The chemical complexity of the cell could prevent rafts from achieving their thermodynamic equilibrium size. Also the cytoskeleton could compartmentalize the cell’s membrane into nanometer-size regions, and therefore the domain sizes cannot exceed the size of the compartments. Finally, a complex sorting of specialized lipids and proteins may be required to assemble lipid rafts.

Cholesterol’s affinity for saturated lipids brings to the forefront other important questions. Cells have both internal and external sources of cholesterol. However, cholesterol’s distribution within the cell varies significantly: 35 to 45% of the lipid component of the plasma membrane (PM) is cholesterol, while it comprises only 0.1% to 2% in the endoplasmic reticulum (ER). How intracellular pathways distribute cholesterol and maintain these compositional differences is not understood. Insight into the mechanisms of these fundamental metabolic pathways of cholesterol is missing due to the

poorly understood transport of cholesterol between the intra-bilayer and inter-cellular membrane compartments and the plasma membrane. Our lack of knowledge concerning both the probability of exchange and the speed of cholesterol exchange is limiting our ability to explain the mapping of cholesterol in the cell, and our picture of cholesterol metabolism. Lipid compositional differences between the membranes within a cell could be partly responsible for the capacity of membranes to absorb cholesterol. This role of lipid composition on cholesterol transport to and from a membrane surface is critical for cholesterol metabolism.

Phase competition also plays an important role in controlling morphology and therefore functionality of multi-component bio-membrane-mimicking aggregates. An important application of this is the crystallization of membrane proteins. In contrast to soluble proteins, the hydrophobic moieties of membrane proteins add a layer of complexity that has resulted in a significantly smaller number of resolved structures than in the case of soluble proteins: 200 vs 60000. The bicelle-based method, a relatively new approach to crystallize membrane proteins, uses mixtures of detergents and membrane-mimicking lipids hosting membrane proteins after being removed (purified) from their native membrane. Crystals of bacteriorhodopsin and some G-protein coupled receptors have been obtained by this method. The key to making it a reliable methodology for a myriad of other membrane proteins is to understand how the lipid-detergent aggregate scaffold promotes the nucleation and growth of protein crystals.

Understanding the underlying physics of these processes requires a detailed knowledge of structure, kinetics and dynamics that neutron and x-ray scattering can provide.

Recent Progress

Lipid rafts: Because in cells the cytoskeleton compartmentalizes the cell membrane into nanometer size regions limiting the domain size to that of the compartments, model, nanometer-sized vesicles, 50 nm and 100nm vesicles made of a binary mixture of lipids was measured to study phase separation as a function of temperature by SANS. The binary mixtures were of structurally similar lipids, DPPC and DLPC, which are two saturated lipids differing in fatty acid chain lengths by 4 carbons: DPPC is 16 carbons long and DLPC is 12 carbons. The headgroup, phosphatidylcholine (PC), in contact with water, is the same for both lipids. This headgroup is a major constituent of cell membranes. The two-phase region in this binary mixture is composed of a liquid phase and a solid phase. DPPC and DLPC de-mix and mix as a function of temperature. The scattering profiles have been modeled using newly developed software in the group. Figure 1 shows data with the corresponding schematics of lipid vesicles where phase separated regions appear as a function of temperature. A fit to one data set is also shown. The software developed by the group gives the user significant flexibility and the ability to fit inhomogeneous vesicles with many domains, including those from membrane protein complexes.

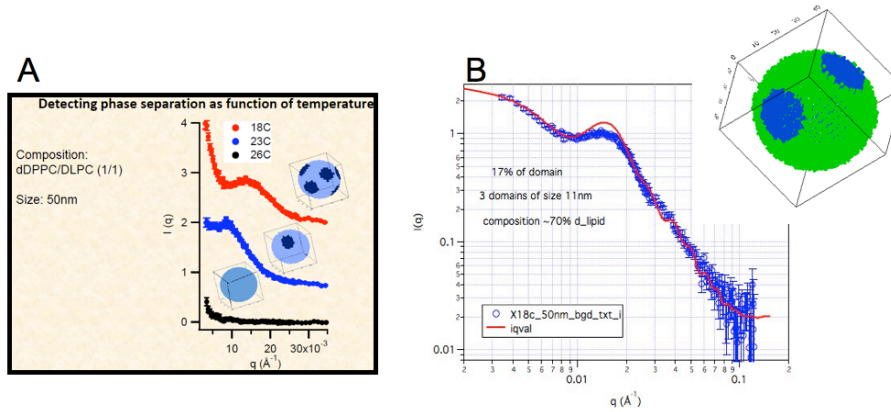


Figure 1. A) Scattering profiles for a 1:1 mixture of DPPC and DLPC with accompanying proposed domain formation model due to temperature induced phase separation. B) Fit to a data set corresponding to a 3:7 mixture of DLPC and DPPC respectively. At 18C the average number of domains is 3, obtained through newly developed software using the IGOR platform.

Cholesterol transfer and flip-flop kinetics in lipid vesicles: The transfer of cholesterol between small, 30 nm radius POPC unilamellar vesicles was obtained using time-resolved, small angle neutron scattering (TR-SANS). This technique allowed results to be obtained for the first time without any chemical alteration of the cholesterol molecule, such as fluorescent chemical tags. The measurements were done using a solvent with the same scattering length density of deuterated POPC, thereby ensuring that cholesterol was the only scattering component in the system. Initially, the cholesterol was only present in half the vesicle population. Over time, cholesterol transferred from these donor vesicles to the acceptor, cholesterol-free vesicles until equilibrium was reached and cholesterol was uniformly distributed among all the vesicles. The scattered intensity as a function of time was observed to decrease, and a two-rate kinetic model was used to fit the data. Additional measurements using cholesterol sulphate in place of cholesterol established that one of these rates corresponds to flipping between bilayer leaflets and the other to exchange between vesicles (figure 2 A). Studying the kinetic rates of the naturally fluorescent cholesterol, DHE, it was found that the chemical differences between DHE and cholesterol have significant effect in their kinetic behavior, and we therefore conclude care must be taken before assuming that transfer rates obtained using chemically tagged molecules correspond to the transfer rates of pure cholesterol (figure 2 B).

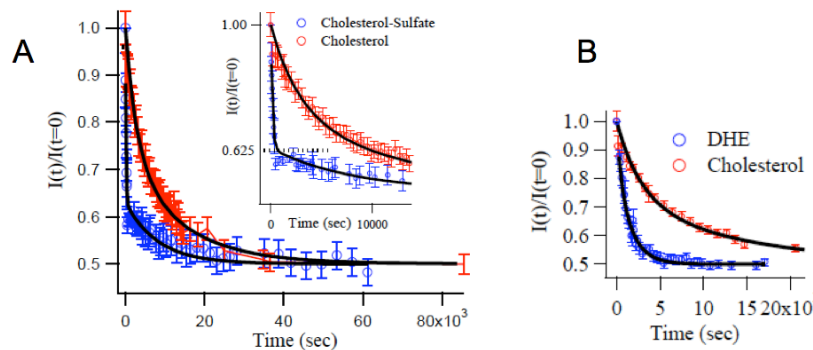


Figure 2. A. Intensity decay for cholesterol sulfate which clearly shows bi-kinetic behavior and which identified one as cholesterol transfer between vesicles and the other as the flipping rate of cholesterol within the bilayer. B. Intensity decay for DHE in contrast to cholesterol (B); the fit shows flipping rates for DHE and Cholesterol to be similar (~220 minutes half life) while the transfer rate is much faster for DHE than it is for Cholesterol (~90 min for cholesterol and 15 min for DHE)

Detergent-lipid mixtures and their potential as scaffolds for membrane protein crystallization: The bicelle-based method has proven to be a stable platform resulting in well-diffracting crystals of G-protein coupled receptors, and other proteins including bacteriorhodopsin. ‘Empty’ bicelles – those devoid of protein– form phase separated, lipid-detergent, disk-shaped aggregates. In proteo-bicelles, formed by mixing proteins with preformed discoidal bicelles, a second type of detergent, octylglucoside or maltoside, is introduced. Octylglucoside and maltoside are commonly used in protocols to extract the proteins from their native environment and stabilize them. In this study we used small angle neutron and x-ray scattering to explore the structure and phase-behavior changes induced by octylglucoside on the disk phase of bicelles. Preliminary results suggest that the new amphiphiles produce elongated aggregates when the ratio of octylglucoside to bicelle corresponds to crystallization conditions. However, further study with salt and higher concentration lipid will truly reveal the lipid scaffold structure during crystallization.

Future Plans

Lipid rafts and protein complexes: With the current software we are now equipped to study both multi-component vesicle systems believed to phase separate. Additionally we will pursue the feasibility of using a neutron spin-echo to measure off-specular reflection from inhomogeneous surfaces (SERGIS)

Cholesterol transfer rates: We will use TR-SANS and reflectivity to measure cholesterol transfer and flip-flop in a number of lipid systems. The results of this work will give insight into the basic mechanism of cholesterol transfer in cellular vesicular pathways and its differing affinity to lipids. The later will help understand the formation of “lipid rafts”.

Membrane protein crystallization in lipidic scaffolds. We intend to understand the roles of amphiphiles in high salt and concentration conditions which produce the meso-structures leading to crystallization.

Publications (FY07-FY09)

“Progress in the Development of Phase-Sensitive Neutron Reflectometry Methods” C. F. Majkrzak, N. F. Berk, P. Kienzle, U. Perez-Salas *Langmuir* 25, 4154-4161 (2009).

Self-Assembly of Conjugated Polymer Networks

K. Weigandt, J. Richards, G. Newbloom and D. C. Pozzo
(dpozzo@u.washington.edu)

Department of Chemical Engineering, University of Washington, Seattle, WA 98195

Program Scope

It is widely recognized that solar energy in the form of photovoltaics needs to take on a central role in resolving our future energy problems. It is also generally accepted that significant efforts are required to develop solar energy technologies that can accelerate the growth and competitiveness of photovoltaics in the renewable energy sector. This project involves a fundamental morphological investigation of self-assembling π -conjugated polymers that can be utilized for the creation of efficient polymer-based solar cells. These types of solar cells could significantly reduce the cost of manufacture through the use of established coating processes facilitating the production of large area devices.

One of the primary factors affecting solar cell performance is the structure of the active layer. This structure is determined largely by the self-assembly of conjugated polymers in solution. Therefore, the performance of polymer solar cells is intimately linked to polymer self-assembly. The main purpose of this research is to obtain a fundamental understanding of poly-3-alkyl-thiophene (P3AT) self-assembly and structure development occurring over multiple length scales and environmental conditions. In particular, we focus on the fibrillar gel phases that are created when conjugated polymers are dissolved at high concentrations (> 1wt%) in solvents of intermediate quality. A central hypothesis driving this research is that the large interfacial area and the inherent interconnectivity that is provided by the gel networks are ideal structural features for device performance. Despite their optimized structure, the rheological properties of these elastic network materials can make it challenging to coat and produce thin films for use in devices. Therefore, we have also developed a new route to generate networks of conjugated polymers inside the confined environment of oil-in-water emulsions. This strategy is aimed at overcoming the intrinsic difficulties of coating gelled materials while also providing for additional structural control through differences in self-assembly in confined environments. In this program we aim to correlate multi-scale structural features of conjugated polymer networks formed in bulk and in confined environments with their rheological, optical and electronic properties. In-situ and ex-situ scattering of neutrons (SANS and USANS) and x-rays (SAXS and WAXS) is used to seamlessly probe structural features in these materials at the molecular, fiber and network levels spanning a wide range of length scales (0.1-10,000 nanometers) and sample compositions. We aim to provide an unequivocal link between the macro-properties and the mesostructure of organogel networks formed from conjugated polymers.

Recent Progress

The project is currently at its early stages but significant progress has already been made towards reaching some of the goals stipulated in the project scope. Current work has primarily focused on the characterization of the network phase of regio-regular poly-3-hexyl-thiophene (P3HT) in aromatic solvents such as toluene, p-xylene and styrene. P3HT

is currently the most commonly used conjugated polymer in organic solar cells and thus it served as a model system to start this research program. We have utilized SANS and USANS to systematically characterize bulk organogels of P3HT over multiple length-scales. Figure 1 shows the complete scattering profile for a typical P3HT sample with the combined SANS and USANS (desmeared) along with a schematic of the structural features that are present at each size range. In the SANS region, the profiles are well approximated by the analytical model for non-interacting polydisperse parallelepiped fibers or ribbons. The model deviates significantly at the USANS range because of the network structure. Models such as the mass fractal can be used to interpret the scattering data in this range. The upturn at the lowest scattering angles is due to inhomogeneities in the gel phase that arise due to the formation of spherulites and micro phase-separation. It is important to point out that the electronic and optical properties of these materials can be greatly affected by structural modification occurring at any of these scales. Therefore, the simultaneous and non-invasive characterization by scattering methods, such as SANS and USANS, is essential. At molecular length scales, optical and electronic properties are directly affected by the crystallinity and conjugation of the polymers. We use wide angle x-ray scattering (WAXS) to characterize the extent of crystallization and to critically compare various possible packing structures to the scattering data. At the same time, at larger network length scales, electronic properties are also strongly affected by the extent and nature of the fiber connections.

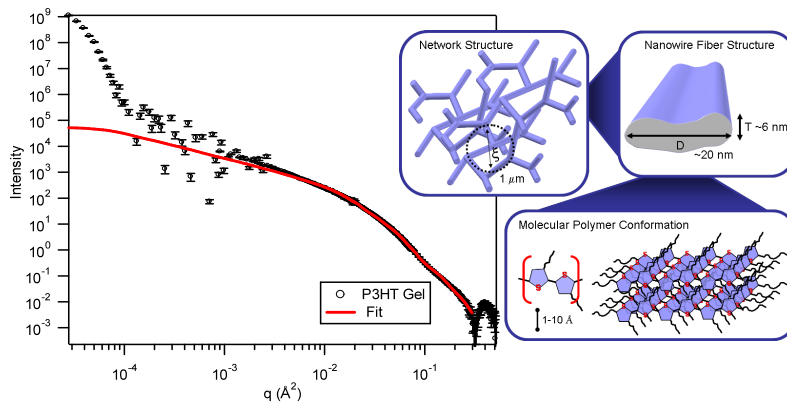


Figure 1: SANS and USANS profiles for P3HT organogel with fit to parallelepiped fiber model. Schematic of structural features.

Rheological, electrical and optical characterization is also performed in-situ and ex-situ along with the scattering experiments in order to directly correlate the structural transitions of the material with variations in the relevant macroscopic properties. Combined rheology and SANS experiments (rheo-SANS) have already been performed to probe the sensitivity of the network structure to the type of temperature profile that is used to induce network formation. It has been found that there exists a large hysteresis between network formation and network dissolution. The rheology of conjugated polymer organogels is also being rigorously compared to rheological models developed for other types of fibrillar gels including those developed for bio-polymers. Ex-situ optical and electrochemical characterization has also been used to decipher the correlation between properties and structure.

We evaluate also the effect of confinement in the self-assembly of P3HT. This is being primarily explored through the formation of organogels within the confined space of oil-in-water emulsion droplets. Figure 2 shows UV-Vis absorbance changes as the temperature is decreased (solvent quality reduced) and the fiber network is formed. The inset in Figure 2 shows that the P3HT emulsions are indeed stable and present clear thermochromic

behavior due to self-association. Neutron scattering presents a unique advantage to the characterization of the structure and self-assembly in emulsion systems, as it is capable of contrast variation. Here, solvents with isotope mixtures are used to eliminate the contribution of the oil-water interface on the scattering signal so that the P3HT contribution is isolated. We have preformed SANS experiments that also suggest that a core-shell structure, rather than a 3D network, forms when the drop size is reduced to sizes on the order of ~ 100 nm. In this structure, P3HT fibers crystallize and form a porous shell close to the oil-water interface. This effect is highly sensitive to the size of the oil droplets, the nature of the stabilizing agent and the mechanism of emulsification. TEM images of the emulsions (Figure 2) confirm the shell structure. This demonstrates that spatial confinement effects can be effectively used to manipulate the structure of these self-assembled materials.

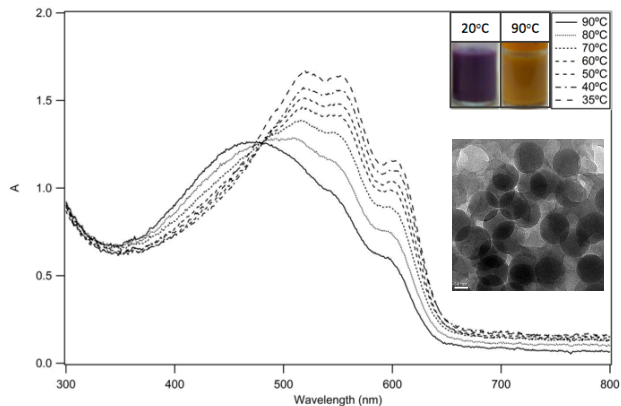


Figure 2: UV-Vis spectra for P3HT emulsions undergoing the self-assembly transition. Inset: TEM image of core-shell emulsion particles.

Future Plan:

Bulk Systems: We will continue to perform the structural evaluation (SANS, USANS and SWAXS) of bulk P3AT systems as a function of molecular parameters. We will evaluate fiber growth, gelation and crystallization kinetics using scattering, thermal analysis and spectroscopy. We also plan to assess single-chain packing inside the nanofibers using contrast variation SANS. Strategies will also be developed for structure manipulation through the application of controlled temperature profiles and external fields. Simultaneous rheological, dielectric and structural (SANS) experiments are also planned to quantify and directly correlate the development of electrical and mechanical properties during self-assembly.

Confined Systems: We will continue to explore and compare self-assembly, crystallization kinetics and network formation in bulk and in confined emulsion systems by performing systematic structural characterization. The effects of emulsion droplet size, molecular weight, polymer concentration, alkyl chain length and solvent type will continue to be explored to decipher their influence over the self-assembly from a fundamental perspective. We will also explore the manipulation of network structure through the application of variable temperature histories to the dispersions. Finally, we plan to explore the effects of adding fullerene n-type semiconductors (e.g. PCBM) to the emulsified systems and to develop effective coating strategies for solar cell applications. We will perform structural (e.g. reflectivity, SANS, TEM and SEM), optical (UV-Vis and fluorescence) and electrical characterization on the coated emulsion films.

Development of New Methods for Studying Nanostructures using Neutron Scattering

Roger Pynn

Indiana University
Department of Physics
Swain Hall West, 3rd Street
Bloomington, IN 47405
rpynn@indiana.edu

Program Scope: The goal of this project is to develop and apply a new interferometric technique that will extend and complement traditional neutron scattering methods in the study of nanostructures. The new method, dubbed Spin Echo Scattering Angle Measurement (SESAME), directly provides a measurement of a spatial correlation function (the Paterson function) in real space, automatically accounts for multiple neutron scattering and may be used to measure either bulk samples or surfaces.

Description of SESAME: About 200 years ago, a British chemist named William Wollaston showed that the two polarization states of light could be split by a pair of birefringent prisms that now bear his name. The action of Wollaston's device is shown in Figure 1a. A pair of Wollaston prisms, combined with an optical polarizer can be used to produce two, spatially-separated, polarized light rays which are coherent with one another and which have a well defined relative phase, ψ , as shown in Figure 1b. An equivalent device, such as those shown in Figures 2b and 2c can be built for neutrons by using triangular regions of magnetic field rather than calcite prisms.

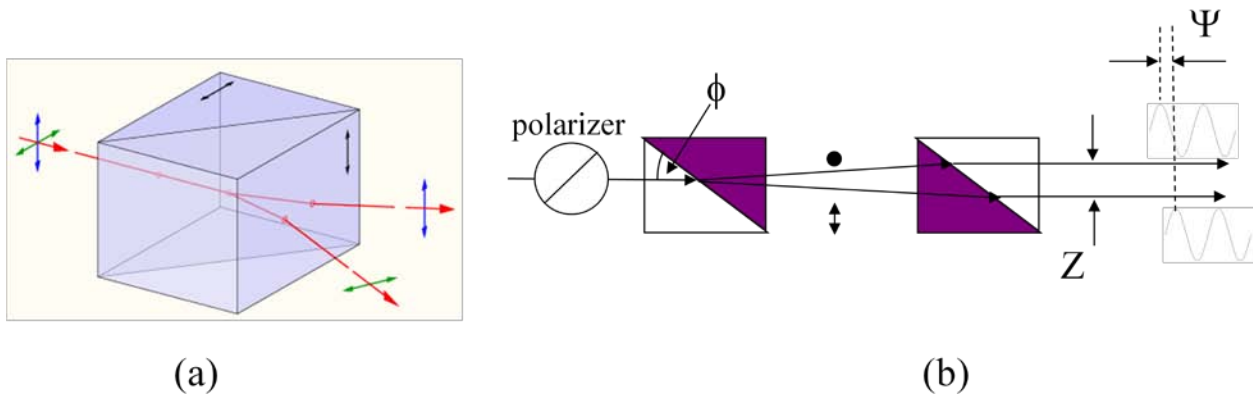


Figure 1: (a) A Wollaston prism made from two pieces of calcite with perpendicular optic axes; (b) A pair of such prisms produces two separated parallel rays with orthogonal polarizations indicated by a dot and a diamond. If the light incident on the first prism is plane polarized at 45° to the optic axis of either calcite crystal, as indicated by the circle with a 45° line to the left of the first Wollaston prism, the two parallel rays will be coherent and separated by a phase angle Ψ .

For SESAME, two neutron Wollaston prisms are used to spatially separate the spin eigenstates of a neutron and another pair of such prisms is used to bring those two states back together again, as shown in Figure 2a, to yield a spin echo. The distance probed in the sample (called the spin echo length) is equal to the separation of the spin states at the sample position and can range from a few tens of nanometers to several microns for reasonably achievable magnetic fields. The measured neutron

polarization turns is the Fourier transform of the slit-smearred neutron scattering function which, in turn, is the Abel transform of the density-density correlation function of the sample.

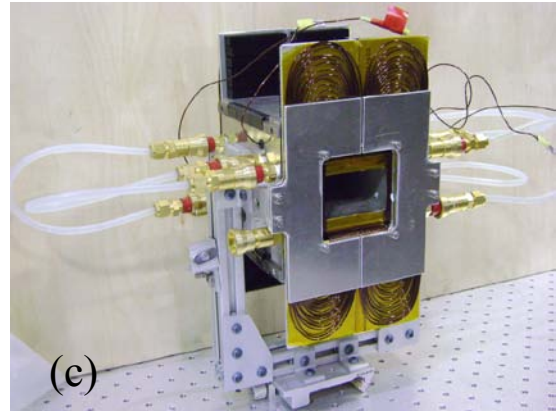
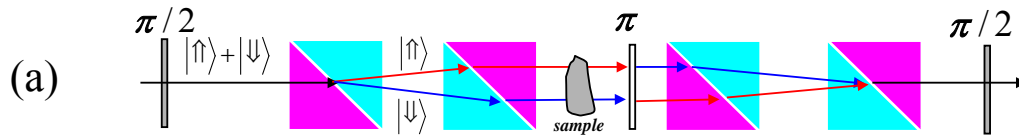


Figure 2: (a) the combination of neutron Wollaston prisms used in our experiments showing the separation of the two neutron spin eigenstates at the sample position; (b) an early version of a neutron Wollaston prism wound using aluminum wire (transparent to neutrons) showing the partially disassembled mu-metal magnetic flux return box; (c) a more recent neutron Wollaston device with water cooling and gaps in the entry and exit faces.

Recent Results

- (a) *Development of neutron Wollaston prisms with smooth magnetic field transitions.* An essential difference between Wollaston prisms for light and neutrons is that it is easy to embed the former in a medium that is not birefringent for light (e.g. air) and which does not therefore cause spatial aberrations of the Larmor phase, Ψ , between the polarization states. This is harder to do for neutrons because the birefringent medium is a magnetic field. To realize the cartoon shown in Fig 2a exactly we would need to contain homogeneous magnetic fields in precisely defined regions of space and embed these in regions of zero magnetic field. This is not easy to achieve. We have resolved this problem by building prisms with gaps for neutrons to enter and exit (Fig 2c). The magnetic field “leaks out” of the gaps but, because of the symmetry of the arrangement in Fig 2a, the aberrations in Larmor phase, Ψ , caused by the field leakage cancel one another almost completely. This effect, in which local and global symmetry is used to cancel aberrations in measurement instruments is a principle that we employ systematically. Our goal is to design magnetic field environments which allow large-area, divergent neutron beams to be used to interrogate nanostructures, thereby increasing the scattered neutron intensity without jeopardizing spatial resolution.

- (b) *Measurement of large in-plane length scales using neutron reflectometry.* To test the ability of SESAME to interrogate relatively long length scales (50 nm – 1000 nm) within a surface, we used the method to measure scattering from silicon diffraction gratings with rectangular and sinusoidal profiles. These measurements have been made both on Asterix at LANSCE using equipment shown in Fig 2c and on the newly installed reflectometer, OFFSPEC, at ISIS which is designed specifically for SESAME. To interpret the measurements, we developed a dynamical theory and found that it accounted for all of the features observed in our experiments on multiple gratings.
- (c) *In collaboration with Dr Wei-Ren Chen of Oak Ridge National Laboratory, we studied the use of SESAME to explore interparticle interactions in colloidal materials.* Although neutron scattering from a colloidal suspension is fully determined by interactions between the constituent particles, information about the shape of these interactions may be spread out over a large range of momentum transfer in measurements of $S(Q)$. SESAME directly measures a real-space correlation function which, as shown in Fig 3a, is expected to be very sensitive to details of the short-range interparticle interaction. Preliminary measurements of $G(Z)$ made on a monodisperse PMMA suspension in preparation for a detailed study of the effects of osmotic compression are shown in Fig 3c. These measurements also confirmed that SESAME results are insensitive to the degree of multiple scattering by the sample, allowing strongly scattering samples to be measured with impunity.

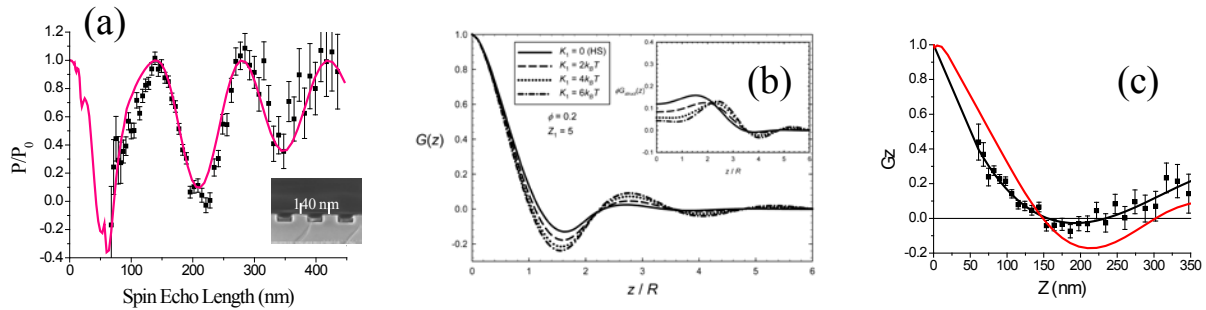


Figure 3: (a) Normalized spin echo polarization measured and calculated for a diffraction grating whose profile, measured by TEM, is shown in the insert; (b) calculated changes in the spatial correlation function, $G(z)$, measured by SESAME for small changes in an attractive Yukawa potential added to a hard-sphere repulsive interaction; (c) preliminary measurements of a 40% concentration of monodisperse PMMA particles in deuterated toluene showing the strong deviation of the measured correlation function from the simple Percus-Yevick hard spheres model.

Future Plans:

- (a) *Colloidal systems:* We plan to apply SESAME to a suspension of 300 nm-diameter, monodisperse PMMA nanospheres with smaller particles added to induce various levels of effective attraction between the PMMA spheres. The system without added smaller particles has been extensively studied by light scattering and shown to be a model hard-sphere system, at least when it is dilute. Because of the correlation function measured with SESAME is expected to be sensitive to interparticle potential, we expect to be able to test the validity of a number of theories of fluid structure.

- (b) *Surfaces*: Now that we have developed an exact dynamical theory for scattering by a diffraction grating and verified that it works using SESAME, we will explore the range of validity of various approximate theories that are used to describe surface scattering, including the DWBA and the Phase Object Approximation.
- (c) *Reflectometry with “Wavy” and “Rough” Surfaces*: Together with collaborators from the Technical University of Munich, we will explore the application of SESAME to measurement of the reflectivity of samples which display either short-range or long-range changes in surface slope that are difficult to measure accurately with conventional reflectometry.

Publications 2008-2010:

The Use of Symmetry to Correct Larmor Phase Aberrations in Spin Echo Scattering Angle Measurement; Roger Pynn, Wai-Tung Hal Lee, Paul Stonaha, Shah Valloppilly, Adam Washington, Brian Kirby, Brian Maranville, and Charles Majkrzak; Rev. Sci. Instrum. **79**, 063901 (2008)

Spin Echo Scattering Angle Measurement at a Pulsed Neutron Source; Roger Pynn, M. R. Fitzsimmons, W. T. Lee, V. R. Shah, A. L. Washington, P. Stonaha, and K. Littrell; J. Appl. Cryst., **41**, 897 (2008)

Pulsed Neutron Beam Control using a Magnetic Multiplet Lens; T. Oku, T. Shinohara, J. Suzuki, R. Pynn, H. M. Shimizu; Nuclear Instruments and Methods **A600**, 1, 100-102 (2009)

Birefringent Neutron Prisms for Spin Echo Scattering Angle Measurement; Roger Pynn, M. R. Fitzsimmons, W. T. Lee, P. Stonaha, V. R. Shah, A. L. Washington, B. J. Kirby, C. F. Majkrzak, and B. B. Maranville; Physica **B 404**, 2582–2584 (2009)

A spin-echo resolved grazing incidence scattering setup for the neutron interrogation of buried nanostructures; J. Major, A. Vorobiev, A. Ruehm, R. Maier, M. Major, M. Mezger, M. Nuelle, H. Dosch, G. P. Felcher, P. Falus, T. Keller, R. Pynn, Rev. Sci. Instrum. **80**, 123903 (2009)

Theoretical studies on the structure of interacting colloid suspensions by spin echo small angle scattering; X. Li, C-Y Shew, Y. Liu, R. Pynn, E. Liu, K. W. Herwig, G. S. Smith, J. L. Robinson, and W-R Chen, J. Chem; Phys., **132**, 174509 (2010)

Dynamical theory calculations of spin-echo resolved grazing-incidence scattering from a diffraction grating; R. Ashkar, P. Stonaha, A. L. Washington, V. R. Shah, M. R. Fitzsimmons, B. Maranville, C. F. Majkrzak, W. T. Lee, W. L. Schaich, and R. Pynn; J. Appl. Cryst., **43**, 455 (2010)

Development of a beam line for spin echo scattering angle measurement at the Low Energy Neutron Source; A. L. Washington, P. Stonaha, R. Ashkar, R. Pynn, V. R. Shah; Presented at International Collaboration on Advanced Neutron Sources (ICANS) (2010) (to be published)

Extended Abstract Grant DE-FG02-08ER46486

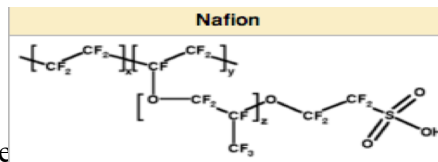
Coherent Transport in Nafion and Other Superprotonic Conductors

George Reiter
Physics Department
University of Houston
Houston Tx 77204-5506
greiter@uh.edu

Program Definition:

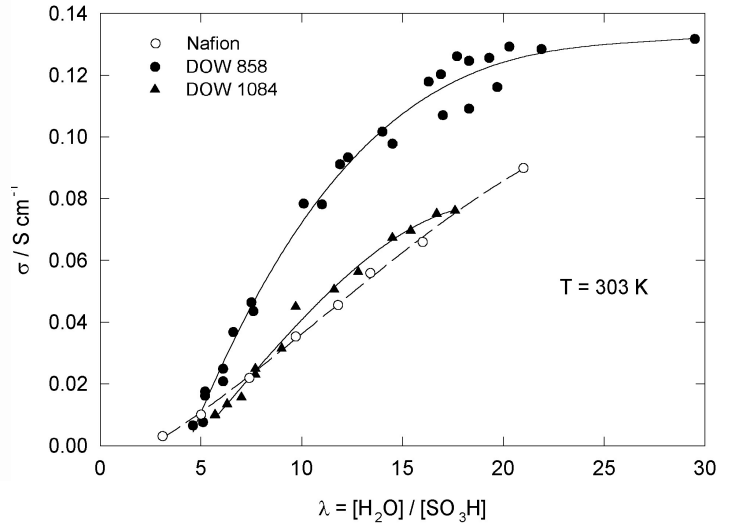
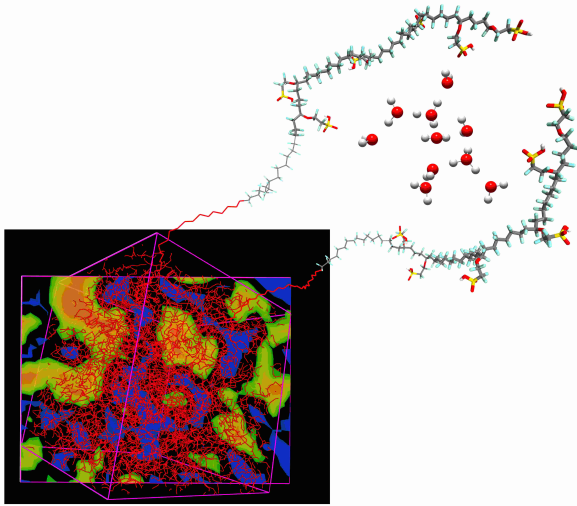
Neutron Compton Scattering, also called Deep Inelastic Neutron Scattering, is a relatively recent local probe of condensed matter systems. The program's intention is to explore what can be learned using it in important hydrogen bonded systems, in particular, water, ferroelectrics, and superprotonic conductors. It provides a direct measurement of the momentum distribution of the protons (and other light ions). In nearly all cases, this is determined by the ground vibrational state of the protons, and hence provides a probe of the effective potential the proton experiences in its local environment. In some cases, the information can be inverted to obtain a direct measurement of the Born-Oppenheimer potential surface for the proton. This has been done and published, in the first such measurement, for $\text{Rb}_3\text{H}(\text{SO}_4)_2$ [1], a superprotonic conductor. In all cases, the measurements is a particularly sensitive probe of the potential energy surface. They are sensitive to quantum coherence. When the proton is in a double or multiple well, and the proton is distributed coherently in the wells, the momentum distribution shows characteristic oscillations, the wavelength of which gives directly the separation of the well. Such oscillations have been observed by us in a powder sample of $\text{Rb}_3\text{H}(\text{SeO}_4)_2$, persisting through the superprotonic transition. A proton that moves coherently through the crystal from one double well to another as the heavy ions move cannot be thought of in the usual terms as a semiclassical particle moving from point to point. It is rather more like a wave diffracting from one well to another as the environment permits. This sort of coherent transport has recently been observed in Nafion, the commercial fuel cell electrolyte, and a related material.

Recent Progress: Nafion is a sulfonated tetrafluorethylene copolymer used as an electrolyte in commercial fuel cells. A multiscale simulation of the structure is shown in the figure below. The hydrophobic backbones of the polymer enclose the water in a spongelike matrix, with the hydrophilic side chains containing the sulphonyl groups extending into the bulk water pockets. Conductivity in the material is due to protons donated from the sulphonyl groups of the polymer to the enclosed water matrix. Within the



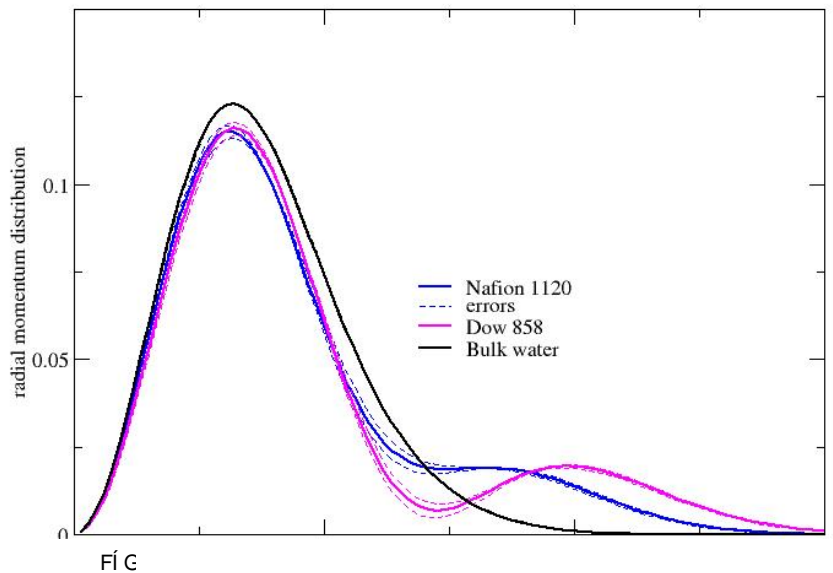
be determined by the same process as in bulk water, the continuous interchange of H_5O_2^+ (Zundelcations) and H_3O^+ (hydronium) structures. One of each of these

configurations is shown in the figure. Recently, a class of similar materials, with shorter side chains(DOW 858, DOW 840, DOW 1084) have been shown to have improved electrical and structural properties with regard to Nafion. The conductivity of two of these compared to Nafion, as a function of the fraction λ of water molecules to sulfonyl groups is shown below.



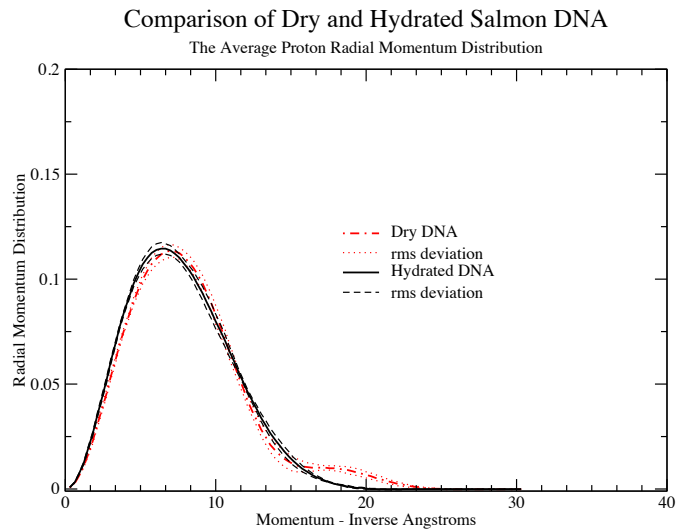
Momentum distribution measurements were made at room temperature on Nafion 1120, the commercial material, and Dow 858, the short side chain version of the polymer, at a water concentration in both cases of $\lambda=14$. The figure below shows that comparison of these two measurements with each other and that of bulk water. It is evident that the quantum state of the protons in the Nafion materials is dramatically different from that of bulk water. The covalent bond has been replaced by a double well effective potential with, in both cases, a separation of the wells of ~ 2 Angstroms. There are more such delocalized protons in the Dow 858 material. The momentum distribution of the Dow material is very similar to the distribution of the protons in water confined in xerogel[2], with pores of 23 Angstrom diameter. The surface there has some similarity in that it is irregular and there are hydroxyl groups projecting into the cavity. Since there is only one free proton for 14 water molecules, it must be that the

Proton Coherence in Nafion and Dow 858



hydrogen bond network is strongly distorted by the presence of the surface to produce momentum distributions such as those above. An attractive hypothesis is that the difference in conductivity is due to the difference in the quantum state of the proton, and that the conductivity in both materials is an example of coherent transport

The delocalization of the protons in water has been observed also by us in connection with biological systems. Reductions in the proton kinetic energy in the bulk of the water surrounding a protein as it unfolds due to raising the temperature have been observed for dilute solutions of lysozyme. It also plays a role in the hydration of DNA. The structural form for dry DNA, the A phase adsorbs about 20 water molecules/base pair in transforming to the biologically active B phase. In the early stages of this process, the reduction in kinetic energy of the protons in the system plays a significant role, and for 6 water molecules/base pair, provides the entire binding energy. The figure to the right, in addition to showing the average reduction in kinetic energy for the system when the 6 water molecules/base pair are present, shows that some of the protons in the dry DNA are in double well potentials.



In addition to the experimental work, we have tested the idea that water can be described as isolated molecules interacting electrostatically through hydrogen bonds. High quality ab initio calculations of the response of isolated molecules to electric fields have been put together with simulations of bulk water, and compared with measured momentum distributions. Although this model holds for dilute water, as in the supercritical phase, it fails significantly for room temperature water. Quantum correlation and electronic overlap effects must be included if the momentum distribution in bulk water is to be explained.

Future plans:

The conjecture on the relationship of the momentum distribution to the conductivity can be explored simply by measuring the momentum distribution at more values of λ and of using other variants of Nafion, such as Dow 1084 to determine if a pattern exists. The effects of coherence can also be tested by replacing the protons with deuterons. Although deuterated Nafion may not be readily available, given the fact that most of the protons we are seeing are those associated with the water molecules, not those donated by the sulfonyl groups, this should not be a problem.

The change of zero point energy with the configuration of proteins in water is going to be further explored by varying the concentration of lysozyme in the water, from high

concentrations, similar to those in living cells, to intermediate concentrations, with separations of the proteins of the order of 100 Angstroms.

The same will be done with both single strand and double strand DNA. We already know from our experiments that there is no noticeable change in the kinetic energy of bulk water as DNA unwinds with temperature, in contrast to the unfolding of proteins. It seems likely that all the changes occur in the water molecules that are the first molecules that are absorbed, and this will be tested by varying the hydration levels.

Ab initio simulations are under way in collaboration with others to determine if the delocalization of the protons can be explained by changes in the Born-Oppenheimer surfaces of individual protons when the water network is strained, or are the result of cooperative interactions between the protons.

Published papers-2007-2009

- (1) D. Homouz, G. Reiter, J. Eckert and R. Blinc, "Measurement of the 3-D Born-Oppenheimer Potential of a Proton in a Hydrogen Bonded System using Deep Inelastic Neutron Scattering: The Superprotonic Conductor $\text{Rb}_3\text{H}(\text{SO}_4)_2$ " *Phys. Rev. Letts.* **98**, 15502 (2007)
- (2) V. Garbuio, C. Andreani, S. Imberti, A. Pietropaolo and G. F. Reiter, Proton quantum coherence observed in Water confined in silica nanopores *J. Chem. Phys.* **127**, 154501 (2007)
- (3) Deuteron momentum distribution in KD_2PO_4 , G. Reiter, A. Shukla, P.M. Platzman and J. Mayers, *New J. Phys.* **10** 013016 (2008)
- (4) Proton momentum distribution of liquid water from room temperature to the supercritical phase C. Pantalei A. Pietropaolo, R. Senesi, S. Imberti, C. Andreani, J. Mayers, C. Burnham, and G. Reiter, in *Phys. Rev. Letts.* **100**, 177801 (2008)
- (5) The vibrational proton potential in bulk liquid water and ice C. J. Burnham, D. J. Anick, P. K. Mankoo, and G. F. Reiter *J. Chem. Phys.* **128**, 15419 (2008)

Novel Molecular Materials for Hydrogen Storage Applications

Maddury Somayazulu (zulu@gl.ciw.edu), Timothy Stroebel, Raja Chellappa,
Viktor V Struzhkin and Russell J Hemley
Geophysical Laboratory, Carnegie Institution of Washington, Washington DC, 20015

Research Scope

The technology of using hydrogen as an environmentally clean and efficient fuel is an active research area worldwide. The key to emergence of a viable global hydrogen economy is the availability of light weight transport and safe storage of hydrogen as a fuel. Hydrogen molecules can bind to the surface of any material either through weak dispersive interactions (physisorption) or through stronger chemical bonding (chemisorption). Storage via physisorption in metal-organic or covalent-organic frameworks and activated carbons is a field that has received a lot of experimental and theoretical attention. Dissociative chemisorption of hydrogen molecules in a number of metal doped carbon and boron based tubular structures has been theoretically predicted and experimentally investigated. It is now becoming evident that using a combination of the two techniques for example with exposed metal ions in frameworks could lead to better retention and rehydrogenation.

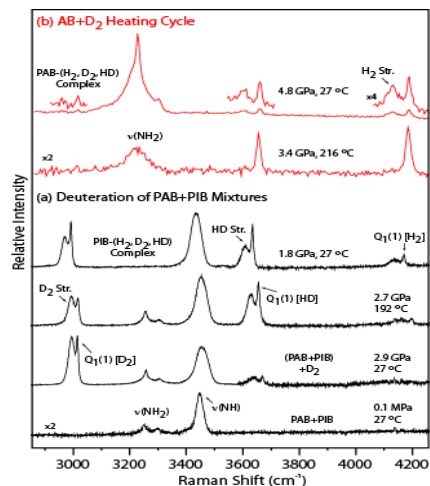
We propose to use high pressure to help design and understand new classes of materials suitable for reversible hydrogen storage. Pressure serves as a unique thermodynamic and chemical variable which can be used to produce new materials. Pressure changes the transition temperatures making the corresponding phenomena accessible at ambient temperatures. For example, we have identified the extraordinary high pressure stability of new compounds in Xe-H₂, SiH₄-H₂, and NH₃BH₃-H₂. While the list of new high hydrogen content compounds synthesized at high pressures continues to grow, studies on hydrogen interaction with covalent organic framework, crown ethers, and B-N-H oligomers in hydrogen, have helped gain insight into storage mechanisms and re-hydrogenation in these materials. In addition, on-going spectroscopic studies on the CO₂-H₂O binary system and the NH₃-H₂-H₂O ternary system at high pressures showed the presence of new clathrates.

By employing a suite of experimental techniques in addition to Raman and synchrotron infrared (IR) spectroscopy measurements, insights into hydrogen interactions with B-N-H compounds and complexes will be obtained using synchrotron x-ray diffraction at the Advanced Photon Source (APS) and neutron diffraction at Oakridge National Laboratory (ORNL), XANES and x-ray Raman scattering at APS. Diamond anvil cells with gas feed-through capabilities up to pressures of 2 kba and temperature range 5 K – 800 K will be modified for investigating hydrogen uptake and release characteristics.

Recent Progress

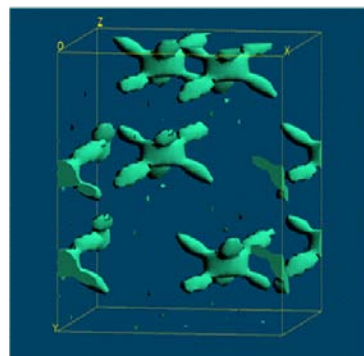
- 1. Chemical hydrides:** B-N-H compounds are gravimetrically efficient due to the light weight elements involved and exhibit bonding characteristics that play a unique role in their ability to interact with H₂ molecules. A promising prototype is ammonia borane (NH₃BH₃) that has a high hydrogen content (19.6 wt. % H and 0.145 kg L⁻¹). High pressure Raman spectroscopy of NH₃BH₃-H₂ mixtures up to 60 GPa reveals unusual pressure-induced complexation and

intermolecular interactions. The behavior of the $\nu(\text{NH}_3)$ modes in the $\text{NH}_3\text{BH}_3\text{-H}_2$ complex indicates a dominant role of the NH_3 functional group in the observed interactions. We suggest that the three dimensional intermolecular dihydrogen bonding network ($\text{N-H}\cdots\text{H-B}$) allows the pressure-aided stabilization of H_2 molecules within the NH_3BH_3 lattice. Our spectroscopic measurements on rehydrogenation of PAB and PIB polymeric species at elevated pressures indicate that hydrogen reuptake can occur via formation of $\text{PAB-(H}_2)_y$ or $\text{PIB-(H}_2)_y$ complexes. PAB and PIB react with H_2 and D_2 at elevated pressures (2–4 GPa) at room temperature by both physical and chemical reactions as revealed by a series of remarkable observations. H_2 can therefore act as a ligand donating its s-bonded electron pair to partially filled p-orbitals in B ($\text{h}^2\text{-H}_2$ model) in the PIB-H_2 complex but electron deficiency of ‘B’ implies no backdonation. Therefore the shift in H_2 stretching modes are not as dramatic as in Kubas complexes.



2. Xenon-hydrogen system:

A suite of x-ray diffraction and optical spectroscopy measurements reveal the formation of a stable compound in the Xe-H_2 binary system. At 4.8 GPa, a unique, hydrogen-rich structure forms that can be viewed as a tripled solid hydrogen lattice modulated by layers of Xe, consisting of xenon dimers. Structure refinements based on new single crystal diffraction techniques provide clear evidence for pressure-induced changes in electron density and the formation of unusual bonding states associated with the xenon dimers and hydrogen molecules.

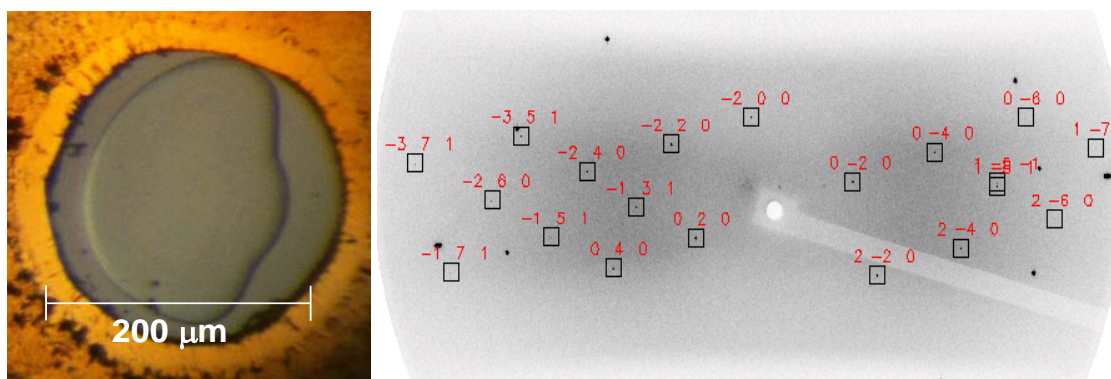


Electron density calculated from the observed structure factors (Beever-Lipson maps) shows the spread of electron density between xenon atoms and in the direction of coordinated H_2 molecules lying within the first coordination sphere of the Xe atoms.

Varying the applied pressure tunes the Xe-Xe distances in the solid over a broad range from that of an expanded xenon lattice (relative to solid Xe at zero pressure) to the distances observed in metallic xenon at megabar pressures. Infrared and Raman spectra indicate a weakening of the H_2 covalent bond as well as the persistence of semiconducting behavior in the compound $\text{Xe(H}_2)_8$ to at least 255 GPa.

3. Silane-Hydrogen system:

We have demonstrated the formation of a novel compound of silane (SiH_4) and H_2 at pressures above 7 GPa that displays markedly stronger intermolecular interaction than previously reported compounds. A complex H-H vibron spectrum with anti-correlated pressure-frequency dependencies and a striking H-D exchange below 10 GPa reveal strong and unusual attractive interactions between SiH_4 and H_2 and molecular bond destabilization at remarkably low pressure. A new range of accessible pressure-driven intermolecular interactions for hydrogen-bearing simple molecular systems, and a new approach to perturb the hydrogen covalent bond are thus possible.



Single Crystal of $\text{SiH}_4(\text{H}_2)_2$ in H_2 medium. The indexed single crystal pattern is on the right.

We observed similar compound formation in $\text{Ge}_3\text{H}_4\text{-H}_2$ system. The dissimilarity between these systems in comparison to $\text{CH}_4\text{-H}_2$ system throws up important questions regarding the stabilizing interactions between these molecular species and the possibility of synthesizing Kubas complexes.

Future Plans

We will explore the full phase diagram of Xe-H_2 and Xe-O_2 and expand these studies to the ternary system $\text{Xe-O}_2\text{-H}_2$. We will continue the exploration of methane like dual systems of hydrogen storage by investigating the ternary systems $\text{CH}_4\text{-SiH}_4\text{-H}_2$; $\text{CH}_4\text{-GeH}_4\text{-H}_2$ and $\text{SiH}_4\text{-GeH}_4\text{-H}_2$. These studies will be performed with a combination of Raman, IR and neutron spectroscopy augmented by neutron scattering measurements at SNAP (IPNS). The mechanics and thermodynamics of rehydrogenation (and deuteration) in ammonia borane, polymeric residues of amino and imido boranes will be investigated using a combination of spectroscopic techniques. Using these measurements and the complementary XANES measurements on boron and nitrogen k edges of retrieved samples as well as *in-situ* x-ray Raman studies at APS. We will pursue DFT calculations that can help construct a comprehensive understanding about the interactions at high pressures in these materials.

Publications (FY07-09)

1. *Pressure-induced phase transitions in LiNH_2*
Raja S Chellappa, Dhanesh Chandra, Maddury Somayazulu, Stephen A Gramsch and Russell J Hemley
J. Phys. Chem. B, **111**, 10785 (2007).
2. *Pressure-induced complexation of $\text{NH}_3\text{BH}_3\text{-H}_2$*
Raja S Chellappa, Maddury Somayazulu, Viktor V Struzhkin, Thomas Autrey and Russell J Hemley
J. Chem. Phys., **131**, 224515 (2009).
3. *High-Pressure Hydrogen Interactions with Polyaminoborane and Polyiminoimino borane.*
Raja S Chellappa, Thomas Autrey, Maddury Somayazulu, Viktor V Struzhkin and Russell J Hemley

- Chem. Phys. Chem., **11**, 93 (2010).
4. *Rheium Reactivity in H₂O-O₂ supercritical mixtures at high pressures.*
Raja S Chellappa, Maddury Somayazulu and Russell J Hemley
High Pres. Res. (in print).
 5. *Novel Pressure-induced interactions in Silane-Hydrogen*
Timothy A Strobel, Maddury Somayazulu and Russell J Hemley
Phys. Rev. Lett., **103**, 065701 (2009).
 6. *Pressure-induced bonding and compound formation in xenon-hydrogen solids*
Maddury Somayazulu, Przemyslaw Dera, Alexander F. Goncharov, Stephen A. Gramsch,
Peter Liermann, Wenge Yang, Zhenxian Liu, Ho-kwang Mao and Russell J. Hemley
Nature Chemistry, **2**, 50 (2010).
 7. *Hydrogen storage in molecular clathrates,*
Struzhkin, V. V., B. Militzer, W. L. Mao, H. K. Mao, and R. J. Hemley
Chem. Rev., **107**, 4133-4151 (2007).

Author Index

Author Index

Abernathy, D. L.	23, 136	Gubarev, M. V.	112
Antropov, V. P.	14	Guidi, T.	23
Armitage, N. P.	1	Guthrie, M.	104
Bagdasarova, Y.	112	Hanson, D.	140
Bauer, E. D.	5, 116	Hanson, Helen A.	124
Boehler, R.	104	Harmon, B. N.	14
Broholm, C.	1	Hemley, Russell J.	155
Bewley, R. I.	23	Hill, J. P.	78
Bulter, P.	140	Hoffmann, Axel	48
Campuzano, J. C.	23	Hücker, Markus.	27
Cava, R. J.	1	Iavarone, Maria	48
Chang, S.	109	Ice, Gene E.	70
Chapon, L. C.	23	Ji, S.	109
Chellappa, Raja	155	Jiang, J. S.	48
Chen, Gang	60	Jiang, Zhang	60
Chen, Sow-Hsin	32	Joyce, J. J.	105
Chen, X.	104	Kanatzidis, M. G.	23
Cheong, S-W.	44	Karapetrov, Goran.	48
Chmaissen, O.	23, 83	Katayama, N.	109
Christianson, A. D.	23, 116	Keiderling, U.	124
Chung, D. Y.	23	Khaykovich, B.	112
Claus, H.	23	Kreyssig, A.	14
Dabrowski, B.	83	Kuhl, Tonya	62
Dai, Pengcheng	9	Laible, P.	140
DeCaro, Curt	60	Lal, Jyotsana	67
Dimitrov, I. K.	124	Laver, M.	124
Durakiewicz, T.	105	Lawrence, Jon	116
Egami, T.	87	Lee, S.-H.	109, 120
Enoki, M.	109	Lee, Young.	56
Faller, Roland.	62	Leighton, Chris	52
Fischer, Jack E.	40	Lin, Z. W.	109
Fitzsimmons, M. R.	91	Ling, X. S.	124
Fouquet, Peter	67	Louca, D.	109, 128
Fujita, M.	109	Lumsden, M. D.	23
Fullerton, Eric E.	95	Lurio, Laurence.	60
Fultz, Brent	99	Ma, Yicong	60
Garg, S.	140	Maccarini, Marco	67
Gentile, T. R.	74, 103	Mackay, Michael E.	66
George, E. P.	87	Majkrzak, C. F.	124
Glyde, Henry R.	40	Makowski, Lee.	67
Goldman, A. I.	18	Manuel, P.	23
Goremychkin, E. A.	27	Mao, D.	104
Graham, K. S.	105	Maranville, B. B.	124
Gu, Genda	27, 109	McQueeney, R. J.	14

Mitchell, J. F.	23	Tulk, C. A.	104
Molaison, J.	104	Vaknin, D.	14
Moncton, D. E.	112	Visani, Cristina	48
Montfrooij, Wouter	132	Wang, CuiHuan.	116
Moreira Dos Santos, A. F.	104	Wang, Xi	124
Morris, J. R.	87	Weigandt, K.	144
Movshovich, R.	5	Wen, J. S.	109
Mukhopadhyay, Mrinmay.	60	Wesolowski, David J.	31
Nagler, Stephen.	68	Worcester, David	60
Nemes, Norbert.	48	Xu, Guangyong.	27, 109
Newbloom, G.	144	Xu, Z. J.	109
Nicholson, D. M.	87	Yamada, K.	109
Norman, M. R.	27	Ye, F.	136
Olamit, J.	91	Yildirim, Taner	40
Osborn, R.	23, 83, 136	Zaliznyak, Igor.	27
Pang, Judy W. L.	70	Zarestky, J. L.	14
Parikh, A. N.	60		
Perez-Salas, U.	136, 140		
Porcar, L.	140		
Pozzo, D. C.	144		
Pradham, N.	104		
Proffen, T.	69		
Pynn, Roger.	147		
Ramsey, B. D.	112		
Reiter, George.	151		
Reznik, D.	23		
Richards, J.	144		
Ronning, F.	5		
Rosenkranz, S.	23, 136		
Russina, M.	124		
Santamaria, Jacobo	48		
Sarrao, J. L.	5		
Sato, T. J.	109		
Shi, J.	124		
Singh, David J.	13		
Singh, S.	91		
Sinha, Sunil K.	60, 95		
Snow, W. M.	74, 103		
Somayazulu, Maddury	155		
Stroebel, Timothy	155		
Struzhkin, Viktor V.	155		
Tchernyshyov, O.	1		
te Velthuis, S. G. E.	48, 136		
Tesanovic, Z.	1		
Thompson, J. D.	5		
Tranquada, John M.	27, 109		

Neutron Scattering Contractors Meeting Participant Listing

Name	Organization	E-Mail
N. Peter Armitage	Johns Hopkins University	npa@pha.jhu.edu
Eric D. Bauer	Los Alamos National Laboratory	edbauer@lanl.gov
Luke Bilbro	Johns Hopkins University	lsbilbro@pha.jhu.edu
Hassina Bilheux	Oak Ridge National Laboratory	bilheuxhn@ornl.gov
Collin Broholm	Johns Hopkins University	broholm@jhu.edu
Robert Cava	Princeton University	rcava@princeton.edu
Sow-Hsin Chen	Massachusetts Institute of Technology	sowhsin@mit.edu
Sang-Wook Cheong	Rutgers University	sangc@physics.rutgers.edu
Omar Chmaissem	Argonne National Laboratory	chmaissem@anl.gov
Pengcheng Dai	University of Tennessee	daip@ornl.gov
Takeshi Egami	University of Tennessee	egami@utk.edu
Michael Fitzsimmons	Los Alamos National Laboratory	fitz@lanl.gov
Eric Fullerton	University of California, San Diego	efullerton@ucsd.edu
Brent Fultz	California Institute of Technology	btf@caltech.edu
Thomas Gentile	National Institute of Standards	thomas.gentile@nist.gov
Henry Glyde	University of Delaware	glyde@udel.edu
Alan Goldman	Ames Laboratory and Iowa State University	goldman@ameslab.gov
Genda Gu	Brookhaven National Laboratory	ggu@bnl.gov
Mikhail Gubarev	Marshall Space Flight Center	Mikhail.V.Gubarev@nasa.gov
Malcolm Guthrie	Carnegie Institution of Washington	Mguthrie@ciw.edu
John Hill	Brookhaven National Laboratory	hill@bnl.gov
Linda Horton	DOE Basic Energy Sciences	linda.horton@science.doe.gov
Dale Huber	Sandia National Laboratory	dlhuber@sandia.gov
Gene Ice	Oak Ridge National Laboratory	icege@ornl.gov
John Joyce	Los Alamos National Laboratory	jjoyce@lanl.gov
Naoyuki Katayama	University of Virginia	nk2u@virginia.edu
Boris Khaykovich	Massachusetts Institute of Technology	bkh@mit.edu
Valery Kiryukhin	Rutgers University	vkir@physics.rutgers.edu
Seyed M. Koohpayeh	Johns Hopkins University	koohpayeh@pha.jhu.edu
Tonya Kuhl	University of California, Davis	tkuhl@ucdavis.edu
Jyotsana Lal	Argonne National Laboratory	jlal@anl.gov
Jon Lawrence	University of California, Irvine	JMLawren@UCI.edu
Young Lee	Massachusetts Institute of Technology	younglee@mit.edu
Christopher Leighton	University of Minnesota	leighton@umn.edu
Xinsheng Ling	Brown University	xsling@brown.edu
Michael E. Mackay	University of Delaware	mem@UDel.Edu
Hokwang (David) Mao	Carnegie Institution of Washington	mao@gl.ciw.edu
Michael Markowitz	DOE Basic Energy Sciences	mike.markowitz@science.doe.gov
Robert McQueeney	Iowa State University	mcqueeney@ameslab.gov
Dean Myles	Oak Ridge National Laboratory	mylesda@ornl.gov
Wouter Montfrooij	University of Missouri	montfrooijw@missouri.edu

Name	Organization	E-Mail
Joreé O'Neal	Oak Ridge Institute for Science and Education	Joree.Oneal@orise.orau.gov
Raymond Osborn	Argonne National Laboratory	ROsborn@anl.gov
Steven Overbury	Oak Ridge National Laboratory	overburysh@ornl.gov
Stephen E. Nagler	Oak Ridge National Laboratory	naglerse@ornl.gov
Keeseong Park	University of Virginia	keeseong@virginia.edu
Michael Pellin	Argonne National Laboratory	pellin@anl.gov
Ursula Perez-Salas	Argonne National Laboratory	perez-salas@anl.gov
Danilo Pozzo	Washington State University	dpozzo@u.washington.edu
Thomas Proffen	Los Alamos National Laboratory	tproffen@lanl.gov
Roger Pynn	Indiana University	rpynn@indiana.edu
George Reiter	University of Houston	greiter@uh.edu
Filip Ronning	Los Alamos National Laboratory	fronning@lanl.gov
Stephan Rosenkranz	Argonne National Laboratory	srosenkranz@anl.gov
John Sarrao	Los Alamos National Laboratory	sarrao@lanl.gov
J. Michael Simonson	Oak Ridge National Laboratory	simonsonjm@ornl.gov
David Singh	Oak Ridge National Laboratory	singhdj@ornl.gov
Sunil Sinha	University of California, San Diego	ssinha@physics.ucsd.edu
Andrei Sirenko	New Jersey Institute of Technology	sirenko@njit.edu
William Snow	Indiana University	wsnow@indiana.edu
Maddury Somayazulu	Carnegie Institution of Washington	zulu@gl.ciw.edu
Oleg Tchernyshyov	Johns Hopkins University	olegt@jhu.edu
Guebre Tessema	National Science Foundation	gtessema@nsf.gov
Suzanne te Velthuis	Argonne National Laboratory	tevelthuis@anl.gov
Zlatko Tesanovic	Johns Hopkins University	zbt@pha.jhu.edu
Thiyaga Thiyagarajan	DOE Basic Energy Sciences	P.Thiyagarajan@science.doe.gov
Joe D. Thompson	Los Alamos National Laboratory	jdt@lanl.gov
John Tranquada	Brookhaven National Laboratory	jtran@bnl.gov
David J. Wesolowski	Oak Ridge National Laboratory	wesolowskid@ornl.gov
Guangyong Xu	Brookhaven National Laboratory	gxu@bnl.gov
Taner Yildirim	University of Pennsylvania	taner@seas.upenn.edu
Juan Yu	University of Virginia	jy8w@virginia.edu
Igor Zaliznyak	Brookhaven National Laboratory	zaliznyak@bnl.gov
Yang Zhang	Massachusetts Institute of Technology	zhyang@mit.edu